Abstract

Tuberculosis is a disease caused by *Mycobacterium tuberculosis*, transmitted from one person to another through inhalation of contaminated aerosols and remains a major threat despite the availability of treatments and prevention globally. Recently, a novel secretion system in *M. tuberculosis* has been identified known as the Type VII secretion system (T7SS) that allows ESX proteins to be secreted by *M. tuberculosis* and other mycobacterial species. In this study, the purified ESX protein complexes: EsxA.EsxB, EsxO.EsxP and EsxG.EsxH were analyzed to observe their effects on two different cell lines; J774.1 macrophages and 16-human bronchial epithelial (16HBE). It was observed that only EsxA.EsxB and EsxO.EsxP bound to the surfaces of J774.1 macrophages and 16HBE, while EsxG.EsxH did not. This observation suggests the possible sharing of receptors that are present on both cell lines. The localization of EsxG.EsxH was investigated by immunofluorescence microscopy of *Mycobacterium marinum*-infected macrophages. EsxG-EsxH was found to be present close to the surface of *M. marinum*, predominantly outside phagosome in infected macrophages. The production of EsxG.EsxH was estimated at 25% and 29% of the total infected macrophages counted at 24- and 48-hours-post-infection (hpi) respectively suggesting the production of EsxG.EsxH was independent to time-length of infection. Not all mycobacteria in infected

macrophages expressed the protein and it was rarely detected in phagosomal bacteria. This rare occurrence did not support the claim of synergism between EsxG.EsxH and Hrs in interrupting the phagolysosomal maturation. Possible co-localisation of EsxG.EsxH with another secreted protein Mpm70 was investigated but these proteins did not co-localise.

Acknowledgement

The acknowledgement is the last piece of my thesis to write but definitely not the least as I would not have been able to accomplish this work without the help of my supervisor, the Head of Postgraduate tutor, family and friends. It has been a great opportunity for me to be able to further my post-graduate education in University of Leicester. It nourished me with new ambient of education system, knowledge and gained a vast experience working with people from a number of different backgrounds.

First of all, I would like to express my deepest gratitude to the Vice-Chancellor of University Putra Malaysia, the Dean and Head of Department of Pathology and Microbiology of Faculty of Veterinary Medicine for having confidence in me to carry out this responsibility and supporting me all this while. I am too much indebted to the Malaysian Government for funding my three and a half-year of education. Without this help, it would be impossible for me to pursue my studies here.

My special thanks goes to my supervisor, Prof. Mark Carr who have accepted me as his student and patiently providing me with knowledge and sharing his experiences in this field throughout the years. Thank you for the guidance and giving me the chance to explore the demanding protein works and confocal microscopy techniques that I should acquire to prepare myself in future. It is a pleasure as well to be working with my two advisors, Prof.

Russell Wallis and Dr. Helen O'Hare who have given me the advices in working with this project. The advices and assistances are much appreciated.

Besides my supervisor, there are a number of people I am grateful to. A big thank you to Assoc. Prof. Dr. Sue Shackleton who has been there motivating me throughout my studies, laboratory members of Prof. Carr especially Dr. Renshaw, Mrs. Sarah Strong, Dr. Nino Iakobacvili and Dr. Richard Cowan who are consistently there for an excellent technical assistance my first ever student, Miss Sade Falowo. It was wonderful having all of you to work with!

To my family and friends, thank you so much for all the loves, care and moral supports and making my daily life fun all the way through. God bless.

"So, verily, with every difficulty, there is relief. Verily, with every difficulty there is relief"

(HQ 94:5-6)

Table of contents

Abstract 1

Acknowledgement 3

Abbreviations: 8

Chapter 1: Literature review 11
1.1 Tuberculosis in general 11
1.2 Treatment and control programs of TB 13
1.3 Disease Transmission 17
1.4 Novel transport systems in mycobacteria 19
1.5 ESX proteins affecting the host immune response 28
1.6 *M. tuberculosis* interactions with pulmonary epithelial cells 35
1.7 Objectives of the study 37

Chapter 2: Protein expression, purification and characterization of ESX protein complexes 39
2.1 Introduction 39
2.2 Methodology 40
2.2.1 EsxA and EsxB of *M. tuberculosis* protein expression and purification 40
2.2.2 EsxO and EsxP of *M. tuberculosis* protein expression and purification 40
2.2.3 EsxG and EsxH of *M. tuberculosis* protein expression and purification 40
2.2.4 EsxG and EsxH of *M. marinum* protein expression and purification 41
2.2.5 SDS Polyacrylamide Gel Electrophoresis (SDS-PAGE) 42
2.2.6 UV circular dichroism spectroscopy 42
2.2.7 Eliminating endotoxin from protein complexes 43
2.3 Results and Discussion 45
2.3.1 Purification of EsxA.EsxB complex 45
2.3.1 (a) Purification of EsxA protein 45
2.3.1 (b) Purification of EsxB protein 49
2.3.2 Purification of EsxO.EsxP (*M. tuberculosis*) 52
2.3.3 Purification of EsxG.EsxH of *M. tuberculosis* protein 58
2.2.4 Purification of EsxG.EsxH (*M. marinum*) 61
2.3.5 UV circular dichroism spectroscopy 64

Chapter 3: Potential immune modulators by Esx proteins in pulmonary environment 70
3.1 Introduction 70
3.2 Methodology 71
3.2.1 Binding of protein complexes to cell membrane of human lung cells 71
3.2.1 (a) Setting up 16HBE cell plate 71
3.2.1 (b) Setting up J774A.1 murine macrophage plate 72
3.2.2 Esx protein complexes of *M. tuberculosis* labelled with Alexafluor 546 (AF546) 73
3.2.3 Confocal microscopy slide preparations and observations 74
3.3 Results and Discussion 76
3.3.1 Binding of protein complexes to cell membrane of human lung cells 76
3.3.1 (a) Labeling of EsxA.EsxB; EsxO.EsxP and EsxG.EsxH protein complexes of M. tuberculosis with AlexaFluor 546 (AF546) 76
3.3.1 (b) Binding of EsxA.EsxB and EsxO.EsxP protein complexes to cell surfaces of J774.1 murine macrophages and 16HBE cells 78
3.3.1 (c) No binding of EsxG.EsxH protein complex to J774.1 murine macrophages cell surface and 16HBE cells 81

Chapter 4: Characterisation of EsxG.EsxH complex of *M. marinum* expression in J774.1 murine macrophages 89
4.1 Introduction 89
4.2 Methodology 91
4.2.1 Production, purification and characterisation of anti-EsxG.EsxH polyclonal antibody 91
4.2.1 (a) Antibody production 91
4.2.1 (b) Purification of polyclonal antibodies from rabbit 2962 sera 91
4.2.1 (c) Anti-EsxG.EsxH M. marinum antibody specificity and sensitivity testing by indirect enzyme-linked immunosorbent assay (ELISA) 92
4.2.2 *Mycobacterium marinum* cultures 93
4.2.2 (a) M. marinum strain DsRed growth 93
4.2.2 (b) Wild type M. marinum growth 94
4.2.2 (c) Single cell suspension of M. marinum 94
4.2.3 Determining the suitable MOI of *M. marinum* for two cell lines infection 95
4.2.3 (a) Viability of J774A.1 macrophages or 16HBE cells 95
4.2.3 (b) Colony forming unit (CFU) of M. marinum in infected J774.1 macrophage 96
4.2.3 (c) Colony forming unit (CFU) of M. marinum DsRed-infected 16HBE cell line 97
4.2.4 ELISA analysis of the expression of EsxG.EsxH in *M. marinum* in infected macrophages 97
4.2.5 EsxG.EsxH *M. marinum* expression in culture 98
4.2.6 Characterisation of EsxG.EsxH protein expression during infection 98
4.2.6 (a) Infected J774A.1 macrophages 98
4.2.7 Expression of EsxG.EsxH complex in 16HBE cell 99
4.2.8 Protein expression in phagosome 100
4.2.9 Imaging 100
4.2.10 Semi quantification of EsxG.EsxH expression in infected J774.1 murine macrophages 100
4.2.11 Co-localisation of EsxG.EsxH with Mpm70 using quantum dot (Qdot)-labelled primary antibodies 101
4.2.11 (a) Conjugating anti-Mpm70 polyclonal antibody with Qdot565 101
4.2.11 (b) Conjugating anti-EsxG.EsxH polyclonal antibody with Qdot655 103
4.2.12 Determining the suitable dilution of labelled antibodies and the use of either DsRed or wild type *M. marinum* without DsRed plasmid for experimental procedure 104
4.2.12 (a) Qdot565-labelled anti-Mpm70 polyclonal antibody optimization 104
4.2.12 (b) Qdot655-labelled anti-EsxG.EsxH antibody optimization 105
4.2.12 (c) M. marinum DsRed versus wild type M. marinum without DsRed plasmid 105
4.2.13 Experimental controls for Qdot analysis 105
4.2.13 (a) Positive controls: Mpm70 and EsxG.EsxH expression in M. marinum 105
DsRed-infected J774.1 macrophages 105
4.2.13 (b) Negative control: Qdot655 reagent on wildtype M. marinum-infected 106
J774.1 macrophages 106
4.2.14 Optimization of experimental protocol 106
4.2.14 Optimized slide preparation protocol 106
4.3 Results and discussion 107
4.3.1 Production, purification and characterisation of anti-EsxG.EsxH polyclonal antibody 107
4.3.2 Determining the suitable MOI of *M. marinum* for two types of cell lines infection 108
4.3.3 ELISA analysis of the global expression of EsxG.EsxH in *M. marinum* in infected macrophages 114
4.3.4 EsxG.EsxH *M. marinum* expression in culture medium 115
4.3.5 Characterisation of EsxG.EsxH protein expression during infection 118

4.3.5 (a) Infected J774A.1 macrophages 118
4.3.6 Protein expression in phagosome 121
4.3.7 The frequency and importance of EsxG.EsxH expression in infected J774.1 murine macrophages 127
4.3.8 No co-localisation between EsxG.EsxH and Mpm70 proteins identified using Qdot-labelling agents 137
General discussion and future work 144
Future work 152
Appendix 154
Bibliography 204

Abbreviations:

AEBSF	4-(2-Aminoethyl) benzosulfonyl fluoride hydrochloride
AIDS	Acquired immunodeficiency syndrome
AMP	Ampicillin
B-cell	Bursa dependent lymphocyte
Bis- Tris	2-[bis(2-hydroxyethyl)amino]-2-hydroxymethyl-propane-1.3-diol
BSA	Bovine serum albumin
CFP-10	Culture filtrate protein, 10kDa
Da	Dalton
DOTS	Direct observed therapy short-course
DTH	Delayed-type hypersensitivity
DTT	1,4,-dithiothreitol
EDTA	Ethylene diaminetetraacetate
ESAT-6	Early secreted antigenic target, 6kDa
ESAT-6/CFP10	The ESAT-6 CFP-10 complex
FCS	Foetal calf serum
HIV	Human immunodeficiency virus
hpi	Hour post-infection
IFNγ	Interferon gamma
IL	Interleukin
INH	Isoniazid
IPTG	Isopropyl-1-thio-β-D-galactoside
KAN	Kanamycin

kDa	Kilo Dalton
LB	Luria-Bertani
LDS	Lithium dodecyl sulphate
MDR	Multiple drug resistant
M. marinum	*Mycobacterium marinum*
MPB	*Mycobacterium bovis* protein
MPM	*Mycobacterium marinum* protein
MPT	*Mycobacterium tuberculosis* protein
Mtb	*Mycobacterium tuberculosis*
OADC	Oleic acid-albumin-dextrose-catalase
OD	Optical density
PAGE	Polyacrylamide gel electrophoresis
PBS	Phosphate buffer saline
PFA	Paraformaldehyde
RD	Region of difference
RPM	Revolutions per minute
SDS	Sodium dodecyl sulphate
TB	Tuberculosis
T-cell	Thymus-dependent lymphocyte
TE	Typsin EDTA
TNFα	Tumour necrosis factor alpha
Tris	2-amino-2-hydroxymethyl-propane-1,3-diol
UV	Ultraviolet
v/v	Volume per volume

w/v	Weight per volume
WCL	Whole cell lysate
WHO	World Health Organisation

Chapter 1: Literature review

1.1 Tuberculosis in general

Tuberculosis (TB), a disease caused mainly by *Mycobacterium tuberculosis* in humans has been around the globe for decades and yet, it remains a major global health problem. Based on the World Health Organisation (WHO) 2013 report, in the year 2012, about 8.6 million people developed TB in which about 1.3 million died from it, including 320 000 deaths, among those were the HIV-positive sufferers. It was estimated that 75 % of the reported cases came from the African regions alone. This showed that TB is a serious matter and unacceptable especially when the disease is treatable and preventable through proper treatment regimes and control measures imposed to the endemic and susceptible countries. For nearly 20 years, WHO has declared TB as a global public health emergency and progress has also been made under the Stop TB Strategy and Millennium Development Goals (MDGs). Via this monitoring effort, the TB mortality rate around the world has been seen to decline each year since then as reported in the year 2012, in which the number was seen to reduce by 45 % since 1990 (WHO, Global Tuberculosis report, 2013).

According to the same resource, there were about 22 high TB burden countries (HBCs) that were identified and these countries accounted for 80% of the world's TB cases. Nonetheless, 7 of these countries successfully met all the 2015 targets for reductions in TB incidence, prevalence and fatality while 4 more are on track by 2015. On the other hand, the African and European continents

have become a more concerning focus points since both regions are still far from achieving the mortality and prevalence targets.

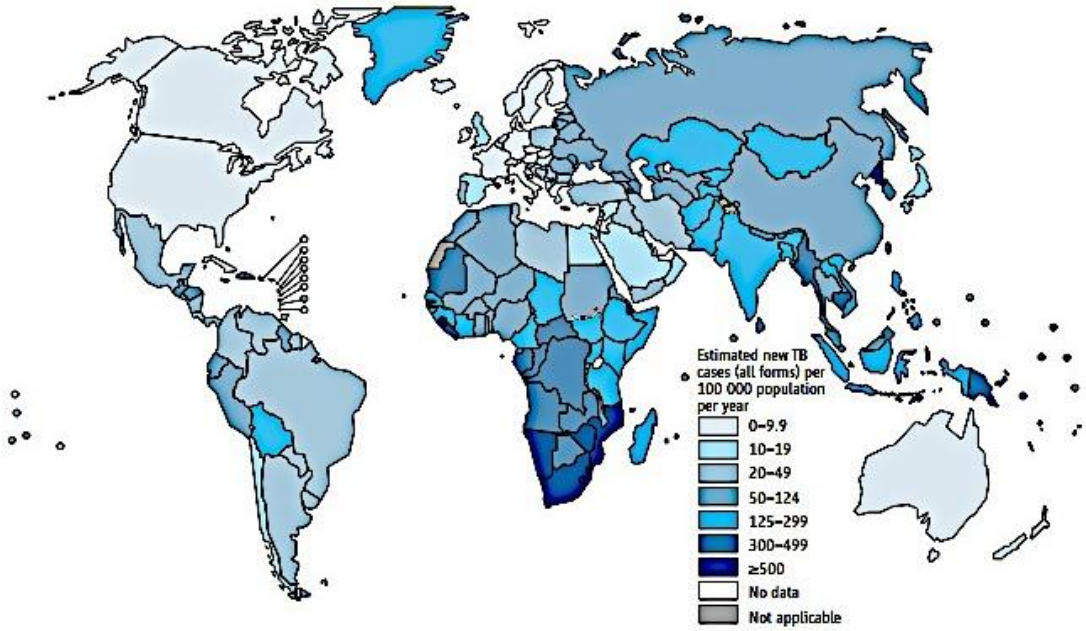

Figure 1.1: Estimated TB incidence rate in 2012. The dark blue colour showed countries with the highest burden of TB incidence where majority of the countries were located in Southern Africa region, which is closely related to the areas where the highest HIV prevalence reported. This figure was taken from World Health Organisation (WHO), Global Tuberculosis report (2013).

A new trend of epidemic occurrence of TB has also been seen to bloom exceptionally in the high-income and/or industrialized countries and this is particularly true with regards to the United Kingdom (UK) [Davidson, JA *et al.,* 2016]. Through UK government policies, a vast number of immigrants and refugees especially from Asian continents swarm the country for working and protection purposes. Along with their migrations, the country is now becoming one of the most TB-prone country though the number of incidence is still at the lowest end and recently has seen to decline in all regions of the country and

among the UK-born and non-UK born population (Davidson, JA *et al.,* 2016). The number of cases and spreading may considerably be reduced with more efficient screening for active and latent TB infection of immigrants from endemic countries at entry (Pareek *et. al*, 2012). In this case, a more fast and cost-effective method should be identified and employed due to the fact that the number of human movements is high every year. And because of this reason, a continuous increase of researches in finding the best way in managing the disease at every aspect has become the main focus in the UK as to keep the number of new cases to the lowest possible.

1.2 Treatment and control programs of TB

Although TB disease is chronic and detrimental for some people, it is important to know that not everyone infected with *M. tuberculosis* will succumb to the severe form of the illness. Depending on host immunity, there are two different conditions that exist, one where majority succumb to latent TB infection while the other one is with active TB disease (Behar, 2013; van Pinxteren *et al.,* 2000; Lalvani *et al.,* 1998). Therefore, the treatment approach for each condition is varied. In most part of the world where TB is a major concern, national programs and operational challenges has been set up under the supervision of the WHO. However, without a strict compliance from the patients, multidrug resistant among TB patients (MDR-TB), to at least rifampin and isoniazid from the first-line anti-TB drugs could develop (Andersen, L *et al.,* 2015). Recently, the extensively drug-resistant TB (XDR-TB) has been identified and leads to a more complicated public health crisis. Patients with active TB not only develop resistance towards the first-line treatment but also showed resistance to the

second-line drugs, which includes at least one fluoroquinolone and one second-line injectable drug (Andersen, L *et al.,* 2015). Hence, an effective treatment care with quality drugs accompanying a thorough diagnosis of MDR-TB and XDR-TB must be handled meticulously. This is because, the treatment for MDR-TB and XDR-TB are relatively costly, time-consuming and the number of treatment options present is limited while the choices generally life-threatening (Wallis, R.S. *et al.,* 2016).

In the United States for example, the number of TB cases was seen to reduce each. From 1993 to 2011 it consistently reduced between 5% and 7% annually seen in both foreign-born and non-foreign-born populations since its resurgence in 1985 to 1992 (Centers for Disease Control and Prevention (CDC), Sixth Edition 2013). Based on the CDC report article on TB Elimination (April 2010), under the National Tuberculosis Indicators Project (NTIP), several objectives have been set. Among the objectives were: to provide a standardize reporting template for each state; to evaluate TB status particularly of immigrants and refugees; and to recommend the initial treatment to people who are free from active TB and are latently infected tested via tuberculin skin test (TST) or interferon gamma release assay (IGRA). This is the regime that the United States has employed as part of their control program (Transmission and pathogenesis of tuberculosis by Centers for Disease Control and Prevention, CDC). Since this program commenced in 2005, a significant number of TB cases have been decreased.

To adhere to a single standard of TB control program through *Mycobacterium bovis* Bacillus Calmette-Guérin (BCG) vaccination to all countries may have seemed to be a feasible method, but based on recent reports pertaining to host protective immune responses following vaccination among populations in African countries and the United Kingdom (UK) provided a new perspective. BCG has been proven to confer variable protection against pulmonary TB in adults. The cytokines and chemokines profiles analyzed using whole blood samples from the respective populations revealed surprising differences in immune responses between the two groups of population. It appeared that the infants vaccinated between 8 to 13 weeks of age were more protected with the released of T helper 1 (Th1)-derived cytokines such as interferon-gamma (IFN-γ), TNF-α, interleukin-1β (IL-1β), IL-12p40 that is more important in granuloma formation; while the Malawian infants vaccinated earlier (3 to 7 weeks of age) showed to produce higher amount of Th2-derived cytokines and growth factors in which were not involved in the general response to TB infection (Lalor *et al.*, 2011). A similar feature has also been observed in African population from other African countries (Randhawa *et al.,* 2011; Finan *et al.,* 2008; Jepson *et al.,* 2001). Gao *et al.* (2005) has reported that between *M. tuberculosis* clinical isolates, there were diversity in gene expression demonstrated and recently, based on single nucleotide polymorphism (SNP) analysis of all *esx* genes on 108 clinical isolates of *M. tuberculosis*, it was shown that out of 23 *esx* genes, 19 of them revealed SNPs some of which identified to involve the stop codons where this could significantly affect the structure and function of a protein (Uplekar *et al.,* 2011).

From this understanding, the dynamic *esx* genes are prone to SNPs and this could explain the likelihood of variation in host immune response. The discrepancies in immune responses could be seen in vaccinated people from one population to another population, which may be contributed by the exposure to different strains of *M. tuberculosis* and/ or vaccinated at different age as mentioned above. This is especially alarming when post-vaccination even showed that the vaccine improves protection against meningeal TB in the children better than the pulmonary type commonly acquired by the adolescents and adults (Kauffman *et al.,* 2010). Hence, a number of reports continue to elaborate on the importance in finding a new vaccine to cater the needs (of the people) depending on the regions where people are prone to contact with different strains of *M. tuberculosis* that may contribute to the variety of immune responses with regards to TB (CDC, 1998; Beresford and Sadoff, 2010). However, in order to produce a new and effective vaccine that could provide consistent immune responses regardless of the origin of the population, it is important to understand the expressed and secreted proteins of the TB in terms of the level of expressions and their ability to stimulate cytokines that specifically involve in initial response to TB infection. Subsequently, from this knowledge, it will lead us to a new and better mechanism of diagnosis, treatment and control of TB.

Another point to consider in order to achieve the target set by the WHO in reducing the number of new and current occurrence of TB, is that strong collaboration is highly needed among the drug regulatory authorities, donors, technical agencies, civil society and pharmaceutical industry. A continuous

research on understanding the pathogenesis of TB is required to assist in developing a new, practical and effective approach in treating, controlling and preventing the disease which is also part of the aim for my study.

1.3 Disease Transmission

Tuberculosis (TB) is a communicable disease where patients with pulmonary TB are the most important and common source of infection. Infection can happen through inhalation of droplets containing 1-5 μm size of particles of *M. tuberculosis* and initiated when active pulmonary TB patients cough the infectious particles into the environment **(Figure 1.2)**. Factors such as the distance between potential host and the patients, the load of inhaled bacteria as well as the potential hosts' immune status plays a major role in assessing the risk of acquiring the disease (Frieden *et al.,* 2003; Hill *et al.,* 2004; Mathema *et al.,* 2008). Post inhalation, the contaminated droplets will travel to the rest of the pulmonary systems such as trachea, bronchi and finally settle in alveolar cells due to their small size. Apart from the terminal alveolar cells, *M. tuberculosis* have been shown to infect other non-phagocytic cells that are present in the alveolar space such as M cells, alveolar endothelial and type I and II pneumocytes (Bermudez and Goodman, 1996; Teitelbaum *et al.,* 1999; Bermudez *et al.,* 2002; Danelishvili *et al.,* 2003; Garzia-Perez *et al.,* 2003; Mehta *et al.,* 2006; Kinhikar *et al.,* 2010).

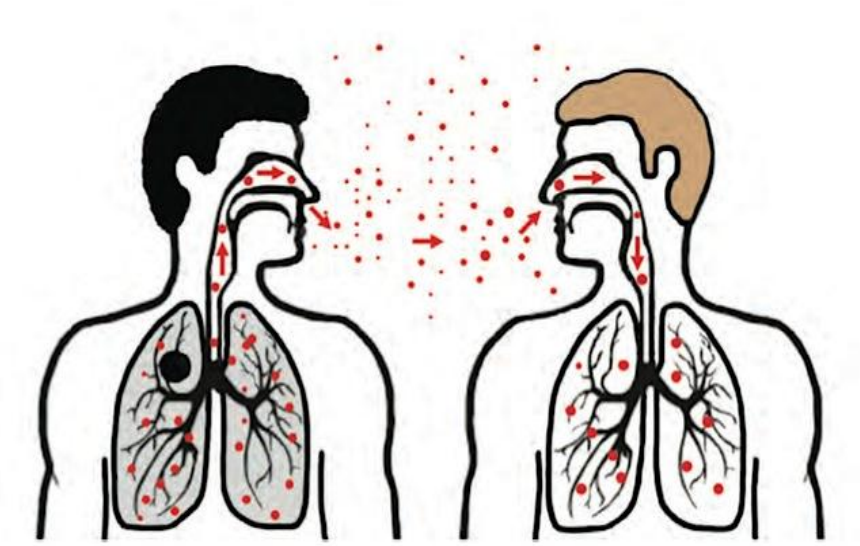

Figure 1.2: Transmission of TB. The pathogen can easily be transmitted from person to person through air. The red dots in this image represent the droplets containing tubercle bacilli. Image above is taken from **www.cdc.gov in "Transmission and Pathogenesis of Tuberculosis" chapter.**

Hence, it is plausible to hypothesize that the first site of interaction between the pathogen and the host is the pulmonary epithelium (Bermudez *et al.,* 1999) through the pathogen secreted protein, lipopolysaccharides or mycolic acids. Yet, there is still a lack of information to suggest which mycobacteria specific secreted protein(s) may lead to the interaction with alveolar epithelial cells if they were in contact and subsequently modulate immune responses to support its existence and growth in the immune cells such as the lung macrophages. Apart from that, even the role of the pulmonary epithelium in any of these pathogenic processes of tuberculosis is still unclear.

1.4 Novel transport systems in mycobacteria

M. tuberculosis, the pathogen of tuberculosis (TB) is typically characterized by the presence of a thick layer of mycolic acids in their cell envelope. The presences of thick protective outer membrane is one of the main reasons mycobacteria survive the harsh conditions including antimicrobial enzymes/ chemicals and mechanical stress. Although it appears benefit the bacteria as a protective shield, it could probably hinder the process of transporting the expressed proteins into the host cell. Thus, it is interesting to understand the mechanism of how the secreted proteins from mycobacteria interact with their environment and/or host cell with the presence of the thick outer membrane.

Protein evolution of pathogenicity was also seen in *Mycobacteria* gene families and they were shown to highly associate with the adaptation to environmental and pathogenic strains. McGuire *et al.* (2012) highlighted the functional importance in their virulence, regulation and variation based on the gene profiles they gathered from 31 organism genomes imported from Tuberculosis Database (TBDB.org). This includes 8 strains of *M. tuberculosis* namely CDC1551, C, Haarlem, H37rv, H37ra, F11, AF2122 and BCG, *M. leprae, M. ulcerans, M. marinum, M. avium 104, M. avium K10, M. sp. MCS, M. sp. KMS, M. smegmatis, M. gilvum, M. vanbaalenii M. abscessus, Norcardia farcinia, Acidothermus cellulolyticus, Rhodobacter sphaeroides, Propionibacterium acnes, and Bifidobacterium longum*. McGuire *et al.* (2012) also observed a number of expansions of known genes particularly those related

to pathogenicity such as the PE/PPE genes, antibiotic resistance genes, as well as the *esx* genes and were able to also predict the most salient candidate to be part of virulence. According to McGuire *et al.,* (2012), both *M. tuberculosis* and *M. marinum* shared similar pathogenicity activities in conjunction with the presence of identical or closely related *esx* genes in both of the mycobacterial species. Hence, the use of *M. marinum* in my study could be used to extrapolate the *M. tuberculosis* pathogenesis as well.

In the past, extensive focus has been made in understanding the mechanism of proteins secreted by the Gram-negative bacteria, particularly the pathogenic species. The studies had led to the identification of various secretion systems employed by the Gram-negative bacteria to transport the virulence factors across their inner and outer cell membrane. The specialized secretion systems identified have been designated as type I to VI secretion system in which each of the secretion systems exhibit a different mechanism during the transportation process as well as the secreted effector molecules that are involved. The one-step type I secretion system for example uses a simple mechanism that spans the whole cell envelope (Holland *et al.,* 2005) where as the two-step type II secretion pathway mediate the folded protein (occurred in periplasm before translocated across outer membrane, OM) to translocate to inner membrane (IM) using Sec- and/or Tat-system assisted by a special structure in IM called secreton (Johnson *et al.*, 2006). On the other hand, type III secretion system uses its special structure called injectisome that forms a channel in order to allow the substrates to cross the entire cell membrane and extended to the recipient cells (Cornelis, 2006). Similar to type III system, the

type IV uses a pilus structure at bacterial cell surface to transfer its substrates directly into host cells (Christie *et al.,* 2005). Type V system appeared to use a simpler two-step mechanism to cross IM using Sec-translocon, and β-barrel translocator (Henderson *et al.,* 2004) in which to date is doubtable for its role as either contiguous with secreted protein or as separate entity that makes it a two-step pathway (Oomen *et al.,* 2004). The type VI secretion system however, is still lacking in details (Mougous *et al.,* 2006; Pukatzki *et al.,* 2007). The schematic diagram summarized the type I to VI secretion system is shown in **Figure 1.3** below.

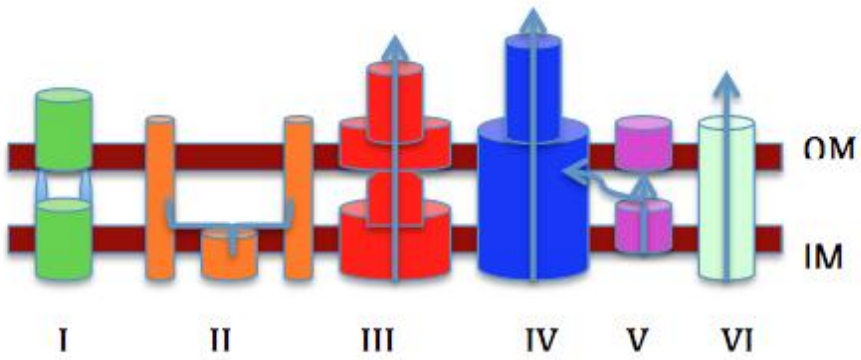

Figure 1.3: Model of Type I-VI secretion systems in bacteria. From left to right, the schematic diagram showed Type I to VI respectively. Note that not all of the secretion systems were required by a single bacterium to secrete the proteins produced as described elaborately in Section 1.4. As for *M. tuberculosis* and other mycobacterial species, a novel secretion system has been identified to assist in secreting the Esx proteins. Image reproduced from Abdallah *et al*. (2007).

In contrast, having a much simpler structure, the Gram-positive bacteria have always been thought to merely traverse their substrates through cytoplasmic and peptidoglycan layer into extracellular environment, hence the lacking in studies related to Gram-positive secretion system systematically. As described thoroughly above, it was mentioned that the type IV secretion system is found not only in Gram-negative bacteria but also in Gram-positive bacteria (Goodfellow and Jones 2012). And recently, a novel secretion pathway has been identified known as the Type Seven Secretion System (T7SS) in Gram-positive bacteria. This specialized transport system was first identified in *M. tuberculosis* H37Rv, phylogenetically belongs to the order of *Corynebacteriales*, a Gram-positive microorganism (Goodfellow and Jones 2012). Meanwhile, there were a few components of T7SS also found in Firmicutes phylum (Abdallah *et al.,* 2007; Pallen 2002). Through this specialized secretion system, the virulence factors are transported across their unique cell envelope into the infected host cells. The ability of mycobacteria to secrete virulence factors allows them to exhibit their pathogenicity, and the virulence factors are commonly displayed on the bacterial cell surface, secreted into the extracellular milieu or injected directly into host cells (Finlay and Falkow 1997). The proteins secreted through T7SS have shown to be lacking in the classical signal peptides that are usually found in proteins secreted by type II, IV and V pathways. Moreover, the secreted proteins via T7SS have been demonstrated to be present in a specific complex (pair dependency) as a functional form (Fortune *et al.,* 2005). The number of researches focusing on the aspect of T7SS has been competitive since and in the meantime, a number of secreted proteins associated with T7SS have also been discovered.

A comparison between the vaccine type mycobacteria, the *M. bovis* BCG and pathogenic species, the *M. tuberculosis* has been made and analyzed by (Zakham *et al.,* 2012; Lew *et al.,* 2011; Galagan *et al.,* 2010; Stahl *et al.,* 1990; Cole 2002; Brosch *et al.,* 2001; Wassenaar 2009). Bacille Calmette-Guérin (BCG) is a live attenuated form of the virulent *M. bovis* TB vaccine and has been administered to people in the endemic and high risk countries with a good record in terms of safety issue (Casanova *et al.,* 1996) since its first used in 1921 (Bloom and Fine, 1994). However, the efficacy of the vaccine varies and in some cases, it was reported to show no efficacy at all (Huebner, 1996). More than a decade ago, several regions of *M. tuberculosis* chromosome that were absent from various BCG substrains have been identified (Mahairas *et al.,* 1996; Philipp *et al.,* 1996; Behr *et al.,* 1999; Gordon *et al.,* 1999). Based on molecular analysis of genetic differences between *M. bovis* BCG and *M. tuberculosis*, of all the missing regions analyzed from RD1 to RD10, it was found that RD1 to RD3 were deleted from BCG strain whilst RD1 was identified to be deleted from all BCG substrains (Mahairas *et al.,* 1996). The mutation of RD1 in all substrains of BCG was seen to be present in the virulent *M. tuberculosis*. The association between loss of about 9.5kb RD1 and mycobacterial virulence and the genes within RD1 has been made since then. The deletion region was identified to compose of 7 genes (Rv3872-Rv3878) as well as causing 2 truncated genes (Rv3871 and Rv3879c) [Cole *et al.,* 1998]. As a consequent of the absence of RD1, the growth of *M. tuberculosis* was seen to be altered and also affect the survivability of mycobacteria in macrophages and its dissemination process

(Lewis *et al.*, 2003), which is similarly seen in the attenuated form of *M. bovis* BCG.

The components of T7SS composed of five gene clusters that are believed to have evolved via gene duplication and these clusters are better known as ESAT6 secretion system (ESX) 1 through 5. Because of gene duplication, most of mycobacteria have a lower number of ESX loci. According to Gey Van Pittius *et al.* (2001), ESX2 and ESX5 evolved relatively recently and only detected in specific subsets of *Mycobacteriaceae*. The ESX5 for example is worthwhile to observe as its presence was reported to coincide with the differentiation between fast and slow growing mycobacteria. Having said that, it is still unknown whether its presence is functionally linked to the slow growing phenotype. Besides the involvement of cluster expansion through gene duplication, the number of ESX loci was reduced also contributed by the deletion events. This is particularly true for ESX1 for instance where pathogenic mycobacteria such as *M. avium* and *M. ulcerans* are deficient in ESX1 (George *et al.,* 1999) despite its importance as a virulent factor. This means that the mycobacteria compensated the loss of ESX1 via different mechanism such as *M. ulcerans* secreting a special toxin that cause cytotoxic to macrophages while *M. avium* producing glycopeptidolipids (GPLs) that are absent in other pathogenic mycobacteria. As for ESX3, it was reported to be essential in a number of mycobacterial species while the ESX4 was identified as the oldest system so far. Above all, only ESX1, ESX3 and ESX5 have been shown to be involved in secreting proteins (Stanley *et al.,* 2003; Abdallah *et al.,* 2006; Siegriest *et al.,* 2009) where there was no report regarding the participation of

ESX2 and ESX4 in protein secretion processes. Table 1.1 showed the summary of the conserved loci present in the T7SS of *M. tuberculosis*, which includes the specific genes expressed the proteins in *esx*A and *esx*B paralogs respectively.

The attenuation of the vaccine strain that was preceded by the deletion of RD1 might have resulted from prolonged *in vitro* growth, which was actuallyseen to have removed majority of ESX1 locus (Simeone *et al.,* 2009; Stoop *et al.,* 2012). Since then, ESX1 has been the widely studied cluster due to its importance in pathology. The first ESX1-associated protein to be identified was the 6-kDa early secreted antigenic target (ESAT-6) or now renamed as EsxA (Sorensen *et al.,* 1995). This small yet highly immunogenic protein is present abundantly in the culture filtrate of *M. tuberculosis*, which is missing from the attenuated live *M. bovis* BCG culture as a result of deletion of region of difference 1 (RD1) [Harboe *et al.,* 1996; Mahairas *et al.,* 1996]. Following the discovery of EsxA, another secreted protein was identified known as the 10-kDa culture filtrate protein (CFP10) or currently known as EsxB (Berthet *et al.,* 1998). It was demonstrated that both proteins, EsxA and EsxB were co-transcribed and formed a tight dimer of 1:1 protein complex that involved in hydrophobic interaction (Renshaw *et al.,* 2002; Brodin *et al.,* 2005; Renshaw *et al.,* 2005) and are dependent on each other for secretion. Furthermore, this protein complex was part of the missing genes in RD1 that were responsible for virulence and was proven through the restoration of RD1 in *M. bovis* BCG enabled the secretion of EsxA subsequently caused the BCG strain to become virulent (Pym *et al.,* 2002; Lewis *et al.,* 2003).

As mentioned before, T7SS comprises of five gene clusters of secretion system, four of which appeared to be homologues of the ESX1 cluster. Not only that, majority of the proteins expressed by the gene clusters exhibit a similar structural characteristic which is forming a stable and tight 1:1 complex with their respective protein partners such as EsxG and EsxH of ESX3; EsxO and EsxP of ESX5; EsxT and EsxU of ESX4; EsxC and EsxD of ESX2 (reviewed by Bitter *et al.,* 2009). Though these specific partners may represent their functional form, through the combination of yeast two-hybrid and biochemical analysis, it was demonstrated that the closely related ESAT6/CFP10 proteins were also able to form a non-genome paired complexes, however incapable of showing binding with more distantly related ESAT6/CFP10 proteins (Lightbody *et al.,* 2004). The proteins identified to form the heterodimeric complexes were the EsxG.EsxR and EsxH.EsxS that could suggest a functional flexibility between closely sequence-related ESAT6/CFP10 protein families.

Although ESX1 was initially identified in *M. tuberculosis*, the gene cluster is also present in other mycobacterial species including *M. marinum, M. kansaii* (Sorensen *et al.,* 1995), *M. leprae* (Cole *et al.,* 2001) and the fast grower mycobacteria, *M. smegmatis* (Flint *et al.,* 2004; Converse *et al.,* 2005; Coros *et al.,* 2008). *M. marinum* has been chosen widely as the model for the purpose of defining the role for paralogous ESX5 system mostly involving the PE and PPE proteins (Abdallah *et al.,* 2006; Abdallah *et al.,* 2007; Abdallah *et al.,* 2008). Not only that, the use of *M. marinum* as an infection model in microscopic analysis has provided a bigger picture in viewing the proteins expression, characteristics and behaviors either in fixed or live preparations. Based on genomic comparison

between *M. marinum* and *M. tuberculosis*, it confirmed the close genetic relationship through identification of 3000 orthologs with an average amino acid identity of 85 % shared between both species, which includes the related-ESX secretion systems and mycobacteria-restricted PE and PPE proteins (Stinear *et al.,* 2008). The genetic similarity has led to the choice of this large genome *M. marinum* in research as a foundation to understand the determinants of tuberculosis pathogenesis particularly when *M. marinum* possessed more *esx* genes (29 *esx* genes) than in *M. tuberculosis* (23 *esx* genes). Other mycobacterial species such as *M. smegmatis* although made up with a large genome (7 Mb), *M. smegmatis* only has three ESX loci and lacking in the key element for mycobacterial pathogenesis, the ESX 1 locus, which is required for granuloma production and bacteria spread between macrophages (Cosma *et al.,* 2003, Guinn *et al.,* 2004, Volkman *et al.,* 2004).

	esxA paralogs		*esxB* paralogs	
Conserved ESX locus	**Inside ESX locus**	**Outside ESX locus**	**Inside ESX locus**	**Outside ESX locus**
ESX-1	***esxA (rv3875)***		***esxB (rv3874)***	
ESX-2	*esxC (rv3890c)*		*esxD (rv3819c)*	
ESX-3	***esxH (rv0288)***	*esxR (rv3019c), esxQ (rv3017c)*	***esxG (rv0287)***	*esxS (rv3020c)*
ESX-4	*esxT (rv3444c)*		*esxU (rv3445c)*	
ESX-5	*esxN (rv1793)*	*esxI (rv1037c), esxL (rv1198),* ***esxO (rv2346c),*** *esxV (rv3619c)*	*esxM (rv1792)*	*esxJ (rv1038c), esxK 9(rv1197),* ***esxP (rv2347c)****, esxW (rv3620c)*

Table 1.1: Overview of *esx* family of *M. tuberculosis*. There were five known conserved ESX loci namely the ESX1 to ESX5 and each locus possessed own pairs of esxA or ESAT6 and esxB or CFP10 paralogs in which the details were stated in the table. Loci in bold were involved in the expression of protein of interest mentioned in this thesis. This table is reproduced from Uplekar *et al.* (2011) whom analyzing the differences in *M. tuberculosis* genomes through the use of SNPs.

1.5 ESX proteins affecting the host immune response

M. tuberculosis has been shown to employ various mechanisms of adaptation to its environment and it is the essential component of its pathogenesis, transmission and maintenance in the host (Schnappinger *et al.,* 2003). Being the most important bacterial control as well as multiplication medium, macrophages have been the most studied and described immune cells with regards to tuberculosis infection. The immune cell responded by

upregulating the synthesis of pro-inflammatory cytokines such as the IL-1β (Montero *et al.,* 2004).

In general, once entering the host cells, mycobacteria primarily would be engulfed by the macrophages, which act as the first line of host cellular defense mechanism against microbial invasion. Over the past decades, researchers have discovered that the pathogenic species of mycobacteria have developed strategies to circumvent the neutralization or killing following the ingestion of mycobacteria from host phagosome biogenesis. As a result of the interference via arresting phagosome maturation and its fusion with lysosome, this mechanism subsequently allows the mycobacteria to enhance their survival within human host cells (Russell, 2011; de Chastellier *et al.,* 2009; Deretic *et al.,* 2006; Russell, 2001).

Abdallah *et al.* (2011) demonstrated that the effector proteins of ESX1 from *M. marinum* were able to affect the subcellular localization and also macrophage cell responses in contrast to ESX5. The observation was made through comparing post-inoculating of ESX1- and ESX5-mutant and wild type of *M. marinum* to macrophage cells independently. The response includes induction of IL-1β as well as inflammasome activation. Despite not participating in such responses, through its effector proteins secreted by the ESX5 system, this system has been shown to induce a caspase-independent cell death following macrophages translocation (Abdallah *et al.,* 2008; Abdallah *et al.,* 2011). The synthesis of IL-1β by macrophages however is dependent on the presence of caspase-1 while caspase-1 requires inflammasome to be activated (Koo *et al.,* 2008; Kurenuma *et al.,* 2009; Carlsson *et al.,* 2010; Mishra *et al.,*

2010). This proves that both ESX1 and ESX5 are dependent on each other to ensure the pathogenic mycobacteria especially *M. tuberculosis* and *M. marinum* to modulate the macrophages responses via regulation among IL-1β, caspase-1 and inflammasome activation that is involved in cell death as seen in Gram-negative bacteria (Labbé and Saleh, 2008).

The EsxA and EsxB have become the major highlight ever since they were recognized to be part of the missing region in *M. bovis* BCG vaccine strain that led to the strain became attenuated. These two proteins has been well characterized structurally (**Figure 1.5**) as detailed in previous *'Novel transport system in mycobacteria'* section of this chapter. A number of studies described that EsxA secreted by the ESX1 pathway in mycobacteria enhances the immune responses compared to its partner, EsxB protein (de Jonge *et al.,* 2007; Hsu *et al.,* 2003). Further studies conducted have shown some considerations that EsxA acts on the host cell membrane, macrophages subsequently caused pore formation to assist the translocation of mycobacteria from an infected cell to a new host cell (de Jonge *et al.*, 2007). However there was slight contradiction to the findings stated by Renshaw *et al.* (2002); Lightbody *et al.* (2004). It was understood in which the characterization of EsxA.EsxB protein complex revealed that the complex was very stable even in harsh environment that closely mimic the condition in phagolysosomal compartment post-engulfing by the macrophages. This suggests that the functional form of EsxA and EsxB is in the form of a complex. Hence, in my study, EsxA.EsxB complex secreted by ESX1 secretion system from *M. tuberculosis* was used as the studied subject. Another surprising observation made by Wang *et al.* (2009) was that the ESAT6

(EsxA) but not CFP10 (EsxB) at higher dosage, at least 1.6 μM concentration capable to inhibit the production of IFN-γ by T cells via mechanism that is independent of cytotoxicity or apoptosis. This finding is important since the current commercially available diagnostic kit for instant the interferon gamma release assays (IGRAs) equipped with anti-IFN-γ antibody is used to screen for both latent and active infection (Kellar *et al.,* 2011) as IFN-γ is known to be critical for activating host defenses (Manca *et al.,* 2001). There will be some variation that should therefore be taken into consideration when developing new drugs, diagnostic kits and vaccines as one reagent may work on some strains but not on the others. The variation in *M. tuberculosis* strains has been described previously in page 23. In addition to EsxA, *M. tuberculosis* through its other virulence factors including lipoarabinomannan were reported to inhibit the maturation of phagosome and NF-κB activation (Lugo-Villarino *et al.,* 2011). For an efficient clearance of mycobacteria in infected host cell, the maturation of phagosome is a crucial step to trigger the coalescent with lysosome, as the enzymes in phagolysosome will continue to digest the mycobacteria (Mehra *et al.*, 2013, Podinovskaia *et al.,* 2013).

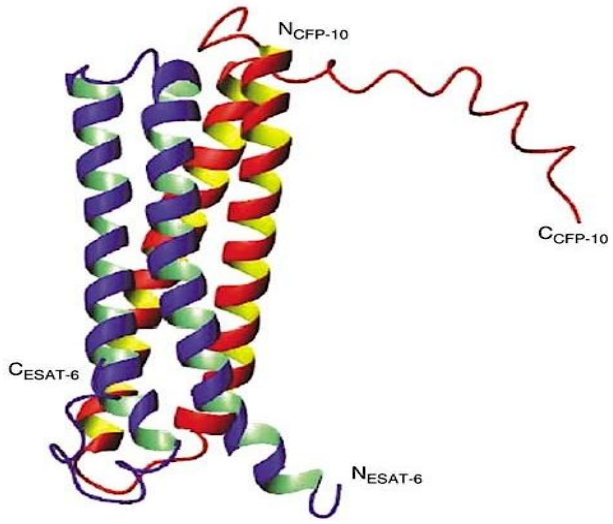

Figure 1.5: The solution structure of EsxA.EsxB. A ribbon representation illustrates two helix–turn–helix hairpin structures formed by individual proteins of EsxA (blue) and EsxB (red) in which the proteins appeared to be anti-parallel to each other and formed a stable four-helix bundle. The C-terminal of EsxB is unstructured is also noticeable (Renshaw *et al.,* 2005).

On the other hand, the ESX3 secretion system of T7SS is predicted to affect the *in vitro* growth of mycobacteria (Sasetti *et al.,* 2003), which is different role as described for the ESX1 secretion system. A delay in growth was demonstrated when ESX3-deficient mycobacteria was left to grow on Middlebrook 7H9 and 7H10 media (Serafini *et al.,* 2009). This could probably be seen as the ESX3 was not essential for mycobacterial growth but the effect of lacking in *esx3* genes only lengthened the time period than a wild type mycobacterial should in normal condition. The delayed in growth was thought to have occurred due to the deficiency in iron and zinc supply post-engulfment by host macrophages. In order to overcome this situation, *M. tuberculosis* must have established a mechanism for it to survive and maintain its growth in an infected cell. The ESX3 gene cluster in *M. tuberculosis*has previously been

shown to be transcriptionally controlled by zinc uptake repressor (Zur) [Maciag *et al.,* 2007] and also the iron-dependent transcriptional repressor (IdeR) [Rodriguez *et al.*, 2002]. As a result, this suggests that the gene cluster might be involved in zinc and iron homeostasis. Lightbody *et al.* (2008) has successfully demonstrated that the proteins, EsxG and EsxH were co-transcribed and form a stable and functional 1:1 complex as predicted by Renshaw *et al.* (2005) that most of the ESAT6 family proteins might exhibit. Despite the similarities between EsxA.EsxB and EsxG.EsxH complexes in terms of the overall backbone fold, EsxG.EsxH structure appeared to have a potential protein interaction on its surface. And in accordance to ESX3 secreted proteins association with zinc homeostasis, Ilghari *et al.*, (2011) furthermore mentioned that the protein complex has high affinity towards zinc ion. This is because, a specific zinc ion-binding site has been identified to present on EsxH. The site is known to conserve across obligate mycobacterial pathogens including *M. tuberculosis* and *M. leprae*. In addition, Ilghari *et al.* (2011) also reported that there was no effect to either EsxG or EsxH when ferum ion was introduced to the ^{15}N-labeled proteins. Although ESX3 has been linked to involve in iron acquisition through mycobactin pathway, the role of its secreted protein, EsxG.EsxH in iron and zinc scavenging and the significances of this protein complex in infected host macrophage cells are still poorly understood.

Another secretion system of T7SS is the ESX5 in which the *esx*5 gene cluster also known to transcribe the EsxO, EsxP, PE and PPE proteins. Just like the other two protein complexes in ESX1 and ESX3 mentioned previously, the EsxO and EsxP also form a tight 1:1 heterodimer and suggested to function as a

complex (Dr. Alharbi, PhD thesis 2012). This protein complex has been well characterized structurally and described by the author and has been demonstrated to bind to the cell surface of murine macrophages, J774.1 as well as U937 monocytes, which could suggest playing an initial role of modulating the immune responses once host cells are infected. Nevertheless, the role of EsxO.EsxP complex is still unclear in contrast to PE/PPE protein. The PE/PPE proteins secretion preceded in the ESX5 secretion system and has been thought to play a major role in virulence and inducing the host immune response. To show the importance of PE and PPE proteins, Gey van Pitius *et al.* (2006) discovered that in mycobacteria that possessed the ESX5 secretion system, these two genes are dominating and highly expanded throughout the genome. A number of observations have been made looking at this secreted *esx5* effector proteins and its association with the secretion of immune cytokine by macrophages through comparison between ESX5 mutant *M. marinum* versus the wild type *M. marinum* (Abdallah *et al.,* 2008; Abdallah *et al.,* 2011; Weerdenburg *et al.,* 2012). Unlike ESX1 secreted proteins that is known to cause virulent in *M. tuberculosis* and *M. marinum*, the ESX5 has shown otherwise. Through the mutation of ESX5 in *M. marinum*, it was identified that the mycobacteria became hypervirulent in adult zebrafish (Weerdenburg *et al.,* 2012). Thus, indicating that with the presence of ESX5-mediated secreted proteins in some mycobacteria, commonly the slow growing pathogenic strains, it established a more moderate yet persistent tuberculosis infection in the model system portraying the chronic condition of tuberculosis.

1.6 *M. tuberculosis* interactions with pulmonary epithelial cells

Although the sequence of the virulent *M. tuberculosis* has been made available through the advancement in molecular and biotechnology, the biology of the pathogen is still poorly understood. With regards to the observation of bacteria-host cell communication, a number of studies using human lung epithelial has been conducted decades ago and continue until today. Studies related to alveolar epithelium involvement particularly in tuberculosis infection using a bilayer alveolar epithelium system have started in 1996. Bermudez and Goodman (1996) have discovered that *M. tuberculosis* was able to invade the lung epithelium and replicates within the type II alveolar cells and this was manifested using electron microscopy. Many pathogenic respiratory pathogens including mycobacteria utilize their own strategies that enable them to establish an infection in host cell. For example, the efficiency of mycobacteria to translocate from one cell to another was evident to be greater when mycobacteria were presented within the macrophages and transported through an infected A549 alveolar epithelium than in uninfected A549 (Bermudez and Goodman, 1996). This approach of translocation appeared to be more efficient probably due to the availability of mode of entrance as well as host responses such as losing the epithelium barrier that has taken place in the infected cell. The mechanism was further explained recently by Babrak *et al.,* (2014), in which any inhaled pathogenic bacteria possibly bind to the respiratory mucosa and then evade the host defences by crossing the mucosal layer, which is often mediated by the interaction with host proteins or modulating the host immune responses. *Streptococcus pneumonia* for instance, possessed PspC, a surface-

exposed bacterial protein to help it to adhere to the host cell membrane through communication with the host glycoprotein, vitronectin (Voss *et al.,* 2013). It was also reported that a number of mycobacterial proteins could facilitate the adherence of the bacteria to the host epithelial surface. The proteins that have been mentioned were fibronectin attachment proteins (FAP), histone-like protein (Hip), heparin-binding hemagglutinin (HBHA) and antigen 85 (Schorey *et al.,* 1996; Pethe 2000; Shimoji *et al.,* 1999).

Through the initial finding of mycobacteria translocation demonstrated by Bermudez and Goodman, Bermudez *et al.* (2002) has established a more refined and well-designed lung epithelial bilayer transwell system. Since then, there has been a growth of interest particularly in studying the different types of pathogens or antigens interaction with the human lung epithelial and their adverse effects on the barrier function (Kusek *et al.,* 2014; Curry-Mc.Coy *et al.*, 2013; Hermanns *et al.,* 2004). Lung injury is usually expected following an introduction to antigen either by pathogenic microbes or even by aspiration of non-self materials and shock. The injuries may become acute or chronic depending on burden of the disease in addition to the time given from infection to treatment. This could lead to a major cause of respiratory failure in critically ill patients. The symptoms usually occurred as a result of interruption to barrier function of the lungs alveolar epithelium and the capillary cells (Ware and Matthay 2001). Dobos *et al.* (2000*)* reported that significant cell monolayer clearing correlated with necrosis and not apoptosis was seen in A549 alveolar epithelium infected with the virulent types of mycobacteria, (Erdman and CDC1551) whereas infection with a virulent mycobacterial species (*M. bovis*

BCG and *M. smegmatis* LR222) did not show any clearing of the monolayer cell. As much as appropriate host immune response is important to defend from *M. tuberculosis* infection, several clinical researches have shown evidences that post-infection may also hold responsible for causing lung injuries especially during an acute inflammatory process. This is due to a complex network among the inflammatory cytokines and chemokines contributed through mediating, amplifying subsequently perpetuating the course of lung injury.

1.7 Objectives of the study

The aim for this study is to characterize the expression of EsxG.EsxH and to find the lead to the role of the expressed protein complex during mycobacterial infection. Therefore, a series of infections in two different cell lines were conducted: the 16HBE (16-human bronchial epithelial cells) and J774.1A murine macrophages; as well as a preliminary study on human lung primary cells (HL204). The purified recombinant *M. tuberculosis* protein complexes were introduced and studied for up to 24- or 48-hours to observe the differences in response on the different cells whether they are up-regulated or down-regulated. Also to understand if the protein complexes modulate immune responses during infection, barrier function was analyzed through measurement of transepithelial electrical resistant, its permeability, and detection of interleukin-8 cytokine. The expression of EsxG.EsxH complex was characterized qualitatively and semi-quantified post-infection with *M. marinum* DsRed to determine the frequency of the protein expression and provide an idea of the importance of the protein complex. From the results, an experiment is conducted in order to scrutinize if the protein complex functions

synergistically with the protein partner, in which we tested first with Mpm70 protein that is known to be expressed by mycobacteria.

Chapter 2: Protein expression, purification and characterization of ESX protein complexes

2.1 Introduction

The plasmids of recombinant protein complexes and the purification methods were received from the previous researchers, Dr. Renshaw, Dr. Al-Harbi, Dr. Ilghari, and Dr. Lightbody respectively. The aim for this chapter is to purify all of the recombinant proteins already transformed in plasmids as tabled below, in order to test our hypothesis that these proteins would bind to mammalian cells. The purified products EsxA.EsxB, EsxO.EsxP and EsxG.EsxH of *M. tuberculosis* were later subjected to conjugation with Alexalfuor 546 to determine the association of these protein complexes with the cell surface of 16HBE. Meanwhile, the purified EsxG.EsxH of *M. marinum* was used to produce a polyclonal primary antibody raised in rabbit. The polyclonal antibody would then be used to track the production of EsxG.EsxH in *M. marinum* strain DsRed-infected J774.1 murine macrophages with the use of anti-rabbit conjugated with Alexafluor 488 secondary antibody. Therefore, it is important to know that the protein was in a complexed form, this was determined through circular dichroism (CD) and purity which was determined by UV-spectrometry and SDS-PAGE following gel filtration technique. All of the protein complexes were kept in suitable buffers so that the proteins are fit for cell infection and primary antibody production.

2.2 Methodology

2.2.1 EsxA and EsxB of *M. tuberculosis* protein expression and purification

The EsxA and EsxB protein expression and purification protocols conducted for this experiment has been established and optimised by Dr. Renshaw described thoroughly in his PhD thesis (2002) without any amendments. The protocols for EsxA and EsxB expression and purification have been included in the Appendix section of this thesis.

2.2.2 EsxO and EsxP of *M. tuberculosis* protein expression and purification

The protocols to express and purify EsxO and EsxP proteins were established and optimized by Dr. Al-Harbi as elaborately described in his thesis (2011) with an amendment. In order to achieve the final concentration of the protein complex close to Dr. Al-Harbi's yield, and not clipped, a change was made to the method. The buffers used throughout the purification steps were kept cool at all times. The bottles holding the buffers were put in a bucket containing ice or ice packs. Similarly, the methods for this experiment have been included in the Appendix section in this thesis.

2.2.3 EsxG and EsxH of *M. tuberculosis* protein expression and purification

The EsxG and EsxH of *M. tuberculosis* protein were expressed and purified using the protocols described by Dr. Ilghari in his paper entitled "Solution structure of the *M. tuberculosis* EsxG.EsxH complex: Functional implications and comparisons with other *M. tuberculosis* Esx family complexes" published in 2011. The full descriptions of the methods were included in the Appendix section.

2.2.4 EsxG and EsxH of *M. marinum* protein expression and purification

The methods implemented for this experiment were based on personal communication and unpublished findings by Dr. Lightbody. The protocols were reproduced without any modification made to express and purify EsxG and EsxH proteins. The details of the methods were included in the Appendix section in this thesis.

Table 2.1: The table below shows the cell, BL21 (DE3) transformed with the proteins sequences cloned in their respective expression vectors or plasmids. In addition, included is the information regarding the protein presence as inclusion bodies or not and whether they were tagged with 6X Histidine.

	EsxA Mtb	*EsxB Mtb*	*EsxO Mtb*	*EsxP Mtb*	*EsxG Mtb*	*EsxH Mtb*	*EsxG M. mar*	*EsxH M. mar*
Plasmid	pET21a-EsxA	pET28a-EsxB	pLEICS05 EsxO	pLEICS01 EsxP	pET23-EsxG	pLEICS01 EsxH	pLEICS01 EsxG	pLEICS05 EsxH
Inclusion body	Y	N	Y	Y	Y	Y	Y	Y
6x His-tagged	N	N	N	Y	N	Y	Y	N

NB: The DNA sequences for EsxO, EsxP, EsxG and EsxH were cloned in pLeics05 and pLeics01 plasmids accordingly and the expression vectors were purchased from the Protein Expression Laboratory (PROTEX), University of Leicester. Dr. Al-Harbi has the cells transformed with EsxO and EsxP expression vectors, while for EsxG and EsxH of *M. tuberculosis*, and EsxG and EsxH of *M. marinum* by Dr. Lightbody. The cells used for the experiments were ready to be used from the glycerol stock culture kept at -80 ^{o}C.

2.2.5 SDS Polyacrylamide Gel Electrophoresis (SDS-PAGE)

For each step of protein expression and purification, the proteins were analysed by SDS-PAGE. 20 µl supernatants from inclusion bodies washes and/or protein samples were combined with 10 µl of 200 mM dithiothreitol (DTT) and 10 µl 4 x NuPAGE LDS sample buffer. Samples were heated for 10 minutes at 70 ^{o}C before being loaded on 4-12 % acrylamide gradient, pre-cast NuPAGE Bis-Tris gels (Invitrogen). Electrophoresis was carried out in MES-SDS Running Buffer (Invitrogen) at a constant 200 volt (V) for 35 minutes. To indicate protein sizes, a Novex Sharp Pre-stained Standard (Invitrogen) ranged from 3.5 kDa to 260 kDa was used throughout the experiments. Protein gel staining was done using 20ml InstantBlue (Sigma) and left on a rocker for at least 15 minutes before destaining with distilled water (dH_2O) for at least 20 minutes on a rocker. The image from the SDS-PAGE gel was taken using a gel doc (BioRad).

2.2.6 UV circular dichroism spectroscopy

The secondary structure of EsxA.EsxB complex was estimated using ultra violet circular dichroism (CD), which was acquired on a Jasco J715 spectropolarimeter. The purified protein complex was prepared at 1 µM in 25 mM sodium phosphate, 100 mM sodium chloride buffer pH6.5. The spectra were recorded from 180 to 250 nm at a scan speed of 20 nm per minute and collected at 1 cm path length cuvette (Renshaw *et al.*, 2002).

The secondary structure of the purified EsxG.EsxH complex was estimated by CD spectroscopy. The protein sample was diluted to the protein concentration of 25 µM in 25 mM sodium phosphate, 100 mM sodium fluoride buffer at room

temperature. The analysis was conducted in a 1 mm path length cuvette at room temperature (25 ^{o}C). The CD spectra were recorded between 190 to 260 nm at 20 nm per minutes scan speed and the results were obtained by a Chirascan Plus™ spectropolarimeter. The method was done following Dr. Lightbody's recommendation in her paper entitled "Characterization of complex formation between members of the *M. tuberculosis* complex CFP-10/ESAT-6 protein family: Towards an understanding of the rules governing complex formation and thereby functional flexibility" in 2008 with the slight modification based on the different spectropolarimeter used in both analyses.

2.2.7 Eliminating endotoxin from protein complexes

The buffers for the experiments were used and prepared specifically for LPS clean up only, where LPS-free/ RNase free sterile bottles and distilled water were used and any beakers for dialysis were washed with 70 % ethanol and then autoclaved to sterilize them. The dialysis tubing used were the Slide-A-Lyzed_G2 tubing 3500 MW which was hydrated with the prepared buffer or pyrogen free water for 2 minutes prior to use. The tabletop was ensured clean by wiping the surface 3 times with 70 % ethanol.

Buffers prepared and used for the removal of LPS from EsxA.EsxB (1-3) and EsxO.EsxP (4-7) were as below:

1. 25mM sodium phosphate, pH7.4
2. 25mM sodium phosphate/ 100mM sodium chloride, pH7.4
3. 25mM sodium phosphate/ 500mM sodium chloride, pH7.4
4. 20 mM sodium phosphate, pH7.4
5. 20 mM sodium phosphate/ 75 mM sodium chloride, pH7.4

6. 20 mM sodium phosphate/ 150 mM sodium chloride, pH7.4

7. 20 mM sodium phosphate/ 500 mM sodium chloride, pH7.4

A new and clean 5 ml HiTrap Q-sepharose column was washed with 10 column volume (CV) of LPS-free water then equilibrated overnight with sodium phosphate buffer only. At the same time, protein samples were dialysed overnight at 4^{o}C in the same buffer preparation. The protein samples were loaded onto the equilibrated column, respectively and the flow-through was collected manually similarly to the steps taken when using AKTA FPLC. For EsxA.EsxB, protein were eluted and collected at 5 CV of 25 mM sodium phosphate/ 100 mM sodium chloride, where fractions collected 15x 1 ml and 2x 5 ml and lastly, elution with 5CV 25 mM sodium phosphate/ 500 mM sodium chloride, pH7.4, fractions were collected as 5x 5 ml. For EsxO.EsxP, the protein was eluted with 5 CV buffer contain 75mM and 150 mM sodium chloride collected as 1 ml fraction in pyrogen-free 1.5 ml microcentrifuge tube. Final elution step with 5 CV buffer contain 500 mM sodium chloride were conducted where 5 ml fractions were collected in 15 ml Falcon tubes. Lastly, the columns were washed with 10 CV distilled water followed by 10 CV of 70% ethanol and the columns were also kept in 70% ethanol. The pooled LPS-free-purified proteins were subjected to SDS-PAGE and filter tips were used for all the pipetting works with the samples.

2.3 Results and Discussion

2.3.1 Purification of EsxA.EsxB complex

2.3.1 (a) Purification of EsxA protein

The expression of EsxA (ESAT6) had shown that the maximum amount of protein produced occurred approximately 4 hours after induction with 0.45 mM IPTG at 37 ^{o}C in an *E. coli*-based expression system. EsxA was produced as insoluble inclusion bodies. The presence of induced EsxA can be seen in the whole lysate fractions around 6.5 kDa marker (Sorensen *et al.,* 1995; Renshaw, *et al.,* 2002). However, EsxA is difficult to see in the lysate supernatant. Prior to purification, since the expression of EsxA in *E. coli* resulted in the production of insoluble inclusion bodies of protein, the insoluble protein was solubilized with 6 M guanidine hydrochloride followed by refolding through the removal of the denaturant via dialysis.

The purification of EsxA was done on a Q-sepharose column and from the result; we could observe fragments or bands between 3.5 and 10 kDa on the SDS-PAGE gel **(Figure 2.3.1,** below) indicating the truncated or clipped EsxA protein. Despite this, the full-length protein was well separated from the truncated form through anion exchange chromatography using Q-sepharose column observed on SDS-PAGE gel **(Figure 2.3.2).** The purification step was conducted twice to isolate only the purified protein (Chromatography in **Figure 2.3.3**). It was noticeable that with the addition of 1 mM EDTA and 100 µM AEBSF in the refolding buffer during the dialysis process appeared to minimize or avoid the occurrence of the truncated protein. The addition of AEBSF acts as

a protease inhibitor stopped the protease activity that might be released from the cells during inclusion body washes steps.

The total protein concentration estimated was around 36.13 µM or 0.358 mg/ml from 1 L of culture and it was done by measuring the absorbance using UV-visible spectrophotometry at 280 nm. The concentration was calculated using extinction coefficient of 17 990 $M^{-1}.cm^{-1}$, which was determined by the number of tryptophan and tyrosine in the protein (Pace *et al.*, 1995; Gill and von Hippel, 1989). The formula for estimating the protein concentration is demonstrated as below:

C= Absorbance at 280 nm/ (extinction co-efficient, ε) (l)

The purified EsxA protein was stable for a few days when keep at 20 ^{o}C or up to 30 days when left at 4 ^{o}C after purification.

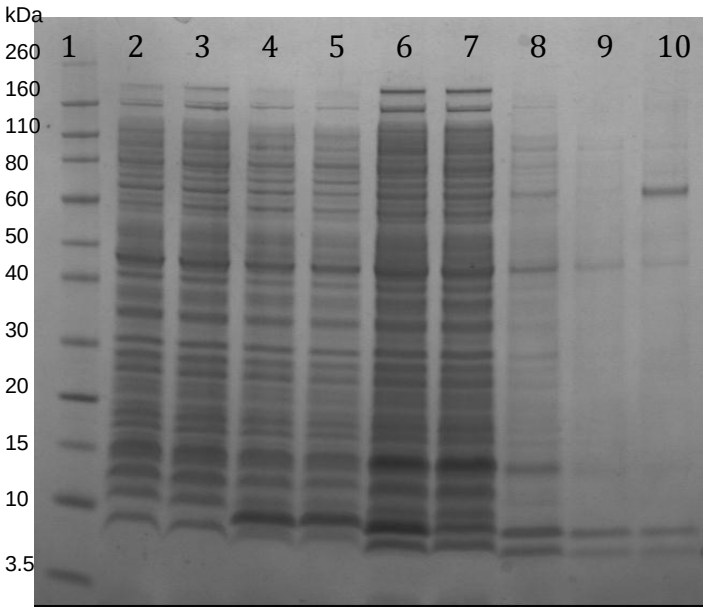

Figure 2.3.1: SDS-PAGE gel showing the pre- and post-induction of *E. coli* BL21 (DE3)-EsxA and its presents in whole cell lysates and post inclusion body washes. Lane 1- protein standard (Novex sharp pre-stained protein standard); 2 and 3- pre-induction samples; 4 and 5- post-induction sample; 6- whole cell lysate; 7- cell lysate supernatant; 8 to 10- first to third inclusion body washes respectively. The protein was seen expressed post-induction with 0.45 mM of IPTG and incubated for 4 hours at 37 ^{o}C on an orbital shaker and also in the whole cell lysates. The protein expression was also observed in the whole cell lysate (lane 6) but not in cell lysate supernatant (lane 7) (personal communications with Dr. Renshaw). Two bands were seen consistently in the inclusion body washes (lane 8 to 10) suggesting the presence of the truncated version of protein expressed in this sample.

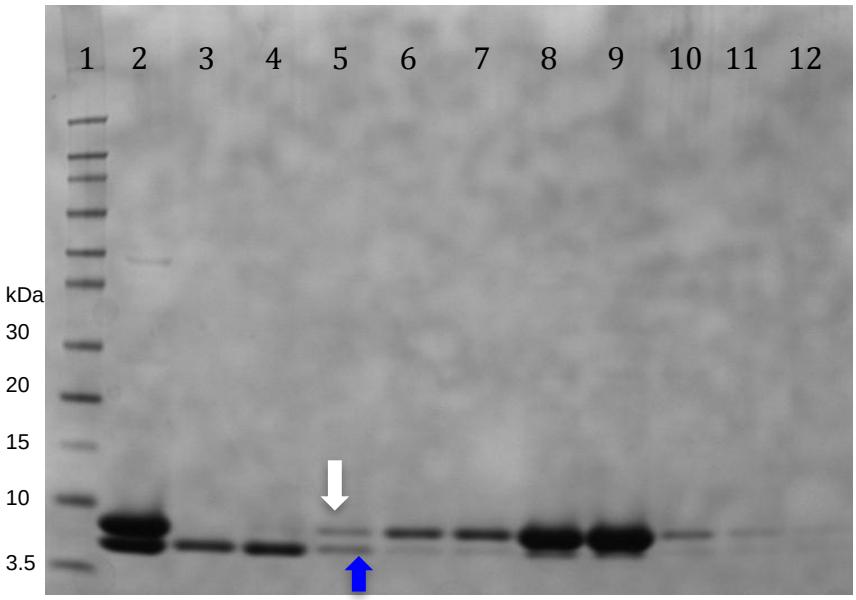

Figure 2.3.2: Purification of EsxA protein by anion exchange chromatography on a Q-sepharose column. Lane 1- Novex pre-stained protein standard, 2- sample load, 3 and 4- flow through, 5 to 12- fractions taken from tubes corresponded to the peaks showed in chromatography. The truncated EsxA was seen present in the flow through during the affinity chromatography (Lane 3 and 4). Faint bands observed in Lane 5 in which the top one was the full length of expressed EsxA (white arrow) and the bottom part (blue arrow) was the clipped or truncated form of EsxA protein. As the step gradient purification step progressed, the full-length was isolated from the truncated form of EsxA. The thicker band presented on the gel indicates more protein concentrated in the corresponded tubes usually observed from 20 to 25 % of elution buffer. The purified full-length protein is seen as a single band weighed around 9 kDa on the gel.

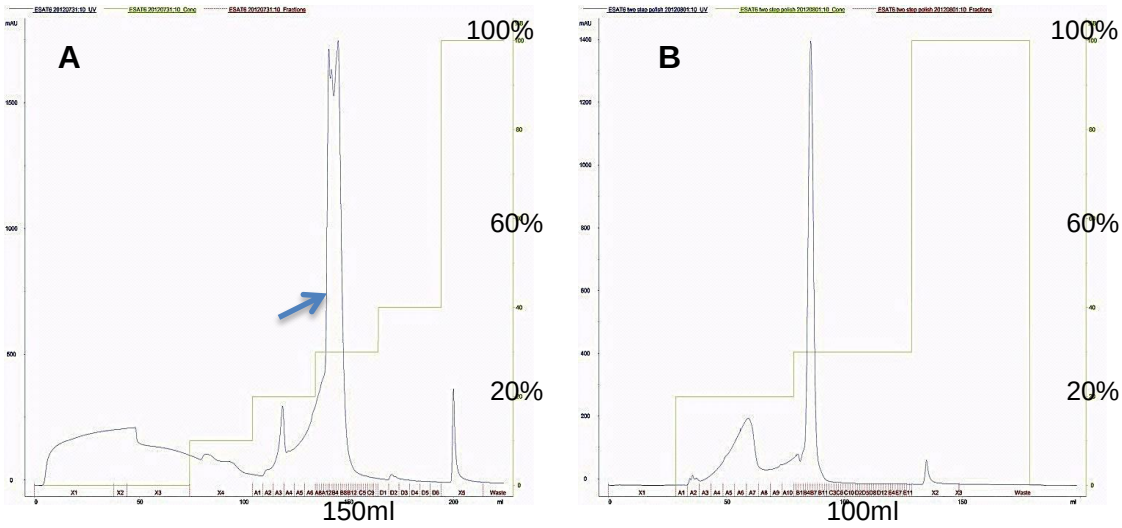

Figure 2.3.3: The purification of EsxA protein on Q-sepharose using step gradient chromatography. Panel A shows the first chromatography for purification of EsxA protein using buffer containing stepwise gradient with increasing concentration of NaCl. Arrow showed where protein was collected and purification was repeated using this sample. While in Panel B, the second chromatography was conducted by applying the same method. About 20 µl of sample were taken from the tubes that corresponded to the peaks seen for SDS-PAGE gel electrophoresis analysis.

2.3.1 (b) Purification of EsxB protein

In contrast, EsxB (CFP-10) protein could be detected in the whole cell lysates and the soluble fractions also could be seen in the lysate supernatants post induction with 0.45 mM of IPTG and found approximately at 14.2 kDa marker (**Figure 2.3.4**) as seen by Renshaw *et al.* (2002) and also observed by Berthet *et al.* (1998). Apart from that, although EsxB appeared to be more resistant to proteolysis, following purification (**Figure 2.3.5**) it was revealed that the protein yielded was approximately half the amount of EsxA (**Figure 2.3.6**) estimated from SDS-PAGE gel. According to personal communications with Dr. Renshaw, the yield of EsxB was less than EsxA based on the intensity of the band observed on SDS-PAGE occurred as a result of structural limitations, in

which it may have caused a none specific proteolytic cleavage and/or exopeptidase activity that may lead to the removal of EsxB during expression in the *E. coli* cell. Despite the hindrance, following the chromatography, the yield of EsxB was estimated about 43.2 µM or 0.47 mg/ml collected from 1 L of culture using the theoretical extinction coefficient of 6 990 $M^{-1}.cm^{-1}$ when measured using UV-*vis* spectrometer at absorbance of 280 nm.

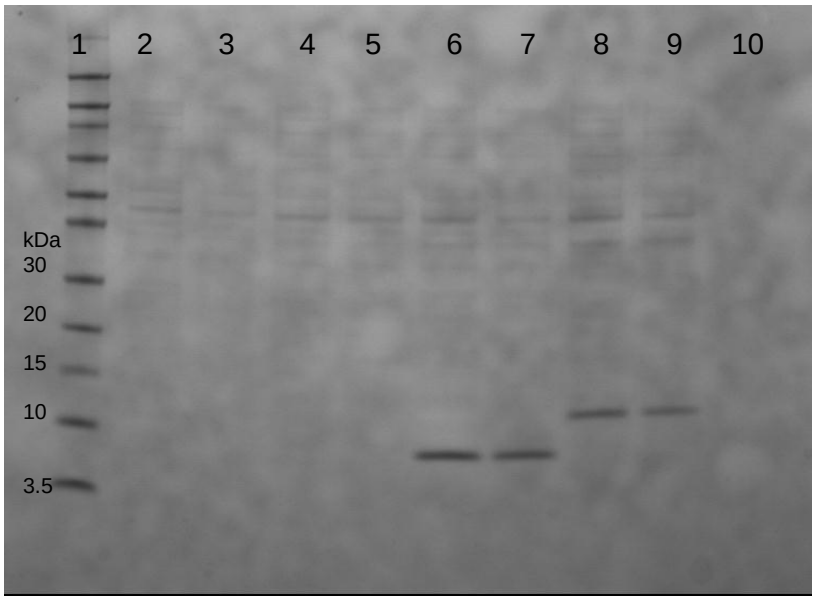

Figure 2.3.4: The bacterial lysates from pre- and post-induction of EsxA and EsxB with 0.45 mM IPTG. Lane 1- protein standard, lane 2 and 3- pre-induction of EsxA, lane 4 and 5- pre-induction of EsxB, lane 6 and 7- post-induction of EsxA, lane 8 and 9- post-induction of EsxB, lane 10- empty lane. After induction and incubating the cells for 4 hours with IPTG, bands were observed indicating the expression of EsxA and EsxB has taken place during the incubation period.

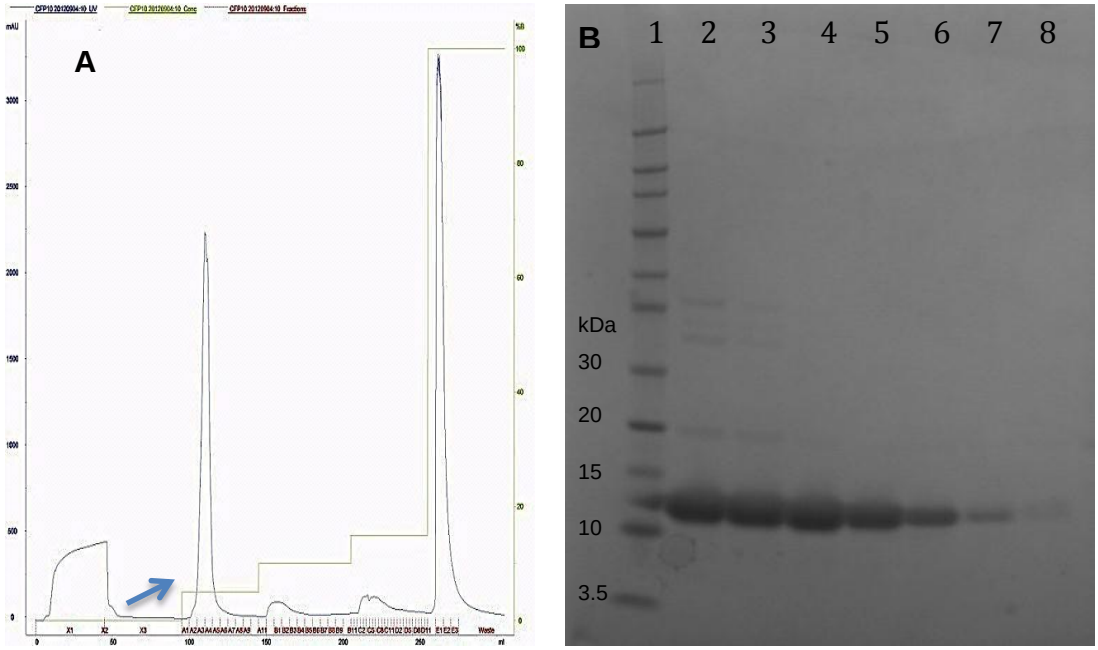

Figure 2.3.5: Chromatography image of second purification for EsxB with piperazine buffer and SDS-PAGE gel post-purification of EsxB. Panel A- chromatography of EsxB has been conducted on a stepwise gradient of increasing NaCl; Panel B- Instant blue stained SDS-PAGE gel showing the purified proteins taken from samples in tubes from the peaks seen on the chromatography (arrow). The evidence of EsxB could be seen from the gel where the bands present at the expected molecular weight of the protein, estimated around 14 kDa.

Based on the report by Berthet, *et al.* (1998), EsxA and EsxB genes were co-transcribed and co-translated (Dillon *et al.*, 2000). The method that we conducted was similar to that optimized by Renshaw *et al.* (2002) previously. The concentration for both proteins was measured and the proteins were mixed thoroughly to prepare a complex of 1:1 ratio. The final concentration of EsxA.EsxB complex was estimated at 18.29 µM in 21 ml or 0.37 mg/ml.

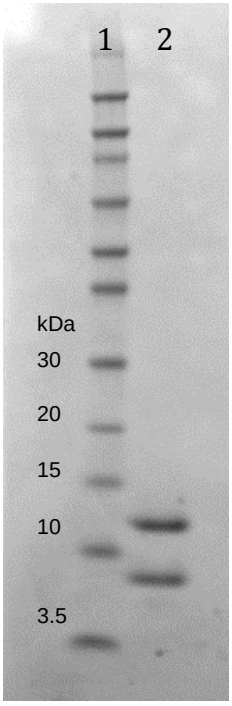

Figure 2.3.6: SDS-PAGE gel showing the EsxA.EsxB complex prepared through combination of 1:1 ratio of each protein of the same concentration. From left to right, lane 1- protein standard and lane 2- EsxA.EsxB complex. Prior to making the protein complex, the two proteins were dialysed against 20 mM sodium phosphate, 100 mM NaCl pH 6.5 overnight for buffer exchange. The protein complex was kept in the same buffer and subjected to lyophilisation, before being stored at -20 ^{o}C until further used.

2.3.2 Purification of EsxO.EsxP (*M. tuberculosis*)

The EsxO and EsxP constructed in pLeics-05 and pLeics-01 respectively were grown in the *E. coli* BL21star (DE3) expression system which was originally prepared and provided by Dr. Al-Harbi who has detailed the methods in his thesis entitled “Characterization of the structural properties and features of *M. tuberculosis* complex proteins linked to tuberculosis pathogenesis” in 2012. The expressed proteins were present as insoluble products and were induced at 0.45 mM of IPTG and incubated for 4 hours at 37 ^{o}C. The insoluble proteins were made as a 1:1.5 ratio complex with an excess of EsxO protein. Prior to the

purification step, the protein complex was solubilized with 6 M guanidine hydrochloride, 25 mM sodium phosphate, 100 µM AEBSF and refolded by dialysis twice against 25 mM sodium phosphate, 200 mM NaCl, 30 mM imidazole pH7.5 to remove all the denaturant. EsxO protein was added in excess to ensure all His_6-tag EsxP was saturated with EsxO, the protein without His_6-tag, to form a complex. The protein complex was then purified using 5 ml Ni^{2+}NTA column by affinity chromatography and the chromatography observed, as shown in **Figure 2.3.7.** Impurities that may originate from nucleic acids, endotoxins or other proteins were removed to finally collect only high level purity if protein complex.

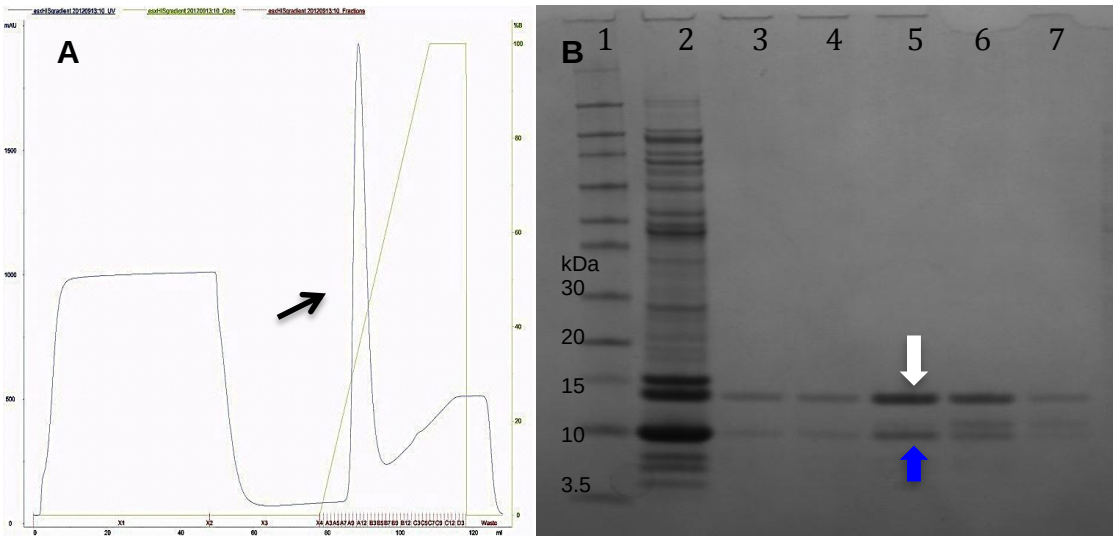

Figure 2.3.7: The purification of EsxO.EsxP complex on Ni^{2+}NTA by affinity chromatography. Panel A showed the chromatogram of linear gradient for the purification of EsxO.EsxP protein complex. Samples from tubes corresponded with peak (black arrow) at gradient were taken for SDS-PAGE gel electrophoresis. Panel B showed the results of SDS-PAGE gel where the expected double bands could be seen clearly as labeled with arrows above. Lane 1-protein standard, 2-sample load, 3 to 7- fractions of protein complex from the tubes corresponded to peaks observed in chromatogram (Panel A, arrow). All of the high molecular weight impurities seen on the gel were removed through this first purification technique. The protein complex was eluted around 172.5 mM imidazole in 20 mM Tris buffer by the linear gradient step of purification method. The two bands represented in white and blue arrow showed the presence of His_6-tag EsxP and EsxO respectively.

Fractions containing His_6-tag EsxO.EsxP complex were pooled and treated with TEV protease to remove the N-terminal His_6-tag. The cleaved His_6-tag was separated from the protein complex by another Ni^{2+}NTA affinity chromatography step **(Figure 2.3.8)** below.

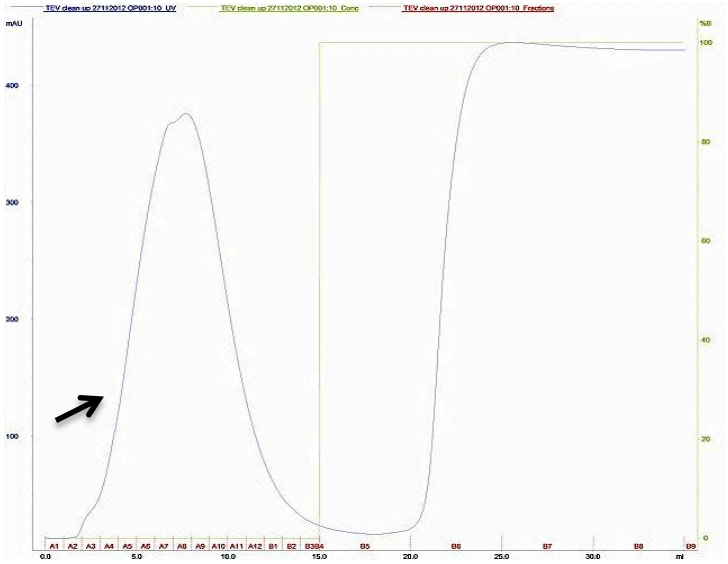

Figure 2.3.8: The chromatogram of Histidine-tag of EsxO.EsxP complex cleaved by TEV protease on a Ni^{2+}NTA using affinity chromatography technique. The fractions before the gradient were collected (arrow), where the EsxO.EsxP complex lacks in histidine tag was determined. The histidine tag was later eluted by imidazole linear gradient step. The protein complex collected was further purified and buffer exchanged by gel filtration.

The protein complex without the presence of His_6-tag was subjected to the final step of purification and buffer exchange via gel filtration **(Figure 2.2.10, Panel B)**. The EsxO.EsxP was evident on SDS-PAGE gel at around 10 kDa (EsxO) and 14 kDa (His_6-tag EsxP) molecular weight. The elution volume of the complex from the gel filtration experiment was seen to be around 70 ml, which is equal to a molecular mass of approximately 20 kDa that is twice of a monomer. This suggests that EsxO.EsxP forms a stable heterodimer and consistent with

the report by Dr. Al-Harbi explained in his PhD thesis (see Bibliography). Furthermore, SDS-PAGE gel stained with Instant Blue, a Coomasie-based staining agent, also suggests that the proteins form 1:1 heterodimer complex **(Figure 2.3.9, Panel C).** The purified protein complex yielded about 14.7 μM in 7 ml or 0.308 mg/ml was determined by UV-visible spectrometer measured at absorbance of 280 nm before the protein sample was concentrated by lyophilisation.

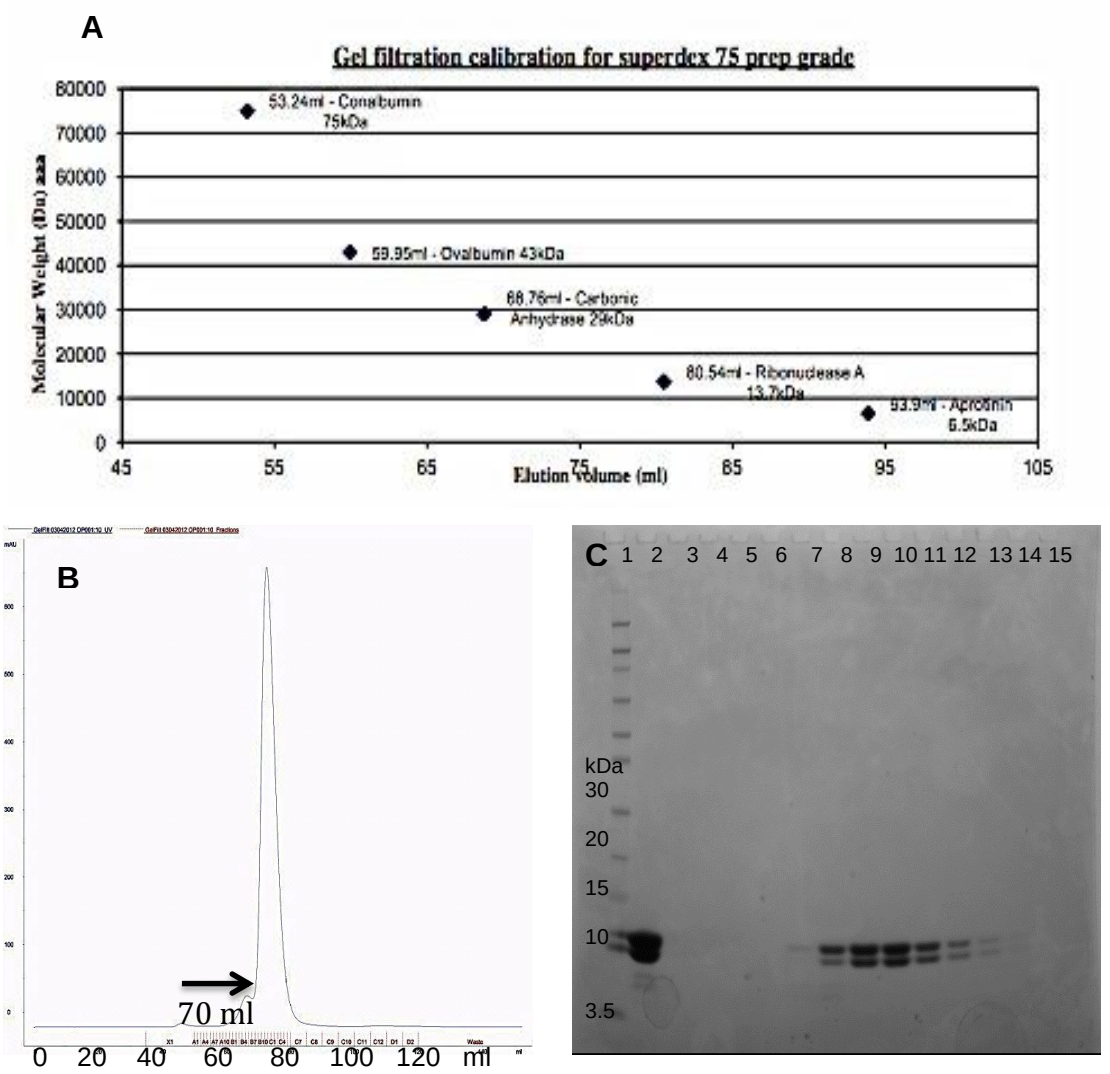

Figure 2.3.9: Purification of EsxO.EsxP complex by gel filtration. Panel A- calibration curve for standard proteins on 120 ml Superdex 75 16/60 prepacked column; Panel B- Chromatography for gel filtration of EsxO.EsxP complex elution profile on a 120 ml Superdex 75 column; Panel C- SDS-PAGE gel showing fractions containing EsxO.EsxP complex. The EsxO.EsxP started to elute at about 70 ml, which is at the expected molecular weight for the protein that is about 20 kDa. Panel C lane 1- protein standard; lane 2- sample load; lane 3- flow through, X1; lane 4 to 7- fractions from B5, B7, B9 and B11 respectively; lane 8 to 13- fractions of EsxO.EsxP complex corresponded with peaks showed in the chromatogram; lane 14 and 15- revealed that no protein complex was observed after C6 fraction, which is around 80 ml onwards.

2.3.3 Purification of EsxG.EsxH of *M. tuberculosis*protein

The EsxG and EsxH constructed in pET23 and pLEICS-01 respectively grown in *E. coli* BL21 (DE3) expression system was originally prepared and provided by the courtesy of Dr. Lightbody. The expressed proteins were present as insoluble products and were best observed at 4 hours post induction with 0.45 mM IPTG incubated at 37 ^{o}C. The presence of induced proteins can be seen in the whole cell lysate fractions around 10 kDa and 12 kDa for EsxG and EsxH respectively following cell lysis and inclusion body washes steps **(Figure 2.3.10)**.

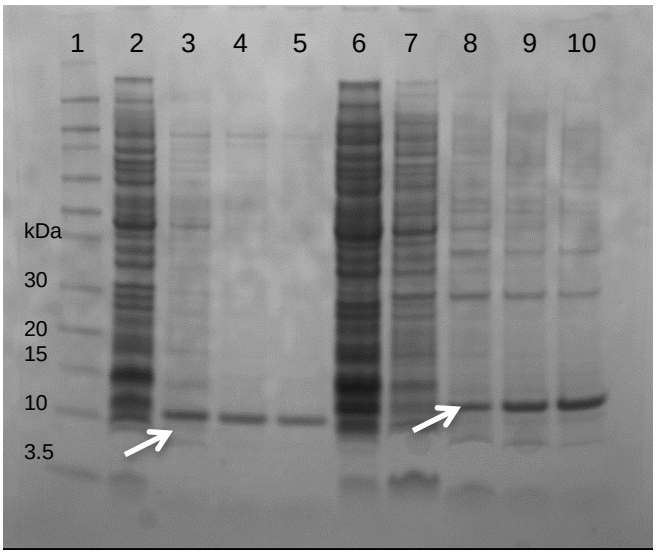

Figure 2.3.10: Post cell lysis and inclusion body washes of EsxG and His-tagged-EsxH proteins. Lane 1- protein standard; lane 2- whole cell lysate; lane 3 to 5- lysate supernatant of EsxG protein; lane 6- whole cell lysate; lane 7 to 10- lysate supernatant of His-tagged-EsxH protein. The proteins were observed in the whole cell lysates and also in the inclusion body washes. Both proteins, EsxG and EsxH were present at the expected molecular weight of about 10 kDa and 12 kDa respectively.

The insoluble proteins were made as a 1:1.5 ratio complex (His_6-tag EsxH to EsxG). EsxG protein was added in excess to ensure all His_6-tag EsxH was saturated with EsxG, the protein without His_6-tag, to form a complex. Prior to purification step, the protein complex was solubilized with 6 M guanidine hydrochloride, 25 mM sodium phosphate, 100 µM AEBSF and dialysed twice against 25 mM sodium phosphate, 200 mM NaCl, 30 mM imidazole pH7.5 to remove all the denaturant. The protein complex was then purified using 5 ml Ni^{2+}NTA column by affinity chromatography and the chromatogram observed as shown in **Figure 2.3.11.**

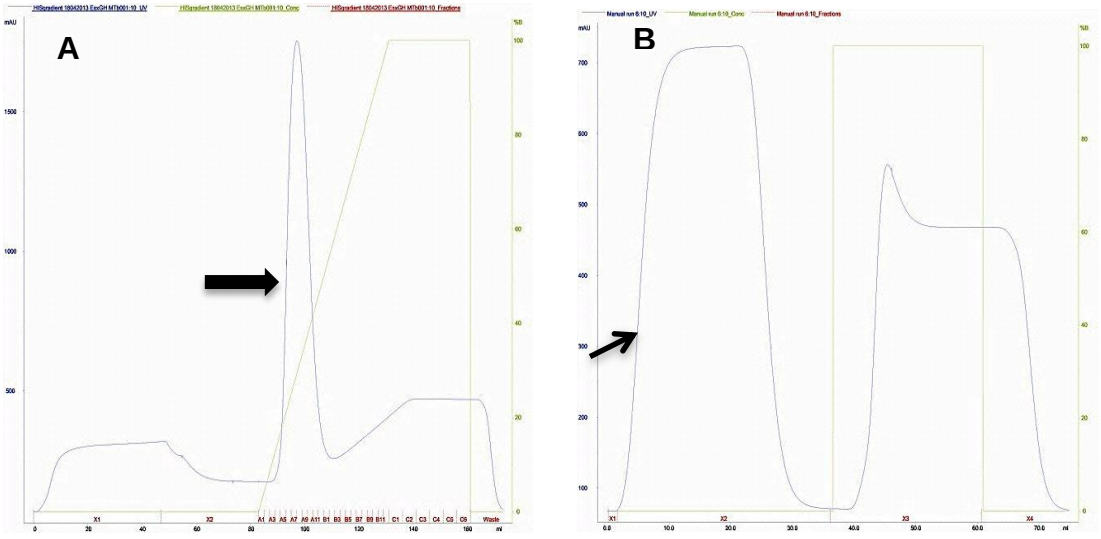

Figure 2.3.11: Chromatography profiles for the purification and Histidine removal of EsxG.ExH *M. tuberculosis* complex on Ni^{2+}NTA column. EsxG.EsxH complex started to elute at around 90 ml on a linear gradient of imidazole (Panel A). The protein complex was collected and pooled from tubes corresponded with the peak at elution (thick arrow) and was then treated with TEV protease to remove the Histidine tag. The purified protein complex was achieved by another cycle of affinity chromatography on Ni^{2+}NTA column. EsxG.EsxH complex was collected at the first 25 to 30 ml (Panel B, thin arrow) while the Histidine tag was eluted afterwards on imidazole gradient.

The protein complex without the presence of His_6-tag was subjected to the final step of purification and buffer exchange via gel filtration **(Figure 2.3.12)**. The EsxG.EsxH complex was evident on SDS-PAGE gel at around 10 kDa protein marker. The elution volume of the complex from the gel filtration experiment was around 75 ml. Furthermore, SDS-PAGE gel stained with Instant Blue, a Coomasie-based staining agent, suggests that the proteins form 1:1 heterodimer complex **(Figure 2.3.12, Panel B).** The purified protein complex yielded about 39.3 µM in 16 ml or 0.79 mg/ml was determined by UV-visible spectrometer measured at absorbance of 280 nm before the protein sample was concentrated by lyophilisation.

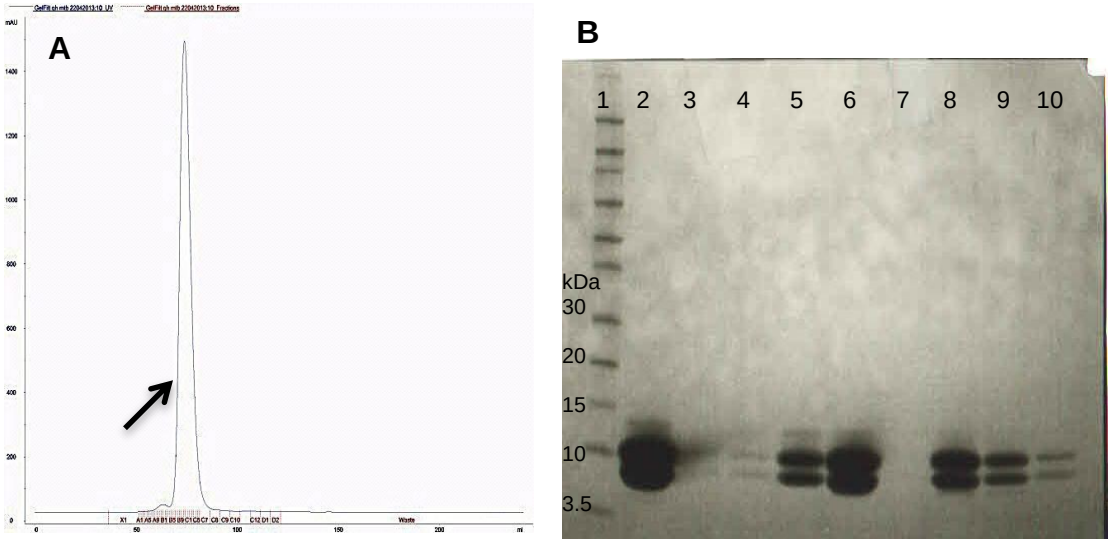

Figure 2.3.12: Chromatogram of gel filtration and SDS-PAGE gel of EsxG.EsxH complex post gel filtration. Panel A showed the chromatogram of EsxG.EsxH gel filtration in which the protein complex was observed to be starting at around 75 ml. Panel B Lane 1- protein standard, lane 2- concentrated sample load, lane 3 to lane 6- A1, B5, B8, B12, lane 7 to lane 10- C9, C3, C5, C7. The intensity of bands stained with Instant Blue on SDS-PAGE gel suggests that the proteins form 1:1 heterodimer complex.

2.2.4 Purification of EsxG.EsxH (*M. marinum*)

The EsxG and EsxH constructed in pLEICS01 and pLEICS05 respectively grown in *E. coli* BL21 (DE3) expression system was originally prepared and provided by Dr. Lightbody. The expressed proteins were best observed at 4 hours post induction with 0.45 mM IPTG incubated at 37 ^{o}C in which the proteins were present as insoluble products. The presence of induced proteins cannot be seen in the whole lysate supernatants but can be seen in the inclusion body washes at around 10 kDa and 14 kDa for EsxH and His-tagged-EsxG respectively **(Figure 2.3.13)**.

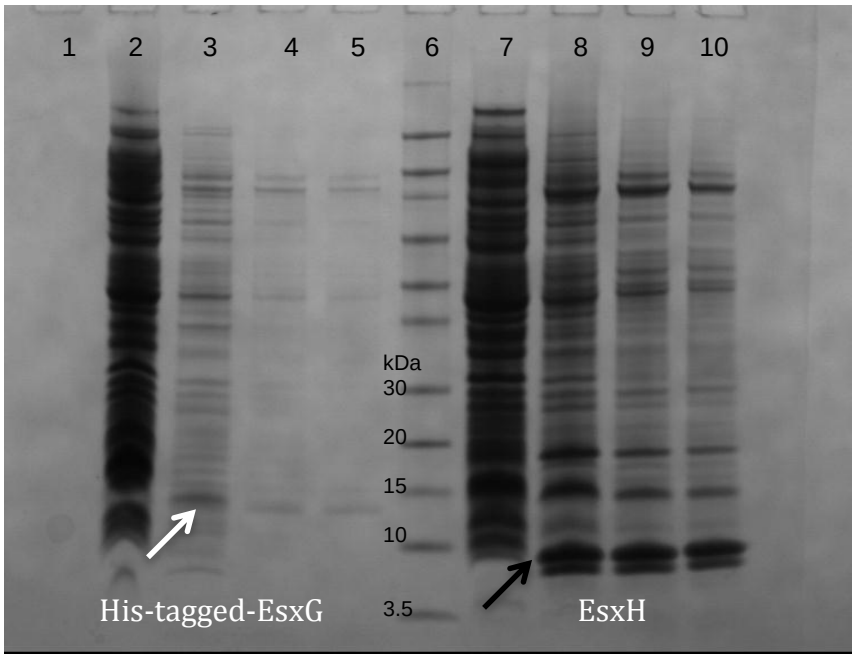

Figure 2.3.13: Post cell lysis and inclusion body washes of cells transformed with His-tagged-EsxG and EsxH proteins. Lane 1- empty lane, Lane 2- whole cell lysate supernatant of His-tag-EsxG; lane 3 to lane 5- lysate of EsxG; lane 6- protein standard; lane 7- whole cell lysate supernatant of EsxH; lane 8 to lane 10- wash 1 to 3. The His-tagged-EsxG (white arrow) was observed in the inclusion body washes (lane 3 to lane 5) as well as in the inclusion body washes of EsxH (black arrow, lane 8 to lane 10).

The insoluble proteins were made as a 1:1.5 ratio complex (His_6-tag EsxG to EsxH) before being solubilized with 6 M guanidine hydrochloride, 25 mM sodium phosphate, 100 µM AEBSF and refolded by dialysis twice against 25 mM sodium phosphate, 200 mM NaCl, 30 mM imidazole pH7.5 to remove all the denaturant. EsxH protein was added in excess to ensure all His_6-tag EsxG was saturated with EsxH, the protein without His_6-tag, to form a complex. The protein complex was then purified using 5 ml Ni^{2+}NTA column by affinity chromatography and the chromatogram observed as shown in **Figure 2.3.14.**

The protein complex without the presence of His_6-tag was subjected to the final step of purification and buffer exchange via gel filtration **(Figure 2.3.14, Panel B)**. The EsxG.EsxH complex was evident on SDS-PAGE gel at around 10 kDa and 12 kDa protein marker. The elution volume of the complex from the gel filtration experiment was seen around 75 ml. Furthermore, SDS-PAGE gel stained with Instant Blue, a Coomasie-based staining agent, suggests that the proteins form 1:1 heterodimer complex **(Figure 2.3.15).** The purified protein complex yielded about 2.97 µM in 6 ml was determined by UV-visible spectrometer measured at absorbance of 280 nm before the protein sample was concentrated by lyophilisation.

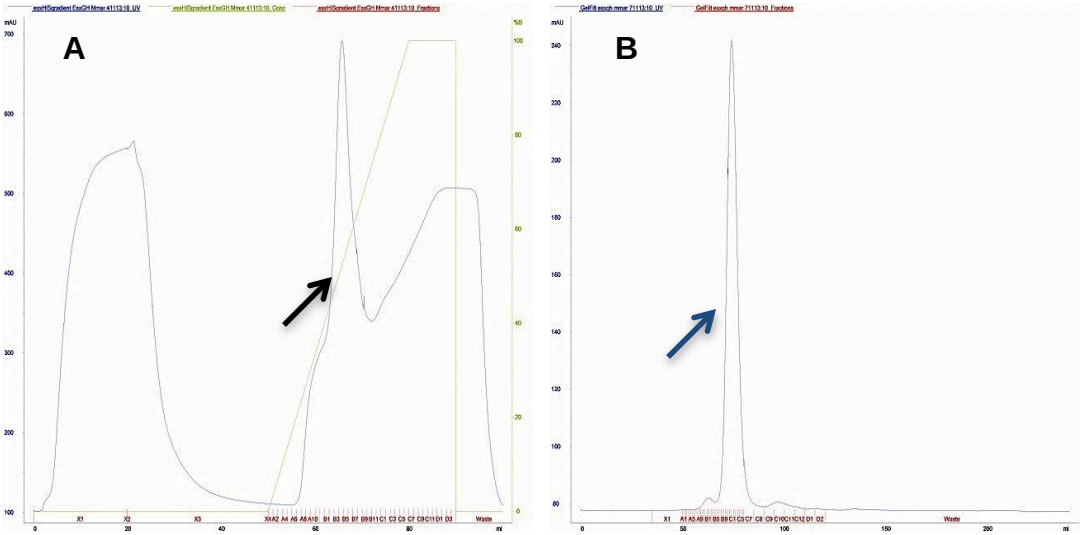

Figure 2.3.14: The chromatograms of EsxG.EsxH *M. marinum* purification on a Ni^{2+}NTA column by affinity chromatography and on a Superdex 75 by gel filtration. Panel A shows the chromatogram of EsxG.EsxH purification where the purified proteins were collected from tubes associated with the peak present at the linear gradient (black arrow). Meanwhile in Panel B shows the chromatogram of gel filtration for the protein complex. The gel filtration step was conducted to remove the heavy and lighter contaminants present in the protein complex and for buffer exchange. Arrow in blue showed the peak where purified protein was collected and pooled.

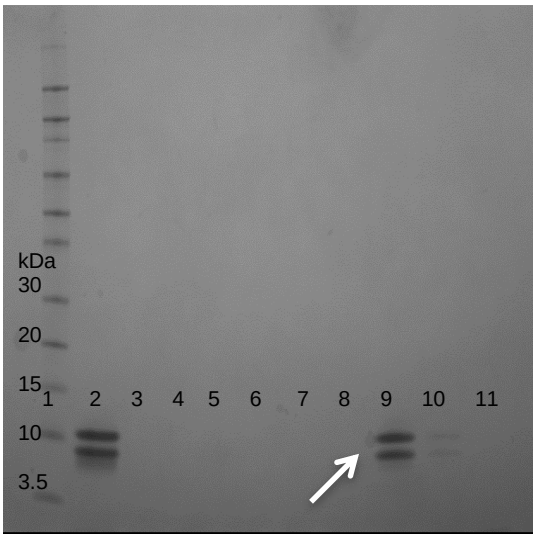

Figure 2.3.15: SDS-PAGE gel showed the purified EsxG.EsxH *M. marinum* post-gel filtration. Lane 1- protein standard, lane 2- sample load of EsxG.EsxH complex, lane 9- the purified protein complex present at the expected molecular weight of around 12- and 10-kDa for His-tagged-EsxG and EsxH proteins respectively (arrow). Based on the intensity of the staining suggests that the complex was made of 1:1 ratio.

2.3.5 UV circular dichroism spectroscopy

Following the purification steps for EsxA and EsxB and complex formation, a far UV circular dichroism spectrum of the protein complex was analysed. A structural content for the complex was performed in 25 mM sodium phosphate, 100 mM NaCl at pH6.5 at 25 ^{o}C illustrating the α- helical content indicated by two negative peaks at approximately 208 nm and 222 nm **(Figure 2.3.16)**.

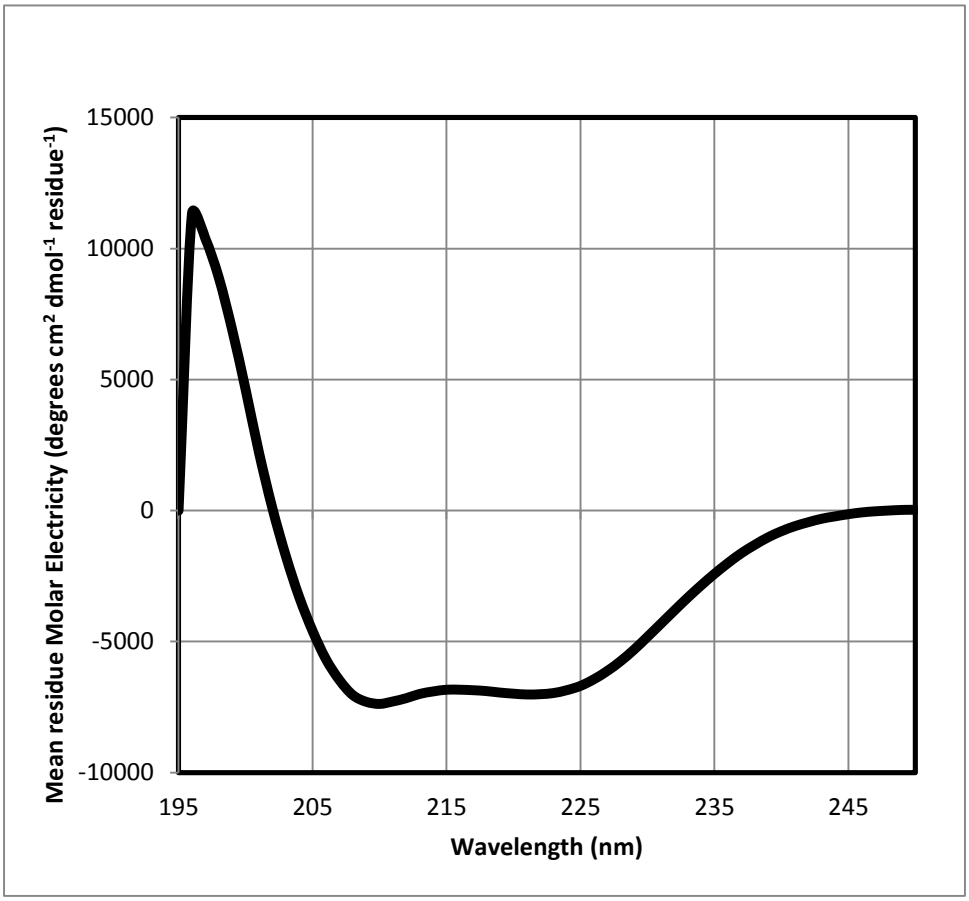

Figure 2.3.16: Far UV circular dichroism spectra acquired from solution of the 1:1 EsxA.EsxB complex at 25 ºC. From the result, it showed that the EsxA.EsxB complex has high α-helical content. This finding was similar to observation made by Renshaw *et al.* (2002) and described by Louis-Jeune *et. al.*, (2012).

UV circular dichroism spectroscopy was also conducted to confirm that the expressed and purified EsxG.EsxH complex was fully folded. The CD spectra obtained from the 25 µM *M. tuberculosis* EsxG.EsxH sample displayed a typical protein with α-helical content. This was illustrated by the presence of two negative peaks at approximately 208 nm and 222 nm on the spectra **(Figure 2.3.17)**.

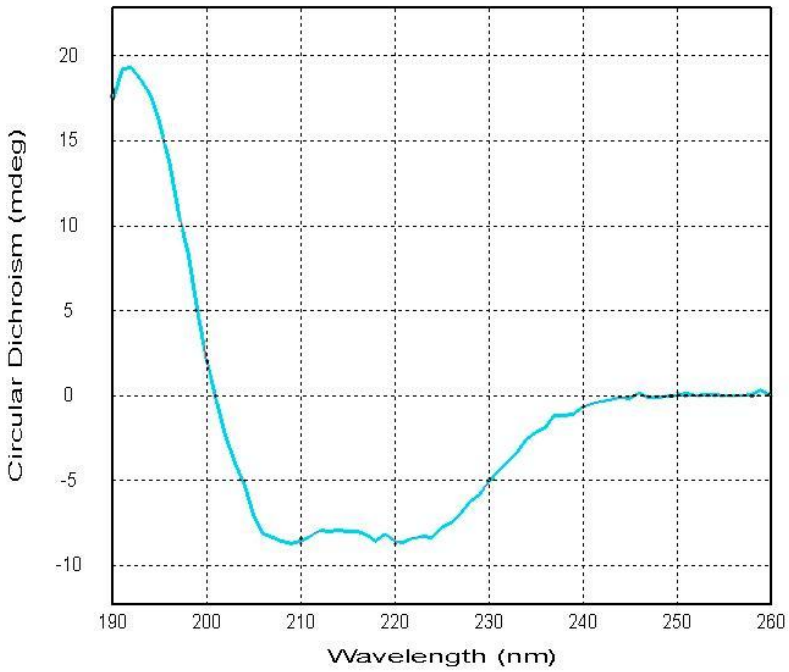

Figure 2.3.17: The CD spectra of *M. tuberculosis* EsxG.EsxH. The spectrum was obtained via a Chirascan Plus™ spectropolarimeter. The scan was recorded between 190 nm to 260 nm at 20 nm per minute scan speed (X-axis). The double minima were observed at approximately 208 nm and 222 nm, which represent the α-helical content of the complex. The spectra were obtained from CHirascan Plus Global 3™ Analysis Software.

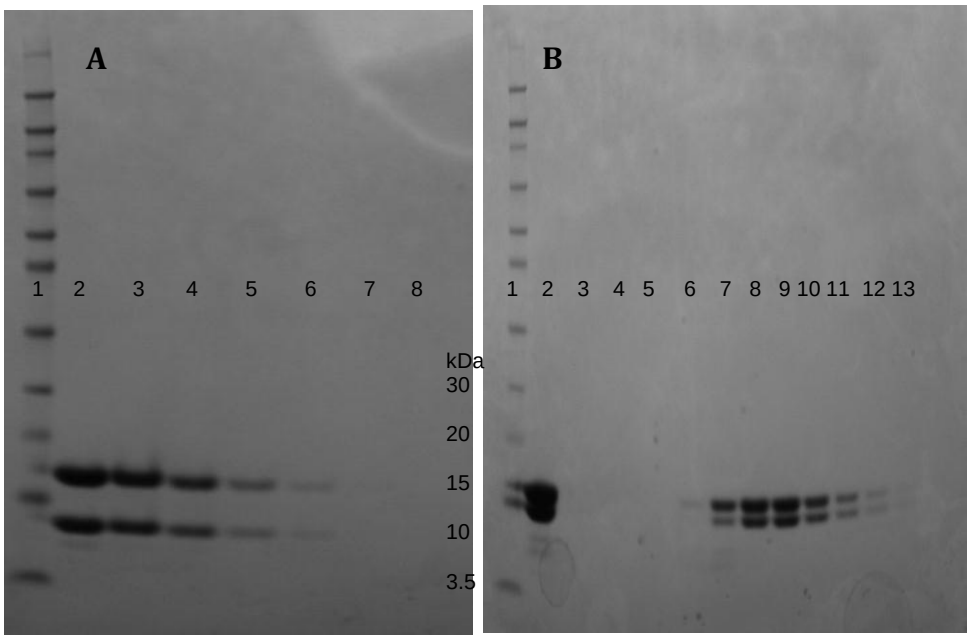

Figure 2.3.18: Post-LPS removal from EsxA.EsxB and EsxO.EsxP complexes manually. EsxA.EsxB (Panel A) and EsxO.EsxP (Panel B) were recovered from the extra purification step for LPS clean up step. The protein complexes were later checked for level of endotoxin present and if required, another purification step would be conducted. However, with the addition of purification step, the tendency of losing the protein is higher which would affect the total amount of protein concentration in our sample. Hence, the level of endotoxin was determined pre-removal of LPS so that unnecessary step would be avoided.

For our experiment, we successfully isolated and purified the recombinant proteins of EsxA and EsxB as well as their paralogous namely the EsxO, EsxP, EsxG and EsxH in the form of complexes. These protein complexes have been well characterized previously by Dr. Renshaw *et al.,* (2002), Renshaw *et al.,* (2005), Dr. Alharbi (PhD thesis) and Dr. Lightbody (personal communication) respectively and the purification steps were conducted based on the researchers' established methodologies described in Renshaw *et al.,* (2005) and Dr. Alharbi's PhD thesis 2012. The purification and characterization of the

protein complexes were made through fast performance liquid chromatography (FPLC) either by ion exchange or affinity technique, followed by gel filtration technique as described thoroughly. All of these proteins were made into a complex by 1:1 ratio with their respective protein partners namely the EsxA.EsxB, EsxO.EsxP and EsxG.EsxH. The purified EsxA.EsxB, EsxO.EsxP and EsxG.EsxH of *M. tuberculosis* and EsxG.EsxH of *M. marinum* protein complexes prepared were all kept in respective buffers of pH6.5. The yields for each protein complex were as follow: 18.29uM/21ml (EsxA.EsxB), 14.7uM/7ml (EsxO.EsxP), 39.3uM/16ml (EsxG.EsxH *M. tuberculosis*) and 2.97uM/6ml (EsxG.EsxH *M.marinum*). Each of the purified protein complexes was seen as a heterodimer on the SDS-PAGE gels and their concentrations were determined by formula mentioned following absorbance reading by UV visible-spectrophotometry. Also, the purity was measured by SDS-PAGE and UV-spectrometer where the peaks of the protein should only be present and detected at 260 nm. This process is critical in cell analysis described in the next chapter in this thesis to ensure that only the protein complex and not other determinants influenced the responses observed. Included, were observations made to determine folded proteins, seen in circular dichroism for EsxA.EsxB and EsxG.EsxH complexes indicated that the prepared protein complexes were fit for the experiment described in the next chapter.

In addition, the protein complexes (EsxA.EsxB and EsxO.EsxP) were purified from lipopolysaccharide (LPS) that could be derived from *E. coli* cell, served as the host expression system. Majority of the lipid that built up the component of outer membrane of Gram-negative bacteria was known to

produce endotoxin that will trigger the host immune response at sub-nanogram levels (Wicks *et al.*, 2008; Cotton et al., 1994). The interaction of LPS with toll-like receptor 4 (TLR4) [Rassa *et al.,* 2002] would stimulate the activation of proinflammatory cytokines (Lee and Iwasaki, 2007; Akira *et al.,* 2006; Chow *et al.,* 1999). The process to achieve LPS-free condition was conducted manually that comprised of purification and dialysis steps using LPS-free reagents preparations. The areas where the experiments were conducted and the instruments used were cleaned thoroughly with 70% ethanol. The end products were tested using limulus amebocyte lysate (LAL) that reacts to bacterial endotoxin or LPS where the LPS level were determined. However, the LPS-free protein was conducted only on protein samples used for trial experiments (EsxA.EsxB and EsxO.EsxP complexes only) in identifying the response of 16HBE towards Esx protein complexes. The LPS-free experiment was not repeated for the second time as the pre-analysis for the presence of LPS showed an acceptable level for used in cell studies. The levels determined to be free from endotoxins were <1 EU/ml and their spike recovery were between 50 and 200 % and their spike were between 1 and 0.01 EU/ml. any amount more than the benchmarks stated here were unacceptable as it showed high level of endotoxin and may affect our results.

Chapter 3: Potential immune modulators by Esx proteins in pulmonary environment

3.1 Introduction

Tuberculosis infection occurs after a prolonged exposure to the *M. tuberculosis* through inhalation of contaminated droplets in which the bacteria later travels to the respiratory tract and settles at the alveolar region. Thus, it is possible that the mycobacterial protein(s) may interact with the pulmonary epithelial as the first interface in the respiratory tract besides the pulmonary defense cells, pulmonary macrophages. We hypothesized that the well-known secreted virulent proteins such as EsxA.EsxB, EsxO.EsxP and EsxG.EsxH would bind to the cell surface of human bronchoalveolar epithelial to trigger the signaling process through modulating the host immune responses in order to establish an infection. The hypothesis was based on the finding reported by Bermudez *et al.,* (1999) that mycobacteria were observed to be able to invade the lung epithelial cell line, though became more efficiently invading the unaffected lung epithelium when mycobacteria were first engulfed by the neighbouring cells or immune cells. In order to prove the hypothesis, the binding between protein complexes and the cell surface of 16HBE cell line were evaluated. Followed by analyzing the barrier function observed via changes of transepithelial electrical resistance (TER) of the polarized lung epithelium and the epithelial permeability, which was explained in detailed in Appendix section. 16HBE is an immortal, differentiated SV-40 transformed bronchial epithelial cell line that forms a polarized cell layer *in vitro* and is widely used as a cell culture model to evaluate drug transportation in pulmonary cells, as the cell line reflecting the barrier properties representative of the airways. Dr. Jane E.

Collins, a senior lecturer in Molecular Cell Biology and also a researcher in epithelial molecular cell biology concerning the innate immune response by different epithelial cells from the University of Southampton has kindly provided us with the 16HBE cells and techniques commonly used in this field.

3.2 Methodology

3.2.1 Binding of protein complexes to cell membrane of human lung cells

3.2.1 (a) Setting up 16HBE cell plate

The methods detailed below were a combination of methods described in Dr. Ray's PhD thesis in 2011 (Bibliography) for the slide preparation while 16HBE cell growth and maintenance was following the protocols established and given by Dr. Collins. The 16HBE cell line was maintained with Minimum Essential Media (MEM) supplemented with L-glutamine; 10 % of FCS and 10 ml/L penicillin/streptomycin. The cells were passaged when the confluence reached between 70 % and 80 %. Cells were washed three times with sterile phosphate buffer saline (PBS) pH 7.4 thoroughly to remove all the serum that may be present in the culture flask. This is because; FCS will deter the action of trypsin EDTA (TE), which was used to detach the cells from the flask in the following step. Next, the cells were incubated for 20 minutes with 1 ml of TE in which the cells would appear rounded and floating after the incubation period. The reaction was stopped by adding 10 ml of supplemented MEM without the antibiotics and thoroughly pipetted to ensure all cells were collected from the flasks. The cell-media mixture was then centrifuged for 7 minutes at 1 200 rpm, 4 ^{o}C. Supernatant was discarded and pellet was resuspended in 10 ml of supplemented MEM without antibiotics. The number of cells was counted using a haematocrit. Two milliliter of cells at 1x10^{5} cell/ml was pipetted onto each well

of 6-well plate containing a sterilized coverslip and incubated at 37 ^{o}C for 24 hours.

3.2.1 (b) Setting up J774A.1 murine macrophage plate

The protocols conducted were conducted without any amendments as described by Dr. Ray in his PhD thesis (Bibliography). The J774A.1 murine macrophages (91051511, ECACC) were grown in Dulbecco's Modified Eagle's Media (DMEM) liquid media (Sigma-Aldrich) supplemented with 10 % foetal calf serum (FCS) [Sigma Aldrich] and 2 mM L-glutamine (Sigma Aldrich) and passaged twice a week until the growth became confluent and the viability percentage was between 70 % and 80 % before they were ready to be used. The murine macrophage cells were scraped using a sterile disposable cell scraper (Fisher Scientific) and centrifuged at 1 000 rpm, 15 ^{o}C for 10 minutes. The supernatant was discarded while the pellet was resuspended with 10 ml pre-warmed supplemented DMEM media. About 100 µl of the resuspended cells were taken out and diluted at 1:1 with 0.4 % trypan blue solution (Sigma Aldrich). From the diluted cell-trypan blue mixture, 10 µl was dispensed onto a counting chamber to determine the cell count and the viability percentage of the cells. Further description on estimating the viability of the cells is explained in a separate section below. The cells were then diluted to 1 x 10^5 cell/ml with the pre-warmed supplemented DMEM media. Prior to dispensing the macrophages, each coverslip was briefly soaked with absolute ethanol and flamed until the ethanol was dried and placed into each well of a 6-well Nunclon Delta Si plate (Fisher Scientific). Two milliliter of 1x10^5 cell/ml was dispensed into each well

and left incubated overnight at 37 ^{o}C where the cells would be at 2 x 10^{5} cells/ml before infection.

3.2.2 Esx protein complexes of *M. tuberculosis* labelled with Alexafluor 546 (AF546)

Prior to labelling, 1 mg of Alexafluor 546 (AF546) NHS ester (succinimidyl ester) [Molecular Probe by Life Technology] in powdered form was dissolved in 100 µl dimethylsulfoxide (DMSO) to make its final concentration at 10 µg/µl as suggested by the manufacturer. The concentration of the purified protein was also measured and the protein concentration should be at least 2 mg/ml for an optimum labelling result (Life Technology). For the labelling steps, the experimental protocols were performed following Dr. Al-Harbi's description in his thesis (2012) [Bibliography]. The AF546 and the EsxA.EsxB, EsxO.EsxP and EsxG.EsxH purified proteins were allowed to mix at a 10:1 dye to protein molar ratio and were left on a rocker at room temperature for an hour or overnight at 4 ^{o}C. The mixtures were transferred to dialysis tube independently and were dialysed separately in buffer consisting of 25 mM sodium phosphate, 100 mM NaCl pH 7.5 twice, between 4 and 6 hours each dialysis in the cold room to remove any excess or unbound dye from the protein-dye mixtures. The conjugated proteins were stored at -20 ^{o}C and viable up to 3 months after conjugation (Life Technology). The degree of labeling (DoL) for each protein-AF546 dye was estimated using the equation below. The best conjugation result determined by DoL would be at 1:1 of protein and dye ratio.

Below is the equation used to estimate the degree of labelling for the fluorophore-conjugated proteins (Life Technology).

$$DoL = \frac{A_{556} \times \text{dilution factor} \times MW_{protein}}{\text{Concentration of protein} \times \varepsilon_{dye}}$$

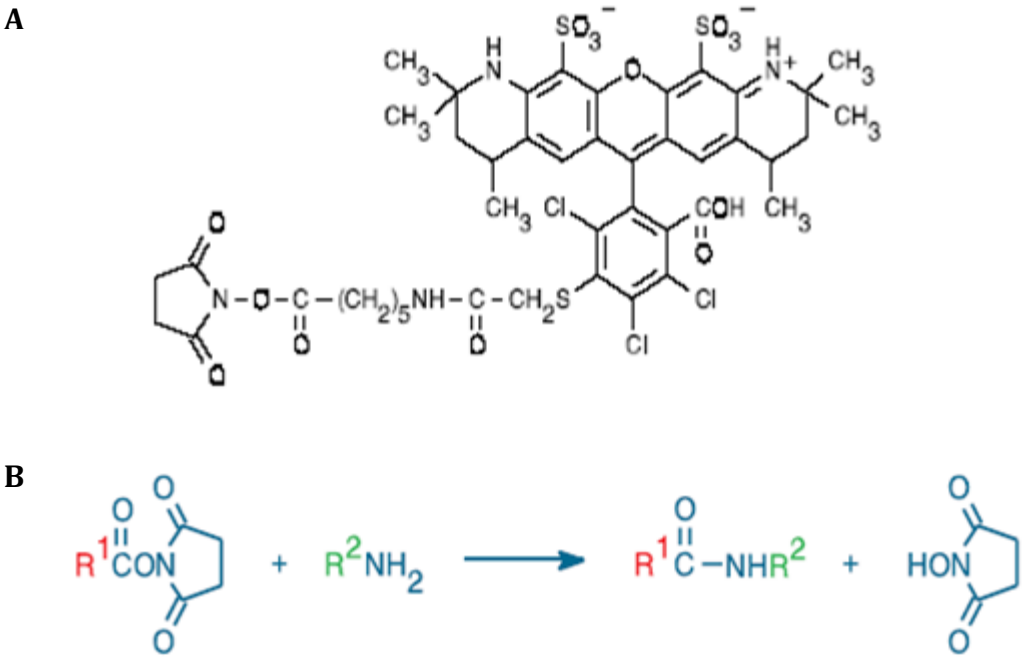

Figure 3.2.1: The reaction of Alexafluor 546 succinimidyl ester with a primary amine. Panel A showed the structure of Alexafluor 546, which was the fluorophore used for labelling the ESX complexes. The primary amine (Panel B) bound to succinimidyl group via the formation of stable amide bond. Images were reproduced from Haugland *et al.,* (2005).

3.2.3 Confocal microscopy slide preparations and observations

The growth of 16HBE cells and J774.1 murine macrophages on sterilized coverslips were prepared as described previously in **section 3.2.1 (a) and (b)** respectively. After an overnight incubation, the cells were incubated with 1 µM labelled protein accordingly and separately for 15 minutes on a rocker and on ice. The subsequent protocol steps were made as described by Dr. Al-Harbi in

his thesis without any changes (see Bibliography). The coverslips were washed twice with phosphate buffer saline (PBS) pH 7.4 before the cells were fixed with 4 % paraformaldehyde (PFA) for 10 minutes at room temperature. Next, the coverslips were treated with 0.2 % Triton X-100 for 1 to 2 minutes at room temperature. Lastly, they were counterstained and mounted with DAPI conjugated with ProLong® Gold Antifade Mountant (Life Technologies) and then the coverslips were adhered to a clean glass slide. For each new step, the coverslips were washed thoroughly twice with PBS. The slides were covered with aluminum foil and left at room temperature for at least 24 hours before viewing using confocal microscope.

The binding signals present on the cell surfaces of J774.1 murine macrophages will serve as a positive control for observations on binding of Esx protein complexes on the surface of 16HBE cell line. The signals from Alexafluor 546 NHS ester dye-labelled protein was produced from the excitation/ emission at 554/ 570 nm.

All of the microscopic observations were conducted using the Olympus confocal microscope provided by the Advance Imaging Unit from the University of Leicester and guided by the Head of the Unit, Dr. Kees Straatman. The images shown in this thesis were all analyzed using the Imaris software (Bitplane, Oxford Instruments) and if the *x, y,* and *z* planes of the images were stacked together that is explained in the respective figures, otherwise the images were taken on a single best Z slice that showed the interaction between protein and host cell surfaces.

3.3 Results and Discussion

3.3.1 Binding of protein complexes to cell membrane of human lung cells

3.3.1 (a) Labeling of EsxA.EsxB; EsxO.EsxP and EsxG.EsxH protein complexes of M. tuberculosis with AlexaFluor 546 (AF546)

The EsxA.EsxB, EsxO.EsxO and EsxG.EsxH of *M. tuberculosis* were conjugated with AF546 succinimidyl ester dye by employing an identical experimental condition as mentioned by Renshaw *et al.,* (2005). The success in conjugating the protein complexes with the fluorophore was determined by measuring the degree of labelling (DoL) for each of the protein complex using the formula stated previously in **Section 3.2.2**. This was done by measuring the absorbance of protein-dye conjugated at 556 nm (the maximum absorbance of AF546 dye) and at 280 nm (absorbance of the protein). The DoL for EsxA.EsxB **(Figure 3.3.1)** was estimated at 1:1, indicating that one fluorophore molecule bound with one protein complex, which is an ideal conjugation result.

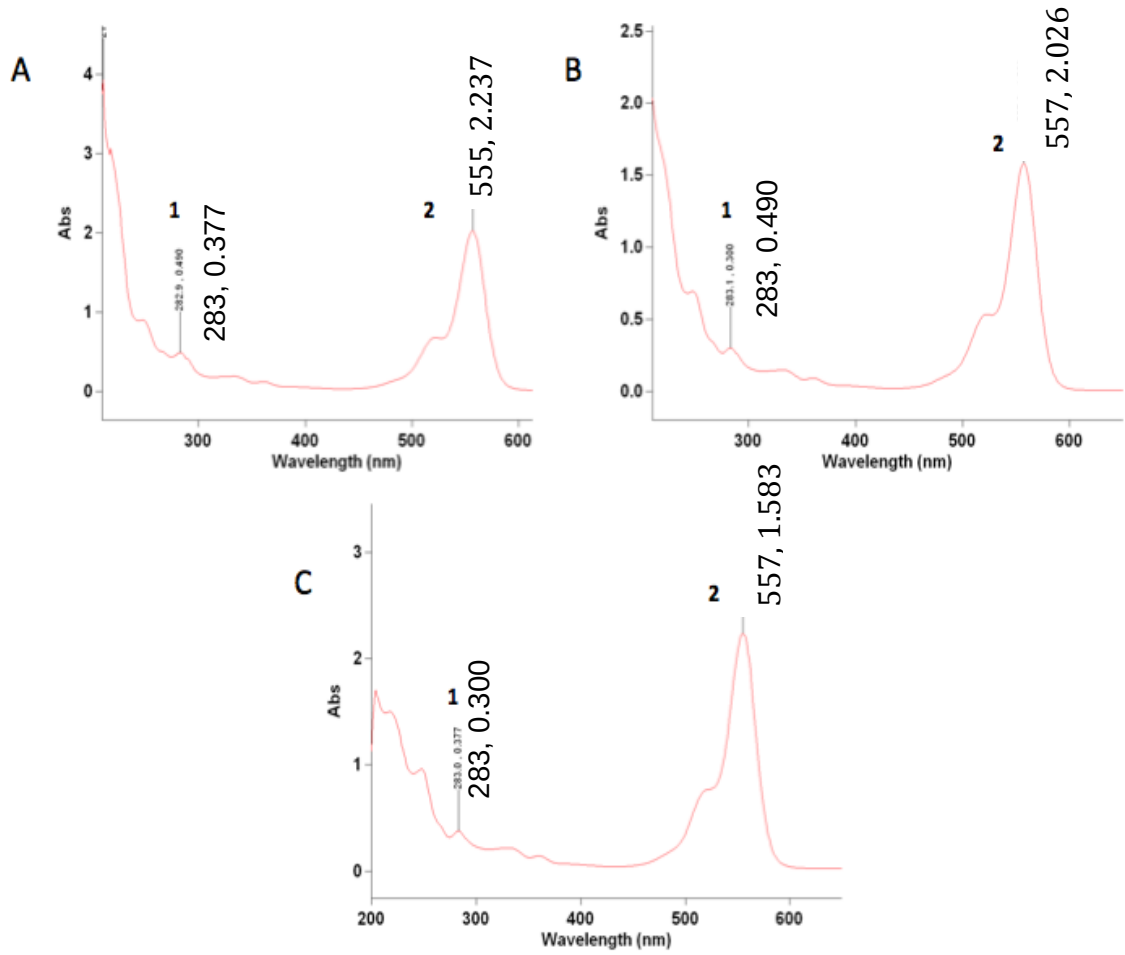

Figure 3.3.1: Determining the degree of labelling (DoL) for protein complexes conjugated with Alexafluor 546 succinimidyl ester. The absorbance of the protein was determined by UV-*vis* spectra at 280 nm (1) while the absorbance for AF546 at 556 nm (2). The conjugated proteins were first dialysed to remove any excess or unbound Alexafluor dye. The peaks presented at two different wavelengths in the figure above suggesting that the protein complexes have successfully conjugated with AF546. Based on the equation detailed in page 71, the DoL was described in the form of ratio for EsxA.EsxB (A), EsxO.EsxP (B), and EsxG.EsxH (C) and has been determined to be at 1:1, 2:1, and 2:1 respectively. The DoLs suggest that one flurophore molecule bound to one protein or two fluorophore molecules bound to one protein accordingly. These findings were consistent with the modification of either one or both of the N-terminals in the protein complexes.

3.3.1 (b) Binding of EsxA.EsxB and EsxO.EsxP protein complexes to cell surfaces of J774.1 murine macrophages and 16HBE cells

In order to determine the possibility of three different Esx protein complexes to the cell surface of lung epithelial cells, the AF546-labelled-protein complexes were introduced independently at 1 µM onto 2 x 10^8 cells/ml culture of 16HBE. For the positive control, the labelled protein complexes were introduced to J774.1 macrophages and for the negative control, AF546-labelled-EsxG.EsxH exposed to J774.1 macrophages was used, both have been described thoroughly by Dr. Al-Harbi in his thesis (see Bibliography). The findings in J774.1 macrophages (positive controls) were used as guidance for the observations in 16HBE cells. Therefore, an identical experimental procedure was performed using 16HBE cells as the host cell to determine if there was any presence of protein complexes bound to the cell surface of the host cell. The above author described his observation as “cap-like”, which refer to the shape of the observed immunofluorescence. Hence, the “cap-like” term is also used in this thesis to describe similar observation, as seen in **Figure 3.3.2a** and **Figure 3.3.2b**.

The “cap-like” characteristic was seen on the cell surfaces of a majority of J774.1 macrophages. Due to the fact that the images were taken at the best focus plane, the representative images below show only some of the J774.1 macrophage cells with signals, indicating protein binding. However, in general, the binding of EsxA.EsxB and EsxO.EsxP was not seen in the majority of 16HBE cells’ surfaces.

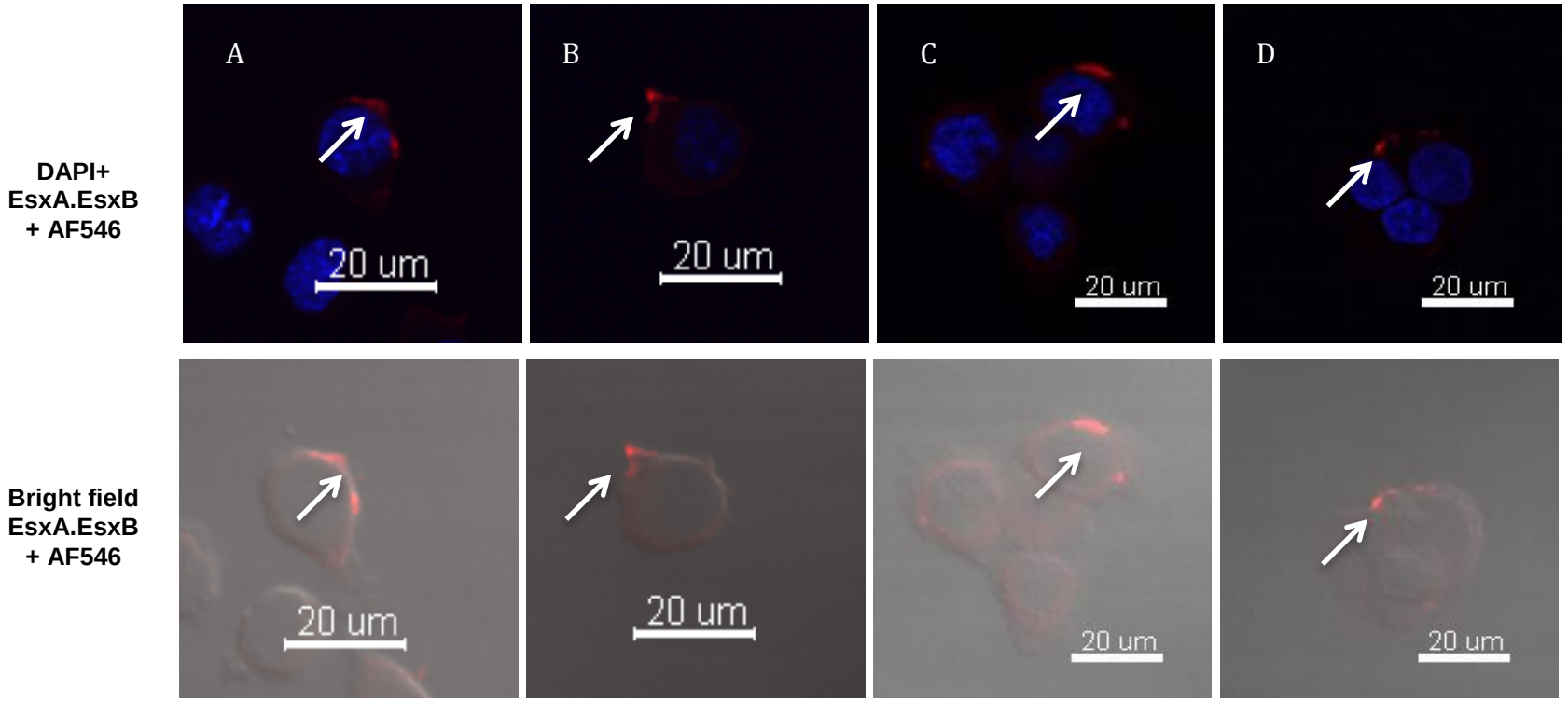

Figure 3.3.2a: Fluorescently labelled EsxA.EsxB at 1 μM **bind to the cell surface of J774.1 macrophages and 16HBE cells.** In above images, the nuclei of both host cells indicated by blue originated from DAPI, signal emitted at 405 nm; while the red discoloration represent the AF546-labelled-EsxA.EsxB complex. On the bright field images, the demarcation of the cell membrane could easily be recognized. The prominent "capping" characteristic was seen clearly in Panel B while in Panel A, C and D appeared like "capping" process were taken place where the signals at receptors are approaching to each other.

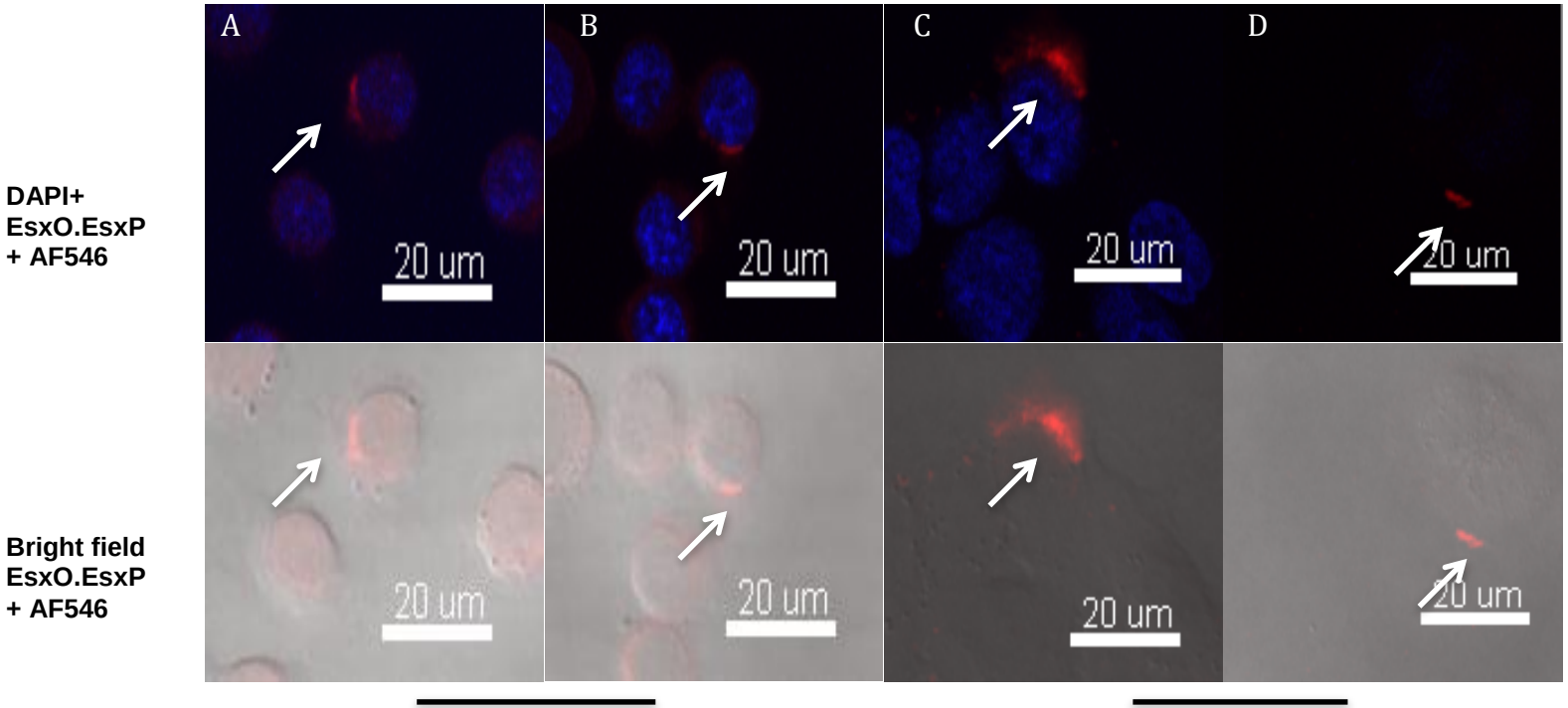

Figure 3.3.2b: Fluorescently labelled EsxO.EsxP complex at 1 μM bind to the cell surface of J774 murine macrophages and 16HBE cells. The nuclei of host cells were showed in blue, while the red signal represent the AF546-labeled-EsxO.EsxP complex. A well-demarcated cell membrane could be seen from the bright field images. A similar "capping" finding as EsxA.EsxB was also seen in cells treated with EsxO.EsxP. The protein was observed to be clustered at a certain area of the host cells indicating a specific binding to the receptor on the cell surfaces has taken place. Images were taken at the best planes to show the cap-like feature.

3.3.1 (c) No binding of EsxG.EsxH protein complex to J774.1 murine macrophages cell surface and 16HBE cells

Renshaw *et al.,* (2005) and Al-Harbi, S. PhD thesis (2012) reported that only EsxA.EsxB and EsxO.EsxP complexes of *M. tuberculosis* were seen to bind to the cell surface of the J774.1 macrophages but not EsxG.EsxH complex. Below are the images taken to investigate the probability of EsxG.EsxH complex binding to the cell surfaces of 16HBE cells. **Panel A of Figure 3.3.2c** shows the results of AF546-labelled-EsxG.EsxH complex in J774.1 macrophage that act as the negative control as it has been known that the protein complex did not bind to the host cell membrane. As expected, there was no binding of the protein complex to J774.1 macrophages. Similarly, when 16HBE exposed to AF546-labelled-EsxG.EsxH complex, it was observed that there was absence of fluorescently labelled EsxG.EsxH signals (red) neither on the cell surface nor within the host cells that could indicate the binding or internalization of the complex. These findings suggest that EsxG.EsxH production was not secreted out from the mycobacteria to bind to cell surface nor cytoplasmic of host cells.

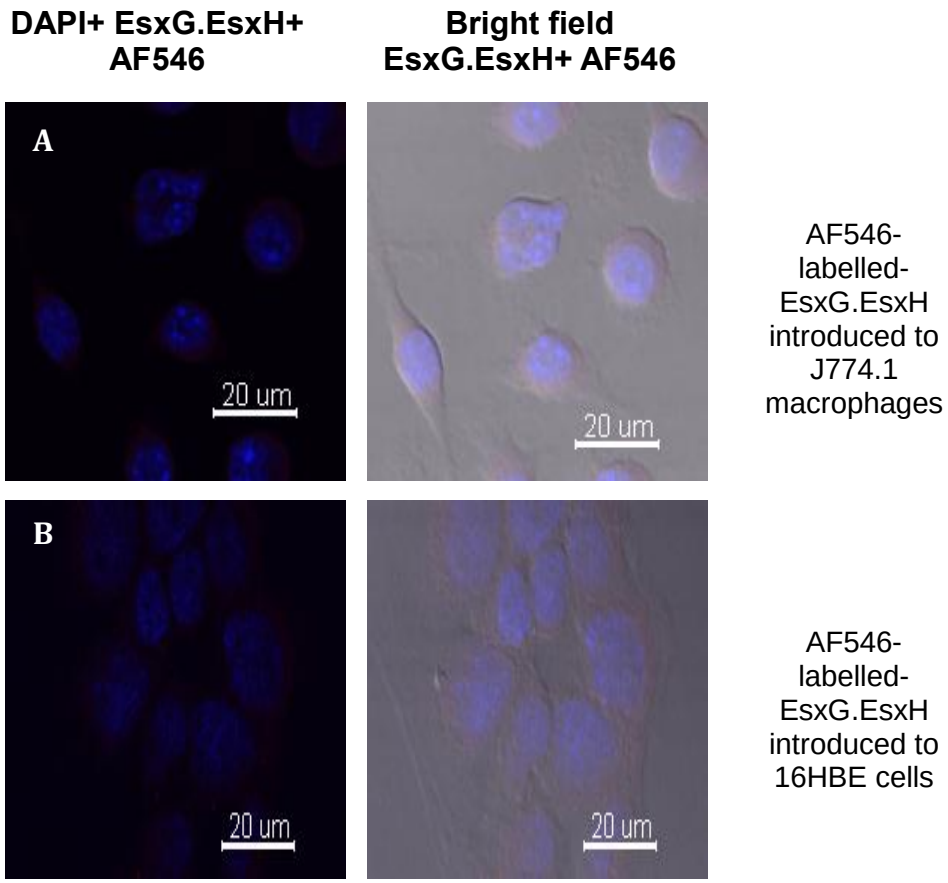

Figure 3.3.2c: EsxG.EsxH complex did not bind to the cell surfaces of J774.1 murine macrophage and 16HBE cell. There were no signals indicated by red colour seen in both cell types, suggesting no binding of EsxG.EsxH on the cell surface of J774.1 macrophage (Panel A) and 16HBE cells (Panel B). The bright blue colours in the photos represent the nuclei stained with DAPI.

There was a possibility for *M. tuberculosis*, through its secreted protein(s) to encounter the lung epithelium first other than secreting its virulence factor(s) only after being engulfed by the lung macrophages. To date, there is no published report available with regards to the binding of any ESX protein complexes to 16HBE cell membrane. However, there were studies showed that the invasion of mycobacteria into a pulmonary cell line (Bermudez and

Goodman (1996); Bermudez *et al.* (2000)). Based on the authors' findings, it has led to our hypothesis that it was plausible that the secreted mycobacterial protein(s) may interact with the pulmonary cells prior to invasion. The primary reason we chose EsxA and EsxB was because these proteins were encoded by genes located at the region of difference 1 (RD1), which was found deleted in the attenuated *M. bovis* BCG strain when compared to *M. tuberculosis* (Lewis *et al.*, 2003; Majlessi *et al.*, 2005; Pym *et al.*, 2002). This showed that the proteins encoded by RD1 are essential in virulence and potent T-cell antigenic targets as reported in a number of published articles (Samten *et al.,* 2009; Renshaw *et al.,* 2005; Lewis *et al.*, 2003; Pym *et al.,* 2002). To further understand the virulence factor that may involve in the invasion of mycobacteria into host cells probably through modulating the host immune responses, initially we looked at three different Esx protein complexes namely, EsxA.EsxB, EsxO.EsxP and EsxG.EsxH binding to 16HBE cell line as those proteins have shown their binding ability with J774.1 murine macrophages.

The positive controls (EsxA.EsxB, EsxO.EsxP bound to J774.1. macrophages) and negative control (EsxG.EsxH did not bind to J774.1 macrophages) and the studied experiments shared the same observation. The presence of high intensity of fluorescence patches indicated by red colour in the confocal microscopy images was found not only on the cell surface of J774.1 macrophages but also on 16HBE cell surface after one hour of exposure to 1 μM of AF546-labelled-EsxA.EsxB and AF546-labelled-EsxO.EsxP complexes respectively. The binding of EsxA.EsxB and EsxO.EsxP also revealed the presence of a special characteristic seen as patches or "cap-like" feature and

this was consistent with the reports by Renshaw P.S., *et al.,* (2005) and Dr. Al-Harbi (Bibliography), respectively. The “cap-like” characteristic on the cell surface of receptors has been reported not only observed in macrophages but also in various receptors such as the insulin, epidermal growth factor, L-selectin, immunoglobulin and immune cell receptors. The unique feature might occur when the host surface receptors interact with complementary ligands. Subsequently lead to signaling pathways activation and aggregation of receptors. As a result, we could see the patch-like structures and when assembled in one pole of the cell; they formed a cap-like feature as seen in the images above (Arhets *et al.,* 1995*;* Arhets *et al.,* 1998). The assembly of molecules is specific for ligand/receptor combinations and has been shown in a number of studies and could be significant for extracellular signal transduction through combination of various signaling elements (Eda *et al.,* 2004; Ilghari *et al.,* 2011; Junge *et al.,* 1999). Coherently, Schnappinger *et al.,* (2003) suggests that the function of the EsxO.EsxP complex might occur before the take-up of *M. tuberculosis* by the macrophage though his report stated that expression of EsxO and EsxP were down regulated via *M. tuberculosis* internalization within the macrophage phagosome. Several previous studies have shown that the formation of the antigen/receptor cluster might be essential for initiating physiological responses in lymphocytes (T-cell and B-cells), such as transcription of genes, release of cytokines and progression of the cell cycle, migration, cell proliferation and antigen-receptor triggered apoptosis *(*Krawczyk and Penninger 2001; Junge *et al.,* 1999; Soderstrom *et al.,* 2005*).*

However, the majority of J774.1 macrophages but only small number of 16HBE cells showed the immunofluorescence signals indicating the binding of the protein complexes to the cell surfaces. The immunofluorescence features, “cap-like” seen in 16HBE were the same as for J774.1 macrophages observed in the previous study by Renshaw *et al.* (2005) and Dr. Al-Harbi in his thesis. Fewer signals were noticed in 16HBE cells, this could be contributed by the nature of the lung epithelial (whether they are normal or cancerous cells) in which they were lined with cell-surface mucins (Packer, LM *et al.,* 2004), which could interrupt the adhesion of protein in our case. Therefore, the immunofluorescence signals could only be seen in a small number of cells. Furthermore, the interaction of EsxA.EsxB and EsxO.EsxP to both cell types also suggests that 16HBE and J774.1 macrophages may have possessed the same receptor on their cell surfaces for each individual protein complex. A significantly reduced signal from the labelled protein following an addition of 20 fold molar excess of unlabelled protein complexes to the labelled protein to create competition for the receptor on host cells was mentioned by Dr. Al-Harbi (Bibliography). These findings suggest that a tight binding occurred between the protein complexes and the target protein on the host cell surfaces, which were very specific and not influenced by the fluorophore used in the experiment.

Previously reported by Dr. Al-Harbi in his PhD thesis (Bibliography), the analysis made post-identification of EsxO.EsxP, EsxA.EsxB and EsxG.EsxH complexes binding to three different cell surfaces namely the J774.1 murine macrophages, U937 monocyte and NIH-3T3 fibroblast cell revealed that only EsxA.EsxB and EsxO.EsxP protein complexes interact with the cell surfaces of J774.1 murine macrophages and U937 monocyte while EsxG.EsxH did not.

There was no binding between the three protein complexes and the fibroblast cell line (NIH-3T3) observed too. Therefore, the binding between the proteins and 16HBE cells contributes to important information since there is no report to date pertaining to the binding of mycobacterial proteins to cell surface of pulmonary cell. In addition, there was also no disruption to the host cells found post-exposure to the proteins as there was absence of lysis of cells observed in cells bound with EsxA.EsxB as claimed by (de Jonge *et al.,* 2007) to possess lytic activity.

The best possibilities of receptors shared between murine macrophages and human epithelial cells were concluded in the table 3.1 below. The information gathered originated from a table from CD marker handbook from BD Biosciences (*www.bdbiosciences.com/go/humancdmarkers*). From the table below, the most salient receptors are probably those related to cell adhesion, signal transduction, cell signalling pathway and regulation of complement cascades. A similar function has been suggested based on surface protein information present on human lung tissues comprises of MRC1, MARCO and MCEMP1 genes. MRC1 for example has been shown to bind to mannose structures on surface of potentially pathogenic microbes while MARCO is part of the innate antimicrobial immune response. MCEMP1 protein that was also present on the surface of human lung cells has been speculated to be involved in immune response. This information was gathered from *www.proteinatlas.org/humanproteome*. However, at this stage, we were unable to point out the exact role EsxA.EsxB and EsxO.EsxP had with regards to their affinity towards cell surfaces of macrophages and lung epithelial cells.

Table 3.1: CD receptors shared by MURINE macrophages and HUMAN epithelial cells

CD	Ligands & associated molecules	Function
CD1d	Lipid, glycolipid Ag	Antigen presentation
CD9	CD63, CD81, CD82, CD315, CD316	Adhesion and migration, platelet activation/co-stimulation, signal transduction
CD13	L-leucyl-B-naphthylamine	Enzymatic activity
CD29	VCAM-1, MAdCAM-1, ECM	Signal transduction, adhesion, differentiation/development
CD39	ATP, ADP	ADP and ATP hydrolysis, neurotransmission regulation
CD40	CD154	Cell adhesion, cell proliferation and signal transduction
CD44	Hyaluronate, collagen, fibronectin, laminin, osteopontin	Cell adhesion
CD46	C3b, C4b, measles virus	Inhibitory complement receptor
CD47	SIRP (CD172), CD61, thrombospondin	Cell adhesion and signal transduction
CD49b	Collagen, laminin, MMP-1	Cell adhesion
CD49c	Fibronectin, collagen, laminin	Cell adhesion
CD49e	Fibronectin, invasion, fibrinogen	Cell adhesion
CD49f	Laminin, invasion	Cell adhesion
CD52		Complement mediated cell lysis and antibody mediated cellular cytotoxicity
CD55	C3b, C4b, CD97, Echovirus	Complement cascade (C3bBb complex) regulation
CD112	CD226, PRR3, afadin	Adhesion
CD118	IFN-alpha, IFN-beta	Differentiation, LIF receptor/co-receptor, proliferation
CD136	MSP, HGFI	Proliferation, anti-apoptosis
CD137	4-1BBL, fibronectin, laminin, vitronectin, collagen VI	Antigen presentation, signal transduction, activation/ co-stimulation, adhesion
CD142	Plasma factor VII/VIIa (FVII)	Differentiation/ development, hemostasis, angiogenesis
CD143	Angiotensin, bradykinin	Enzymatic activity
CD164	CXCR4	Adhesion, proliferation and differentiation of hematopoietic stem and progenitor cells
CD166	CD6	Activation/co-stimulation, adhesion

CD193	CCL3, 5, 7, 8, 11, 14, 15, 24, 26, HIV-1	HIV receptor/co-receptor, chemotaxis
CD213a2	IL-13	Functions as a decoy receptor for IL-13, binding with high affinity but unable to induce a signal. Reduces the biological effects of IL-13
CD217	IL-17A, IL-17F, IL-17RC, IL-RB	Associates with IL-17RC to form receptors for IL-17A, IL-17F, and IL-A/F heterodimers, promoting inflammatory responses. Associates with IL-17RB to form the receptor for IL-17E (IL_25), suppressing Th17 responses and promoting Th2 responses
CD220	Insulin, IGF-2	Insulin receptor. Causes internalization and degradation of insulin and stimulates glucose uptake
CD221	Insulin-like growth factor 1 (IGF-1), IGF-II, insulin	Receptor for IGF-I and II. Mediates mitogenic and anti-apoptotic signals
CD222	IGF-II, TGF-β latency-associated peptide (LAP), Proliferin, Prorenin, Plasminogen, Leukemia inhibitory factor (LIF), Herpes simplex virus, Thyroglobulin, Retinoic acid, Cathepsin B, D, L, CD87	Internalizes various extracellular ligands and directs them to lysosomes. Associates with cd87 to activate latent TGF-B. Binding IGF-II stimulates insulin secretion. Mediates proliferin-induced angiogenesis.
CD227	CD54, CD169, Selectins; Grb2, -Catenin, GSK-3	Involved in cell-cell interactions and adhesion. May confer cell surface protection by protruding from cell surface. Cytoplasmic tail is involved in many cell signaling pathways.
CD230	CD230 (homophilic binding); N-CAM (CD56)	Implicated in copper binding, oxidative stress homeostasis, cell survival, signal transduction. Abnormal isoform PrPsc causes neuropathology.
CD334	aFGF, FGF20	Cancer, muscle development

Chapter 4: Characterisation of EsxG.EsxH complex of *M. marinum* expression in J774.1 murine macrophages

4.1 Introduction

EsxG and EsxH proteins are part of the proteins produced by ESX3 of T7SS of mycobacteria. In the previous chapter, it was shown that EsxG.EsxH complex did not bind to the cell surface of J774.1 macrophage, U937 monocyte and 16HBE lung cells, although the protein complex known to be produced by mycobacteria. According to Serafini *et al.,* (2009), Siegrist *et al.*, (2009), and Sassetti *et al.*, (2003), ESX3 appeared to be important and essential in most pathogenic strains and that without it, the growth of mycobacteria is delayed and was thought to play a role in iron and zinc homeostasis. This could suggest that by manipulating and understanding the ESX3 cluster secreted protein(s), we may be able to understand the direct or indirect involvement of ESX3 expressed proteins in TB pathogenesis. In non-pathogenic mycobacteria such as in *M. smegmatis* however, ESX3 proteins did not appeared to be important. In the case of *M. smegmatis,* the bacterium possessed a different mechanism that enable it to minimise the effect from the absence of the protein cluster and continued to grow optimally by acquiring iron via a different siderophore pathway (Siegrist *et al*., 2009). Besides that, *esx3* locus has been seen as a focus of potential vaccine efforts since ESX3 is able to produce potential T-cell antigens (Sweeney *et al.*, 2011). It was shown that mycobacteria could generate a prominent protective bactericidal immunity after *M. smegmatis* Δ *esx*3 was inoculated and infected in mice. Billeskov *et al.*, (2007); Hervas-Stubbs *et al.*, (2006); Majlessi *et al.*, (2003) revealed that EsxG and EsxH of ESX3 were able to generate CD4 and CD8 T-cell responses in mice and humans following

infection which is consistent with earlier reports by Aagaard *et al.,* (2003), Skøjt *et al.*, (2002), and Skøjt *et al.*, (2000) which showed that ESX3 is responsible as a potent T-cell antigen in mycobacteria-infected human and cattle. Therefore, we hypothesized that the EsxG.EsxH complex was produced after invading into host cells and that the production would be significant as it was reported to be important for the bacterial growth and manipulating the host's immune responses. Here, the importance of the protein complex was evaluated through the usage of confocal microscopy and semi-quantitative analysis after characterizing the expression of EsxG.EsxH in J774.1 murine macrophages and 16HBE cell. In addition, we looked at the possibility of co-localization between EsxG.EsxH and Mpm70 protein, also secreted by mycobacteria species.

4.2 Methodology

4.2.1 Production, purification and characterisation of anti-EsxG.EsxH polyclonal antibody

4.2.1 (a) Antibody production

An anti-EsxG.EsxH polyclonal antibody 2962 was produced by Cambridge Research Biochemicals (CRB) using their custom antibody production service. The company was provided with 10 ml of purified EsxG.EsxH *M. marinum* in a solution of 25 mM sodium phosphate, 100 mM sodium chloride, pH 6.5 for immunization of two rabbits. During an 11-week immunization course, CRB provided pre-immune sera to assess the suitability of the rabbits as candidates for antibody production, as well as test bleeds at week 5 and 7 of the course for sensitivity and specificity testing by ELISA. The final bleed was provided after 11 weeks and the IgG fraction purified using a pre-packed Protein A column (GE Healthcare).

4.2.1 (b) Purification of polyclonal antibodies from rabbit 2962 sera

A pre-packed 5 ml Protein A Sepharose column (GE Healthcare) was equilibrated with 10 column volume (CV) of filtered, degassed phosphate buffer saline (PBS) pH 7.4 (Oxoid). 7 ml of polyclonal sera from rabbit 2962 was diluted at 1:1 with PBS and any insoluble material removed by centrifugation at 4 000 x *g* for 10 minutes. The supernatant was collected and loaded onto the pre-equilibrated Protein A column and the flow-through was collected. Ten (10) CV of PBS was applied to wash away any unbound material from the column, while the bound material was eluted using 5 CV of 100 mM sodium citrate pH 2.8. One milliliter (1 ml) fractions were collected into 1.5 ml microcentrifuge

tubes containing 450 ul 1 M Tris-HCl pH 9.0. This neutralized the pH of the eluted sample to around 7.2. The A_{280} (Cary 50 Bio UV-Visible Spectrophotometer) of the eluted samples was used to create an elution profile and the purity of polyclonal IgGs, and the purity of the antibodies analysed on SDS-PAGE gel. The appropriate fractions were pooled together and the total IgG content quantified at A_{280}.

4.2.1 (c) Anti-EsxG.EsxH M. marinum antibody specificity and sensitivity testing by indirect enzyme-linked immunosorbent assay (ELISA)

The indirect ELISA method to determine the sensitivity and specificity was conducted following the protocols from Abcam as described below.

i) Coating antigen to 96-well microtitre plate

The purified EsxG.EsxH *M. marinum* protein complex was diluted to a working concentration of 1 nM with sterilized PBS. The antigen was further diluted at 10 fold dilution. The wells of a 96-well PVC microtitre plate (Thermo Scientific) were coated with 50 µl of diluted antigen. Each dilution was done in triplicate. The plate was covered with an adhesive plastic (Thermo Scientific) and incubated at 4 ^{o}C overnight. Then the coating solutions were removed and washed 3 times with 200 µl sterilized PBS. The solutions were removed by flicking the plate over a sink while the remaining drops were removed by patting the plate on a clean paper towel. The same method was done using EsxA.EsxB and EsxO.EsxP protein complexes to test for the antibody specificity.

ii) Blocking

Each coated well was blocked with 200 µl of 5 % bovine serum albumin (BSA) [Sigma Aldrich] in PBS and left incubated at least 2 hours at room temperature or overnight at 4 ^{o}C. The plate was then washed 2 times with 200 µl PBS.

iii) Incubation with primary and secondary antibody

A 100 µl of diluted antibody (1:100) was added to each well and covered with adhesive plastic. The plate was incubated overnight at 4 ^{o}C to obtain a strong signal. Following that, the plate was washed 4 times with PBS and later wells were added with 100 µl donkey anti-rabbit secondary antibody conjugated with alkaline phosphatase (ALP) [Sigma Aldrich] diluted at 1:100 with 1 % BSA. The plate was incubated for 1 to 2 hours at room temperature before being washed 4 times with PBS.

iv) Detection

A 100 µl of substrate solution, p-Nitrophenyl-phosphate (pNPP) [Thermo Scientific] was dispensed into each treatment well with a multichannel pipet (ARENA).

4.2.2 *Mycobacterium marinum* cultures

4.2.2 (a) M. marinum strain DsRed growth

M. marinum strain expressing the red fluorophore DsRed (pMSP12:DsRed, selected for by addition of 50 µg/ml kanamycin) *M. marinum* DsRed glycerol stock was grown in five milliliter starter culture media containing sterilized 7H9 broth (BD Difco^{TM} Middlebrook broth) and 15 % v/v glycerol (Fisher Scientific)

supplemented with 10 % w/v of albumin-dextrose-catalase (ADC), 5 % v/v Tween-80 (Fisher Scientific) and 25 µg/ml kanamycin (Thermo Scientific) and incubated at 31 ^{o}C for two weeks. After that, two milliliter of starter culture was taken out and added to a 100 ml of 7H9 broth, ADC, Tween-80 and KAN mixture preparation. The culture was allowed to grow at 31 ^{o}C until the optical density (OD) at A_{600} (WPA biowave CO8000 Cell Density Meter) reached between 0.5 and 0.8 in which the incubation usually takes about 5 days to achieve the desired OD. This is the exponential growth phase of bacteria, which is suitable to be used for infecting the macrophages.

4.2.2 (b) Wild type M. marinum growth

A loopful of wild type *M. marinum* strains from glycerol stock was grown in five milliliter starter culture media containing sterilized 7H9 broth (BD Difco™ Middlebrook broth) and 15 % v/v glycerol (Fisher Scientific) supplemented with 10% w/v albumin-dextrose-catalase (ADC) and 5 % v/v Tween-80 (Fisher Scientific) and incubated at 31 ^{o}C for two weeks. Since the growth was more rapid than the DsRed strain, only one milliliter of starter culture was taken out and added to a 100 ml of 7H9 broth supplemented with ADC and Tween-80 broth preparation. The culture was allowed to grow at 31 ^{o}C until the optical density (OD) at A_{600} (WPA biowave CO8000 Cell Density Meter) reached between 0.5 and 0.8, which is the exponential growth phase where the incubation usually takes about 5 days to achieve the desired OD.

4.2.2 (c) Single cell suspension of M. marinum

The 100 ml of wild type or DsRed strain of *M. marinum* culture was centrifuged (Eppendorf centrifuge 5810R) at 2 500 x *g*, 15 ^{o}C for 10 minutes.

The supernatant was discarded and the pellet was washed 3 times with 30 ml sterilized phosphate buffer saline (PBS) pH 7.4 (Gibco, Life technologies). For each wash, the cells were subjected to centrifugation at 2 500 x *g*, 15 ^{o}C for 10 minutes. After the final wash, pellets were resuspended in 10 ml sterilized PBS before being passed through a 22-G needle (Terumo) attached to a sterile 5 ml syringe (Terumo) slowly and gently for five times. Lastly, the suspension was spun down at 1 000 rpm for 2 minutes. The supernatant now consists of single cell suspension of *M. marinum* and was transferred carefully into a clean 15 ml falcon tube (Corning CentriStar) without disrupting the pellet at the bottom of the falcon tube. A 10 µl of the cell suspension was pipetted onto a counting chamber (Hawksley) for cell counting. The counting chamber was put upside down on the light microscope stage (Olympus) in which the top part was facing the light source in order for ease of observation. The number of *M. marinum* was counted using 40X objective lens. Multiplicity of infection (MOI) of 0.5 was chosen and used throughout the macrophages infection while MOI of 20 was used for 16HBE infection and the plates were incubated at 32.5 ^{o}C at 2 time points (24 hours and 48 hours). The MOI was chosen on the basis of infectivity and also initial microscopic observation and evaluation, which will be mentioned below.

4.2.3 Determining the suitable MOI of *M. marinum* for two cell lines infection

4.2.3 (a) Viability of J774A.1 macrophages or 16HBE cells

The cells from J774.1 murine macrophages and/ or 16HBE cells were grown as described in Chapter 2. About 10 µl of cells was taken and pipetted on 1 side of the counting chamber for total cell count. In another 1.5 ml sterilized tube, the cells were diluted at 1:1 with trypan blue to count for viable and non-

viable cells. Live cells would not be stained while the dead cell will be stained blue due to its inability to pump out the dye. The total number of viable and non-viable counted should be around the total number of unstained cells counted to avoid any technical flaw, which was also observed and counted at the same time. Viability of the cells can be estimated from the stained cells as below:

$$\text{Viability of cells (\%)} = \left(\frac{\text{Total number of viable cells counted}}{\text{Total number of cell counted (unstained)}} \right) * 100$$

4.2.3 (b) Colony forming unit (CFU) of M. marinum in infected J774.1 macrophage

This experiment was conducted following the method described by Ramakrishnan *et al.,* 1994 and Ray, A. PhD thesis 2010. J774.1 macrophages were seeded at $1x10^5$ cell/ml in a 48-well Corning Cell bind cell culture multi-well plate (Sigma Aldrich) and incubated overnight at 37 ^oC. The cells were infected with the wild type and DsRed strains of *M. marinum* respectively at MOI of 0.5, 5.0 and 20 and incubated at 34 ^oC for 24-, 48-, 72-, 96- and 120-hours. This method was conducted to observe the differences in number of *M. marinum* growing at different dilutions ($x10^{-1}$; $x10^{-2}$; $x10^{-3}$; $x10^{-4}$ and $x10^{-5}$) over the period of time respectively and was done in triplicate. After the incubation period, the cells were washed three times with sterile PBS pH 7.4 before lysing with 200 µl of 0.01 % v/v Triton X-100 (Sigma). The cells at the bottom of the well were scraped thoroughly and transferred to a 96-well plate and diluted accordingly with supplemented 7H9 broth. About 10 µl of undiluted (neat) and diluted cells were dropped onto a 7H10 agar (BD Difco™ Middlebrook agar) supplemented with 15 % v/v glycerol with or without 25 µg/ml kanamycin depending on which

strain was used. The plates were incubated for 2 weeks before colonies were counted.

$$CFU = (A \times 10^{n}) \times 0.1$$

Legend: A is the total number of colonies counted; n is the dilution and 0.1 is the total volume in milliliter.

4.2.3 (c) Colony forming unit (CFU) of M. marinum DsRed-infected 16HBE cell line

The 16HBE cells were seeded at $1x10^5$ cell/ml in a 48-well Corning Cell bind cell culture multiwell plate and incubated overnight at 37 ^oC. The cells were infected with *M. marinum* DsRed at MOI of 0.5, 5.0 and 20 and incubated at 34 ^oC for 24-, 48-, 72-, 96- and 120-hours. The method to determine the *cfu* of *M. marinum* DsRed post infection with 16HBE cells was the same as mentioned previously for infection in J774A.1.

4.2.4 ELISA analysis of the expression of EsxG.EsxH in *M. marinum* in infected macrophages

50 ml of J774A.1 murine macrophages at $2x10^5$ cells/ml were grown for 4 days and infected with *M. marinum* at MOI of 0.5. These cells were harvested by centrifugation at 2 000 x *g*. The cell pellet was lysed using 1 ml RIPA buffer comprising of 50 mM Tris-HCl, 150 mM NaCl, 10 mM $MgCl_2$, 0.1 % w/v SDS; for 20 minutes on ice. The samples were then sonicated using Misonix Sonicator 3000 for 2 minutes, in cycles of 20 seconds on, 20 seconds off before being centrifuged for 20 minutes at 4 000 x *g*. The soluble fraction was taken and absorbance at 280 was measured. Another set of 50 ml of uninfected macrophages underwent the same process and act as the negative control. The

ELISA technique was used to tract the global expression of EsxG.EsxH in infected macrophages at 48 hours post infection and the concentration was estimated using a standard which is the EsxG.EsxH protein complex prepared at concentrations between 0.1 to 1.0 nM.

4.2.5 EsxG.EsxH *M. marinum* expression in culture

An amount of 1000 µl of *M. marinum* culture was pipetted into a 1.5 ml microcentrifuge tube and was spun down at 1 000 x *g* for 2 minutes. The supernatant was removed while the pellet was resuspended and incubated with primary antibody (2962) diluted at 1:100 with 0.1 % w/v BSA for 1 to 2 hours at 30 ^{o}C. The cells were then centrifuged and washed 3 times with 1 ml of PBS. Next, cells were incubated with donkey anti-rabbit secondary antibody conjugated with Alexafluor 488 (Invitrogen) diluted at 1:100 in 0.1 % w/v BSA for an hour. About 300 µl of the mixture was taken and spread loop on a sterile coverslip using a disposable loop. The coverslip was left to air dry and mounted with ProLong® Gold Antifade Mountant directly labeled to a nucleic acid dye, diamidino-2-phenyindole (DAPI) [Life Technologies, Thermo Fisher Scientific] on a clean microscope glass slide (Thermo Scientific). The slide was kept at room temperature.

4.2.6 Characterisation of EsxG.EsxH protein expression during infection

4.2.6 (a) Infected J774A.1 macrophages

The J774A.1 murine macrophages were grown at 1x10^{5} cells/ml as described previously in Chapter 3. The coverslips, on which the macrophages were adhered to, were transferred to a Nunc 8-well plate (Thermo Scientific) where the coverslips were subjected to fixation, permeabilisation, blocking and

staining with appropriate fluorescent dye(s). The coverslips were washed with 1 ml sterile PBS pH 7.4 after each step. The slides were first fixed using 4 % paraformaldehyde (PFA) [Sigma Aldrich] for 10 minutes at room temperature. Next, the slides were treated with cold 0.2 % v/v Triton X-100 for 5 minutes to disrupt the membrane of the cells in order for the antibodies and fluorophores to act on the specific proteins. Before addition of antibodies, the slides were blocked with 5 % w/v BSA for an hour at room temperature to minimise any possible non-specific binding. Rabbit polyclonal anti-EsxG.EsxH antibody (2962) was added at 1:100 dilution in 1 % w/v BSA and incubated overnight at 4 ^{o}C. After that, donkey anti-rabbit IgG H&L conjugated with Alexafluor 488 (Life Technologies) was added at 1:100 dilution in 1 % w/v BSA and left at room temperature for an hour. The cells were counterstained and mounted with ProLong® Gold Antifade Mountant (Life Technologies) directly labeled with DAPI and slides were allowed to rest 24 hours up to 6 days at room temperature in dark before imaging. By incubating the slides over a period of time at room temperature, may improve the refractive index and also resulted in reduction of photobleaching occurrence.

4.2.7 Expression of EsxG.EsxH complex in 16HBE cell

The experimental protocol conducted for 16HBE cells infected with *M. marinum* strain DsRed was following the method described previously for infecting J774 murine macrophages with the same bacterium. This includes the number of cells/ml of 16HBE cells and the reagents used. The only different for this experiment was the MOI used was much higher, which was 20.

4.2.8 Protein expression in phagosome

A fluorescent membrane dye, $DiIC_{18}$ (5)-DS (Life Technologies) was added at 2 µg/ml in the slides preparation both on controls and infection sets before the fixation step. The slides were left incubated for an hour at 34 ^{o}C. The rest of the experimental procedures were conducted as mentioned previously in 4.2.6 section.

4.2.9 Imaging

Slides were observed using an Olympus FV1000 confocal laser-scanning microscope with 60X objective. All the images were analysed using Imaris 7.2.3 software (Bitplane, Oxford Instruments).

4.2.10 Semi quantification of EsxG.EsxH expression in infected J774.1 murine macrophages

Slides were prepared using the same protocol as mentioned before. The total number of cell were counted manually and infections by *M. marinum* were categorised as below:

Category	**Number of *M. marinum* counted per cell**
Low	1-5
Medium	6-10
High	11 and above

Graphs were plotted to see the correlations or a pattern between protein expressions and the number of cells infected by the mycobacteria.

4.2.11 Co-localisation of EsxG.EsxH with Mpm70 using quantum dot (Qdot)-labelled primary antibodies

4.2.11 (a) Conjugating anti-Mpm70 polyclonal antibody with Qdot565

The labelling process was conducted following the manufacturer's recommendations provided with the purchased of *SiteClick Qdot565* kit (Life Technologies). The steps include antibody concentration and buffer exchange; modification of antibody carbohydrate domain by β-galactosidase; azide attachment to the exposed carbohydrate; purification and concentration of azide-modified antibody and conjugation with DIBO-modified label and purification. The steps were portrayed as in the flow chart below **(Figure 4.2.1).** The Qdot antibody labelling kit came with several components included were: a small antibody concentrator, reparation buffer, collection tube, β-galactosidase, UDP-GalNAz, Tris pH7.0, buffer additive, β-1,4-galactosyltransferase (GalT), large antibody concentrator, and DIBO-modified label. The small antibody concentrator was first rinsed with 450 µl dH_2O by centrifugation for 6 minutes at 5 000 x g. About 125 µl of 1 mg/ml anti-Mpm70 antibody was added both to the small concentrator and to the 500 µl preparation buffer in order to dilute the antibody. The solution was then centrifuged at 5 000 x g for 6 minutes and the flow through was discarded. Another centrifugation at same speed and time was subjected again after adding 450 µl of preparation buffer and the centrifugation was stopped only after the antibody volume was about 50 µl. The centrifugation time was made shorter (about 3 minutes) to avoid the antibody from becoming too concentrated. In order to collect the concentrated antibody, the small antibody concentrator was inverted into the collection tube and centrifuged for 3 minutes at 1 000 x g and approximately 50 µl of antibody should be yielded in

the collection tube. To the antibody, 10 µl of β-galactosidase was added and the tube was sealed with parafilm and incubated for 4 hours at 37 ^{o}C. This step is meant to modify the antibody carbohydrate domain to allow azide attachment in the next step. Next, the antibody was mixed with an azide modification solution composed of dH_2O, Tris buffer pH7.0, buffer additive, GalT enzyme and incubated overnight at 30 ^{o}C. After an overnight incubation, 1 ml of 1X Tris buffer was added by diluting the 20X Tris buffer stock with dH_2O, to the large antibody concentrator after removing the conical collection tube from it. The antibody concentrator was centrifuged for 10 minutes at 1 200 x g and the flow through was discarded. About 1.75 ml of 1X Tris pH7.0 and 250 µl of azide modified antibody prepared before was transferred to the large concentrator and centrifuged for 6 minutes at 1 200 x g and the flow through was discarded. Another 1.8 ml of 1X Tris buffer was added to the large concentrator and continued with centrifugation for 10 minutes at 1 200 x g. Again, the flow through was discarded and the latter step was repeated once more. After that, 1.8 ml of 1X Tris buffer was added to it and centrifuged for 10 minutes at 1 400 x g. Centrifugation was continued at 1 400 x g for 5 minutes until the volume in the concentrator about 100 µl. The last step for the Qdot565 labeling technique was adding the 50 µl of Qdot DIBO-modified label to the azide-modified antibody in a 1.5 ml centrifuge tube. The reaction was vortexed and briefly centrifuged and incubated overnight at 25 ^{o}C. The conjugated antibody was stored at 2-8 ^{o}C and protected from light. The optimal working concentration was determined by performing a series of dilutions.

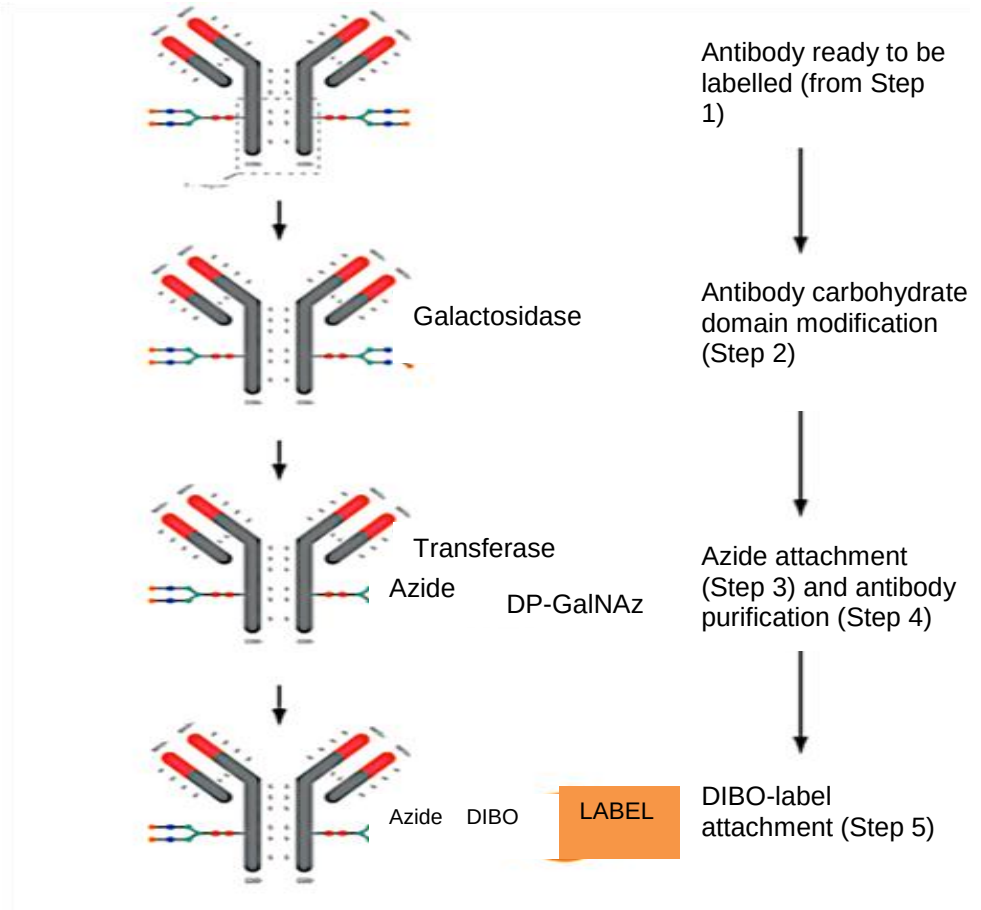

Figure 4.2.1: Summarized steps for antibody labelling using SiteClick Qdot antibody labelling kit. The flow chart above was extracted from Thermofisher SiteClick Qdot labeling manual.

4.2.11 (b) Conjugating anti-EsxG.EsxH polyclonal antibody with Qdot655

The labelling process was conducted following the manufacturer's recommendations provided with the purchased *SiteClick Qdot655* kit (Life Technologies). The steps were as described in 4.2.11 (a).

4.2.12 Determining the suitable dilution of labelled antibodies and the use of either DsRed or wild type *M. marinum* without DsRed plasmid for experimental procedure

4.2.12 (a) Qdot565-labelled anti-Mpm70 polyclonal antibody optimization

The J774A.1 murine macrophages were infected at $1x10^5$ cells/ml with *M. marinum* wild type without DsRed plasmid at MOI of 0.5 as described similarly in **Chapter 3** of this thesis. The coverslips, on which the macrophages were adhered to, were transferred to a Nunc 8-well plate (Thermo Scientific) where the coverslips were subjected to fixation, permeabilisation, blocking and staining with appropriate fluorescent dye. The coverslips were washed 5 times with 1 ml sterile PBS pH 7.4 after each step. The coverslips were fixed using 4% w/v paraformaldehyde (PFA) [Sigma Aldrich] for 10 minutes at room temperature. Next, the coverslips were treated with cold 0.2 % v/v Triton X-100 for 5 minutes to disrupt the membrane cells' in order for the conjugated antibodies to act on the specific proteins. Before addition of the antibodies, the coverslips were blocked with 5 % w/v BSA for an hour at room temperature to prevent any possible non-specific binding. The Qdot565-labelled-anti-Mpm70 antibody was added at dilutions of 1:100; 1:200 and 1:500 separately in 1 % w/v BSA and incubated overnight at 4 ^oC. After the overnight incubation, they were washed with 1X PBS. After that, the coverslips were left on the hood for drying, and were mounted with ProLong® Gold Antifade Mountant (Life Technologies) and attached onto clean glass slide and were allowed to rest between 24 hours and even up to 6 days at room temperature in the dark before imaging. By incubating the slides over a period of time at room temperature, it may improve the refractive index and also resulted in reduction of photobleaching occurrence.

4.2.12 (b) Qdot655-labelled anti-EsxG.EsxH antibody optimization

The slides were prepared as described in **section 4.2.12 (a).** The dilutions made for Qdot655-labelled-anti-EsxG.EsxH antibody were 1:100 and 1:200.

4.2.12 (c) M. marinum DsRed versus wild type M. marinum without DsRed plasmid

The slide preparations for this experiment remained the same as described in **section 4.2.12 (a)**. The only difference was the addtion of another set of infection on macrophages with wild type *M. marinum* without DsRed plasmid to compare with *M. marinum* DsRed strain-infected macrophages.

4.2.13 Experimental controls for Qdot analysis

4.2.13 (a) Positive controls: Mpm70 and EsxG.EsxH expression in M. marinum DsRed-infected J774.1 macrophages

The positive controls for this experiment include the detection of EsxG.EsxH complex in infected J774A.1 murine macrophages with *M. marinum* DsRed (method as described previously in **section 4.2.6 (a)**; Mpm70 protein in infected J774A.1 murine macrophages with *M. marinum* DsRed using similar method mentioned in 4.2.6 (a) except the antibody applied was anti-Mpm70 polyclonal antibody diluted at 1:500; anti-rabbit-AF488 conjugated secondary antibody was applied at 1:1000 to detect the presence of Mpm70 protein-anti-Mpm70 primary antibody complex. The method used in this experiment for the detection of Mpm70 protein was taken from Dr. Ray, A.'s Ph.D thesis (Bibliography).

4.2.13 (b) Negative control: Qdot655 reagent on wildtype M. marinum-infected J774.1 macrophages

The J774A.1 murine macrophages were infected at 1x10^5 cells/ml with *M. marinum* wild type without DsRed plasmid at MOI of 0.5 as described similarly in **section 4.2.6 (a)** in this thesis. However, the infected cells for the negative control were treated with the unconjugated labelling agent at 1:500 dilutions, similar to the dilution used in the experimental controls with conjugated proteins to see if there was any non-specific binding to either the host cell or mycobacteria.

4.2.14 Optimization of experimental protocol

4.2.14 Optimized slide preparation protocol

The slides were prepared as described thoroughly in **section 4.2.12 (a)** with adjustments only made to the antibodies used in which for this experiment, the Qdot655-labelled-anti-EsxG.EsxH and Qdot565-labelled-anti-Mpm70 antibodies were added at 1:200 respectively in 1 % BSA in a single preparation tube. The rest of the protocols remained the same that includes the fixation, permeabilisation and washes in between the new step introduced to the infected cells.

4.3 Results and discussion

4.3.1 Production, purification and characterisation of anti-EsxG.EsxH polyclonal antibody

In order to detect and determine the expression of EsxG.EsxH in an infected host, the first step was to produce and purify as well as to characterize anti-EsxG.EsxH antibody. The validity of final purified antibody product from rabbit serum was measured by its specificity and sensitivity using the ELISA method. The recombinant EsxG.EsxH protein complex was seeded onto a 96-well plate at a concentration ranged from 0 to 1 nM in PBS while the antibody was maintained at 1:100 dilutions or 0.22 mg/ml. The result for the purified protein was repeated twice to ensure consistency. The ELISA assay showed that the purified antibody was able to detect the protein complex as low as 0.1 nM in concentration. The reason only one dilution has been chosen is because in preliminary microscopy experiment, there was no distinct signal seen at 1:500 dilution of primary antibody. Employing the reading from EsxG.EsxH results, a standard curve was made and a comparison has been conducted with EsxA.EsxB and EsxO.EsxP protein complexes **(Figure 4.3.1)**. The result showing that the antibody does not cross-react with other protein complexes. This means that the anti-EsxG.EsxH polyclonal antibody was specific in detecting EsxG.EsxH of *M. marinum*.

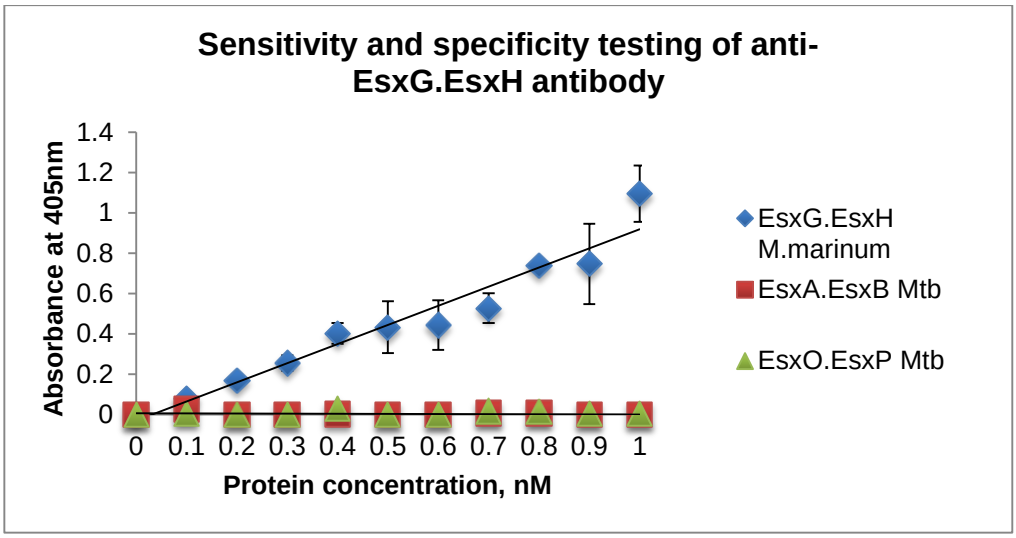

Figure 4.3.1: The ability of the polyclonal anti-EsxG.EsxH primary antibody to specifically distinguish only EsxG.EsxH protein complex. The antibody was able to detect as low as 0.1 nM protein concentration and both parameters were determined by ELISA method. Standard deviation was used as error bar. Our polyclonal primary antibody did not seem to be sensitive in detecting EsxA.EsxB and EsxO.EsxP of ESX1 and ESX5 family clusters respectively, which made it reliable to be used for detection tool.

4.3.2 Determining the suitable MOI of *M. marinum* for two types of cell lines infection

M. marinum has been widely used as a model to represent *M. tuberculosis* infection *in vitro* (Ramakrishnan *et al.*, 1994; Stamm *et al.*, 2003) and *in vivo* (Cosma *et al.*, 2006; Davis *et al.*, 2009). In addition to the similar genetic make up (Lew *et al.,* 2011; Galagan, 2010); the ability to grow in short period of time that is within a week has also enabled *M. marinum* to be chosen as a suitable candidate in understanding the disease transmission and pathology of *M. tuberculosis* infection. In these confocal microscopy studies, we employed the fluorophore-expressing mycobacteria as has been conducted before by Stamm *et al.*, 2003; van der Wel *et al.*, 2007; Hagedorn *et al.*, 2009;

Ray, A. PhD thesis 2010. The different multiplicity of infection (MOI) of *M. marinum* per macrophage cell defining was preceded before continuing our microscopy experiment. Infections at various MOI levels were left incubated at 34.5 ^{o}C for five days and was sampled or counted for each day; Day 1 until Day 5. This evaluation is important to exhibit the optimal MOI and maximum day of infection suitable for observation of the protein expression. **Figure 4.3.2** below showed an example of *M. marinum* growth at various dilution factors on a 7H10 agar plate. In this representative image and based on our observation, we could see that was almost no growth at most instances in all three replicates with the highest dilutions observed at 72 hpi. The ability to survive or grow was reduced dramatically probably due to the death of the mammalian host cell (J774.1 murine macrophage), which may be due to limited amount of nutrient available after left incubated for 5 days. Thus, the maximum incubation period chosen to perform the experiment for microscopy observation was 48 hours.

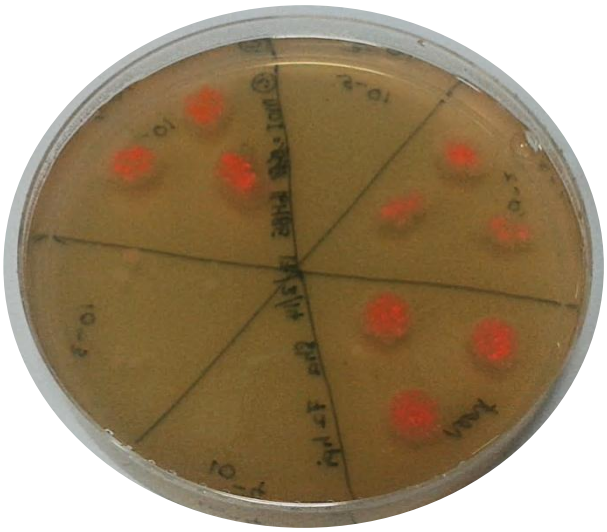

Figure 4.3.2: A representative photo of 7H10 plate with the growth of *M. marinum* DsRed at different level of dilutions after infecting 16HBE cells for 72 hours. A single plate of 7H10 agar was divided into 6 sections as shown in the photo. It comprised of neat (no dilution performed), 10^{-1},10^{-2},10^{-3}, 10^{-4},10^{-5} and 10^{-6} dilution of infected 16HBE infected with respective MOIs. We conducted and labeled similarly to all the three replicates for J774.1 macrophage infected with *M. marinum* DsRed strain.

The *M. marinum* DsRed strain infecting J774.1 macrophage with different dilution factors that has been left cultured on 7H10 agar plate was counted **(Panel A of Figure 4.3.3)** to estimate cfu. From the graph below, we could see that the cfu/ml was increasing from D1 and reached maximum at D2 but the number of cells showed continuous reduction from D3 till D5. A similar pattern of mycobacterial growth was seen in both MOIs; 0.5 and 5.0 except that for MOI 5.0 plateaued after D4. We continued with the use of *M. marinum* DsRed at MOI 0.5 to view the expression of EsxG.EsxH complex in the set of infection with J774.1 macrophages. At MOI of 0.5, we could distinguish the expression better in single bacterium infecting the host cell thus led us to be able to semi-quantify them later. If infection was allowed at higher MOI as mentioned in previous

studies by Stamm *et al.*, (2003); van der Wel *et al.*, (2007) such as MOI of 10 for *M. tuberculosis* and *M. marinum*, it would be difficult for us to count the signals and the pathogen. Our preliminary trial performed in J774.1 macrophages infected with *M. marinum* DsRed at MOI 0.5 rarely showed the presence of a prominent EsxG.EsxH signal indicating the protein expression as there was no reference to refer to date. Thus, we decided to continue with infection at MOI 0.5 to decipher and understand the pattern of EsxG.EsxH expression in a single mycobacterium cell as well as in a densely infected host cell.

We also performed an identical experimental procedure for 16HBE cells infected but tested with different MOI of *M. marinum* DsRed strain. We have chosen two MOIs these were 0.5 and 20 (**Panel B of Figure 4.3.3).** MOI of 0.5 was chosen to be tested because we wanted to standardize the method and was comparable for both cell types while MOI 20 was tested based on previous study by McDonough and Kress (1995), where the authors demonstrated cytotoxicity in lung epithelial following TB infection using *M. tuberculosis* MOI at 20 in A549 lung cell line. Our analysis as shown in the graphs below was consistent with McDonough and Kress's finding when *M. marinum* DsRed was used at MOI 20. The ability of *M. marinum* to infect the host cell at MOI 20 was 2 to 3 times higher than at MOI 0.5, even after three days post-infection, which were at its optimum. After D3, the colony-forming unit dropped drastically which may similarly be related to lack of nutrient for the host cell to survive and allow the infection within the cell to continue. Therefore, we decided to conduct our experiment using 16HBE infected with *M. marinum* DsRed at MOI of 20 and

incubated for 48 hours so that it can be comparable to J774.1 macrophage infection.

Macrophages, originates from its precursor cells, the monocytes and together these two tissues are the building blocks of the 'mononuclear-phagocyte system' as they shared their origin, morphology and functions that includes rapid phagocytosis. The function as a phagocyte that internalize the antigens could be the main reason the macrophage showed higher infectivity with *M. marinum* since D1 of infection when compared to 16HBE lung cell line. Van Furth, R. *et al.*, (1972) has described that the study on 'mononuclear-phagocyte system' has started as early as 1972 and the dynamic functions of phagocytic cells researches has grown since. On the other hand, 16HBE lung cells, lacking this function component and thus delayed in allowing the infection to happen. A number of studies have postulated that mycobacteria-infected alveolar macrophages and stimulated the cell to invade the lung tissues more efficiently which results in remodeling to the site of infection and developed a cellular mass called tubercle or granuloma (Ulrichs and Kaufmann 2006; Flynn and Chan 2005; Algood *et al.*, 2005; Algood *et al.*, 2003) than mycobacterium directly invading the lung tissues (Bermudez and Goodmann 2002). Therefore, the ability of J774.1 macrophage to be infected by *M. marinum* was observed to be higher in comparison to 16HBE cell due to the nature of the macrophage cell itself as a phagocytic cell.

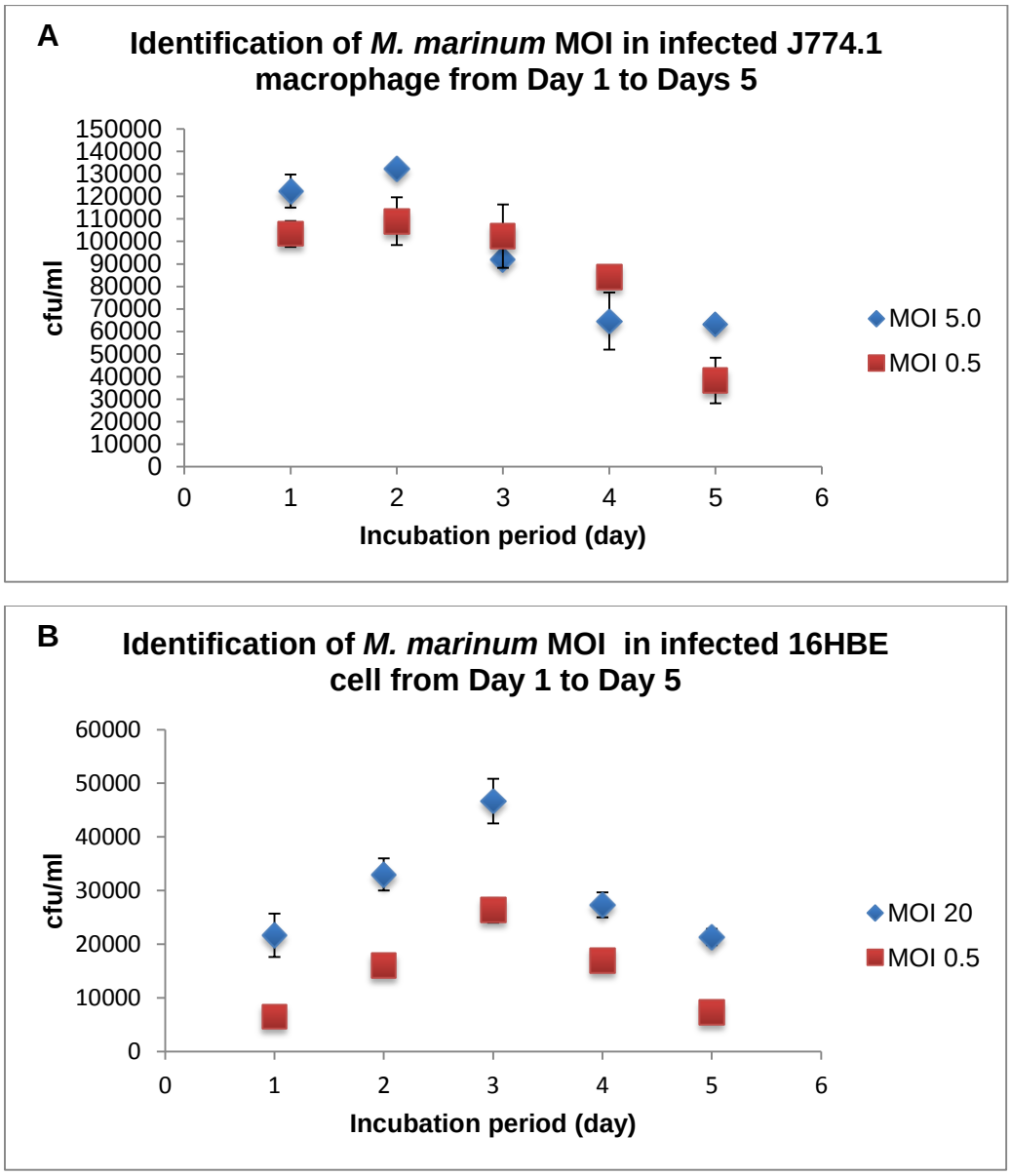

Figure 4.3.3: The identification of optimal MOI of *M. marinum* DsRed in infected J774.1 macrophages for microscopy analysis. Panel A showed the infectivity of *M. marinum* DsRed from Day 1 to Day 5 at two different MOI. MOI of 0.5 was chosen for the experiment involving J774 murine macrophages based on comparison with the initial confocal results. Whilst panel B, was an estimation of infectivity and viability of the bacteria infecting pulmonary 16HBE cells. The results showed that with an increased number of bacteria infecting the cells, the infectivity was improved until Day 3 before the viability dropped at Day 4. Hence, MOI of 20 has been chosen for infecting 16HBE cells. Standard deviation was used as the error bar in both graphs.

4.3.3 ELISA analysis of the global expression of EsxG.EsxH in *M. marinum* in infected macrophages

After the preliminary result was screened to look at the protein expression, a global expression of EsxG.EsxH protein was also determined. ELISA assay was conducted using samples obtained from 50 ml cultures of 48 hours-infected J774.1 macrophages and 16HBE cells at MOI of 0.5 and 20, respectively to estimate the global expression of EsxG.EsxH expression in *M. marinum*-infected macrophages. *M. marinum* DsRed was left to infect continuously without any washing step included after the first three hour of infection when employed to macrophages and lung epithelial cells (Dobos *et al.*, 2000). The variable for this analysis is the MOIs. Primarily, it was predicted that the more bacteria infecting a cell, the more protein would be expressed. Notably, the protein expression was determined to be higher in 16HBE cells than in J774.1 macrophages **(Figure 4.3.4)** via ELISA**.** This result contradicted with the result showed in **Figure 4.3.3** in which it appeared that *M. marinum* DsRed was more effectively infecting J774.1 macrophages than 16HBE even when compared with two extreme MOIs between these two cell types. From the global expression results, the requirement for the protein is higher hence the EsxG.EsxH expression was seen more in 16HBE cells although less number of cells infected with mycobacteria.

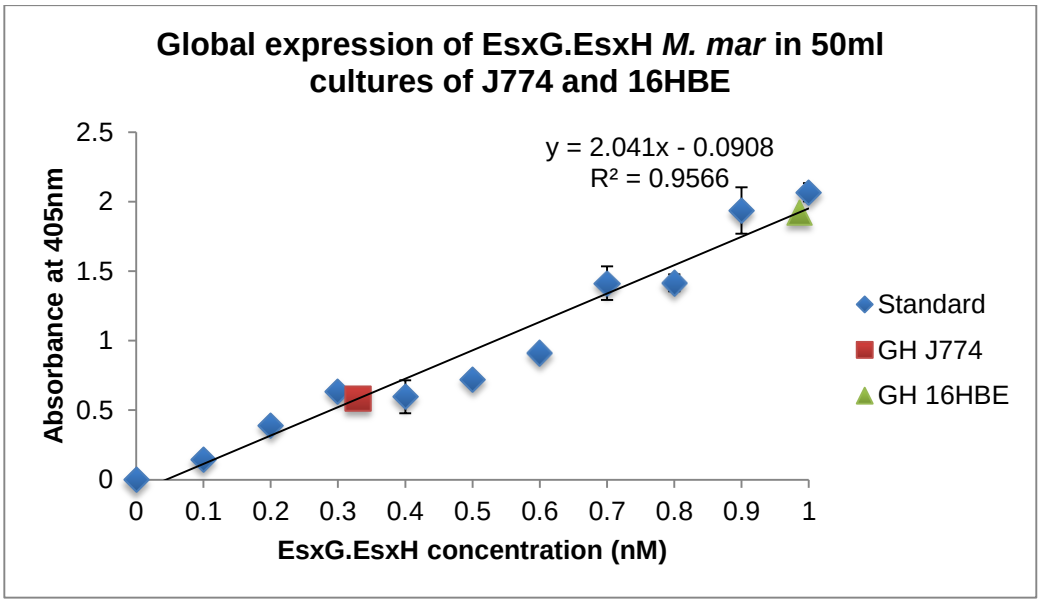

Figure 4.3.4: ELISA analysis of the global expression of EsxG.EsxH in *M. marinum* in infected macrophages. The protein expression in J774 and 16HBE were determined at 0.33 nM (red square) and 0.9 nM (green triangle) respectively based on the determined standard. The presence of EsxG.EsxH in a collective growth of infected macrophage and 16HBE was to confirm that the mycobacteria were expressing the protein in the two host cells and that true positive was also seen microscopically when the antibody employed to the coverslip-infected cells. Standard deviation was used as error bar.

4.3.4 EsxG.EsxH *M. marinum* expression in culture medium

There was an initial doubt of losing the protein complex *in vitro* with incubation at 34.5 ºC, as it was difficult to locate the signals from the preliminary trial microscopy slides. In addition to that, there was also no published report with regards to EsxG.EsxH expression in murine macrophages to confirm this situation. Therefore, to rule out the possibility of the protein complex was loss in culture medium, the expression of EsxG.EsxH complex *in vitro* was conducted. Our finding revealed that some fluorescent signals were found scarcely produced by a small number of bacteria indicating the expression of EsxG.EsxH *in vitro*. The production of the signals was homogenously covering the

mycobacteria as seen before in our preliminary trial. However, since the protein expression seen in this experiment was very low and the proteins were highly associated with the bacteria, we concluded that most, if not the entire, of the protein complex was not loss in the culture filtrate as showed in **Figure 4.3.5** below. Another experimental step that could be added to enhance the conclusion is to examine if the supernatant of *M. marinum* culture contain any EsxG.EsxH using ELISA method.

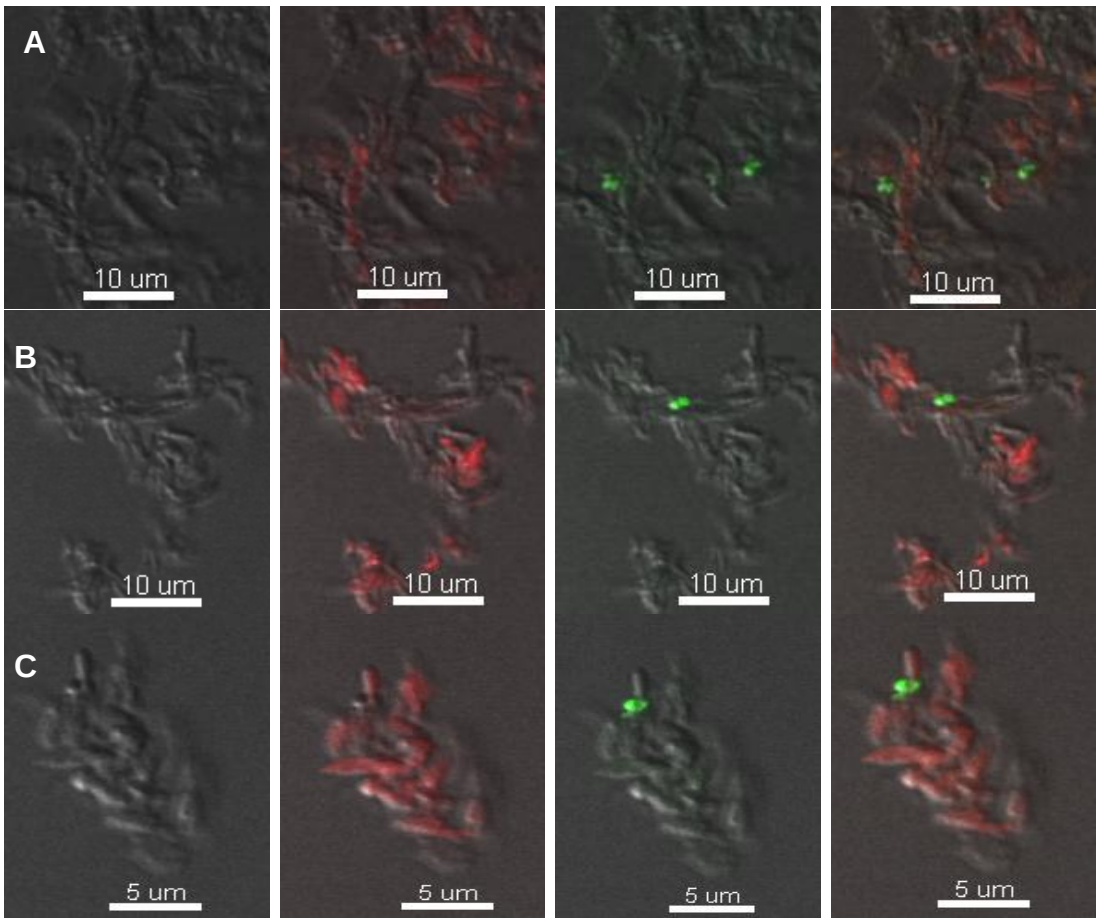

Figure 4.3.5: EsxG.EsxH of *M. marinum* expression in 7H9 broth. The mycobacterial culture that was incubated at 34.5 ^{o}C was spun down and treated with Triton X-100 and washed with PBS before treated with polyclonal anti-EsxG.EsxH antibody raised in rabbit. The green fluorescent signal seen above was due to the secondary antibody raised against rabbit conjugated with AF488, which detected and adhered to the polyclonal primary antibody. The green signals showed in images above suggesting the presence of EsxG.EsxH complex expressed by *M. marinum* that expressed DsRed (red). However, the protein expression was rarely detected and appeared as above. The protein expression feature from the above observation was similar to the one we have seen in preliminary infection slides mentioned in previous section. Any unbound secondary antibodies were removed through PBS washes. Panel C image was magnified at 120X. Images were taken with combination Z slices.

Based on this microscopy observation, apparently there were an infrequent or low number of protein complex expressions by *M. marinum in vitro*. By looking at this result, we were assured with our pilot findings as a true positive signal and at this stage, we could say that the protein complex expression was low. In order to characterize EsxG.EsxH complex expression in infected macrophages, we conducted our experimental analysis in infected J774.1 murine macrophages and 16HBE cells using the same optical density, between 0.6 and 0.8, which is the growing phase for mycobacterium. The O.D could be achieved after five days of incubation.

4.3.5 Characterisation of EsxG.EsxH protein expression during infection

4.3.5 (a) Infected J774A.1 macrophages

Subsequent to determining the specificity and sensitivity of anti-EsxG.EsxH primary antibody and the suitable MOIs for two different cell types, this experiment was conducted to verify our hypothesis that EsxG.EsxH complex was expressed in the infected cells. First, we shall characterize the protein expression in *M. marinum* DsRed infected-J774.1 murine macrophages and was demonstrated 48-hour post infection.

An infection with *M. marinum* DsRed strain was set up in J774.1 murine macrophages for 48 hours. Next, the cells were washed, fixed with paraformaldehyde, permeabilized and treated with the primary polyclonal antibody and secondary antibody before mounted with ProLong® Gold Antifade conjugated to DAPI, a nucleic acid stain. The images below in **Figure 4.3.6** showed the observations presented in I, II and III. The blue signal we saw

suggesting the macrophages nucleus (A) while the red channels (B) indicates *M. marinum* DsRed. Here we could see several levels of infection by mycobacteria. Some J774.1 macrophages contained 1 to 5 mycobacteria cells; some had between 6 and 10 while others may have more than 10 or showed no infection at all. Panel C consists the most important part of the study. The green signals emitted in the images signified the EsxG.EsxH complex expression in the infected macrophages. The expressed protein was not only seen in macrophages containing highly infected mycobacteria but also in low number of mycobacteria infection. Panel D has a clearer view of the association between the protein complex expression and mycobacteria. In Panel D (I) and (III), we could see the presence of the expressed protein complex in densely infected macrophages. Panel D (I) for example showed few mycobacteria expressed EsxG.EsxH despite burdened with high infection whereas in Panel D (II), more mycobacteria cells producing EsxG.EsxH in highly infected macrophage. However, not all of the mycobacteria in the infected cell producing the EsxG.EsxH protein complex.

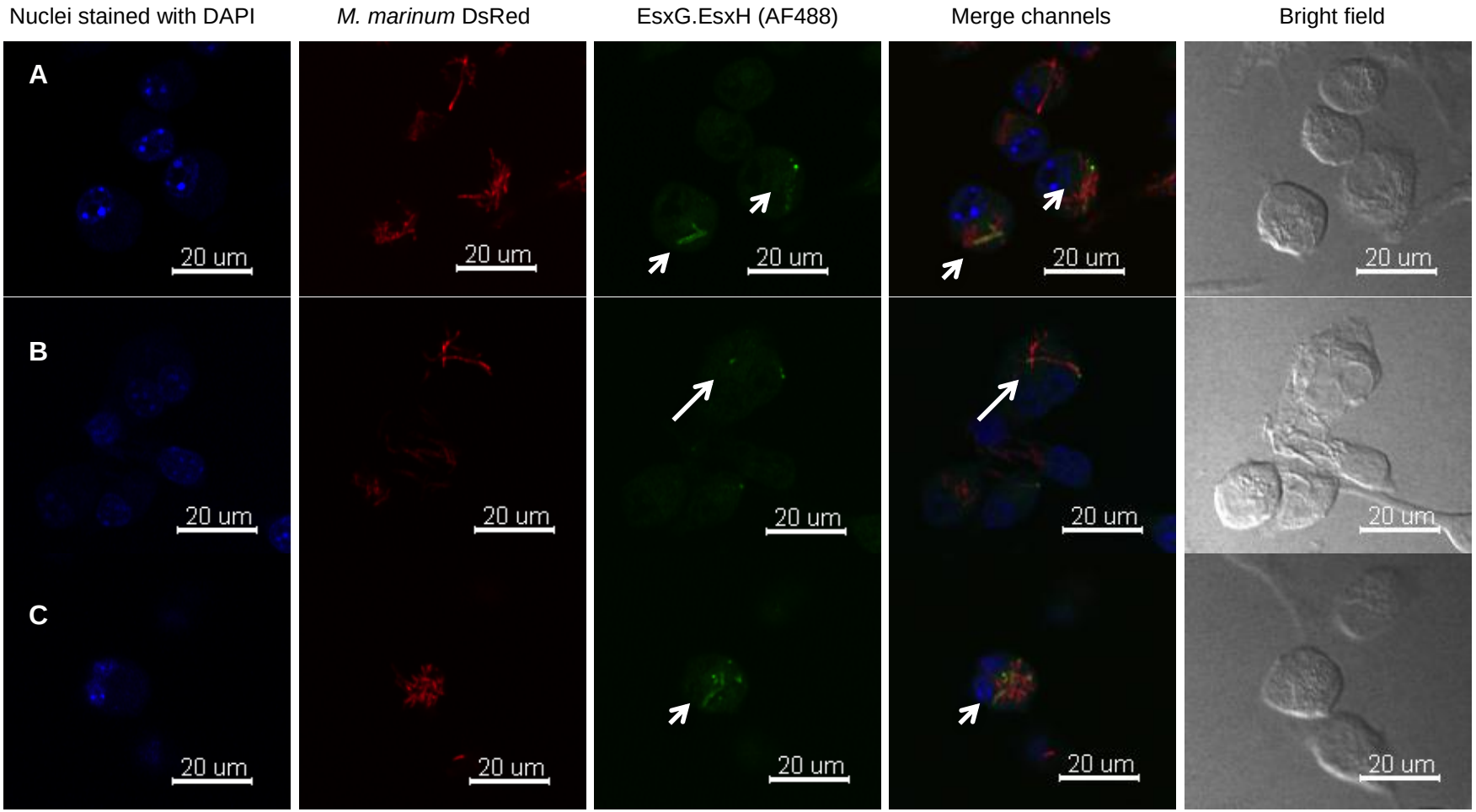

Figure 4.3.6: EsxG.EsxH expression in *M. marinum* DsRed-infected J774.1 macrophages. Panels A, B and C showed mixture of medium, low and high level of infection per macrophage, respectively and their association to EsxG.EsxH expression at 48-hours (merge channels). At each infection level, EsxG.EsxH was detected and appeared to be covering the whole bacterium (short arrows) and at polars only (long arrows). Images were from the best frame.

Another important point to be considered was the appearance of the protein expressed in cells observed in every microscopy analysis and they were very consistent. In some instances, the signal appeared to be covering the whole mycobacteria or surrounding the periphery of mycobacteria as shown Panel C with short white arrows. With others, the signals may be observed at two polar of a bacterium (long white arrow in Panel C). The polar localization of EsxG.EsxH complex expression in mycobacteria was not the only protein to be seen in this manner. The polar localization of expressed EsxG.EsxH complex was consistent with previous study by Carlsson *et al.*, (2009). The team has looked at another ESX1 secreted substrate, Mh3864, a partially cell wall associated post-translocation also localized to mycobacterial poles, with Mh3864 observed at only one pole, which was associated with actin tail. But, for EsxG.EsxH we noticed that the protein complex localized at both ends of mycobacteria.

4.3.6 Protein expression in phagosome

The common appearance of EsxG.EsxH expressed in J774.1 macrophages covering the whole mycobacterium raised an important question whether the protein was actually secreted after residing in the phagosome. To address this possibility, *M. marinum* DsRed infecting the J774.1 macrophages was incubated with a special dye, $DiIC_{18}$ (5)-DS for an hour. The dye, once applied to cells, would diffuse laterally within the plasma membrane. Lipophilic carbocyanine $DiIC_{18}$ (5)-DS is a far-red fluorescent, which contain sulfonate groups and is highly fluorescent and quite photostable when incorporated into

membranes. By applying this dye, we were able to visualize the phagosome-bacteria association. Nonetheless, the detection was difficult to determine because the dye is a far-red fluorescent dye, which was not detectable by naked eyes. So, the detection started with identifying the green fluorescent signal indicating the presence of the protein complex and from there, we viewed it through FV1000 software in order to observe the different channels set at different wavelengths.

Our findings revealed that there were very rare occasion to appreciate the correlation between the EsxG.EsxH protein expressions with phagosome. In most examples, the associated protein expression presents in phagosome were the ones that were closer to the cell membrane of the J774.1 macrophages. **Figure 4.3.7** below shows an example of mycobacterium that expressed the EsxG.EsxH complex present in a phagosome (white arrow). The mycobacterium (red in Panel A) is located very close to the cell membrane of macrophage. The phagosome was indicated by magenta (Panel B) while the green signal signified the production of the EsxG.EsxH complex. In this same figure, we could see the protein expressed but was not present within phagosome (yellow arrow). The number of infected macrophage with EsxG.EsxH present in the phagosome counted was only 2 out of 800 to 1 000 infected macrophages estimated. The data on estimated number of cells infected were shown in **Figure 4.3.10** and **Figure 4.3.11**. Since the expression of EsxG.EsxH was not profound, we did not continue to compare it with the total number of *M. marinum* DsRed within the phagosome.

The EsxA.EsxB complex has been proposed to dissociate from each other in a very acidic environment such as in the phagosome (de Jonge *et al.,* 2007) although Renshaw *et al.*, (2005) determined that the solution structure of this complex formed a stable tight 1:1 complex. The complex also showed to withstand an extreme pH and will only destabilized at pH 4.5 (Lightbody *et al.*, 2008). Therefore, the finding indicated that even in low pH environment such as in mature phagosome, the complex should function as a complex and not as an individual protein during the course of infection. In addition to that, the protein complex has been claimed to play a role in host cell lysis activity through formation of pores in host cell membranes (Smith *et al.,* 2008; Hsu *et al.*, 2003). Although this may become the underlying reason for our finding, earlier report by Renshaw, *et al.* contradicts with both assumptions. Renshaw *et al.'s* argument supported by his findings that the surface of protein complex has a uniform distribution of positive and negative charges thus provide no clue of any possible hydrophobic patch and that his result clearly inconsistent with the feature of a membrane-spanning pore. Knowing that EsxG.EsxH possessed a very similar characteristic to EsxA.EsxB such as in this case, it was impossible to suggest that EsxG.EsxH did as how de Jonge *et al.* and Hsu *et al.* had explained.

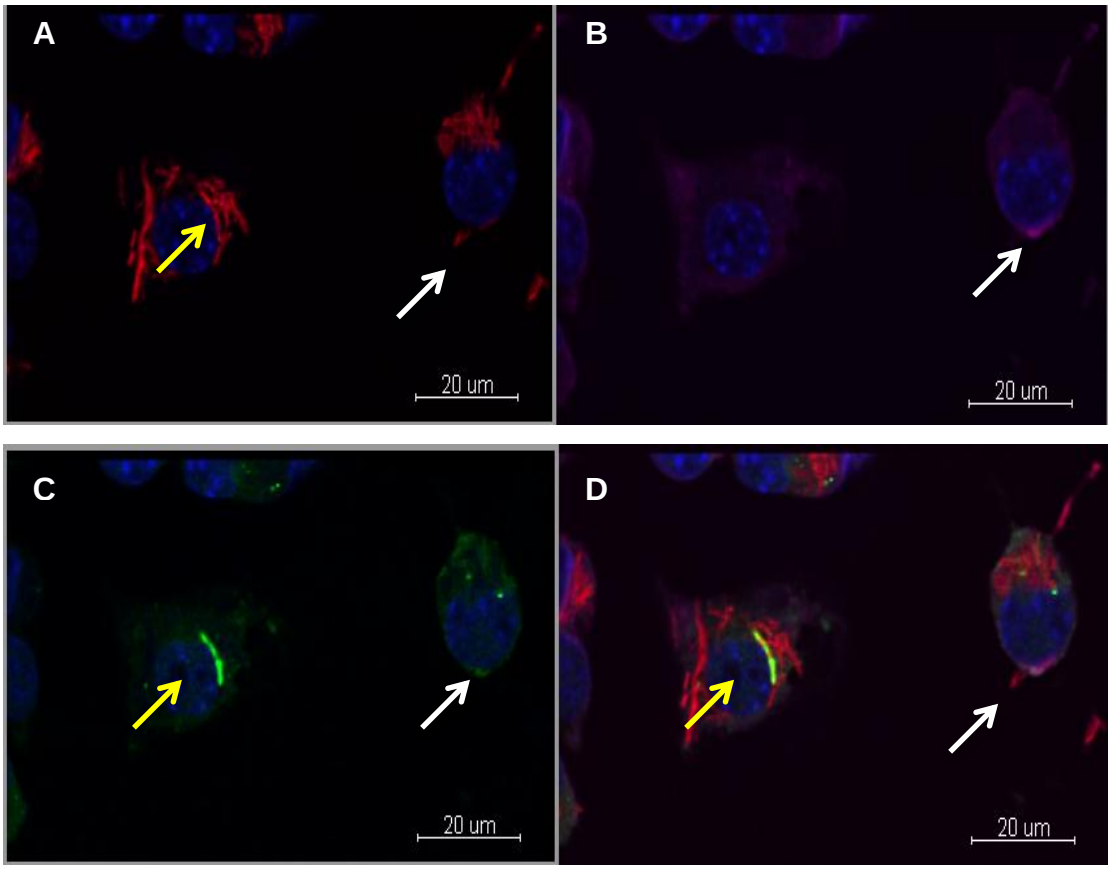

Figure 4.3.7: *M. marinum* DsRed producing EsxG.EsxH engulfed by the phagosome in 48 hpi-infected-J774.1 macrophages. Panel A showed *M. marinum* DsRed (red) infecting J774.1 macrophages with the blue signal indicated the nucleus of macrophages stained by DAPI. The macrophages cells were densely infected by mycobacteria. Panel B revealed the phagosome membrane (purple) present within the J774.1 macrophage cells, which was associated with the bacteria showed by white arrow in Panel D. The related bacterium also observed to express EsxG.EsxH protein (green signal, white arrow) as shown in Panel C. In addition in Panel C, there was EsxG.EsxH expression (yellow arrow) but did not present in phagosome. Images taken at combined Z slices.

The image below is the best example of one of the interesting findings that we occasionally found. The EsxG.EsxH complex was produced by a mycobacterium located at the position of either entering or leaving the infected macrophage. Half of the mycobacteria was presented inside the host cell while the other half was still outside **(Figure 4.3.8; white arrow)**. This observation has also been seen by Ray, A. in his study and suggesting the ejectosome structure during the course of infection. In this same infected host cell, we could also appreciate the expression of EsxG.EsxH by the same bacteria where its ejectosome structure was detected using $DiIC_{18}$ (5)-DS dye. Apparently, the green signal indicating the protein complex merely present within the cytoplasm of host cell while the membrane staining for ejectosome was seen outside the host cell. Recently, the phagosomal escapes of *M. marinum* and *M. tuberculosis* excluding *M. avium* have been associated with the formation of the ejectosome, an actin-based structure (Hagedorn *et al.*, 2009). The researchers claimed that *M. tuberculosis* and *M. marinum* are able to spread via this non-lytic mechanism with an intact mycobacterial ESX1 secretion system. This could also suggest that the production of EsxG.EsxH complex does not only rely upon post entry into the macrophages but also possibly just before escape from the host cell.

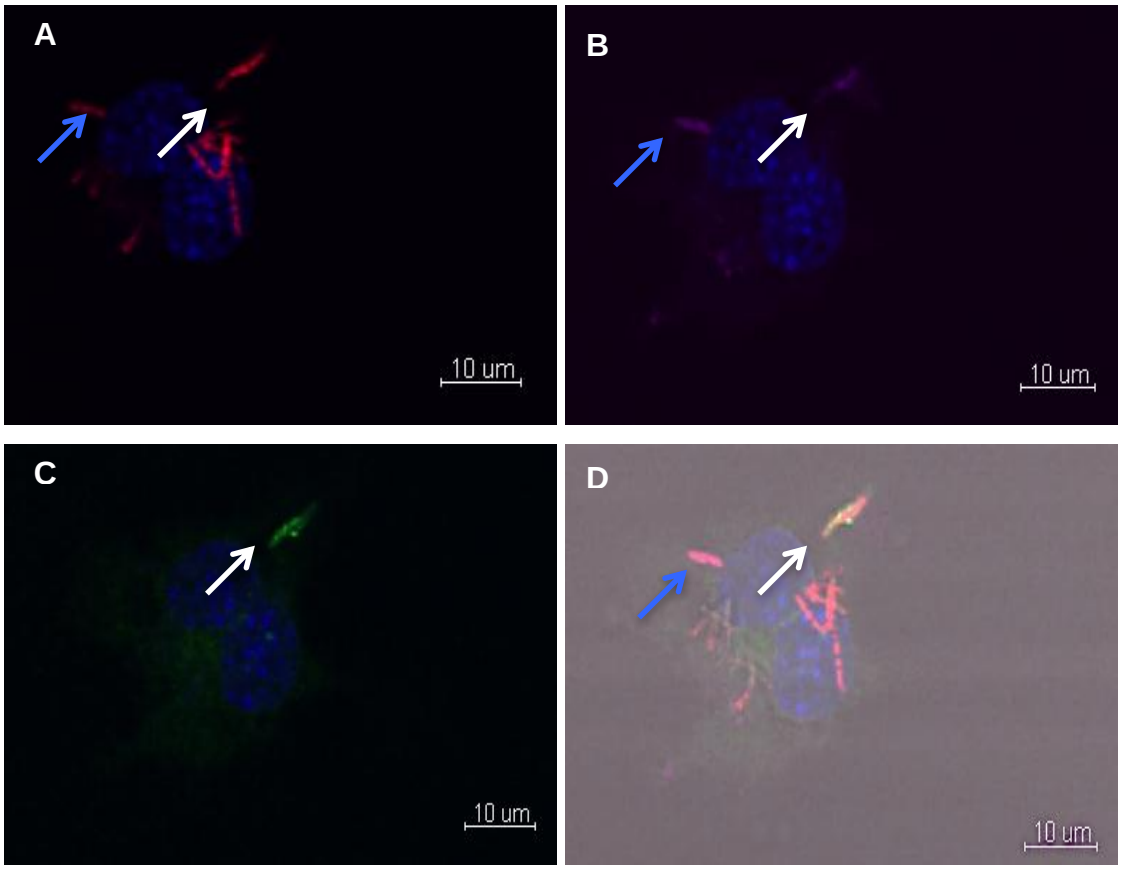

Figure 4.3.8: The bacteria present within the J774.1 macrophage phagosomes were noted to be located close to the cell membrane of macrophages. As mentioned previously, the blue, red (Panel A), purple (Panel B) and green signals (Panel C) were representing the nucleus of J774.1 macrophages, *M. marinum* DsRed, phagosome and EsxG.EsxH complex respectively. In this image, we displayed two different situations where the blue arrows showed mycobacterium engulfed by phagosome, while the white arrows demonstrated the *M. marinum* DsRed expressing EsxG.EsxH protein was also present within phagosome as clearly represented in Panel D. However, this scenario was infrequently seen throughout the experimental setting.

4.3.7 The frequency and importance of EsxG.EsxH expression in infected J774.1 murine macrophages

Mycobacteria are intracellular microorganism and most of their genomic properties were devoted towards functions that enable them to establish infection either the latent or progressive type in infected individuals. The lesion caused by *M. tuberculosis* is usually characterized by the formation of granulomas, one of the mechanisms adopted by *M. tuberculosis* to support the persistence of its viability. As mentioned previously in the Introduction part of this chapter, ESX3 that also secretes EsxG and EsxH has been suggested to produce prime T-cell (CD4 and CD8) against mycobacteria antigens following the migration of dendritic cells containing the engulfed bacilli. The specific immune response migrated back to the infected site guided by chemokines produced by the infected cells. This results in accumulations of various immune cells and endothelial cells that trigger the formation of granulomatous lesion (Bodnar *et al.*, 2001; Gonzalez-Juarrero *et al*., 2001) and suggest the importance of ESX3 secreted proteins in host immune responses.

In conjunction with our previous screening and the analysis mentioned before, we tried to look at the frequency of its expression in infected macrophages. Therefore, semi quantification analysis was conducted to interpret the frequency of EsxG.EsxH protein expression when J774.1 macrophages were infected with *M. marinum* DsRed at MOI of 0.5 for 24 and 48 hours. With the same experiment, we were also able to study the levels of infection that occurred at two different time points. In addition to that, it will enable us to understand the relationship between levels of infection and

EsxG.EsxH protein expression; whether the protein complex was expressed more at low (1-5 bacteria) or medium (6-10 bacteria) or highly (>10 bacteria) infected J774.1 macrophages. Apart from that, we would like to emphasize on understanding and correlating our findings with the information gathered regarding its importance in TB.

The total macrophages were first counted, followed by mycobacteria and lastly the green signals representing EsxG.EsxH expression. The counting was done manually and the total number of macrophages counted must not be less than 1 000 cells in order to get a better picture of the protein expression. This is because, based on a number of observations made previously; the protein expression was very infrequent. **Figure 4.3.9** below showed a representative image of EsxG.EsxH complex expressed in infected macrophages used to semi-quantified the protein expression.

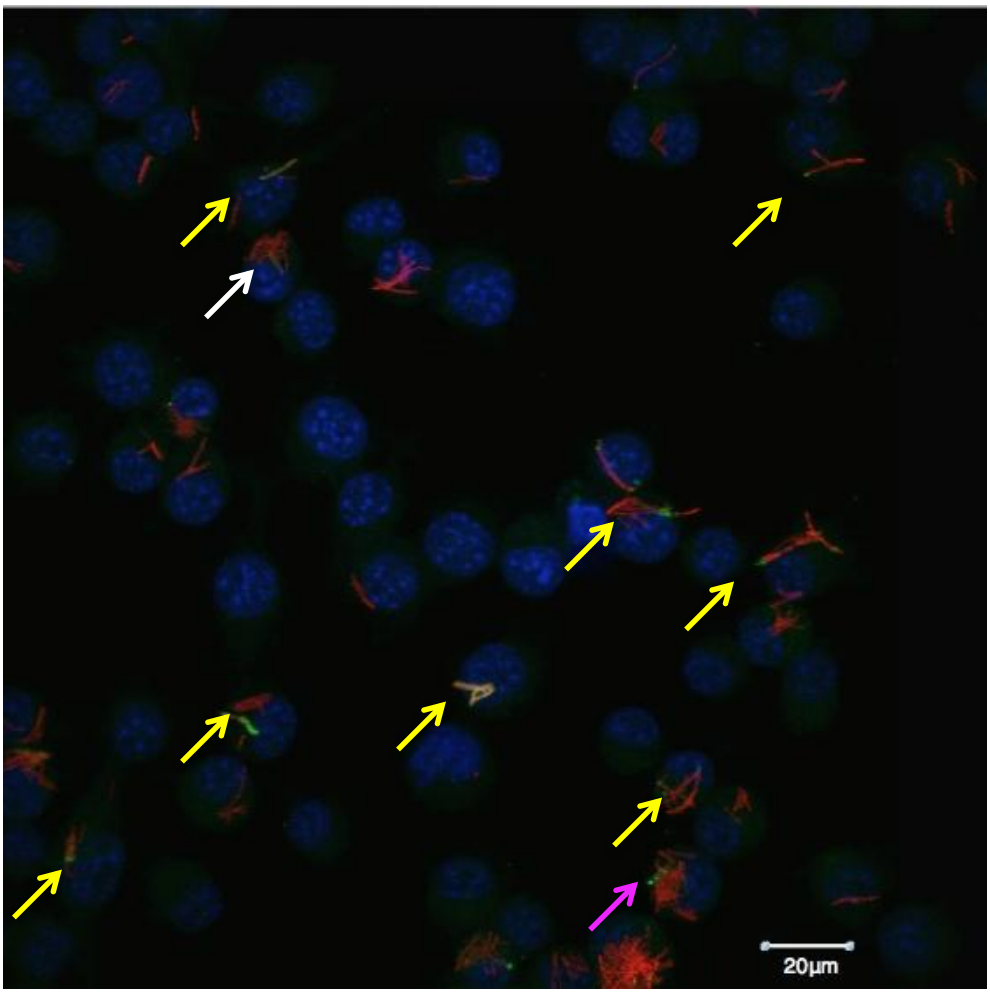

Figure 4.3.9: The expression of EsxG.EsxH complex observed in three different categories of infected J774.1 macrophages after 24 hours. In this image, we could see mixture groups of infected macrophages with or without protein complex expressed in. All arrows presented above were the host cells containing the expressed protein. The yellow arrow showed a low category of infection occurred in an infected macrophage while the white and purple arrows represent medium and high category respectively. There were a lot of low infected host cells seen to express EsxG.EsxH at 24hpi in comparison to other groups. There were also other infected cells that did not show any protein expression by the mycobacteria. The image was taken from combined Z slices.

At 24 hpi **(Figure 4.3.10),** the percentage of macrophages being infected with bacteria was 52.7% out of 1636 cells counted and about one fourth or 24.7% appeared to produce signals indicating the expression of EsxG.EsxH complex. Out of the total number of signal produced, only two cells were identified to be present within phagosome. At this time point, it was calculated that the low level of infection category was predominant compared to other categories. However, it did not relatively reflect the EsxG.EsxH protein expression yet as we too conducted another observation at 48 hpi. The frequency of protein complex expressed at low-infection macrophages were about 1:5 meanwhile for densely-infected macrophage cells showed about 50% or one cell would have protein expression in every two macrophage cells. Remarkably, this number is quite promising so as for medium level of infection category, signals were estimated around 1:3 **(Panel C and D).** Up to this stage we could conclude that at 24 hpi, the pattern for EsxG.EsxH protein produced was noticed to be higher with the increased in the number of mycobacteria cells infecting a J774.1 macrophage.

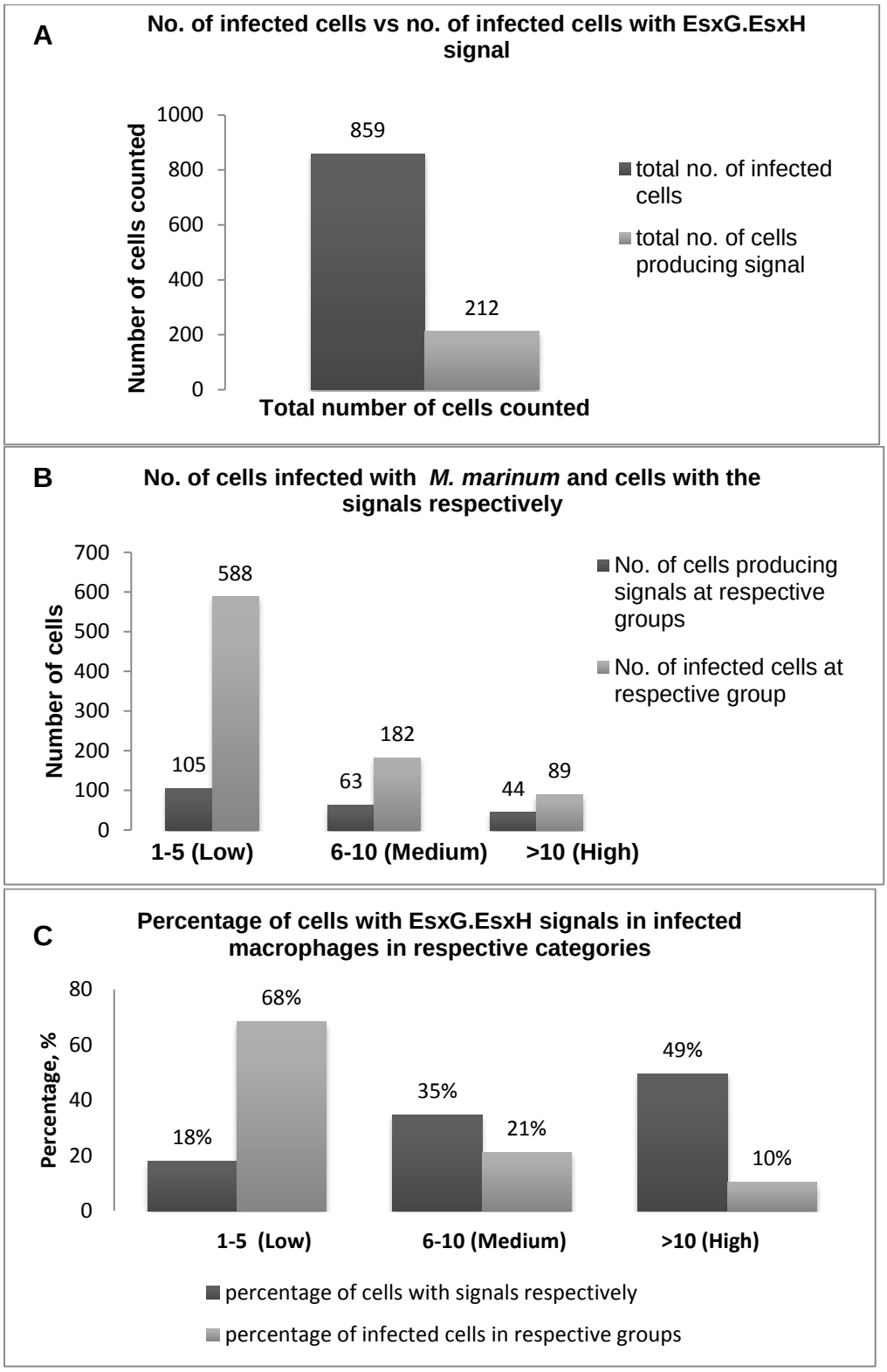

Figure 4.3.10: Semi quantification of EsxG.EsxH observed at 24hpi. The total number of macrophages counted was 1636, which composed of 859 of infected and 777 uninfected macrophages. About 25% of estimated infected macrophage cells produced EsxG.EsxH (Panel A) and could be considered as high and important during course of infection. Infected cells were categorized accordingly (Panel B) and the relatedness of EsxG.EsxH expression was determined in percentage (Panel C).

We also conducted the same quantification technique for J774.1 macrophages infected with *M. marinum* DsRed for 48-hour **(Figure 4.3.11),** as infected macrophages growth reached its maximum at this time point. We hypothesize that more protein expression would be viewed as mycobacteria may require more nutrients to survive (Serafini *et al.*, 2009; Siegrist *et al.*, 2009; Sassetti *et al.*, 2003) and a more diverse level of infections would become more prominent. From the overall observation made, a similar result showed, wherein only two signals were seen to be present in phagosome. A total of 1572 J774.1 macrophages were counted where about 75% of the macrophages were infected with *M. marinum* DsRed while 393 out of 1572 were uninfected macrophages. There was a small increase in percentage of signals demonstrated which was about 5.3%. We could speculate that the increased number of infected J774.1 macrophage cells might was minimal. Looking at the level of infection trend on the other hand, it appeared that there was a huge different from 24hpi outcome. The numbers of J774.1 macrophage cells infected by mycobacteria at various level of infection were of no different **(Panel B).** There was no significant difference among each other categories and the cells seemed to expose to mycobacteria evenly as more time was allowed for an infection to occur. At 48 hpi, the EsxG.EsxH protein was seen to be expressed more in highly infected J774.1 macrophages than in lower number of mycobacteria infecting a macrophage cell **(Panel C and Panel D).**

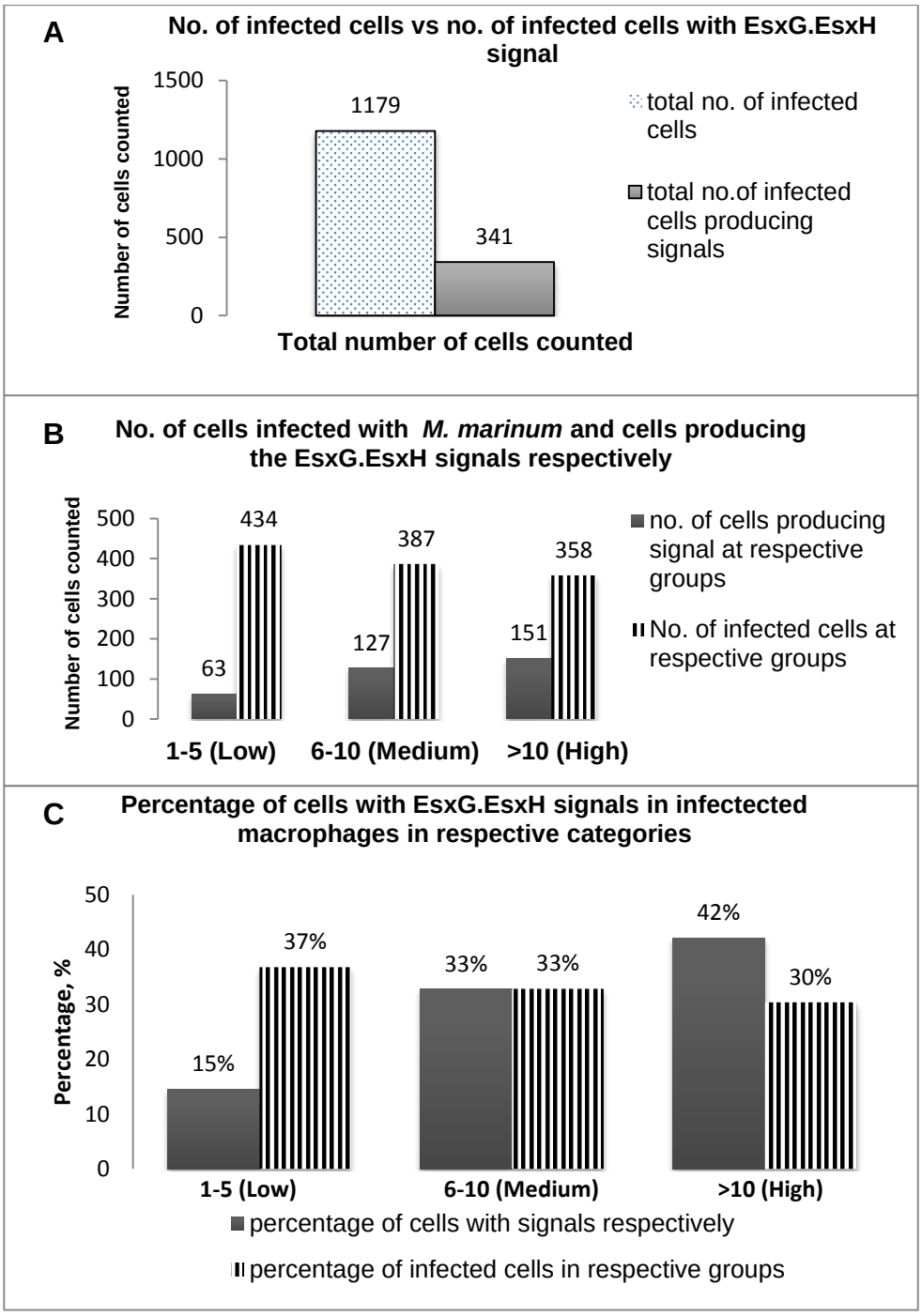

Figure 4.3.11: Semi quantification of EsxG.EsxH observed at 48hpi. Total of 1572 macrophages counted where 1172 were infected with *M. marinum* while 341 did not. About 25% of infected macrophages showed to express EsxG.EsxH (Panel A), which was similar to observation made at 24hpi. The correlation between protein expression and level of infection was also determined (Panel B and C), in which Esxg.EsxH expression was greatest at high level of infection.

We knew that *M. tuberculosis* was a facultative pathogen that causes a chronic disease and able to sustain most of its cell cycle in a non- or slowly replicating state. Once the bacterium resumed its replication, it could transmit itself to a new host. However, there would possibly be metabolic adaptations to and recover from hypoxia, which was relevant condition to link with the dormant state, yet the virulent remained viable for decades and tolerant to almost all first and second line of TB treatments (Warner and Mizrahi 2006; Xie *et al*., 2005) while maintaining at least five times lower of ATP levels than its replicating stage (Rao *et al.,* 2008; Weinstein *et al.*, 2005). All in all, the metabolic changes throughout the course of infection starting from mycobacteria entrance till exit from cell cycle remain incomplete. From our analysis, the production of EsxG.EsxH complex could have related to the mycobacterial metabolic activity involved in its life cycle. The protein expression was seen more in densely infected cells regardless of the span of incubation time. We did not allow the infection further or more than 48 hours as the infectivity dropped after that, up to this point we could only conclude that the protein expression is not necessarily produce all the time. When we compare EsxG.EsxH complex with two other mycobacterial proteins known for their frequent expression in macrophages, it appeared that EsxG.EsxH complex was more common than RpfA expression (Iakobachvilli, N., PhD thesis 2014) but less common than Mpm70 protein (Ray, A., PhD thesis 2010). The common findings shared by these three proteins was their presence in phagosome was rare or almost absent throughout the course of infection up to 72 hours for Mpm70 case and 48 hours for EsxG.EsxH and RpfA.

From the microscopic studies of EsxG.EsxH expression in *M. marinum*-infected macrophages suggest that the protein complex is only expressed in a relatively small subset of mycobacteria at any specific time point, perhaps suggesting only a transient requirement for this protein complex, and/or significant heterogeneity within the bacterial population as seen in *in vitro* microscopy observation described earlier in this chapter. Apart from that, EsxG.EsxH complex is infrequently seen expressed in phagosome localized mycobacteria. Since the protein complex is seen to localize on the surface of expressing bacteria suggests that it could possibly be a potential cell surface-binding partner. In order to confirm this hypothesis, another experimental procedures could be conducted through studies such affinity-purification coupled to mass spectrometry and yeast-two-hybrid (Gavin *et al.,* 2011; Gavin *et al.,* 2006; Fields and Song, 1989) that have been known to provide successful result in determining protein-protein interactions. Other than these high-throughput studies, there are also low-throughput experiments such as pull-downs, co-immunoprecipitation, mutational analysis and protein arrays (Zhu and Synder, 2001; Hall *et al.,* 2007) in which many of the interested domain-motifs interactions have been discovered (Blikstad and Ivarsson, 2015).

The ability of EsxG.EsxH protein complex to express in mycobacterium-infected murine macrophages suggests the needs of the protein complex during the course of infection. The characteristic features of the protein expression have been determined earlier in this chapter aiding the identification for the following experiment. As described by Ilghari *et al.* (2011), the special characteristic of EsxG.EsxH in comparison to EsxA.EsxB, the former possessed

a cleft suggesting the presence of a functional binding site, which is absent in EsxA.EsxB complex (**Figure 4.3.12).** The well-characterized protein expressed by mycobacteria, Mpm70, was tested as the protein partner. The expression feature of Mpm70 during infection in macrophages appeared similar to EsxG.EsxH plus both proteins did not seem to be present in phagosome. Hence, Mpm70 was chosen, as the first protein to determine the protein partner for EsxG.EsxH and the co-localization was determined through confocal microscopy using quantum dot-labelled-antibodies.

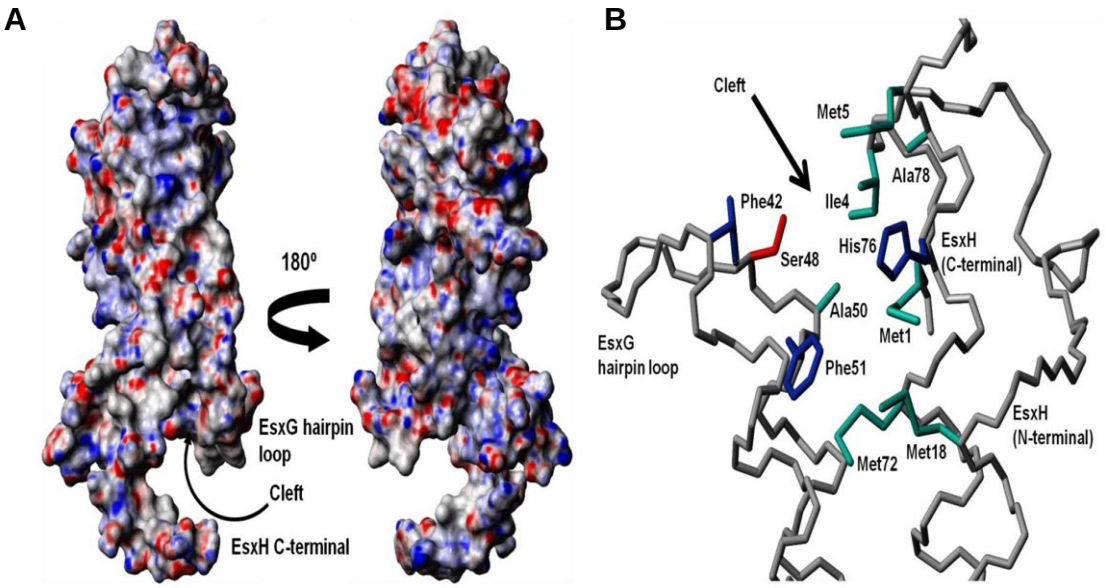

Figure 4.3.12: The surface view of EsxG.EsxH protein complex and the presence of the cleft found between the loop that links the EsxG and C-terminal arm of EsxH that suggest a functional binding site on the protein complex. Image was extracted from Ilghari *et al.* (2011).

4.3.8 No co-localisation between EsxG.EsxH and Mpm70 proteins identified using Qdot-labelling agents

Prior to conducting this experiment, a series of optimization steps have been conducted and described in the Appendix section of this thesis. The optimizations included; were suitable dilutions for both Qdot-labelled-antibodies and the type of mycobacteria used to finalize the experimental protocol. The microscopy observations were made together with the assistance of Dr. Kees Straatman from the Advance Microscopy Unit, University of Leicester, who had worked with Qdot before. Below are the images that were often observed during the microscopy analysis.

In **Figure 4.3.13** below, both signals indicating the presence of Mpm70 protein (green) and EsxG.EsxH (yellow) expression were seen in the same mycobacterium. Although they did not appear to co-localize with each other, both of the proteins could be seen present at the same time in the same mycobacterium. However, this occurrence was rare. A more common observation noticed from this experiment was either Mpm70 or EsxG.EsxH present in the host cell at any single time or both of the proteins were found together but produced by different mycobacteria in the same host **(Figure 4.3.14)**.

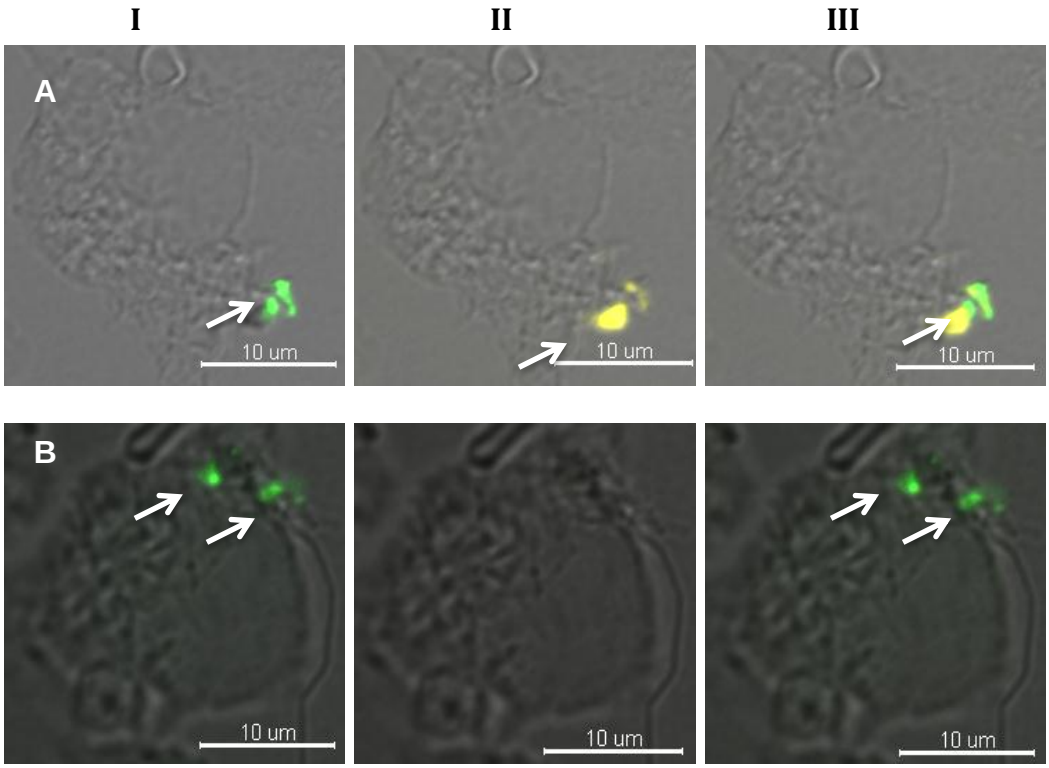

Figure 4.3.13: Expression of EsxG.ExsH and Mpm70 in wild type *M. marinum*-infected J774.1 macrophages. The green signals present in the images above indicate the expression of Mpm70 protein and was detected using the Qdot565-labelled-anti-Mpm70 antibody shown in Panel A. However, the signal was seen from mycobacteria present outside the broken host cell. Meanwhile, the yellow signals observed in Column II in Panel A suggesting the expression of EsxG.EsxH protein when Qdot655-labelled-anti-EsxG.EsxH antibody was employed. When the two channels were merged, it appeared to be produced by the same mycobacteria. One of the yellow signals was produced at polar region of mycobacteria and this finding is consistent with our finding for the expression of EsxG.EsxH that has been mentioned earlier. Also, there was an overlapping of signals seen in Panel A Column III that could suggests an association or co-localization between the two proteins. As for Panel B, there was only Mpm70 protein expressed present in the infected cell and it proved that the association between the two proteins are not necessarily present at all time.

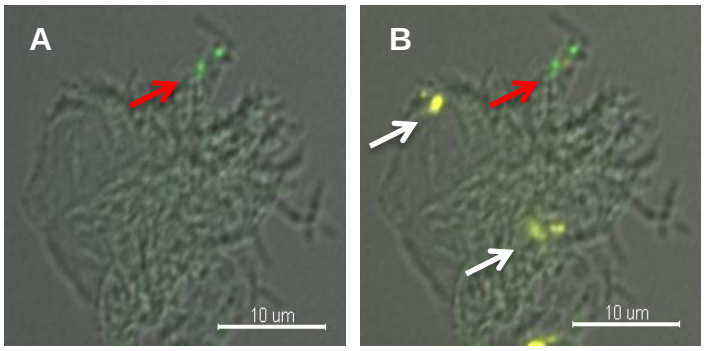

Figure 4.3.14: EsxG.EsxH and Mpm70 proteins were expressed by different mycobacteria within the same host cell. The production of Mpm70 protein was observed as a green signal (red arrows) in Panel A and Panel B above. More of EsxG.EsxH proteins (white arrows) were expressed in this heavily infected macrophage, showed as yellow signal in Panel B. In this image, we could observe the expression of both proteins by different mycobacteria infecting the single infected macrophage. Although this finding is different from previously described observation, it showed that there was a possibility of co-localization occuring (however it was not frequently found in the infected host cell). A more common scene found was that either the proteins were separately produced by the same infected macrophage or they were produced separately by different macrophages.

The observations made may suggest the intermittent needs for both proteins in a single infected host cell at a single time point. However, the role for the need of having both the proteins present at the same time is yet to be determined, in addition to learning which protein is responsible for co-localizing to EsxG.EsxH to complete the puzzle of the cleft present in between EsxG and EsxH. Although the production of EsxG.EsxH could only be seen for a short period of time or presumably in the early stage of infection, we still could not disregard its importance in TB infection as well as based on the number of EsxG.EsxH complex estimated particularly when the complex was seen to be expressed mostly in densely infected host cells (J774.1 macrophages). A further

analysis using zebrafish as a host model would be a good option to identify and demonstrate the virtual expression of EsxG.EsxH as well as to postulate the protein production with time.

In summary, chapter 4 described the effort to characterize the expression of EsxG.EsxH complex in *M. marinum*-infected-J774.1 murine macrophages as the host model and to determine its possible co-localisation activity with Mpm70 through a series of confocal microscopic examinations. The objective was achieved using different fluorescence conjugation reagents and preparation techniques as well as semi-quantitative method to analyse the frequency of EsxG.EsxH expression at 24- and 48-hour post infection. In order to pursue with the protein detection, anti-EsxG.EsxH polyclonal antibody was produced using the purified recombinant protein of EsxG.EsxH complex of *M. marinum* and tested for its sensitivity and specificity. The antibody could determine the presence of EsxG.EsxH protein as low as 0.1 nM at 1:100 antibody dilutions, which is at 0.22 mg/ml or 0.15 μM of anti-EsxG.EsxH antibody. The specificity of the polyclonal antibody was exhibited when the same antibody concentration was tested against EsxA.EsxB and EsxO.EsxP of *M. tuberculosis*, and was unable to detect the presence of both protein complexes even at 1 nM of protein concentration.

Initially, optimization of MOI and the immunofluorescence protocol was conducted and MOI of 0.5 was chosen for the analysis and was used throughout the experiments related to *M. marinum*-J774 murine macrophages infection. The production of EsxG.EsxH complex was observed in infected J774.1

macrophages but not in every infected cell consistently. The signals observed appeared in two forms: the protein complex either covering the whole cell or present at both ends of the mycobacteria with the former occurring more commonly than the latter. This was followed by the determination of EsxG.EsxH expression in phagosomes in which a special fluorescent dye was employed ($DiIC_{18}$ (5)-DS) that emit far-red fluorescence when interacting with plasma membrane. Unfortunately, the signals that indicated the presence of EsxG.EsxH were not seen within phagosome. In a very rare occasion, the protein complex was observed to be present in phagosome. Between 700 and 900 of macrophages infected with *M. marinum* DsRed, only 2 signals of EsxG.EsxH complex were detected. This showed how uncommonly the protein production is associated with phagosome. This finding actually contradicted with the claimed made by a number of studies previously that suggested EsxH synergistic interaction with Hrs protein leads to prevention of coalescence between phagosome and lysosome. As a result, mycobacteria could escape from enzymatic lysis in phagolysosome compartment (Mehra *et al.*, 2013). The frequency of EsxG.EsxH protein expressed in infected cells was determined in which more than 800 cells out of 1636 cells were infected, where it was estimated about 1 cell in every 4 infected cells showed positive signal for EsxG.EsxH expression at 24-hpi. However, the expression of protein complex was no different when observed at 48-hpi, only the spread of protein expression among the three group classifications (low, medium and high) was seen more evenly distributed in 48 hours compared to 24-hpi. This could suggest the occurrence of a more transient requirement for this protein complex within the bacterial population. Apart from that, this finding also revealed that EsxG.EsxH

complex production is more common found than previously reported RpfA protein but less common than Mpm70 protein expression in *M. marinum*-infected J774.1 murine macrophages. The frequency of EsxG.EsxH complex expression was seen as moderate throughout 48-hpi suggests some degree of importance of the protein complex during the course of infection.

Further investigation was conducted in looking at Mpm70 as the possible protein partner for EsxG.EsxH complex with Mpm70 protein. As mentioned previously, Ilghari *et al.* suggested that EsxG.EsxH possessed a cleft that links EsxG and EsxH that is suitable for the binding of a protein, in which the specific protein has not been identified to date. The characteristic feature of Mpm70 is similar to the expression of EsxG.EsxH in an infected macrophage. In addition, it was also determined that both of the proteins expressed by the *M. marinum* DsRed were not express in the phagosomal compartment. Although these characteristics did not strongly support the possibilities of the two proteins working synergistically, however, it was worthwhile to try and understand the similarities in the features shown by both proteins microscopically. An attempt was carried out through the implementation of quantum-dot (Qdot) technology. There were reports available claiming that this technology was able to produce a prominent signal even at low concentration of Qdot. For this experiment, we have changed the method of slide preparation to avoid the possibilities of anti-rabbit secondary antibody to recognize the conjugated primary antibody that would lead to false positive. This is the factor that needs to be eliminated as both of the primary antibodies were collected from rabbit serum. Due to this reason too, the previous co-localization seen was unnecessarily true and has

led to the implementation of Qdot labelling technique to both of the prepared primary antibodies. An intriguing finding was observed in which both of the proteins were seen expressed in an infected macrophage. Although they may not appear to be co-localized with each other, a rare phenomenon was also spotted where both of the proteins were expressed in the same mycobacterium that infected the same macrophage. Unfortunately, due to limited experimental time, we could not conduct this experiment further to observe more of this scenario and try to search for more possible co-localization between EsxG.EsxH complex and other ESX family proteins that will be more valuable as they would be secreted by the same secretion system, T7SS.

General discussion and future work

Recently, a novel secretion system has been identified in *M. tuberculosis* and has been classified as the Type Seven Secretion System (TSSS) by Bitter *et al.,* (2010). The first protein secreted by the secretion system identified was ESAT 6 or currently known as EsxA. Following the finding, more *M. tuberculosis* proteins from the ESX family of proteins had been recognized to be secreted by TSSS. This showed the importance of ESX proteins for *M. tuberculosis* particularly in their involvement in TB pathogenesis. The virulence of EsxA.EsxB for example had been shown through comparative genomic analysis between virulent *M. tuberculosis* (H37Rv) with the attenuated vaccine type, *M. bovis* BCG that proved the missing genes in *M. bovis* BCG were the reason of it becoming less virulent and the missing genes included were the *esxA* and *esxB* genes. The discoveries of other esxA and esxB paralogs resulted in a number of increasing interest to undermine the role they may have and/ or share.

Therefore, prior to understanding the role of Esx proteins, we initially performed purification of four (4) recombinant Esx protein complexes namely EsxA.EsxB, EsxO.EsxP and EsxG.EsxH of *M. tuberculosis* and EsxG.EsxH of *M. marinum* each representing ESX1, ESX5 and ESX3 family protein. The purification protocols together with the amendments where necessary, and were described in length in the Appendix section as other researchers have conducted them before, who were also mentioned and acknowledged in the respective section. It was important to ensure that the protein complexes

were fit for determining the responses by 16HBE cells post-introduction to the protein complexes. In order to achieve it, lipopolysaccharide (LPS) was removed by implementing the gradient step purification technique, which was performed manually. All of the instruments and media used were maintained pathogen-free as much as possible. However, this step was prepared one time for the protein complexes used in preliminary experiments only and not for the actual experiments as the pre-analysis LPS value was maintained between 1 and 0.01 EU/ml. Nevertheless, we did not test for the distilled water used to dilute the buffers and the protein complexes to the desired concentrations. This may have affected our results. In future, it would be best to use the medium in which the cells grow to maintain a pyrogen-free environment, as well as to reduce as much as possible the changes to the cells that could be the result of external factors such as diluting agent.

Chapter 3 revealed the answer to the question, whether or not the protein complexes bound to the cell surfaces of 16HBE cells? Previously, Dr. Al-Harbi in his thesis showed the ability of the EsxA.EsxB and EsxO.EsxP to bind to the cell surfaces of J774.1 macrophages and U937 monocyte but not to fibroblast cell (NIH-3T3). However, the exact interaction site(s) was not determined. In conjunction with another finding by Goodman and Bermudez (1999) that revealed the ability of mycobacterium to invade human lung cell has led to our intention in determining if the EsxA.EsxB, EsxO.EsxP and EsxG.EsxH of *M. tuberculosis* bind to the surface of 16HBE that may contribute to the invasion of the mycobacterium. As expected, a similar observation was made between the control (J774.1 macrophages) and

16HBE. The similarities included not only the ability of EsxA.EsxB and EsxO.EsxP to be bound to the cell surface of 16HBE but also portrayed the unique characteristic of cap-like feature, which was described by Dr. Al-Harbi in his findings (PhD thesis). The unique feature may happen when the host surface receptors interact with complementary ligands. The assembly of molecules is specific for ligand/receptor combinations and has been shown in a number of studies may be significant for extracellular signal transduction through combination of various signalling elements (Eda *et al.,* 2004; Junge *et al.,* 1999). This observation has not been mentioned anywhere before in literature and we concluded that these two Esx protein complexes were able to interact with receptors present on monocytes, macrophages as well as human bronchial epithelial cell. Nevertheless, the “cap-like” characteristic on the cell surface of receptors has been observed previously in macrophages and in various receptors such as the insulin, epidermal growth factor, L-selectin, immunoglobulin and immune cell receptors (Arhets *et al.*, 1998; Arhets *et al.,* 1995). A table consisting of information on CD receptors shared between human epithelial and mouse macrophage were presented in Chapter 3. The most salient receptors that the protein complexes shared, were those involved in antigen presentation, signal transduction, chemotaxis and cell survival. This was supported by numerous reports on EsxA.EsxB in particular suggesting that the possible role of EsxA.EsxB complex was in inducing immune responses during TB (Renshaw *et al*., 2005; Lewis *et al.,* 2003; Pym *et al,* 2002).

Subsequently, we wished to explore whether the studied protein complexes anticipated in modulating the host immune system and/or affecting the lung epithelial barrier as part of an invasion mechanism following their adherence to the cell surface of 16HBE. The same experimental procedures were repeated on the primary lung cell line, HL204 to observe and compare the effects caused by the Esx protein complexes. However, this section of the studies were moved to Appendix section due to lack of proper controls and also the use of untested samples for LPS. In order to understand the flow of the continuation of the study, we shall discuss the second part of the study in this paragraph. First, the response by 16HBE towards EsxA.EsxB, EsxO.EsxP and EsxG.EsxH showed no significant difference (p>0.05) between medium and buffer controls and the different concentrations of protein. The trend observed was very similar among them suggesting either the buffers were affecting the results or that this was the actual responses influenced by the proteins per se. The lack in concluding the result was contributed by the use of non-LPS-removal-buffers and -distilled water. In addition, the absence of LPS as one of the controls made it difficult to rule out if the response was influenced by the presence of LPS not only to the TER but also IL8 analysis. As for the experiment conducted using HL204 primary pulmonary cells, a distinctive feature was found on all of the cells treated with controls and Esx protein samples. The HL204 primary cells were observed to produce very viscous and thick mucous that made sampling almost impossible. The viscosity led to the accidental extraction of cells present on the transwell filter when sampling. This could lead to false TER readings and evaluation of barrier integrity due to the interrupted cells.

Or, there was also the probability that the apical medium was sampled less and led to loss of the overall picture of detail aimed for. Hence, the implementation of primary lung cells was stopped after the trial experiment using HL204 to avoid any false positive or false negatives to the outcomes. Nevertheless, the apical mediums collected were centrifuged and the sediments were kept for cell count. After 24 hours of exposure to protein complexes, a mixture of necrotic and apoptotic cells were observed using light microscopy. However, there was no specific trend or association seen between protein concentrations and cells counted. This result may not reflect the actual condition due to the possibilities mentioned above.

Chapter 4 explained the expression of EsxG.EsxH complex post uptake by J744.1 macrophages. In chapter 3, we concluded that EsxA.EsxB and EsxO.EsxP complexes interacted with the cell surfaces of 16HBE but not EsxG.EsxH. Based on a number of previous studies reported on the possible roles that EsxG.EsxH complex may offer such as its connection with synergistic effect with HRS protein to prevent phagosome-lysosome interaction leading to lysis of the bacteria through the activity of enzymatic reaction in phagolysosome (Mehra *et al*., 2013); its potential as a subunit vaccine (Sweeney *et al*., 2011). However, based on our observation, the number of EsxG.EsxH signals present in an engulfed *M. marinum* was rare, that it did not reflect the role of EsxG.EsxH in preventing phagolysosome formation as suggested previously by Mehra *et al*. (2013). The expression of EsxG.EsxH was seen consistent when compared with two different time periods of infection i.e. at 24- and 48-hours, which was estimated at 25 and

29 % respectively. The greatest protein expression observed at 24-hpi and 48-hpi was seen to be in high infection category although a more evenly spread of infection and protein expression was seen at 48-hpi compared to 24-hpi. This could possibly be contributed by the number of infection among different groups of infection (low, medium and high) that occurred at the two different incubation period. In order to improve the findings, we could also include another step in the slide preparation protocol. After inoculating J774.1 macrophages with *M. marinum* DsRed and incubated for 3 hours (Anes *et al.,* 2006), the infected cells should undergo thorough washing to wash away mycobacterium that failed to penetrate or be engulf by the macrophages. This would ensure the number of mycobacterium was a constant factor. Earlier, the quantification of EsxG.EsxH expression in 50 ml of 48 hours-*M. marinum* DsRed-infected-macrophages was determined to be 0.33 µM. Under confocal microscopy observation, the expression of EsxG.EsxH seen was more likely to be transient in occurrence and was supported through the findings mentioned by Tufariello *et al*., 2016; Tinaztepe *et al.,* 2016; Siegriest *et al.,* 2009. According to the authors, the iron-acquisition by EsxG.EsxH is important for mycobacterium to survive in host cells post-infection in which its production may not be required all the time. Tufariello *et al.,* (2016) also suggested that PE5.PPE4 worked synergistically with EsxG.EsxH in siderophore-mediated iron uptake. Elimination of EsxG or EsxH affects the secretion of PE5 (encoded within the locus) and PE15.PPE20 (encoded outside the locus) in which the latter has been associated with virulence functions rather than iron uptake. Either way, the two pairs of PE.PPE proteins require EsxG.EsxH to facilitate their

secretion making EsxG.EsxH important in both functions: as a metal scavenging mediator and possibly in virulence. In order to perceive a better understanding at protein expression level in infected host cells, other methods that could have been employed were quantitative real-time polymerase chain reaction (qRT-PCR) and Northern blotting. The information that would be gathered from isolating the mRNA transcripts of EsxG.EsxH genes could lead to a more accurate estimation of protein expression using DNA probes (Adamski *et al.,* 2014; Gao *et al*., 2011; Zheng *et al.,* 2006). Through the use of techniques mentioned, we would be able to determine EsxG.EsxH expression variation, if the protein complex was up-regulated or down-regulated in a normal growth medium and iron-deficiency medium.

The structural analysis of EsxG.EsxH complex by Ilghari *et al.,* (2011) revealed that there was a cleft on the surface of hydrophobic EsxG.EsxH complex. The author also suggested that it could be a binding site for protein-protein interaction. Following this finding, we were interested in determining the protein that would be responsible in the interaction. The first protein chosen was Mpm70 in which the co-localization experiment was initiated by labelling the primary anti-Mpm70 antibody with fluorophores. Several labelling methods and agents were performed to exclude unnecessary noise and mislabelling until finally we concluded the analysis using antibody labelled with quantum dot (QD) labelling. The major challenge for this part was the use of antibodies raised in the same host (rabbit) as there were high chances of false positive co-localisation if we used the conventional way of detection (primary and conjugated secondary antibodies applied to detect

both proteins at the same time). Through the used of QD565- and QD655-labelled anti-Mpm70 and anti-EsxG.EsxH antibodies respectively, we could conclude that there was no co-localisation found between the two proteins. However, there are other methods that could be used to screen for co-localisation between EsxG.EsxH with other potential proteins especially those secreted through the ESX secretion systems. Methods such as yeast-two-hybrid (Y2H) and microarray have been reported to be highly reliable could be employed to achieve the goal.

Future work

Due to lack of time to further explore issues regarding the association or co-localization between EsxG.EsxH complex with other secreted proteins of *M. tuberculosis* as their possible protein partner, the expansion for experiment for Chapter 5 pertaining to this objective can be done. In order to achieve this aim, the use of protein microarray could be employed. This experimental method has been widely performed and known to be powerful and versatile tool for the identification of enzyme activity, protein-protein and protein-nucleic acid interactions (Pandey and Mann, 2000; Emili and Cagney, 2000). We hope to observe EsxG.EsxH protein specifically bind to a range of different proteins or a specific protein, which can be identified in this manner, and in some instances to improve the effectiveness, protein microarray is coupled with mass spectrometric (Walter *et al.,* 2000).

From the experiments we have conducted, we know that EsxG.EsxH complex was not express in the phagosome but predominantly in the cytoplasmic compartment (Chapter 4). Although the frequency of the protein complex was noticed to be infrequent but increased with time due to increase in the number of mycobacteria following multiplication within the macrophages, this indicator might suggest the intermittent requirement of the protein complex during infection. Because of this reason, we want to explore the expression of the protein complex through live imaging of infected zebrafish embryo with *M. marinum*. The questions that we wanted to ask are: Is there possibility for

aggregation of macrophages i.e. production of granuloma? Does the protein complex participate in bacterial spread from cell to cell?

In addition to the above questions, we wanted to also discover the role of EsxG.EsxH complex by comparing between the wild type *M. marinum*, and EsxG.EsxH mutant *M. marinum*. The mycobacteria will then be inoculated in laboratory animal such as TLR4-deficient-mice and the progress of the disease will be followed. The reason of using this type of mice is to reduce, if not, to remove the chances of TLR4 activated by the presence of endotoxins, which in return affecting the data analysis. Lung from the mice can be taken for histopathology while blood samples can be used to determine a range of cytokines secreted by the host during the course of infection. From there, we hope to understand which pathway does the protein complex trigger to probably modulate the host immune system for survival. Similar method can also be employed using purified EsxG.EsxH or other purified protein complexes such as EsxA.EsxB and EsxO.EsxP rather than using live mycobacteria to achieve the same aim.

Appendix

A. Isolation and purification of Esx protein complexes

These experiments were conducted to collect the purified Esx protein complexes for anti-EsxG.EsxH polyclonal antibody production and determining the binding ability of Esx proteins namely EsxA.EsxB, EsxO.EsxP and EsxG.EsxH complexes to the cell surface of 16HBE. The results could be found in Chapter 2 of this thesis.

Methodology

a) Expression and purification of EsxA

The following experimental protocols for purification of EsxA and EsxB were repeated as described by Renshaw *et al.,* (2001).

Escherichia coli cells transformed with EsxA expression vector, pET21a were grown on Luria-Bertani (LB) agar (Melford) supplemented with 100 µg/ml ampicillin (AMP) and incubated at 37 ^{o}C overnight (Stuart Scientific Incubator SI 18). A few colonies were inoculated into LB broth (Melford) supplemented with 100 µg/ml AMP at 37 ^{o}C, 200 rpm in an orbital shaker (New Brunswick Scientific Excela E24 incubator shaker series) and left overnight to grow. The starter culture was then spun down at 5 000 rpm and the cell pellet was resuspended with supplemented LB broth and was transferred to another vessels containing 2 x 500 ml of LB broth with 100 µg/ml AMP and incubated at 37 ^{o}C, 200 rpm on an orbital shaker until the cell optical density reached between 0.6 and 0.8 when measured at A_{600} (WPA biowave CO8000 cell density meter). Next, the cells were induced with isopropyl-1-thio-B-D-galactoside (IPTG) [Sigma Aldrich] to a

final concentration of 0.45 mM. During pre-induction and post-induction steps, about 200 µl and 100 µl samples were taken from grown cultures respectively. The volume difference was mainly due to the normalization according to cell density and the samples were analyzed by SDS-PAGE to observe for protein production. After 4 hours of incubation, cell were harvested by centrifugation at 5 000 rpm for 20 minutes at 4 ^{o}C (Beckman JLA 8.1000 rotor, Beckman Coulter Avanti J-20XP centrifuge). The cell pellet can be kept at -20 ^{o}C or used directly for the next step. The harvested cell pellet was lysed in 50 ml Bugbuster HT protein extraction reagent (Novagen) with the addition of hen egg albumin lysozyme (Sigma) at concentration of 100 µg/ml and left incubated on a rocker for 20 minutes at room temperature. The cell pellet was collected by centrifugation at 12 000 rpm for 30 minutes at 4 ^{o}C (Beckman JA 25.50 rotor, Beckman Coulter Avanti J-30I centrifuge). The inclusion bodies were homogenized using 3 ml hand-held glass homogenizer in wash buffer made up of 50 mM Tris, 10 mM ethylenediaminetetraacetic acid (EDTA), 0.5 % Triton X-100 at pH 8.0 for 2 minutes and centrifuged at 12 000 rpm for 10 minutes at 4 ^{o}C. This process was repeated for at least three times or until the supernatant appeared clear. EsxA inclusion bodies was solubilized in resolubilization buffer containing 6 M Guanidine-Hydrochoride (Gdn-HCl), 1 mM EDTA, 100 µM 4-(2-Aminoethyl) benzenesulfonyl fluoride hydrochloride (AEBSF) [Sigma Aldrich] prior to refolding via dialysis twice against buffer comprising of 25 mM sodium phosphate, 100 mM NaCl, 1 mM EDTA PH6.5 initially for 4 hours followed by overnight dialysis at 4 ^{o}C. A 5 ml Q sepharose column was used to purify the protein on a Fast Performance Liquid Chromatography (FPLC) [AKTA] using a stepwise gradient of increasing NaCl concentration. Prior to usage, the Q-

sepharose column was equilibrated overnight with 25 mM sodium phosphate, 100 mM NaCl, 1 mM EDTA buffer pH 6.5. EsxA eluted at 150 mM NaCl while the purity of the protein was judge to be greater than 95 % pure by SDS-PAGE. The purification by stepwise gradient chromatography was conducted twice in order to collect only the purified protein product.

b) Expression and purification of EsxB M. tuberculosis protein

Escherichia coli BL21 (DE3) cells transformed with the EsxB-pET28a-based expression vector were grown in LB agar broth containing 40µg/ml kanamycin overnight. A few single colonies were taken and grew in 2 x 50 ml LB broth supplemented with 40 µg/ml kanamycin overnight at 37 ^{o}C on an orbital shaker. Cell pellets from these two cultures were collected through centrifugation at 5 000rpm. The cell pellet were then resuspended with about 5 ml of fresh sterilized LB broth and transferred to 2 x 500 ml of LB broth supplemented with 40 µg/ml kanamycin. The cells were allowed to grow until the OD reached between 0.6 and 0.8 at 600 nm before 0.45 mM of IPTG were added to each vessel. The cells were then left for 4 hours of incubation at 37 ^{o}C on orbital shaker and then harvested after the induction step. The cells can either be kept at -20 ^{o}C until used or directly processed as detailed below. The cell pellets were lysed with Bugbuster HT with 100 uM AEBSF was added following the lysis incubation period. The soluble fraction consisting EsxB was dialysed against 20 mM Tris and 1 mM EDTA buffer pH 8.0. The initial purification of the protein was carried out on a 5 ml Q sepharose column pre-equilibrated with the Tris/ EDTA buffer pH 8.0. The column was washed with a stepwise gradient of increasing NaCl concentrations and EsxB was eluted in the

75 mM NaCl wash. Fractions with EsxB were pooled and dialysed against 20mM piperazine and 1 mM EDTA buffer pH 5.8. The sample was then applied to a pre-equilibrated 5 ml Q-sepharose column with the piperazine/ EDTA buffer. Again, stepwise increasing NaCl column washes was applied to the column with EsxB eluting in the 50 mM NaCl wash and was judged to be greater than 95 % pure by SDS-PAGE.

c) EsxA.EsxB 1:1 complex

The concentrations of both purified proteins were estimated by spectrophotometry and were mixed to 1:1 ratio to form a stable complex. Both of the proteins and complex were kept in 20 mM sodium phosphate, 100 mM sodium chloride buffer pH6.5.

d) EsxO and EsxP of M. tuberculosis protein expression and purification

The following experimental protocols were reproduced from Al-Harbi's PhD thesis (2011) with slight changes in which the protein samples were kept cool at all time. The buffers used in purification steps were also kept cool in ice.

Escherichia coli cells transformed with EsxO and EsxP in pLeic05 and pLeic01 vector respectively were grown on LB agar containing 100 µg/ml AMP and incubated overnight at 37 ^{o}C (Al-Harbi S, PhD thesis 2010). A few single colonies were selected and grown in 2 x 50 ml LB broth supplemented with 100 µg/ml AMP for each cell and incubated at 37 ^{o}C overnight on an orbital shaker. The cells were then spun down for 20 minutes at 5 000 rpm and the cell pellets were collected. The cell pellets were first resuspended with about 5 ml of LB broth before transferred to 2 x 500 ml LB broth supplemented with 100 µg/ml

AMP for each cell. The cultures were grown at 37 ^{o}C until the OD measured at 600 nm between 0.6 and 0.8 before induced with 0.45 mM IPTG. The cell cultures were incubated for 4 hours at 37 ^{o}C on an orbital shaker. The cells were again spun down and the pellet were collected and either kept at -20 ^{o}C or process immediately. The pellets that were collected previously were subjected to inclusion body washes to extract the proteins as they were initially found to be insoluble. The presence and concentrations of each protein were estimated by SDS-PAGE. The cell pellets for EsxO and EsxP collected from the last inclusion bodies washes were mixed with resolubilization buffer containing 6 M guanidine HCl, 25 mM sodium phosphate separately. After the concentration of each protein were estimated, the proteins were made as a complex at 1:1 ratio complex and mixed on rocker at 4 ^{o}C for 20 minutes before dialysed overnight at 4 ^{o}C against buffer comprising of 25 mM sodium phosphate, 200 mM sodium chloride, 30 mM imidazole pH7.4. The protein complex was then subjected to purification on a 5 ml Ni^{2+}NTA column by affinity chromatography and was eluted by 25 mM sodium phosphate, 200 mM sodium chloride, 500 mM imidazole buffer pH7.4. Histidine-tag on EsxP would bind to Ni^{2+}NTA column used during the purification process in which later the histidine tag was removed by TEV protease through another affinity chromatography step. The protein complex, lacking of histidine-tag was finally purified on a 120 ml Superdex75 column by gel filtration and the purity was determined by SDS-PAGE gel and its concentration was measured by UV-visible spectrophotometry. The purified EsxO.EsxP complex was kept in 25 mM sodium phosphate, 150 mM sodium chloride buffer pH6.5.

e) EsxG and EsxH of M. tuberculosis protein expression and purification

The following experimental protocols were reproduced from Ilghari *et al.* (2011).

A loopful of glycerol stocks of *E. coli* cells transformed with EsxG and EsxH insert in pET23 and pLeic01 vector respectively, were streaked onto LB agar supplemented with 100 µg/ml AMP and were incubated at 37^{o}C overnight. The next day, 2-3 colonies of bacteria were taken and cultured into 2 x 50 ml LB broth supplemented with AMP antibiotic and left incubated at 37^{o}C overnight in an orbital shaker incubator. Each flask containing bacterial culture was transferred to a clean 50 ml falcon tube and the cells were spun down at speed of 5 000 rpm for 30 minutes. The supernatant was discarded while the pellet was resuspended with LB broth before all the resuspended material was poured into a 500 ml LB broth supplemented with 100 µg/ml AMP until the OD measured between 0.6 and 0.8 at absorbance 600 nm. Then, the cells were induced with 0.45 mM IPTG and continued with incubation for 4 hours at 37 ^{o}C. The cells were harvested by centrifugation and the pellets collected were subjected to cell lysis in 50 ml Bugbuster HT with the addition of 100 µg/ml lysozyme. The lysis was allowed to occur for 30 minutes at room temperature on a rocker. In order to extract the proteins as both proteins appeared to be insoluble from the SDS-PAGE gel observation of pre- and post-induction samples, inclusion body washes was conducted with 50 mM Tris, 10 mM EDTA, 0.5 % Triton X-100 buffer used as the wash buffer. The concentrations of proteins were estimated by SDS-PAGE gel and the proteins were made as a 1:1 complex before being purified on 5 ml Ni^{2+}NTA column by affinity chromatography. Prior to purification, in separate tubes, the collected cell pellets were solubilized using 25 ml of 6 M guanidine HCl, 1 mM EDTA, 100 µM AEBSF

and dialysed against 25 mM sodium phosphate, 200 mM sodium chloride, 30 mM imidazole buffer pH 7.4 overnight at 4 ^{o}C. During the purification process, the histidine tag on EsxP would bind to the column and the protein complex was eluted by gradient of 25 mM sodium phosphate, 200 mM sodium chloride, 500 mM imidazole buffer pH 7.4. The histidine-tag-protein complex fractions were pooled, then mixed with TEV protease and dialysed overnight in 25 mM sodium phosphate, 200 mM sodium chloride, and 30 mM imidazole buffer pH 7.4 to remove the histidine-tag. The protein solution was purified again on a 5 ml Ni^{2+}NTA column by affinity chromatography using the same base and elution buffers (25 mM sodium phosphate, 200 mM sodium chloride, 30 mM imidazole buffer pH 7.4 and 25 mM sodium phosphate, 200 mM sodium chloride, 500 mM imidazole buffer pH 7.4 respectively). The protein complex with the absence of histidine-tag was subjected to the final step of purification on a 120 ml Superdex75 column through gel filtration step and the purity was determined by SDS-PAGE. The protein complex was kept in the gel filtration buffer comprising of 25 mM sodium phosphate, 100 mM sodium chloride pH6.5.

f) EsxG and EsxH of M. marinum protein expression and purification

The experimental protocol was conducted following personal communication and unpublished findings by Dr. Lightbody.

E. coli BL21 (DE3) transformed with EsxG and EsxH in pLeic01 and pLeic05 vector respectively were grown on LB agar containing 100 µg/ml AMP and incubated overnight at 37 ^{o}C. The next day, 2-3 colonies of bacteria were taken and cultured into 2 x 50 ml LB broth supplemented with AMP antibiotic and left incubated at 37^{o}C overnight in an orbital shaker incubator. Each flask containing

bacterial culture was transferred into a clean 50 ml falcon tube and the cells were spun down at the speed of 5 000 rpm for 30 minutes. The supernatant was discarded while the pellet was resuspended with LB broth before all the resuspended material was poured into a 500 ml LB broth supplemented with 100 µg/ml AMP until the OD measured between 0.6 and 0.8 at absorbance 600 nm. Then, the cells were induced with 0.45 mM IPTG and continued with incubation for 4 hours at 37 ^{o}C. For inclusion body washes, first, both cell pellets were lysed using 50 ml Bugbugster HT, added with 100 µg/ml lysozyme and incubated at room temperature on a rocker for 30 minutes. Any remaining DNA in the lysates (observed as a very thick mucous-like solution) were digested using combination of 5 mM $MgCl_2$ and 1 mg/ml of bovine DNAse I (Sigma) and incubated at room temperature on a rocker for another 30 minutes. The cells were then spun down by centrifugation at a speed of 12 000 rpm at 4^{o}C for 30 minutes. Both cell pellets were washed at least three times with wash buffer comprised of 50 mM Tris, 10 mM EDTA and 0.5% triton X-100 pH 8.0. After each wash, the cells were centrifuged at 12 000 rpm at 4^{o}C for 10 minutes. After the last wash, the pellets were resuspended in resolubilisation buffer consisting of 6 M guanidine HCl, 1 mM EDTA and 100 µM AEBSF. The resuspended solutions were left in the cold room for 20 to 30 minutes to mix. In order to prepare them into a 1:1 complex mixture, SDS-PAGE gel electrophoresis was conducted to estimate the proteins concentrations. After that, the soluble protein complexes were dialysed in dialysis buffer made up of 25 mM sodium phosphate, 200 mM NaCl and 30 mM imidazole pH 7.4 twice initially for 4 hours and then was left overnight for dialysis at 4^{o}C. The protein complex was loaded into a 50 ml Superloop (GE Healthcare) for purification on an AKTA FPLC

system. The 6XHis-tagged EsxG.EsxH recombinant protein complex was purified using a 5 ml N Ni^{2+}NTA column (GE Healthcare). The purification was carried out using a base buffer of 25 mM sodium phosphate, 200 mM NaCl and 30 mM imidazole pH 7.4 with the elution buffer comprising of the same sodium phosphate and NaCl concentrations but with 500 mM imidazole pH7.4. To elute the bound protein, the elution buffer was applied to the column in a linear gradient manner. A constant flow flow-rate of 2 ml/min was set during the purification. The eluted proteins were analysed on NuPAGE SDS-PAGE gel. In order to remove the His tag, TEV protease cleaved was performed. The purified fractions containing the protein complex were pooled then mixed with 1 mM DTT and 7.5 U/ µl His tagged TEV protease (provided by Dr. Xiaowen Yang, University of Leicester) and dialysed into a buffer containing 25 mM sodium phosphate, 200 mM NaCl and 30 mM imidazole pH 7.4. The protein complex again were purified using pre-equilibrated 5 ml Ni^{2+}NTA column to separate the protein complex from His tag and the His tagged TEV protease. Fractions containing untagged EsxG.EsxH complex was collected and pooled after being determined by SDS-PAGE gel and finally purified from high and low molecular weight contaminants using a 120 ml Sephadex75 gel filtration column. The buffer used was 25 mM sodium phosphate, 100 mM NaCl pH 6.5 at a constant flow rate of 1 ml/ml. The protein concentration was measured at absorbance 280 nm.

B. Effects of Esx protein complexes on the integrity of human lung epithelial barrier

The evaluation of the effects and possible roles of Esx protein complexes on human lung epithelial barrier were made following the findings of EsxA.EsxB and EsxO.EsxP bound on the cell surfaces of 16HBE cell line while EsxG.EsxH did not. In addition, using 16HBE cell line as host model we also explore on how these protein complexes may influence the immune responses. We hypothesize that EsxA.EsxB protein could stimulate the transepithelial electrical resistance (TER) of the lung cells based on its properties as an antigen that is essential in tuberculosis pathogenesis as mentioned in numerous published articles (Renshaw *et al.* 2005; Hasan *et al.*, 2009; Xu, 2009). ESX1 cluster that encoded EsxA.EsxB proteins has been known to be involved in causing full virulence in tuberculosis infection by *M. tuberculosis* and we presumed that ESX5 cluster, which responsible to secrete EsxO.EsxP, also play similar role as the EsxA.EsxB protein. Being the latest ESX region identified phylogenetically, ESX5 has been associated to virulence in *M. marinum*, the fish pathogen (Abdallah *et al.*, 2009; Abdallah *et al.*, 2006) and was also thought to be responsible in cell death *M. tuberculosis* related pathogenesis (Abdallah *et al.*, 2011). To date, there was no information regarding this particular protein complex of ESX5 specific role. However, other secreted proteins from this cluster, the PE/PPE proteins have been well described. Therefore, we try to understand the role of not only the EsxA.EsxB complex but also EsxO.EsxP as well as the EsxG.EsxH complex when interact with human pulmonary cells and modulating the immune system or manipulating the epithelial cells after establishing an infection. In order to achieve the objectives, we first look at the

possibility of contact between the protein complexes and the cell surface of 16HBE, which is the human pulmonary cell line used as the study model. Then, we proceed with assessing the integrity of lung epithelial barrier and lastly, analyzing the cytokine released from the communication between the proteins and lung cells.

Methodology

a) 16HBE culture

Most of the experiments were performed using 16HBE cell line and prepared as detailed in **section 3.2.1 (a)** in this thesis. For the analysis of epithelium barrier function estimated by transepithelial electrical resistance (TER) expressed in ohm (Ω), the methods were conducted following protocol by Grainger et *al.,* (2006) with some modifications includes the type of cell used and its medium where 16HBE cell was seeded onto the Transwell filters (Corning) with a 0.4 µm pore diameter inserted on a 24-well plate (Corning). During cell growth, the medium (MEM) was changed every other day until the cells reached confluence, which was viewed under a light microscope. The confluence of 70% to 80% usually observed between 5 to 7 days post cultured with resistance measured greater than 150 $\Omega.cm^2$. The TER was measured with the use of an EVOM voltmeter and a STX2 electrode (World Precision Instruments).

b) Coating the Transwell filter with 16HBE cells

The culturing of 16HBE cell line protocol was conducted following method optimized by Dr. Emily Swindle group from the University of Southampton who

has been employing the cell line looking at the impact caused by allergens to lung tissue barrier. The transwell plate consists of two compartments: a 24-well plate and the twelve removable sterile filters in the middle of the plate. Firstly, the filter compartment was coated with 50 µl of 1:10 dilution of collagen I bovine (Life Technologies) and incubated for 30 minutes at 37 ^{o}C. This step is crucial as it is to allow adherence of 16HBE cells to the filter. After the incubation, the collagen was removed by pipetting and the plate was left to dry. About 500 µl of pre-warmed Minimum Essential Medium (MEM) liquid with Earle's Salts with stable glutamine (PAA, UK) supplemented with 10 % fetal bovine serum heat inactivated (PAA, UK) and 10 ml/L penicillin/streptomycin (Sigma Aldrich) was added to the basolateral (bottom) part of the plate fitted with filters. The antibiotic was added to prevent bacterial contamination. The plate was left incubated at 37 ^{o}C; 5 % CO_2 to warm. About 200 µl containing $7.5x10^5$ of 16HBE cells diluted with supplemented MEM was dispensed carefully onto the apical compartment of the filter. The plate was incubated in 37 ^{o}C; 5 % CO_2 incubator. Transepithelial Electrical Resistance (TER) was measured prior to media change on day 2 (D2) and day 5 (D5). Commonly, the cells are ready to be used between D5 and D7. Meanwhile, the empty top and bottom rows (without the filters) were filled with 1 ml of Hank's Balance Salt Solution with phenol red (HBSS) (Life Technologies), buffer that designed for cells maintained in non-CO2 ambient while phenol red function as an indicator if the pH in the cell environment changes from neutral to acidic (yellow) as described by the manufacturer referring to Hanks and Wallace publication in 1949. The colour changes could also indicate that the medium requires a replacement.

c) Coating the Transwell filter with HL204 primary cell

The steps for culturing the primary bronchial epithelial cell were made based on Xiao *et al.,* (2011) with modifications from Gray *et al.,* (1996). The primary human lung cell, HL204 has been maintained with 300 µl starvation medium at the basolateral layer and none on the apical layer. There was a thick mucous covering the surface of the cell. About 100 µl pre-warmed TER medium was aliquoted to each allocated well of 24-welll Transwell plate and left for 15 minutes at 37 ^{o}C; 5 % CO_2 incubator to acclimatize. TER was measured as mentioned previously. After that, the apical media was removed carefully using pastette. For primary cell, there was high production of thick mucus observed and created some degree of resistance during pipetting. About 300 µl pre-warmed starvation medium was dispensed to the basolateral well. The plate was then left incubated overnight at 37 ^{o}C, 5 % CO_2. Treatments were prepared accordingly in starvation medium as described below. The treatments composed of protein complexes at different concentrations: 1 µM, 0.1 µM, and 0.01 µM. About 100 µl of each treatment were dispensed to the apical part.

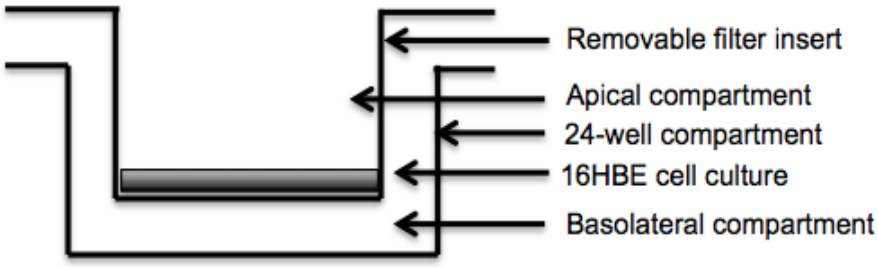

Figure B1: A schematic diagram showed 16HBE cell line cultured on transwell plate. The top (apical) compartment/ chamber was filled with the culture of lung epithelial cell line (16HBE). Both apical and bottom (basolateral) chamber were filled with MEM medium. Treatments containing Esx protein complexes in MEM medium were dispensed carefully and gently at the apical compartment.

d) Measurement of transepithelial electrical resistance (TER)

The protocol for this experiment has been well described by Grainger *et al*., (2006) with some amendments in terms of cell type used in addition to the treatments described below. Cells were treated with different protein samples (EsxA.EsxB; EsxG.EsxH and EsxO.EsxP complexes) at a dose-dependent manner; the medium and buffer controls were incubated at 37 ^{o}C for 3-, 6-, 24-hour. After 3 hours of incubation period, the apical treatment was pipetted out and kept in a sterile 1.5 ml microcentrifuge tubes (Eppendorf) and replaced with fresh media to reduce the effect of the buffer to the cells. The TER was measured with an epithelial volt ohmmeter (EVOM) with STX2 electrode at each time interval. For the HL204 cell, TER was measured at 0, 6 and 24-hour post exposure to the tested samples. The raw readings were deducted with 150; the background reading measured using the same probe. For the positive and

negative controls, polyinosinic:polycytidylic acid (poly I:C) and TNF-α were used in addition to medium and buffer for each protein complex for controls.

Table B1 showed stock concentrations of purified Esx protein complexes of *M. tuberculosis*. Dilutions were prepared from the working concentration of 1 μM diluted from the concentrated protein stock. All of the freeze-dried protein complex samples were first dissolved with sterilized distilled water and further diluted to appropriate concentration for the concentration-dependent experiment.

ESX protein complexes	**Concentrations (μ M)**	**Buffers (pH6.5)**
EsxA.EsxB	18.29	20 mM sodium phosphate/ 100 mM sodium chloride
EsxO.EsxP	14.7	25 mM sodium phosphate/ 150 mM sodium chloride
EsxG.EsxH	39.3	25 mM sodium phosphate/ 100 mM sodium chloride

e) The16HBE cells permeability after ESX proteins introduction determined by FITC-dextran

Following the assessment of TER, the investigation was continued with determining the integrity of the epithelial barrier after exposing the cells to the protein complexes. The passage of uncharged molecules across confluent cells on filter insert was measured with a fluorescein isothiocynate (FITC)-conjugates 4 kDa dextran (Sigma Aldrich). About 900 μl of basolateral experimental medium and 250 μl of apical 2 mg/ml FITC-dextran medium was applied to 16HBE cells and incubated for 3 hours at 37 ^{o}C. Triplicate basolateral medium samples were

collected and assayed on a 96-well Nunc plate (Fisher Scientific UK Ltd). A standard curve of FITC-dextran in medium (2 to 0.03125 mg/ml) was simultaneously run in duplicate. The fluorescence was measured on a fluorimeter at excitation and emission wavelengths of 485 nm and 530 nm, respectively using a Fluoroskan Ascent FL2.5 reader (Thermo Fisher, London, United Kingdom). The basolateral measurements were corrected for dilution factor by dividing the volume of the basolateral medium by the volume of the apical medium and multiplying the readings by this number.

f) Measurement of cytokine secretion by sandwich enzyme-linked immunosorbent assay (ELISA)

The media from the apical and basolateral components aspirated by pastette with care and supernatants were collected by centrifugation at 1 500 rpm for 10 min at 4 ^{o}C. The supernatants were then transferred to a fresh tube and stored at -80 ^{o}C until further use. Quantification of IL-8 secretion was assessed based on the manufacturer's protocol (Thermo Fisher Scientific). All conditions were measured in duplicate and the concentration of IL-8 excreted from the cells was estimated using the standard curve conducted simultaneously.

g) Determining the changes in TER of HL204 cell post-exposure to protein complexes

Measurement of TER for HL204 primary cells were conducted as described previously in **3.2.5.**

h) Cell count for HL204 after introduction to medium and protein complexes

The apical mediums collected at 6- and 24-hour were centrifuged at 3 000 rpm for 7 minutes. Supernatant were separated carefully from the cell pellet. About 25 µl of sterile PBS was added into each tube and cells were resuspended thoroughly. A volume of 10 µl was aspirated transfer to a haematocrit for cell counting. In addition, the overall observations were taken into account such as the shape of the cells and the presence of apoptotic cells or debris.

Results and Discussion

d) Changes in transepithelial electrical resistance (TER) post-exposure to ESX protein complexes on 16HBE cells

The ability of EsxA.EsxB and EsxO.EsxP complexes to bind to human pulmonary epithelial surface has been evidence and described previously in Chapter 3 in this thesis. The investigation was continued with evaluation of the barrier integrity of the treated polarized cell layer with Esx protein complexes, respectively through determining the changes occurred measured by TER and permeability test (Waters *et al.,* 1997; Kim *et al.,* 2005). The 16HBE cell line was used as the host model and the three Esx protein complexes in MEM medium mentioned previously were incubated with the host cells up to 24 hours. The

16HBE lung cells were grown on a sterilized filter where the growth of the cells were maintained with culture media on apical and basolateral surfaces to create a barrier function mimicking our natural state of pulmonary system. In order to investigate the changes in epithelial barrier, TER was measured at 0-, 3-, 6- and 24-hour post-treatment with Esx proteins. As for the controls include the medium, buffers, poly I:C and TNF-α were also applied to 16HBE.

Figure B2 showed the analysis for all the controls conducted in which revealed that the TER for all of the controls dropped consistently after 20 hours post-exposure to the treatments. No significant change (p>0.05) seen in cells exposed to TNF-α when comparing other controls to medium control. In addition, the permeability test using FITC-dextran as the determinant in host cells 20-hour-post-exposed to the respective treatments mentioned above, showed that cells treated with TNF-α was similar to the medium response. This showed that TNF-α did not cause any significant change to the integrity of 16HBE as compared to poly I:C tested at 2 different concentration. Relatively, the higher concentration of poly I:C, the higher the changes could be observed in the barrier integrity of 16HBE cell line as expected.

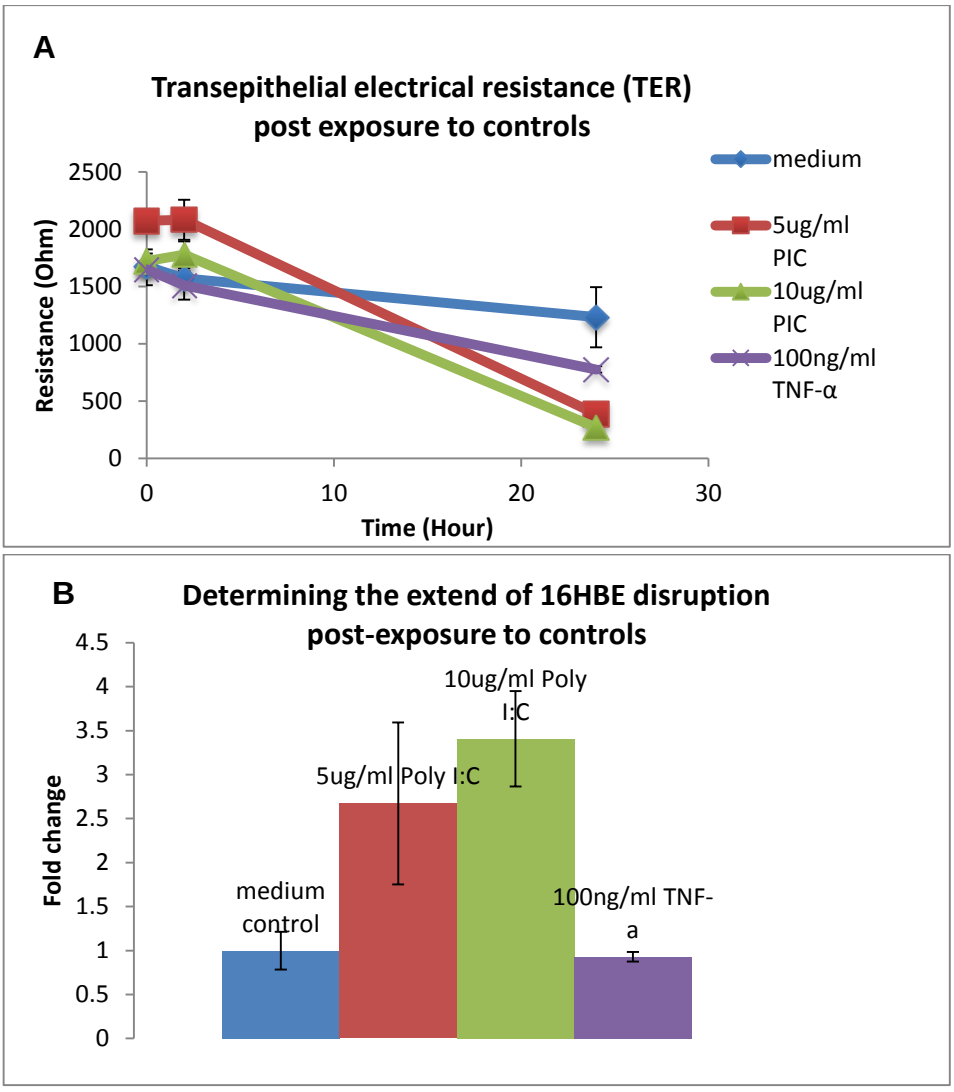

Figure B2 showed the responses of 16HBE post-exposure to control treatments, respectively exhibited in TER (A) and permeability analysis (B). All of the TER readings showed a dropped post 20-hour exposure to the treatments. As expected, the integrity of 16HBE barrier were disrupted significantly while TNF-α did not show any significant change when compared to medium control. This result validated the usage of 16HBE cell line to observe any changes in TER and barrier integrity when introduced to the protein treatments.

In comparison, the Esx protein complexes used as treatments, a transient dropped in TER were seen after 3 hours of treatment in all treated samples including the media and buffer controls (**Figure B3**). These findings could suggest an occurrence of disruption towards 16HBE cells either from the treatments or merely due to technical incompetency. Surprisingly, after 6 hours of incubation, the TER readings were seen to show an increased before becoming plateau afterwards. However, the decreased in TER readings from 6 hours onwards were insignificant and the pattern maintained within the mean baseline resistance of 16HBE cells, which was estimated to be around 2681 ± 280 ohm/cm^2 indicating that host cells could still able to sustain their physiologic barrier with tight intercellular junction and actively absorbed sodium for its physiologic function (Zhang *et al.,* 1997; Kim *et al.,* 1991). As observed before and explained in Chapter 3, there was absence of binding of EsxG.EsxH complex to the cell surface of 16HBE cells, however, there were changes to the TER observed. Instead of exhibiting similar observation as per medium control, the 16HBE cells treated with EsxG.EsxH complex showed a continuous dropped after 6 hours of exposure, which was identical to the other protein treatments observations (**Figure B3, Panel A)**. Meanwhile, the medium control showed a steady reduction in TER probably due to lack of nutrient supplied to the cells subsequently causing the cells to lose its viability. It was also observed that there were changes in all buffer controls used, therefore it was thought that the differences in TER estimated might be contributed by the buffers in which the proteins were stored rather than the protein effects (**Figure B3, Panel A-C**). The TER changes in cells treated with protein complexes were consistent with the

TER changes seen in cells treated with the respective buffers. However, among the three different buffers used, the closest trend of changes to the medium control was the EsxO.EsxP buffer, which composed of 25 mM sodium phosphate, 150 mM sodium chloride pH 6.5 probably contributed by the concentration of sodium chloride used was similar to physiologic. If this experiment required another attempt, it is highly recommended to investigate the responses using protein complexes stored in buffer with 150 mM sodium chloride and the dilutions were made using medium instead of distilled water to reduce the possibility of external factors influencing the final outcomes. Besides that, the time of sampling and measurement of TER could be taken earlier such as 30 minutes, 1- and 2-hour post-exposure to protein treatments. The duration of exposure versus the cell responses towards antigens may provide a different finding since our TER results showed recovery of TER after 6 hours of exposure in which we probably loss some important information at less than 6 hours of protein treatments.

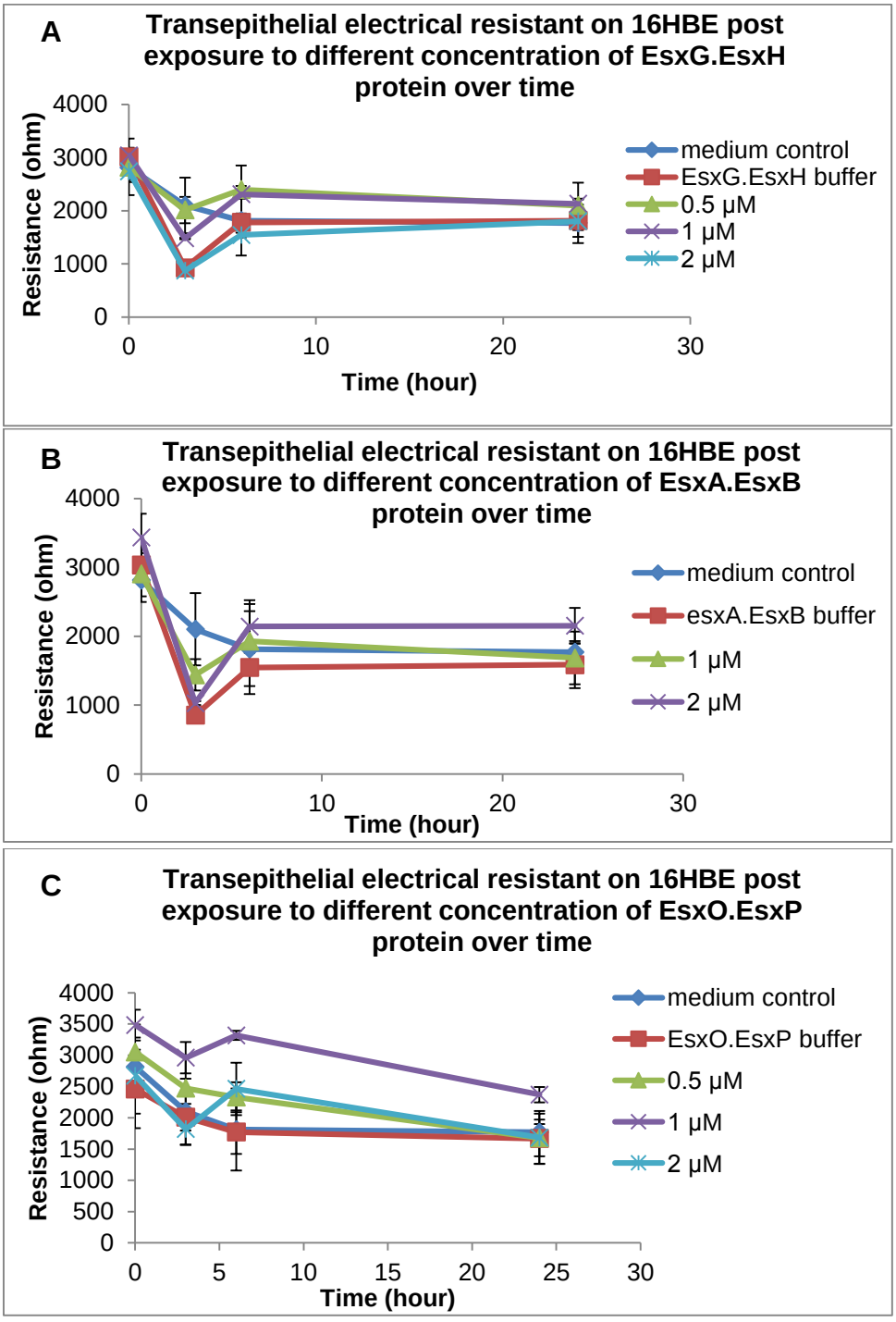

Figure B3 showed TER changes in 16HBE cells exposed to different concentrations of *M. tuberculosis* Esx protein complexes observed for 24 hours. All of the readings were measured at 0-, 3-, 6- and 24-hour post-introduction to treatments where the TER readings expressed in ohm, Ω. Panel A-C showed the cells responses exposed to EsxG.EsxH, EsxA.EsxB and EsxO.EsxP complex, respectively. A steep decreased was observed in the first 3 hours of introduction and continued to drop 6 hours onwards.

e) Assessment of epithelial barrier integrity

To further assess the integrity of 16HBE barrier, the cells were treated with FITC-conjugated 4 kDa dextran added at the apical layer. The influx of FITC-conjugated 4 kDa dextran into basolateral space was measured to determine the permeability of our treated 16HBE after 24 hours of introduction to ESX protein complexes. The permeability was analyzed by the dissipation of the reagent across the apical epithelial monolayers to the basal chamber using Fluoroskon Ascent FL2.5 reader (Rezaee *et al.*, 2011; Hardyman *et al.*, 2013). From the **Figure B4** below, as predicted, the control buffers used for each protein complex were seen to cause an effect to the integrity of 16HBE cells barrier. This result is highly association with the findings observed for TER analysis for all of the control buffers mentioned above. This could probably indicate the disruption to the host cell barrier caused by the buffers and the protein treatments. However, there was no difference in permeability of the cells after 24 hours exposure to the treatments when the treatments including the buffer controls were compared to medium control. It was intriguing to see that EsxG.EsxH at higher concentration (1- and 2- μM), the ability of 4 kDa FITC-dextran to permeate through the host cells were similar to observation made on medium control, which contradicted with TER analysis for the protein at both concentrations. The undisturbed tight junction could also suggest the absence of substances such as toxin; as seen in certain intestinal pathogens like *as C. difficile, Bacteroides fragilis,* and *enteropathogenic E. coli,* that capable of disrupting the tight junction (Sears, 2000).

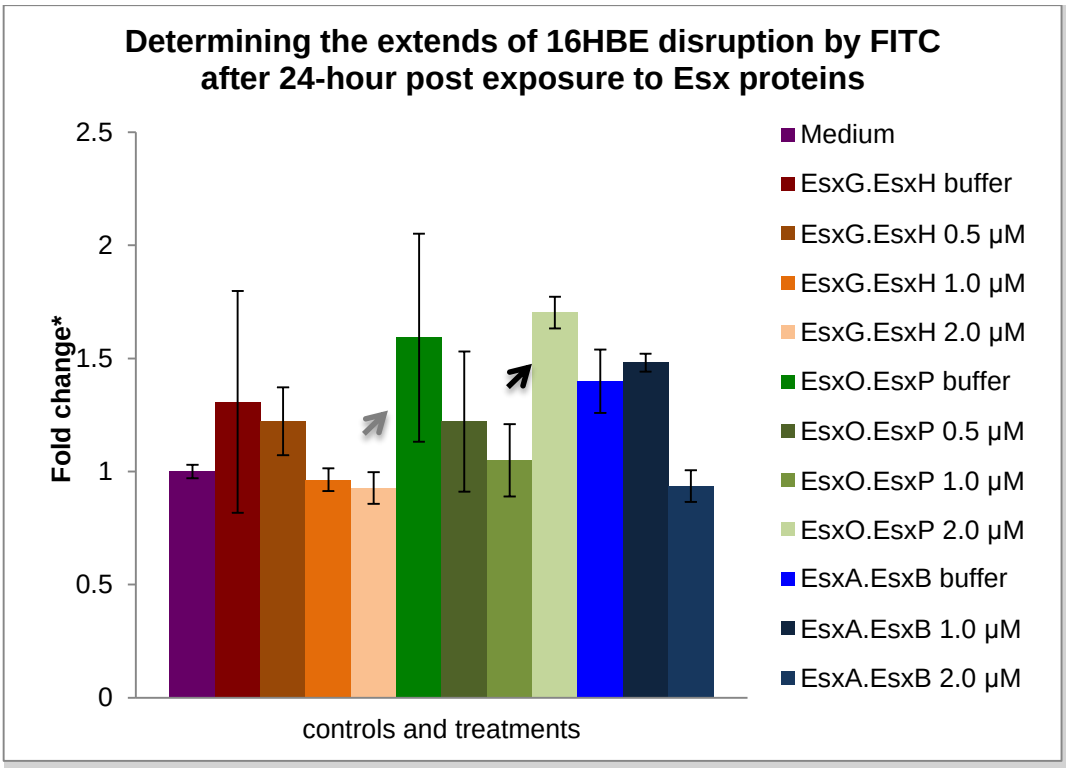

Figure B4 showed the effects of ESX protein complexes to the permeability of 16HBE cells expressed relative to medium control (purple bar). Analysis was made using basolateral medium of 16HBE cells collected post 24 hours of exposure to the respective tested samples. There was no significant difference in the disruptions of barrier integrity observed in all cells with various tested samples prepared at different concentrations. Although it may appeared that EsxO.EsxP at concentration of 2 µM and its buffer (black and gray arrows respectively) affecting the permeability of host cell, however, the differences may due to the buffer than the protein complex.

f) Secretion of IL-8 from 16HBE apical and basolateral medium post introduction to ESX proteins

For this experiment, the supernatants from basolateral and apical media were collected at 3- and 24-hour post-exposure to Esx protein complexes and medium and buffer controls. The supernatants were used to investigate the involvement of IL-8 in 16HBE cells after encountering the tested samples. To determine the presence of IL-8 at the basolateral and apical layer of 16HBE

culture plate, a commercially available sandwich ELISA detection kit was used. A recombinant human IL-8 and anti-IL-8 antibody were provided by the manufacturer (**ThermoFisher Scientific, UK**) and a standardized control was prepared to assist in identifying and estimating the concentration of IL-8 in the supernatant samples **as shown in Figure B5**.

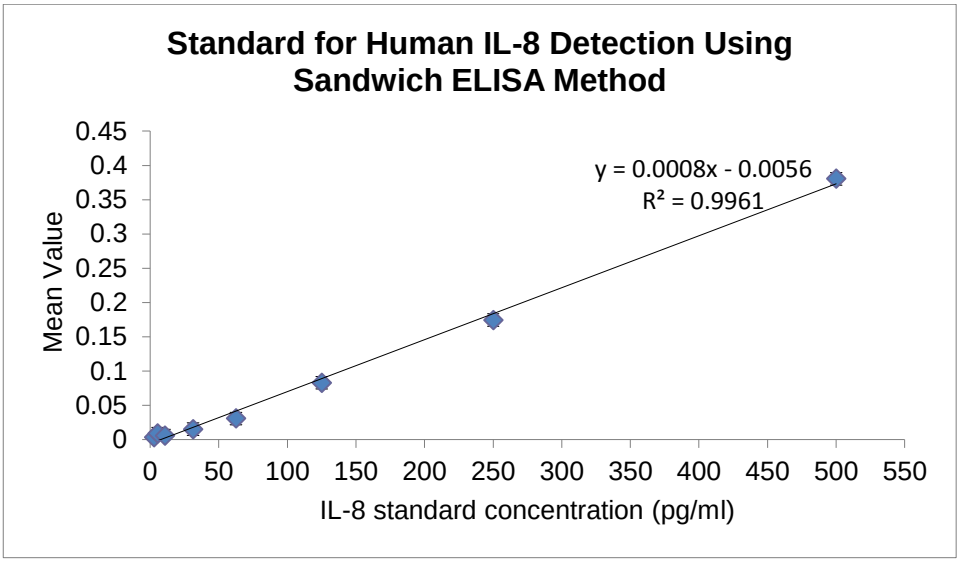

Figure B5 showed standard curve prepared to determine the presence of IL-8 using the Human IL-8 Sandwich ELISA detection kit. The standard curve composed of mean value of absorbance (A_{550}-A_{450}) for its Y-axis while the concentration for its X-axis. From this standard curve, the concentration of IL-8 for each treated samples 3- and 24-hour were determined. The findings for apical and basolateral were displayed in the graphs described below.

Interleukin 8 (IL-8), a chemokine or chemotactic factors is produced by various kind of cells including macrophages, epithelial cells, respiratory smooth muscles and endothelial muscles (Browning *et al.,* 2000; Govindaraju *et al.,* 2008; Fernando *et al.,* 2011) after encountering with antigen(s). During persistent colonization by pathogenic bacteria, alveolar macrophages will be repeatedly activated especially in cystic fibrosis patients. As a result, lung epithelial cells responded by releasing various inflammatory mediators. In this

experiment, the initiation and amplification of innate and inflammatory responses to vast insults could be contributed by the first interface, which is the lung epithelium (Cheng *et al.*, 2007; Martin *et al.*, 1997; Stadnyk 1994). Our findings revealed that at 24 hours post-exposure to tested samples, the amount of IL-8 secreted in cells treated with EsxA.EsxB, EsxO.EsxP and EsxG.EsxH protein complexes were approximately between 900 to 1200 pg/ml in basolateral supernatants (**Figure B6 Panel A**) while in apical supernatants, IL-8 concentration detected were approximately 400 to 500 pg/ml. This chemokine production was consistent to a number of studies conducted previously by employing purified proteins such as ESAT-6 and ESAT-6-like proteins (Boggaram *et al.*, 2013) as well as live avirulent, H37Ra and virulent mycobacteria, H37Rv (Lin *et al.*, 1998; Wickremasinghe *et al.*, 1999) using A564 pulmonary cell line as host model. In these studies, the researchers found out that the concentration of IL-8 produced by the host cells were stabled after 24 hour of exposure to pathogens and/ or their secreted proteins. The concentration of IL-8 between pre-treatment and 24 hours however, did not appear to have a significant different. For medium and buffer controls, it was observed that the level of IL-8 slightly dropped while the cells exposed to studied proteins showed an insignificant increased.

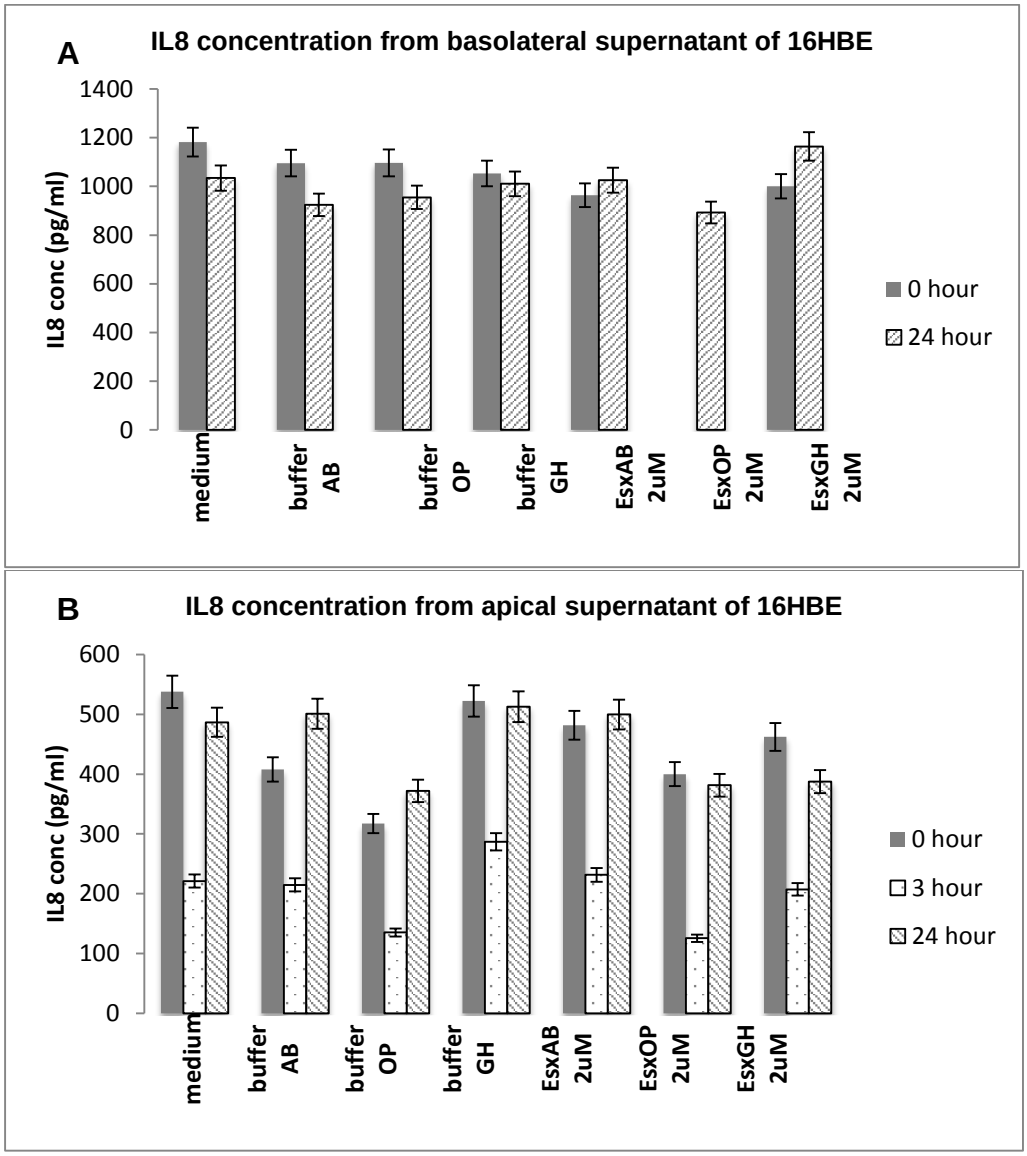

Figure B6 showed the production of IL-8 by 16HBE exposed to Esx protein complexes. 50 µl of basolateral samples were tested for the presence of IL-8 using the IL-8 detection kit. **Panel A** showed the concentration of IL-8 estimated and based on the standard curve**.** There was no significant difference of IL-8 production detected in the basolateral compartment at pre-treatment and 24-hour post treatment. To analyze the differences in IL-8 released at the basolateral and apical compartments, **Panel B** showed the amount of IL-8 present in the apical supernatant, expressed in pg/ml. the concentrations of IL-8 were lower than those detected in basolateral supernatants. A drastic drop in IL-8 was seen at 3-hour post-exposure to tested samples but increased or recovered close to pre-treatment values at 24-hours. Standard deviation used as error bar.

As suggested by Lin, Y. *et al.* (1998) based on reports by Kurashima, K., *et al.* (1997); Zhang, Y. *et al*. (1995) and Antony, V.B. *et al.* (1993), it appeared that the production of this chemokine depends on anatomic sites in which Kurashima *et al.* and Zhang *et al.*, found that patients with pulmonary tuberculosis showed high IL-8 concentration in bronchoalveolar lavage fluid (BAL) while patients with tuberculous pleuritis did not show an elevated concentration of IL-8 (Antony *et al.,* 1993), which means that there is possibility to see an effect of IL-8 production depending on the type of cells used in a study. Without the addition of sample treatments where only media were added to the 16HBE cells grown on transwell system, the concentration of IL-8 at 0-hour could be detected (Fan *et al.,* 2014; Eckmann *et al.,* 1993) to be at least 1000 pg/ml from basolateral supernatants and 450 pg/ml in apical supernatants. The report by Wickremasinghe *et al.* (1999) also discussed on the effect of culture media used to grow mycobacteria-infected monocytes towards the production of IL-8, although an extra purification measures has been conducted via gel filtration and multiple dialysis and finally followed by determining lipopolysaccharide (LPS) (Dempsey *et al.,* 2007) using limulus amebocyte assay (Wang *et al.,* 2009; Wang *et al.,* 2012). Hence, it is important to compare the changes in IL-8 concentration level between treatments and medium control. In addition, it also proven that 16HBE cell line able to secrete IL-8 as described by many researchers, previously (Lindén, 1996; Massion *et al.,* 1995). Of note, all of the media at 0-hour were collected and replaced with fresh media with or without buffers and protein treatments from both compartments.

A study by Linden *et al.,* (1999) has demonstrated that β-adrenoceptor activations modulates the release of IL8 in 16HBE cells that caused by TNF-α, the pro-inflammatory cytokine. The increase in the level of concentration of IL-8 seen in our experiment probably correlated with the introduction of treatments to the host epithelial, as described by Kurashima *et al.* (1997) and Zhang *et al.* (1995), which leads to the activation of β-adrenoceptor that causes the secretion of TNF-α that results in the release of IL8. It was also observed that more IL-8 twas recovered from basolateral compartment than from the apical space that is polarized on the transwell microporous membrane could indicate that IL-8 was preferentially secreted by basolateral surface [Eckmann *et al.,* (1993)]. According to Levine (1995); Kwon *et al.*, (1995); Cromwell *et al.*, (1992); Coulter (2000), the chemokines released act as the second messengers that convey signal for the recruitment of inflammatory cells to the infection site subsequently, in response to inflammatory cytokines, the principal chemokines, IL-8 and IL-1β were released by the lung epithelial cells. Mukaida (2003) also reported that IL-8 plays a potent role in pathogenesis of either acute or chronic lung diseases. An increasing concentration of IL-8 on apical surface was seen at 24-hour when compared to 3-hour post-exposure to treatments but, when they were compared to medium control, the 24-hour analysis did not show any significant changes in the amount of secreted IL-8. Apparently, the production of IL-8 showed an insignificant increased after 24 hours exposed to treatment samples as the TER readings showed recovery from 6 hours post-exposure onwards. The analysis for permeability of 16HBE cells using FITC-dextran as the detection agent also showed no significant different in all tested samples and controls determined at 24 hours which further supports the findings observed in this experiment.

g) Changes in TER post-exposure to ESX proteins in HL204 human primary lung cells

The effects of Esx protein complexes on primary cells, HL204 were investigated and all of the experimental protocols were identical and repeated as described previously for 16HBE cells experiments. However, the concentrations of tested treatments used in this experiment were lower than those employed for 16HBE. The findings showed below were the results from the preliminary investigation. When determining the transepithelial electrical resistant (TER) for HL204 after applying the purified Esx protein complexes, surprisingly, the TER readings taken from cells exposed to tested samples were all improved over the studied times (**Figure B7, Panel A and Panel B**). More interestingly, they were about 2 times higher than their pre-treatment (0-hour) measurements. This observation was also true for medium control except after 24 hours, where the TER reading appeared to be decreased. An interesting feature was observed on HL204 where there was a thick mucus layer noticed covering the top of the cell and as a result, it was difficult to sample the apical medium. This finding was comprehensively different from observation made on 16HBE. Since the human airways possessed innate and adaptive immune responses, the mechanism of defense could also include the production of mucous, which could contribute to host resistance to *M. tuberculosis* infection (Harriff *et al.,* 2014) as we observed in this experiment.

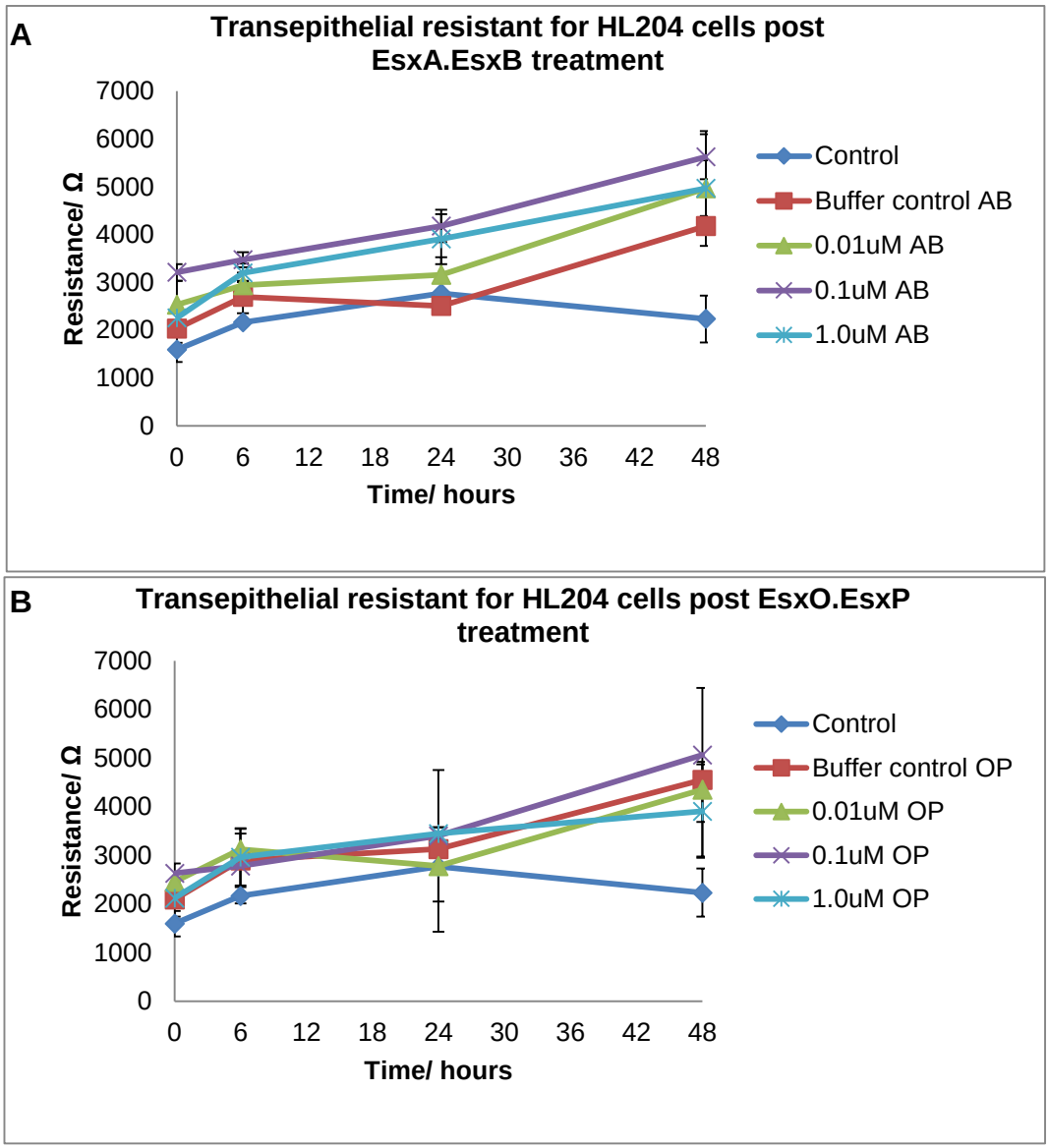

Figure B7 showed changes in TER of HL204 after exposed to ESX protein complexes time-concentration dependent manner. The response of HL204 towards the exposure to EsxA.EsxB (**Panel A**) and EsxO.EsxP (**Panel B**) were different from observation made in 16HBE cells. The TER readings for all treatments seemed to increase post introduction of treatments and the readings were higher than the initial measurements. This is also true regardless of the different concentrations imposed to the cells. Meanwhile, the TER for medium control (control) dropped gradually after 6 hours incubation.

h) Detection of cells from collected HL204 apical medium

According to a number of studies, the infection caused by *M. tuberculosis* commonly leads to necrosis than apoptosis (Abdallah *et al., 2007).* There were a mixture of necrotic and apoptotic cells observed under light microscopy. An increase trend of cell counted for cells treated with EsxA.EsxB and EsxO.EsxP complexes were seen as showed below. The pattern was seen as a dose-dependent and increased with time of exposure **(Figure B8)**.

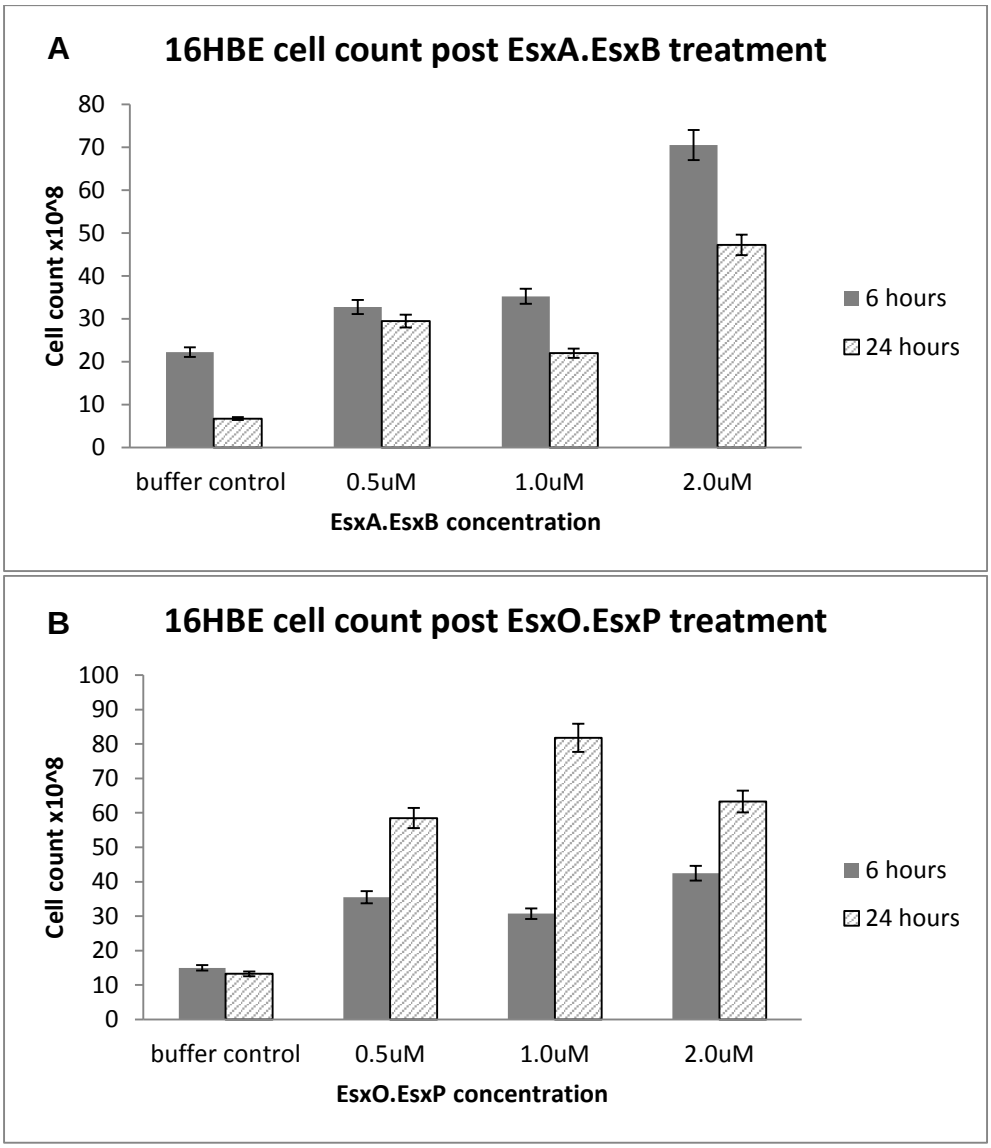

Figure B8 showed the disruption to HL204 primary cells at 6- and 24-hour post-exposure to EsxA.EsxB and EsxO.EsxP proteins. In Panel A, there was an increased in cells counted from apical medium in dose-dependent and with time. As for cells treated with EsxO.EsxP protein, we believed the similar pattern could be seen however, due to technical inefficiency during pipetting the thick apical medium, some cells might be disrupted and caused an increased in cell count for buffer control and cell with 0.01 μM.

In accordance to the promising results shown by the binding of the protein complexes to 16HBE cell surface, the possible effect on 16HBE epithelial was explored through the analysis of integrity of the lung epithelial barrier. The first part of the analysis involved the measurement of transepithelial electrical resistant (TER), which provides a general picture of the status of the epithelial barrier. Despite the presence of interactions between EsxA.EsxB and EsxO.EsxP with the cell surface of 16HBE cells observed, there was no evidence found to show an effect of Esx family protein complexes to the integrity of lung epithelial barriers, which argues against a pore forming cell lysis activity for Esx protein complexes. In addition, consistent with the report by Antony *et al.,* 1993, IL-8 cytokine was also not significantly detected post-exposure to the protein complexes. This could suggest two possibilities either the type of cells did not responded well with the tested protein samples or it was true negative observed in which the protein complexes did not involve in elevating IL-8 release that commonly secreted in response to inflammation in lung diseases. In Chapter 3, we also attempted to learn whether ESX protein complexes, EsxA.EsxB and EsxO.EsxP participate in modulating the immune responses on lung epithelial, primary cells, HL204 were also employed. Similar to experimental procedures conducted using 16HBE cell line, a distinctive feature found was for all of the cells where the cells produced very viscous mucous that made sampling almost impossible. This is because there was high chance of extracting the cells on the transwell filter that may lead to false TER readings and evaluation of barrier integrity due to the interrupted cells. Or, there is also probability that the apical medium was sampled less and leads to loss of the overall picture of details aimed for. Hence, the implementation of primary lung

cells was stopped after this trial experiment to avoid any false positive or false negative to the outcomes. Nevertheless, the apical mediums collected were centrifuged and the sediments were kept for cell count. After 24 hours of exposure to protein complexes, a mixture of necrotic and apoptotic cells was observed using light microscope. However, there was no specific trend or association seen between protein concentrations and cell counted. This result may not reflect the actual condition due to the possibilities mentioned before. Nevertheless, the results could be enhanced and supported with appropriate controls included throughout the experiments.

C. Trial experiments to determine the co-localisation of EsxG.EsxH and Mpm70

Methodology

a) Conjugating anti-Mpm70 and anti-EsxG.EsxH polyclonal primary antibodies with APEX AF647 antibody labelling kit

The antibody labeling kit consists of an APEX antibody-labeling tip that contains resin at the bottom of the tip. A gentle tap to settle all the resin was applied followed by hydrating the resin with 100 µl of wash buffer provided together in the kit, using a pipette. The Apex antibody-labeling tip was then applied directly to the pipette and the wash buffer was pushed gently into a clean microcentrifuge tube without disturbing the resin bed. The hydrated resin bed volume is about 10 to 15 µl. About 10 µl of 10 µg (1 µg / µl) IgG antibody solution (anti-Mpm70/EsxG.EsxH antibody) was applied to the top of the resin using the elution syringe provided in the kit. The antibody was pushed onto the column and a drop may elute from the tip and this eluent was discarded. A

reactive dye consisting of 2 µl of DMSO and 18 µl of labeling buffer (given together in the kit) was applied to the resin and the solution was pushed carefully. A small amount of dye may elute and this eluent was also discarded as waste. The tip was then left for 2 hours incubation at room temperature or 4 ^{o}C if left overnight. After incubation, the APEX tip was washed twice with 50 µl each with wash buffer by pushing the buffer through the tip into a microcentrifuge tube. In a clean microcentrifuge, 10 µl of neutralization buffer (provided in the kit) was added. The APEX tip was positioned on the microcentrifuge tube containing neutralization buffer and 40 µl of elution buffer (given in the kit) was added to the top of the resin. The labeled antibody was eluted using microcentrifuge pipette into the neutralization buffer and mixed properly. The manufacturer recommended that the buffer to elution buffer should be kept at 1:4 to ensure the correct pH. The covalently labeled antibody solution was dialysed with PBS then aliquoted and kept at -20 ^{o}C until further used. The final concentration of the antibody was estimated about 0.15 µg / µl.

b) Slide preparation with AF647-labelled anti-Mpm70 polyclonal antibody

The J774A.1 murine macrophages were infected at 1x10^{5} cells/ml with *M. marinum* DsRed at MOI of 0.5 as described previously in Chapter 3. The coverslips, on which the macrophages were adhered to, were transferred to a Nunc 8-well plate (Thermo Scientific) where the coverslips were subjected to fixation, permeabilisation, blocking and staining with appropriate fluorescent dye. The coverslips were washed with 1 ml sterile PBS pH 7.4 after each step. The slides were first fixed using 4 % paraformaldehyde (PFA) [Sigma Aldrich] for 10 minutes at room temperature. Next, the slides were treated with cold 0.2 %

Triton X-100 for 5 minutes to disrupt the membrane cells in order for the antibodies and fluorophores to act on the specific proteins. Before addition of antibodies, the slides were blocked with 5 % BSA for an hour at room temperature to prevent any possible non-specific binding. Rabbit polyclonal anti-EsxG.EsxH antibody (2962) was added at 1:100 dilution while the AF647-labeled-anti-Mpm70 antibody was also added at 1:500 in 1 % BSA to the slides and left for incubation overnight at 4 ^{o}C. After overnight incubation, donkey anti-rabbit IgG H&L which was conjugated with Alexafluor 488 (Life Technologies) was added at 1:100 dilution in 1 % BSA and then left at room temperature for an hour. This would enable us to detect the presence of EsxG.EsxH as the secondary antibody would bind to anti-EsxG.EsxH primary antibody. The cells were counterstained and mounted with ProLong® Gold Antifade Mountant (Life Technologies) directly labeled with DAPI and the slides were allowed to rest between 24 hours and even up to 6 days at room temperature in the dark before imaging. By incubating the slides over a period of time at room temperature, it may improve the refractive index and also resulted in reduction of photobleaching occurrence.

c) Slide preparation withAF647- labelled anti-EsxG.EsxH polyclonal antibody

The protocol used in preparing the slides was the same as described above **(Section B page 190)** with some amendments where the usage of the antibodies involved. The primary antibodies used for this experiment after blocking with 5 % BSA step was unconjugated anti-Mpm70 polyclonal antibody was added at 1:500 dilution and the AF647-labelled-anti-EsxG.EsxH antibody was added at 1:100 diluted in 1 % BSA and incubated overnight at 4 ^{o}C. After

overnight incubation, donkey anti-rabbit IgG H&L which was conjugated with Alexafluor 488 (Life Technologies) was added 1:1000 dilution in 1 % BSA and left at room temperature for an hour. This would enable us to detect the presence of Mpm70 through the binding of secondary antibody to specific receptor of anti-Mpm70 primary antibody. The cells were counterstained and mounted with ProLong® Gold Antifade Mountant (Life Technologies) directly labeled with DAPI and the slides were allowed to rest between 24 hours and even up to 6 days at room temperature in the dark before imaging.

d) Conjugating anti-Mpm70 polyclonal antibody with Alexafluor 647 Succinimidyl Esters (NHS esters) using conventional method

The purified anti-Mpm70 antibody at concentration of 2 mg/ml was dialysed overnight against 500 ml fluorescence buffer composed of 25 mM sodium phosphate/ 100 mM sodium chloride; pH 7.5. The antibody was then mixed thoroughly with 25 µl mixture of 1mg of AF647 fluorophore powder diluted in 50 µl of dimethylsulfoxide (DMSO), and was left on the rocker overnight at 4 ^{o}C. The antibody labeled with AF647 solution was further dialysed against 2 L of fluorescence buffer to remove any excess dye. Absorbance was measured at A_{280} and A_{651} to estimate the final protein concentration and the degree of labeling (DOL). The conjugated antibody was kept at -20 ^{o}C and viable up to 3 months post labeling, as suggested by the manufacturer (Thermofisher). The DOL was expressed as mole dye per mole protein and was estimated using the below formula provided by the manufacturer:

$$(A_{651} \times \text{dilution factor}) / (\varepsilon_{647} \times M_{antibody})$$

Based on the manufacturer's recommendation, a good degree of labeling reading should be between 2 and 6 mole dye per mole protein.

e) Slide preparation

The slides of infected J774A.1 murine macrophages with *M. marinum* at MOI of 0.5 were conducted as described in **Section (c)** in this chapter.

Results and Discussion

c) Infected J774.1 macrophages with the presence of Mpm70 and EsxG.EsxH using AF647 labelled-anti-Mpm70 antibody

The anti-Mpm70 antibody was labelled with AF647 using a commercially available APEX AF647 antibody labelling kit from ThermoFisher, UK. The degree of labelling however, could not be determined but the experiment was still continued in which the presence of Mpm70 was observed in positive control set while there was no signal seen in the negative control set. The final concentration of the labelled antibody was made merely by estimation.

In the **Figure C1**, Panel A (I, II and III) showed green signals indicating the presence of EsxG.EsxH complex in three different infection levels (high, medium and low respectively) by *M. marinum* in J774.1 macrophage cell. The EsxG.EsxH complex was detected through the used of anti-rabbit secondary antibody conjugated with AF488 binding to anti-EsxG.EsxH primary antibody. Meanwhile, in Panel B (I, II, and III), the assigned yellow signals were detected from the AF647-labelled anti-Mpm70 antibody. These signals were not strong enough to confirm the co-localization of Mpm70 with EsxG.EsxH complex.

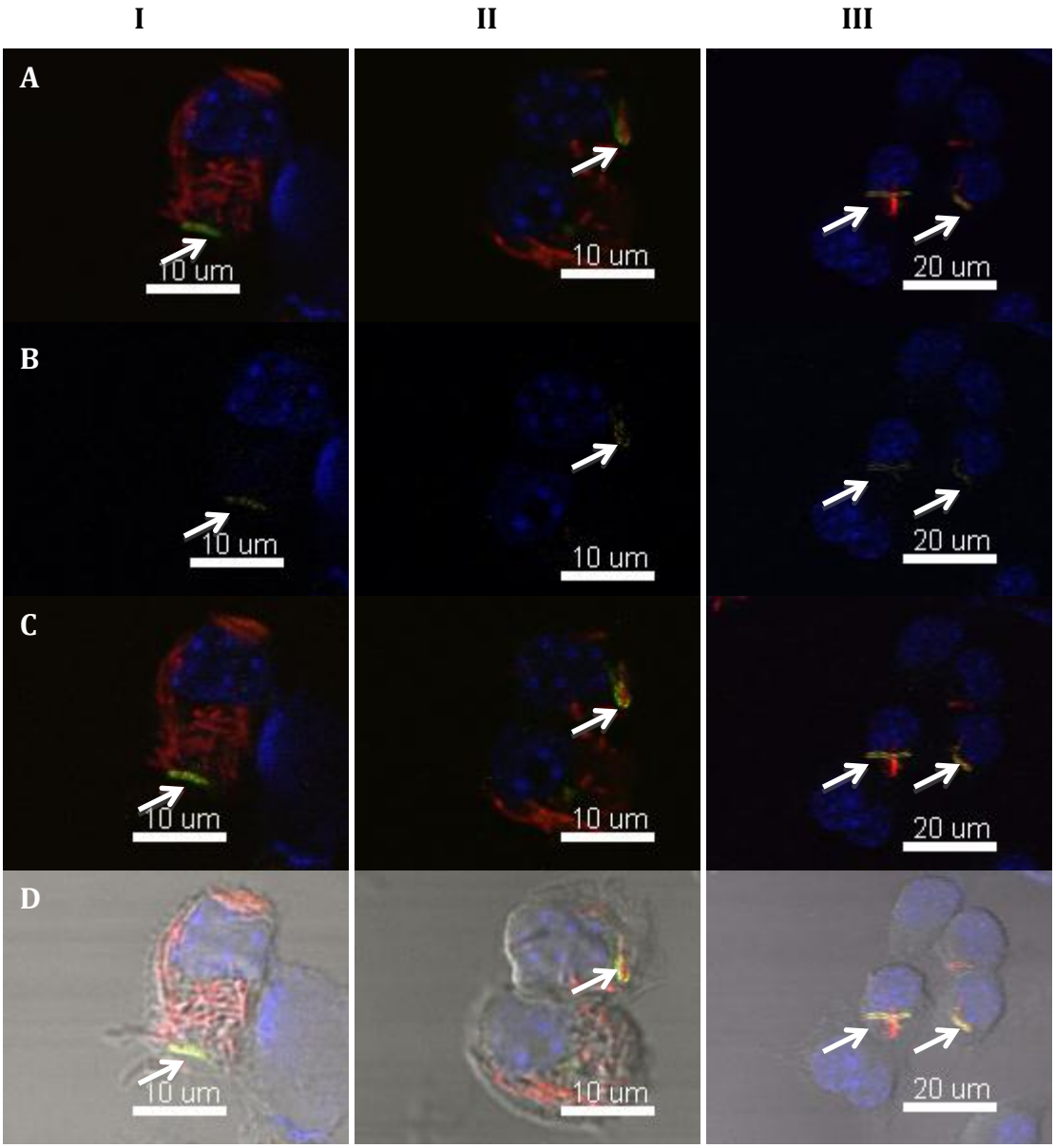

Figure C1 showed co-localisation between EsxG.EsxH *M. marinum* and Mpm70 using anti-Mpm70 antibody labeled with AF647. Panel A with green signals indicating the presence of EsxG.EsxH complex in the *M. marinum* DsRed-infected J774.1 macrophages. EsxG.EsxH was detected by the use of anti-rabbit secondary antibody conjugated with AF488 that bound to anti-EsxG.EsxH antibody. Panel B showed the assigned yellow signal for AF647-labelled-anti-Mpm70 antibody. The signals were not strong to clearly show the association between the two proteins. Panel C are images from merge channels for blue channel (DAPI for nucleus staining), the red channel for *M. marinum* DsRed, green for AF488 and far-red for the labeled-antibody. Panel D also showed merge channel images on a bright field-view.

d) Infected J774.1 macrophages with the presence of Mpm70 and EsxG.EsxH using AF647-conjugated-anti-EsxG.EsxH antibody

Another microscopy analysis was also conducted using AF647-labelled-anti-EsxG.EsxH and anti-Mpm70 primary antibody and anti-rabbit secondary antibody conjugated with AF488 to detect the co-localisation of EsxG.EsxH and Mpm70. In comparison our previous microscopic observation described above (page 179)**,** here, the backgrounds from green signal were prominent within the cytoplasm of macrophages, which deter the detection of Mpm70 though the methods conducted for both experiments were kept the same. The assigned yellow signals indicating the presence of EsxG.EsxH were seen consistently with the presence of Mpm70 protein at most instances. Due to the presence of high backgrounds, another labeling technique was conducted, which was elaborately described above.

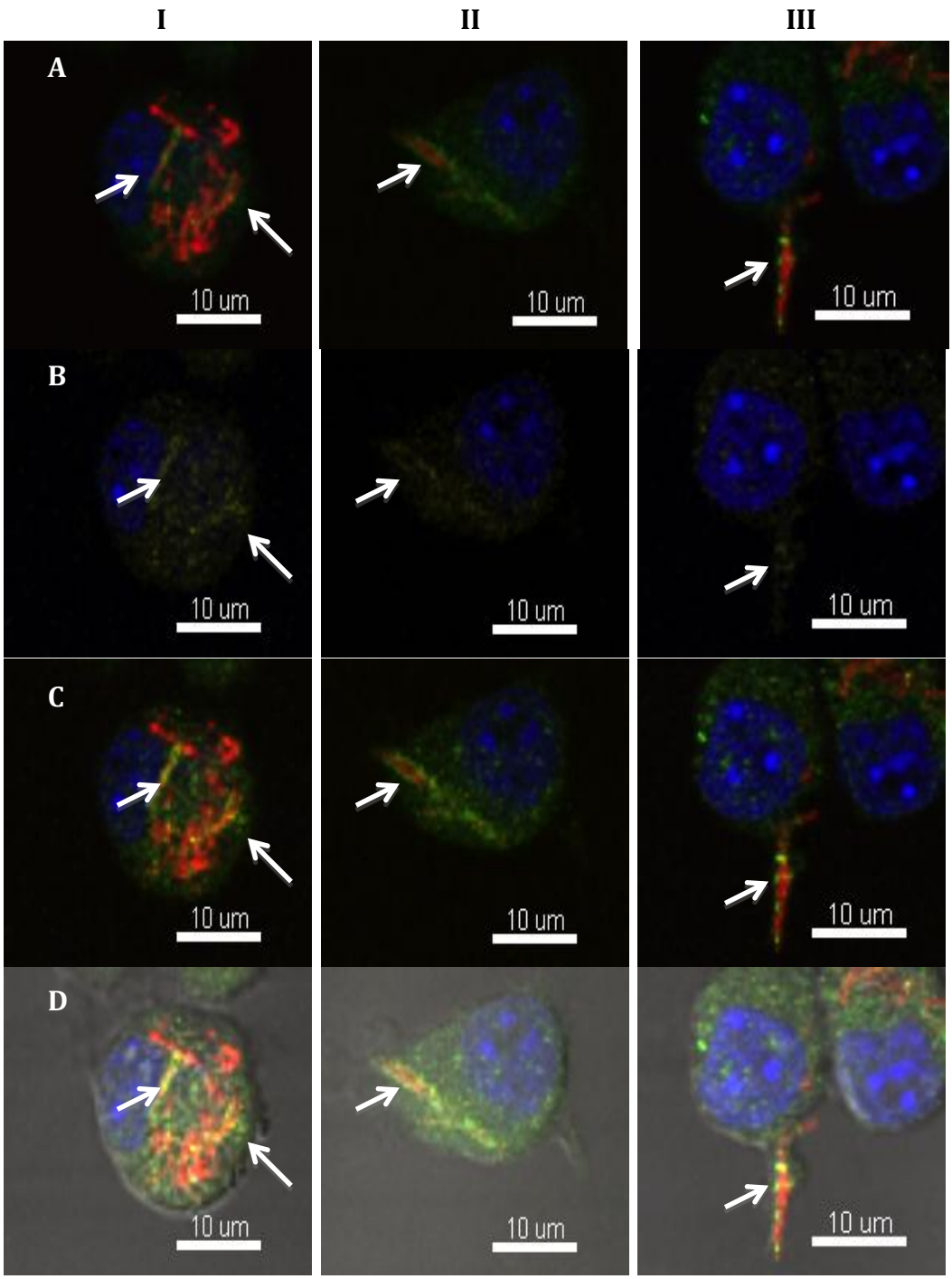

Figure C2 showed co-localisation of EsxG.EsxH with Mpm70 using AF647-labelled-anti-EsxG.EsxH. The nuclei of J774.1 macrophages was stained with DAPI (blue), *M. marinum* DsRed (red), Mpm70 (green) and EsxG.EsxH (yellow) respectively. Column I, II and III were selected to show the association between the proteins. There was also an evidence of ejectosome (Column III, arrow), an actin-based structure mentioned by Hagedorn *et al*. The presence of Mpm70 (A) and EsxG.EsxH (B) were best seen in merged channels in C and D.

e) Pilot experiment primary antibody labelling with AF647 fluorophore using conventional approach

As we could see in Column I and II for Panel A to D in **Figure C3**, there were signals produced indicative of association or co-localization between EsxG.EsxH (green) and Mpm70 proteins (yellow) regardless the level of of infection in J774.1 macrophages. Note that for Column I and II, the signals for both proteins were highly associated with each other except for one labelled with the orange arrow, significant characteristic of a “footprint” for Mpm70 protein.

However, for Part I and II of the microscopy results using a directly Alexafluor-labelled primary antibody to detect one protein and AF488-conjugated secondary anti-rabbit antibody to detect the second protein possessed a risk of overlapping in protein detection. This could be due to the origin of anti-EsxG.EsxH and anti-Mpm70 primary antibodies, which were both raised in rabbits that led to recognition of both antibodies, hence resulted in the apparent co-localization seen in the experiments, therefore we opted for an alternative method of implementing quantum dots-antibody labelling to overcome this issue.

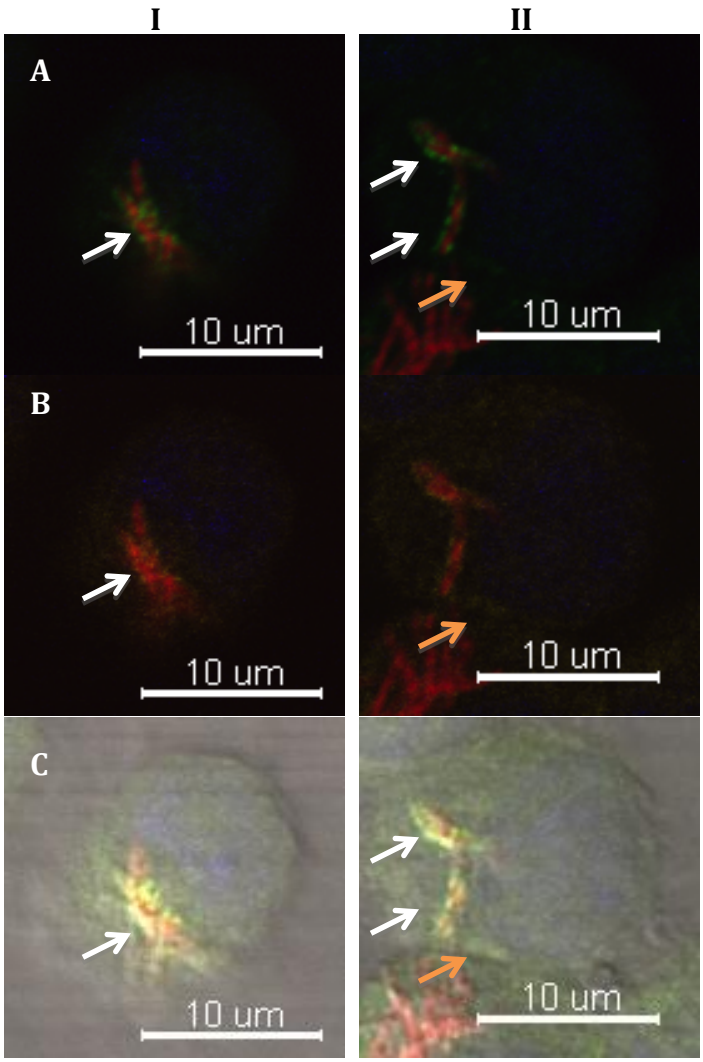

Figure C3 showed co-localisation of EsxG.EsxH with Mpm70 in *M. marinum* DsRed-infected J774.1 macrophages using AF647-anti-Mpm70 antibody labelled conventionally. Panel A (I and II) indicate the expression of EsxG.EsxH using anti-rabbit secondary antibody conjugated with AF488 (green) while in Panel B (I and II) showed Mpm70 signals detected and presented as yellow signals. The association between the two proteins were showed in white arrows. In addition, there was also presence of "footprint" showed by orange arrow, which is one of characteristics of Mpm70 protein. The footprint is better demonstrated in Panel C, were the images from merged channels presented in the bright-field channel.

f) Optimisation of quantum dot-labelled-antibodies dilutions and option for mycobacterium for infection in J774.1 macrophages

(i) Qdot565-labelled-anti-Mpm70 polyclonal antibody optimization

Initially, the optimisation was done to determine the dilution factor for the Qdot-labelled-anti-Mpm70 antibody. Three different dilutions were employed to both labelled polyclonal antibodies- 1:500, 1:200 and 1:100. At 1:500, there was a lacking of signal observed while at 1:100 dilution, high amount of non-specific backgrounds were seen within the cytoplasm of host cells **(Figure C4, Panel I).** Ultimately, the antibody dilution of 1:200 was chosen because of the non-specific background within the cytoplasmic of J774.1 macrophages was minimized and the signals produced were still evident and prominent **(Figure C4, Panel II).** Since we could view the signal within the macrophages, this has proven that the QD-labelled antibody was able to translocate into the cytoplasm of macrophages and detecting the expressed protein by the mycobacteria. Surprisingly, all of the *M. marinum* DsRed infecting the J774.1 macrophages were detected to produce Mpm70 protein in which has never been observed and described before by Ray, A., 2010.

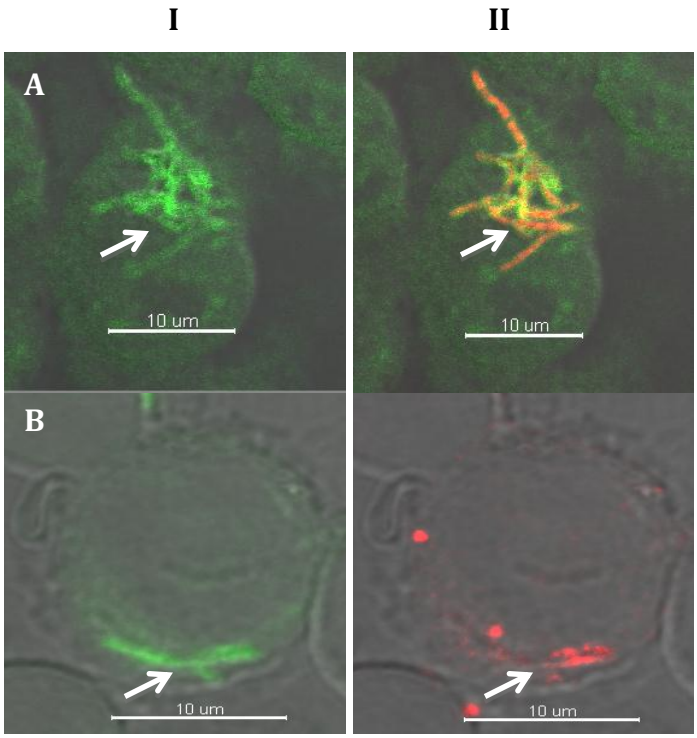

Figure C4 showed optimisation for Qdot565-labelled-anti-Mpm70 antibody in *M. marinum* DsRed-infected macrophages. Panel A (I and II) showed 1:100 dilution preparation of labelled anti-Mpm70 antibody while in Panel B (I and II) is the representative image of the labelled anti-Mpm70 antibody at 1:200 dilution. The backgrounds within the cytoplasm of macrophages were reduced at 1:200 in which the latter dilution was used throughout the experiment. Column II of Panel A is the image inclusive of merged channels. Meanwhile, Column II Panel B showed only the channel for *M. marinum* DsRed. The differences is meant to show that the high chances of overlapping spectrum between the Qdot565 and DsRed could happen as Qdot is known to have a broader excitation spectrum than that of normal Alexafluor.

(ii) Qdot655-labelled-anti-EsxG.EsxH antibody optimization

We tested with different dilutions for Qdot655-labelled-anti-EsxG.EsxH antibody. The dilutions were set at 1:100, 1:200 and 1:500; ultimately, 1:200 dilution was chosen and used throughout the experiment. As shown in **Figure C5**,

backgrounds can be seen not only within but outside of the host cells too when anti-EsxG.EsxH was used at 1:100 and the backgrounds were minimized at 1:200 dilution.

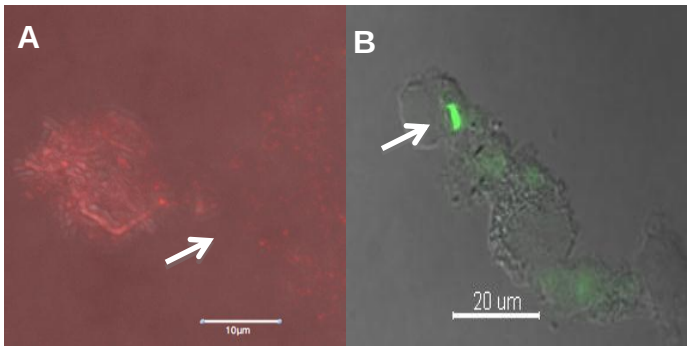

Figure C5 showed optimisation of the dilution factor for Qdot655-labelled-anti-EsxG.EsxH antibody in wild type *M. marinum*-infected macrophages. The images above showed the result after employing two different dilutions of the Qdot655-labelled anti-EsxG.EsxH antibody. Panel A was the example of image taken when the labelled antibody was used at 1:100 dilution. The signal was represented by red in colour. Notice that there was high level of background present not only within the host cell but also outside the host cell (arrow). The images in Panel B with labelled antibody used at 1:200 dilutions presented with a more well-defined signal (arrow) and background was minimized. The signal for this image was represented in green colour. Hence, a lower concentration of labelled antibody at dilution of 1:200 was chosen to be used throughout this experiment.

(ii) *M. marinum* DsRed versus wild type *M. marinum* without DsRed plasmid

Following the observation mentioned above, we decided to employ wild type *M. marinum* without the DsRed plasmid to remove the chances of false positive of AF565 signal through the broad excitation spectrum that may overlap with DsRed wavelength spectrum. **Figure C6** portrayed the results from employing

M. marinum DsRed (Panel A) and the wild type (Panel B). Both images were presented on bright field.

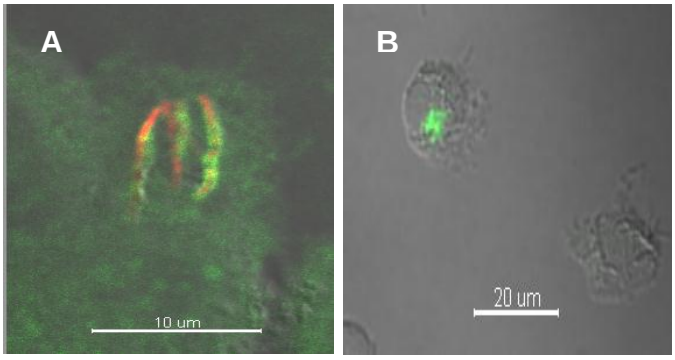

Figure C6 showed the differences in microscopic analysis of two different types of *M. marinum.* Panel A is the image that often observed when Qdot565-labelled-anti-Mpm70 antibody was used to detect the expression of Mpm70 in the host cells infected with *M. marinum* DsRed. Each bacterium within the cells appeared to express the protein although it was known that Mpm70 expression was uncommonly seen as such. When the wild type without the presence of DsRed plasmid was used, the possiblity of spectrum overlapping or photobleaching was successfully excluded. A more common feature was observed as previously mentioned by Ray, A. (2010). Both images were examples from applying Qdot565-anti-Mpm70 antibody at to the set of infections and the protein signals showed in green.

g) The experimental controls for Qdot analysis

Figure below were the representative images of positive controls for both protein expressions, the Mpm70 and EsxG.EsxH in *M. marinum* DsRed-infected murine macrophages. The Mpm70 in Panel A was seen as “bead-like” signals present at the periphery of mycobacteria whilst EsxG.EsxH protein complex was seen often as covering the whole mycobacteria (Panel B).

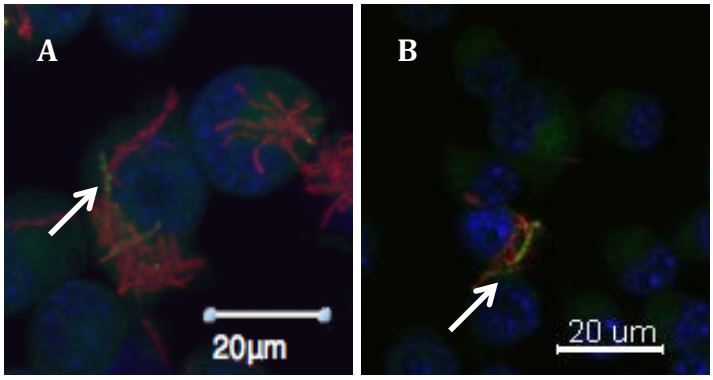

Figure C7 showed positive controls of *M. marinum* DsRed-infected J774.1 macrophage. Panel A, Mpm70 protein (green) was expressed in highly infected host cells. Meanwhile in Panel B, we could see the expressed EsxG.EsxH protein complex (also in green) in the infected host cells. The red signals observed in both panels represented *M. marinum* expressing DsRed and the blue signal were the nuclei of the macrophages stained with DAPI.

Figure C8 is the negative controls where only the Qdot labelling agents were applied to the cells. No signal was present for both labelling agents indicating that the agents did not bind non-specifically to neither the host cells nor the wild type *M. marinum*. This information is important to exclude false positive due to the non-specific binding of the agents to the mycobacteria and host cells.

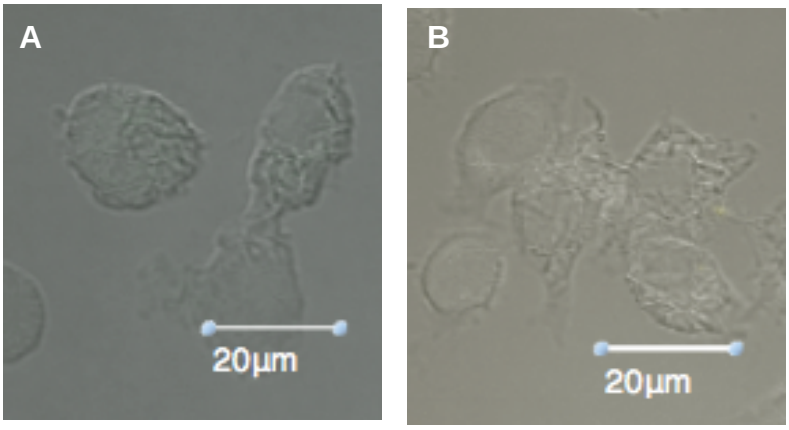

Figure C8 showed representative images of negative control using wild type *M. marinum*-infected J774A.1 treated with Qdot labelling agents only. Panel A showed J774A.1 murine macrophages infected with wild type *M. marinum* and Qdot565 was applied to rule out non-specific binding of the labelling agent to either macrophage or mycobacteria. No signal was found indicating no non-specific binding occurrence. In Panel B, a similar procedure was conducted using Qdot655 for the same objective. Again, there was no signal in the prepared set of infection.

Bibliography

1. Aagaard, C, Govaerts, M, Okkels, LM, Andersen, P, Pollock, M (2003). Genomic approach to identification of *Mycobacterium bovis* diagnostic antigens in cattle. *Journal of Clinical Microbiology* 41: 3719-3728.

2. Abdallah, AM, Bestebroer, J, Savage, ND, de Punder, K, van Zon, M, Wilson, L, Korbee, CJ, van der Sar, AM, Ottenhoff, TH, van der Wel, NN, Bitter, W, Peters, PJ (2011). Mycobacterial secretion systems ESX-1 and ESX-5 play distinct roles in host cell death and inflammasome activation. *Journal of Immunology* 187: 4744-4753.

3. Abdallah, AM, Gey van Pittius, NC, Champion, PA, Cox, J, Luirink, J, Vandenbroucke-Grauls, CM (2007). Type VII secretion-mycobacteria show the way. *Nature Review Microbiology* (5): 883-891.

4. Abdallah, AM, Savage, ND, van Zon, M, Wilson, L, Vandenbroucke-Grauls, CM, van der Wel, NN, Ottenhoff, TH, Bitter, W (2008). The ESX-5 secretion system of *Mycobacterium marinum* modulates the macrophage response. *Journal of Immunology* 181: 7166-7175.

5. Abdallah, AM, Verboom, T, Hannes, F, Safi, M, Strong, M, Eisenberg, D (2006). A specific secretion system mediates PPE41 transport in pathogenic mycobacteria. *Molecular Microbiology* (62): 667-679.

6. Abdallah, AM, Verboom, T, Weerdenburg, EM, Gey van Pittius, NC, Mahasha, PW, Jimenez, C, Parra, M, Cadieux, N, Brennan, MJ, Appelmelk, BJ, Bitter, W (2009). PPE and PE_PGRS proteins of *Mycobacterium marinum* are transported via the type VII secretion system ESX-4. *Molecular Microbiology* 73: 329-340.

7. Adamski, MG, Gumann, P, Baird, AE (2014). A method for quantitative analysis of standard and high-throughput qPCR expression data based on input sample quantity. *PLoS One* 9(8): e103917.

8. Akira, S, Uematsu, S, Takeuchi, O (2006). Pathogen recognition and innate immunity. *Cell* 124:783-801.

9. Algood, HMS, Chan, J, Flynn, JL (2003). Chemokines and tuberculosis. *Cytokine Growth Factor Rev* 14: 467-477.

10. Algood, HM, Lin, PL. Flynn, JL (2005). Tumor necrosis factor and chemokine interactions in the formation and maintenance of granulomas in tuberculosis. *Clinical Infectious Diseases* 41(suppl 3): S189-S193.

11. Anes, E, Peyron, P, Staali, L, Jordao, L, Gutierrez, MG, Kress, H, Hagedorn, M, Maridonneau-Parini, I, Skinner, MA, Wilderman, AG, Kalamidas, SA, Kuehnel, AG, Griffiths, G (2006). Dynamic life and death interactions between *Mycobacterium smegmatis* and J774 macrophages. Cellular Microbiology 8(6): 939-960.

12. Antony, VB, Godbey, SW, Kunkel, SL, Hott, JW, Hartman, DL, Burdick, MD, Strieter, RM (1993). Recruitment of inflammatory cells to the pleural space. Chemotactic cytokines, IL-8, and monocyte chemotactic peptide-1 in human pleural fluids. *Journal of Immunology* 151(12): 7216-7223.

13. Arhets, P, Gounon, P, Sansonetti P, Guillén, N (1995). Myosin II is involved in capping and uroid formation in the human pathogen *Entamoeba histolytica*. *Infection and Immunity* 63(11): 4358-4367.

14. Arhets, P, Olivo, JC, Gounon, P, Sansonetti, Guillén (1998). Virulence and functions of myosin II are inhibited by overexpression of light meromyosin in *Entamoeba histolytica. Molecular Biology of the Cell* 8: 1537-1247.

15. Babrak, L, Danelishvili, L, Rose, SJ, Kornberg, T, Bermudez, LE (2014). The environment of "*Mycobacterium avium* subsp. *homonissuis*" microaggregates induces synthesis of small proteins associated with efficient infection of respiratory epithelial cells. *Infection and Immunity* 83(2): 625-636.

16. Behar, SM (2013). Antigen-specific CD8+ T cells and protective immunity to tuberculosis. *Advances in Experimental Medicine and Biology* 783: 141-163.

17. Behr, MA, Wilson, MA, Gill, WP, Salamon, H, Schoolnik, GK, Rane, S, Small, PM (1999). Comparative genomics of BCG vaccines by whole-genome DNA microarray. *Science* 284: 1520-1523.

18. Beresford, B, Sadoff, JC (2010). Update on research and development pipeline: tuberculosis vaccines. *Clinical Infectious Diseases* 50 (supplement 3): S178-S183.

19. Bermudez, LE, Goodman, J (1996). *Mycobacterium tuberculosis* invades and replicates within type II alveolar cells. *Infection and Immunity* 64(4): 1400-1406.

20. Bermudez, LE, Goodman, J, Petrofsky, M (1999). Role of complement receptors in uptake of *Mycobacterium avium* by macrophages *in vivo*: evidence from studies using CD18-deficient mice. *Infection and Immunity* 67: 4912-4916.

21. Bermudez, LE, Sangari, FJ, Kolonoski, P, Petrofsky, M, Goodman, J (2002). The efficiency of translocation of *Mycobacterium tuberculosis* across a bilayer of epithelial and endothelial cells as a model of the alveolar wall is a consequence of transport within mononuclear phagocytes an invasion of alveolar epithelial cells. *Infection and Immunity* 70: 140-146.

22. Berthet, FX, Rasmussen, PB, Rosenkrands, I, Andersen, P, Gicquel, B (1998). A *Mycobacterium tuberculosis* operon encoding ESAT-6 and a novel low-molecular-mass culture filtrate protein (CFP-10). *Microbiology* 144: 3195-3203.

23. Billeskov, R, Vingsbo-Lundberg, C, Andersen, P, Dietrich, J (2007). Induction of CD8 T cells against a novel epitope in TB10.4: correlation with mycobacterial virulence and the presence of a functional region of difference-1. *Journal of Immunology* 179(6): 3973-3981.

24. Bitter, W, Houben, EN, Bottai, D, Brodin, P, Brown, EJ, Cox, JS, Derbyshire, K, Fortune, SM, Gao, LY, Liu, J, Gey van Pittius, NC, Pym, AS, Rubin, EJ, Sherman, DR, Cole, ST, Brosch, R (2009). Systematic genetic nomenclature for type VII secretion systems. *PLoS Pathogens* 5: e1000507.

25. Blikstad, C, Ivarsson, Y (2015). High-throughput methods for identification of protein-protein interactions involving short linear motifs. *Cell Communication and Signaling* 13: 38-47.

26. Bloom, BR, Fine, PEM (1994). “The BCG experience: implications for future vaccines against tuberculosis.” Tuberculosis: pathogenesis, protection, and control. *ASM Press, Washington DC* pp: 531-557.

27. Bodnar, KA, Serbina, NV, Flynn, JL (2001). Fate of *Mycobacterium tuberculosis* within murine dendritic cells. *Infection and Immunity* 69(2): 800-809.

28. Boggaram, V, Gottipati, KR, Wang, X, Samten, B (2013). Early secreted antigenic target of 6kDa (ESAT-6) protein of *Mycobacterium tuberculosis* induces interleukin-8 (IL-8) expression in lung epithelial cells via protein kinase signaling and reactive oxygen species. *Journal of Biological Chemistry* (288): 25500-25511.

29. Brodin, P, de Jonge, MI, Majlessi, L, Leclerc, C, Nilges, M, Cole, ST, Brosch, R (2005). Functional analysis of early secreted antigenic target-6, the

dominant T-cell antigen of *Mycobacterium tuberculosis*, reveals key residues involved in secretion, complex formation, virulence, and immunogenicity. *Journal of Biological Chemistry* 280: 33953-33959.

30. Brosch, R, Pym, AS, Gordon, SV, Cole, ST (2001). The evolution of mycobacterial pathogenicity: clues from comparative genomics. *Trends in Microbiology* 9: 452-458.

31. Browning, DD, Diehl, WC, Hsu, MH, Schraufstatter, IU, Ye, RD (2000). Autocrine regulation of interleukin-8 production in human monocytes. *American Journal of Physiology and Lung Cell Molecular Physiology* 279: L1129-L1136.

32. Carlsson, F, Joshi, SA, Rangell, L, Brown, EJ (2009). Polar localization of virulence-related Esx-1 secretion in mycobacteria. *PLoS Pathogens* 5:e1000285.

33. Carlsson, F, Kim, J, Dumitru, C, Barck, KH, Carano, RA, Sun, M, Diehl, L, Brown, EJ (2010). Host-detrimental role os Esx-1-mediated inflammasome activation in mycobacterial infection. P*LoS Pathogens* 6(5): e1000895.

34. Casanova, JL, Blanche, S, Emile, JF, Jouanguy, E, Lamhamedi, S, Altare, F, Stéphan, JL, Bernaudin, F, Bordigoni, P, Turck, D, Lachaux, A, Albertini, M, Bourrilon, A, Dommergues, JP, Pocidalo, MA, Le Deist, F, Gaillard, JL, Griscelli, C, Fischer, A (1996). Idiopathic disseminated bacillus Calmette-Guérin infection: a French national restrospective study. *Pediatrics* 98(4 Pt 1): 774-778.

35. Castro-Garza, J, King, CH, Swords, WE, Quinn, FD (2002). Demonstration of spread by *Mycobacterium tuberculosis* bacilli in A549 epithelial cell monolayers. *FEMS Microbiology Letters* 212: 145-149.

36. Centers for Disease Control and Prevention (CDC). Development of new vaccines for tuberculosis recommendations of the advisory council for the elimination of tuberculosis (ACET). Report on August 21, 1998/47(RR13): 1-6

37. Cheng, DS, Han, W, Chen, SM, Sherrill, TP, Chont, M, Park, GY, Sheller, JR, Polosukhin, VV, Christma, JW, Yull, FE, Blackwell, TS (2007). Airway epithelium controls lung inflammation and injury through the NF-kappa B pathway. *Journal of Immunology* 178(10): 6504-6513.

38. Chow, JC, Young, DW, Golenbock, DT, Christ, WJ, Gusovsky, F (1999). Toll-like receptor-4 mediates lipopolysaccharide-induced signal transduction. *Journal of Biological Chemistry* 274(16): 10689-10692.

39. Christie, PJ, Cascales, E (2005). Structural and dynamic properties of bacterial type IV secretion system (review). *Molecular Membrane Biology* 2291-2): 51-61.

40. Coker, R (2004). Compulsory screening of immigrants for tuberculosis and HIV. *British Medicine Journal* 328: 298-300.

41. Cole, ST (2002). Comparative and functional genomics of the *Mycobacterium tuberculosis* complex (review). *Microbiology* 148(10): 2919-2928.

42. Cole, ST, Brosch, R, Parkhill, J, Garnier, T, Churcher, C, Harris, D, Gordon, SV, Eiglmeier, K, Gas, S, Barry III, CE, Tekaia, F, Badcock, K, Basham, D, Brown, D, Chillingworth, T, Connor, R, Davies, R, Devlin, K, Feltwell, T, Gentles, S, Hamlin, N, Holroyd, S, Hornsby, T, Jagels, K, Krogh, A, McLean, J, Moule, S, Murphy, L, Oliver, K, Osborne, J, Quail, MA, Rajandream, MA, Roger, J, Rutter, S, Seeger, K, Skelton, J, Squares, R, Squares, S, Sulston, JE, Taylor, K, Whitehead, S, Barrell, BG (1998). Deciphering the biology of *Mycobacterium tuberculosis* from the complete genome sequence. *Nature* 393: 537-544.

43. Cole, ST, Eiglmeier, K, Parkhill, J, James, KD, Thomson, NR, Wheeler, PR, Honore, N, Garnier, T, Churcher, C, Harris, D, Mungall, K, Basham, Brown, D, Chillingworth, T, Connor, R, Davies, RM, Devlin, K, Duthoy, S, Feltwell, T, Fraser,

A, Hamlin, N, Holroyd, S, Hornsby, T, Jagels, K, Lacroix, C, Maclean, J, Moule, S, Murphy, L, Oliver, K, Quail MA, Rajandrean, MA, Rutherford, KM, Rutter, S, Seeger, K, Simon, S, Simmonds, M, Skelton, J, Squares, R, Squares, S, Stevens, K, Taylor, K, Whitehead, S, Woodward, JR, Barrell, BG (2001). Massive gene decay in the leprosy bacillus. *Nature* 409: 1007-1011.

44. Converse, SE, Cox, JS (2005). A protein secretion pathway critical for *Mycobacterium tuberculosis* virulence is conserved and functional in *Mycobacterium smegmatis*. *Journal of Bacteriology* 187: 1238-1245.

45. Cornelis, GR (2006). The type III secretion injectisome. *Nature Rev Microbiology* 4(11): 811-825.

46. Coros, A, Callahan, B, Battaglioli, E, Derbyshire, KM (2008). The specialized secretory apparatus ESX-1 is essential for DNA transfer in *Mycobacterium smegmatis*. *Molecular Microbiology* 69: 794-808.

47. Cosma, CL, Klein, K, Kim, R, Beery, D, Ramakrishnan, L (2006). *Mycobacterium marinum* Erp is a virulence determinant required for cell wall integrity and intracellular survival. *Infection and Immunity* 74: 3125-3133.

48. Cotton, M, Baker, A, Saltik, M, Wagner, E, Buschle, M (1994). Lipopolysaccharide is a frequent contaminant of plasmid DNA preparatinos and can be toxic to primary human cells in the presence of adenovirus. *Gene therapy* 1: 239-246.

49. Coulter, KR, Knoell, DL, Hard, J, Wewers, MD, Allen, ED, Castile, RG (2000). Induction of interleukin-8 release by lung epithelium with cystic fibrosis epithelial lining fluid is marginally affected by inhibitors of interleukin-1 beta. *The Journal of Pharmacotherapy* 20(1): 64-74.

50. Cromwell, O, Hamid, Q, Corrigan, CJ, Barkans, J, Meng, Q, Collins, PD, Kay, AB (1992). Expression and generation of interleukin-8, IL-6 and granulocyte-macrophage colony-stimulating factor by bronchial epithelial cells and enhancement by IL-1β and tumor necrosis factor-α. *Immunology* 77: 330-337.

51. Curry-Mc.Coy, TV, Venado, A, Guidot, DM, Joshi, PC (2013). Alchol ingestion disrupts alveolar epithelial barrier function by activation of macrophage-derived transforming growth factor beta1. *Respiratory Research* 14:39.

52. Danelishvili, L, McGarvey, J, Li, YJ, Bermudez, LE (2003). *Mycobacterium tuberculosis* infection causes different levels of apoptosis and necrosis in human macrophages and alveolar epithelial cells. *Cellular Microbiology* 5(9): 649-660.

53. Davis, JM, Ramakrishnan, L (2009). The role of the granuloma in expansion and dissemination of early tuberculosis infection. *Cell* 136: 37-49.

54. de Chastellier, C, Forquet, F, Gordon, A, Thilo, L (2009). Mycobacterium requires an all-around closely apposing phagosome membrane to maintain the maturation block and this apposition is re-established when it rescues itself from phagolysosomes. 11(8): 1190-1207.

55. de Jonge, MI, Pehau-Arnaudet, G, Fretz, MM, Romain, F, Bottai, D, Brodin, P, Honoré, N, Marchal, G, Jiskoot, W, England, P, Cole, ST, Brosch, R (2007). ESAT-6 from *Mycobacterium tuberculosis* dissociates from its putative chaperone CFP-10 under acidic conditions and exhibits membrane-lysing activity. *Journal of Bacteriology* 189(16): 6028- 6034.

56. Dempsey, EC, Cool, CD, Littler, CM (2007) Lung disease and PKCs. *Pharmacological Research* 55: 545-559.

57. Deretic, V, Singh, S, Master, S, Harris, J, Roberts, E, Kyei, G, Davis, A, de Haro, S, Naylor, J, Lee, HH, Vergne, I (2006). *Mycobacterium tuberculosis*

inhibition of phagolysosome biogenesis and autophagy as a host defense mechanism. *Cellular Microbiology* 8: 719-727.

58. Dillon, DC, Alderson, MR, Day, CH, Bement, T, Campos-Neto, A, Skeiky, YA, Vedvick, T, Badaro, R, Reed, SG, Houghton, R (2000). Molecular and immunological characterization of *Mycobacterium tuberculosis* CFP-10, an immunodiagnostic antigen missing in *Mycobacterium bovis* BCG. *Journal of Clinical Microbiology* 38(9): 3285-3290.

59. Dobos, KKM, Spotts, EA, Quinn, FD, King, CH (2000). Necrosis of lung epithelial cells during infection with *Mycobacterium tuberculosis* is preceded by cell permeation. *Infection and Immunity* 68: 6300-6310.

60. Eckmann, L, Kagnoff, MF, Fierer, J (1993). Epithelial cells secrete the chemokine interleukin-8 in response to bacterial entry. *Infection and Immunity* 61(11): 4569-4574.

61. Eda, S, Yamanaka, M, Beppu, M (2004). Carbohydrate-mediated phagocytic recognition of early apoptotic cells undergoing transient capping of CD43 glycoprotein. *The Journal of Biological Chemistry* 279(7): 5967-5974.

62. Emili, AQ, Cagney,G (2000). Large-scale functional analysis using peptide or protein arrays. Nature Biotechnology 18: 393-397.

63. Eoh, H, Rhee, KY (2012). Multifunctional essentiality of succinate metabolism in adaptation to hypoxia in *Mycobacterium tuberculosis*. *Proceedings of the National Academy of Science USA* 110(16): 6554-6559.

64. Fan, L, Wang, Q, Fuente-Núñez, CDL, Sun, FJ, Xia, JG, Xia, PY, Hancock, REW (2014). Increased IL-8 production in human bronchial epithelial cells after exposure to azithromycin-pretreated *Pseudomonas aeruginosa in vitro. FEMS Microbiology Letter* 355: 43-50.

65. Fernando, RI, Castillo, MD, Litzinger, M, Hamilton, DH, Palena, C (2011). IL-8 signaling plays a critical role in the epithelial-mesenchymal transition of human carcinoma cells. *Cancer Research* 71(15): 5296-5306.

66. Ferrari, G, Langen, H, Naito, M, Pieters, J (1999). A coat protein on phagosomes involved in the intracellular survival of mycobacteria. *Cell* 97: 435-447.

67. Fields, S, Song, O (1989). A novel genetic system to detect protein-protein interactions. Nature 340: 245-246.

68. Finan, C, Ota, MO, Marchant, A, Newport, MJ (2008). Natural variation immune responses to neonatal *Mycobacterium bovis* bacillus Calmette-Guerin (BCG) vaccination in a cohort of Gambian infants. *PLoS One* 3: e3485.

69. Finlay, BB, Falkow, S (1997). Common themes in microbial pathogenicity revisited. *Microbiology and Molecular Biology Rev* 61: 136-169.

70. Flint, JL, Kowalski, JC, Karnati, PK, Derbyshire, KM (2004). The RD1 virulence locus of *Mycobacterium tuberculosis* regulates DNA transfer in *Mycobacterium smegmatis. Proc Natl Acad Sci USA* 101: 12598-12603.

71. Flynn, JL, Chan, J (2005). What's good for the host is good for the bug. *Trends in Microbiology* 13: 98-102.

72. Fortune, SM, Jaeger, A, Sarracino, DA, Chase, MR, Sassetti, CM, Sherman, DR, Bloom, BR, Rubin, EJ (2005). Mutually dependent secretion of proteins required for mycobacterial virulence. *Proceedings of the National Academy of Science USA* 102: 10676-10681.

73. Frieden, TR, Sterling, TR, Munsiff, SS, Watt, CJ, Dye, C (2003). Tuberculosis. *Lancet* 362(9387): 887-899.

74. Galagan, JE, Sisk, P, Stolte, C, Weiner, B, Koehrsen, M, Wymore, F, Reddy, TBK, Zucker, JD, Engels, R, Gellesch, M, Hubble, J, Jin, H, Larson, L, Mao, M, Nitzberg, M, White, J, Zachariah, ZK, Sherlock, G, Schoolnik, GK (2010). TB database 2010: Overview and update. *Tuberculosis (Edinb)* 90(4): 225-235.

75. Gao, Q, Kripke, KE, Saldanha, AJ, Yan, W, Holmes, S, Small, PM (2005). Gene expression diversity among *Mycobacterium tuberculosis* clinical isolates. *Microbiology* 151: 5-14.

76. Gao, W, Zhang, W, Meldrum, DR (2011). RT-qPCR based quantitative analysis of gene expression in single bacterial cells. *Journal of Microbiology Methods* 85: 221-227.

77. Garzía-Pérez, BE, Mondragón-Flores, R, Luna-Herrera, J (2003). Internalization of *Mycobacterium tuberculosis* by macropinocytosis in non-phagocytic cells. *Microbial Pathogenesis* 35(2): 49-55.

78. Gavin, AC, Aloy, P, Grandi, P, Krause, R, Boesche, M, Marzioch, M, Rau, C, Jensen, LJ, Bastuck, S, Dümpelfeld, B, Edelmann, A, Heutier, MA, Hoffman, V, Hoefert, C, Klein, K, Hudak, M, Michon, AM, Scelder, M, Schirle, M, Remor, M, Rudi, T, Hooper, S, Bauer, A, Bouwmeester, T, Casari, G, Drewes, G, Neubauer, G, Rick, JM, Kuster, B, Bork, P, Russell, RB, Superti-Furga, G (2006). Proteome survey reveals modularity of the yeast cell machinery. *Nature* 440: 631-636.

79. Gavin, AC, Maeda, K, Kuhner, S (2011). Recent advances in charting protein-protein interaction: mass spectrometry-based approaches. *Current Opinion in Biotechnology* 22(1): 42-49.

80. George, KM, Chatterjee, D, Gunawardana, G, Welty, D, Hayman, J, Lee, R, Small, PL (1999). Mycolactone: a polyketide toxin from *Mycobacterium ulcerans* required for virulence. *Science* 283: 854-857.

81. Gey van Pittius, NC, Gamieldien, J, Hide, W, Brown, GD, Siezen RJ, Beyers AD (2001). The ESAT-6 gene cluster of *Mycobacterium tuberculosis* and other high G+C Gram-positive bacteria. *Genome Biol 2: Research*. 0044.1-0044.18.

82. Gey van Pittius, NC, Sampson, SL, Lee, H, Kim, Y, van Helde, PD, Warren, RM (2006). Evolution and expansion of the *Mycobacterium tuberculosis* PE and PPE multigene families and their association with the duplication of the ESAT-6 (*esx*) gene cluster regions. *BMC Evolution Biology* 6: 95.

83. Gill, SC, von Hippel, PH (1989). Calculation of protein extinction coefficients from amino acid sequence data. *Analytic Biochemistry* 189(2): 319-326.

84. Goodfellow, M, Jones, AL (2012). Order *Corynebacteriales* ord. nov. *Bergey's Manual of Systematic Bacteriology, Springer Verlag, New York* 5: 235-243.

85. Gonzalez-Juarrero, M, Turner, OC, Turner, J, Marietta, P, Brooks, JV, Orme, IM (2001). Temporal and spatial arrangement of lymphocytes within lung granulomas induced by aerosol infection with *Mycobacterium tuberculosis*. *Infection and Immunity* 69(3): 1722-1728.

86. Gordon, SV, Brosch, R, Billault, A, Garnier, T, Eiglmeier, K, Cole, ST (1999). Identification of variable regions in the genomes of tubercle bacilli using bacterial artificial chromosome arrays. *Molecular Microbiology* 32(3): 643-655.

87. Govindaraju, V, Michoud, M, Ferraro, P, Arkinson, J, Safka, K, Valderrama-Carvajal, H, Martin, JG (2008). The effects of interleukin-8 on airway smooth muscle contractin in cystic fibrosis. *Respiratory Research* 9: 76-87.

88. Grainger, CI, Greenwell, LL, Lockley, DJ, Martin, GP, Forbes, B (2006). Culture of Calu-3 cells at the air interface provides a reprentative model of the airway epithelial barrier. *Pharmaceutical Research* 23(7): 1482-1490.

89. Guinn, KM, Hickey, MJ, Mathur, SK, Zakel, KL, Grotzke, JE, Lewinsohn, DM, Smith, S, Sherman, DR (2004). Individual RD1-region genes are required for export of ESAT-6/CFP-10 and for virulence of *Mycobacterium tuberculosis*. *Molecular Microbiology* 51(2): 359-370.

90. Hagedorn, M, Rohde, KH, Russell, DG, Soldati, T (2009). Infection by tubercular mycobacteria is spread by non-lytic ejection from their amoeba hosts. *Science* 323: 1729-1733.

91. Hall, DA, Ptacek, J, Synder, M (2007). Protein microarray technology. *Mechanisms of Ageing and Development* 128: 161-167.

92. Harriff, MJ, Cansler, ME, Toren, KG, Canfield, ET, Kwak, S, Gold, MC, Lewinsohn, DM (2014). Human lung epithelial cells contain *Mycobacterium tuberculosis* in a late endosomal vacuole and are efficiently recognized by $CD8^{+}$T cells. *PLOS Pathogens* 9(5): e97515.

93. Harboe, M, Oettinger, T, Wiker, HG, Rosenkrands, I, Andersen, P (1996). Evidence for occurrence of the ESAT-6 protein in *Mycobacterium tuberculosis* and virulent *Mycobacterium bovis* and for its absence in *Mycobacterium bovis* BCG. *Infection and Immunity* 64: 16-22.

94. Hardyman, MA, Wilkinson, E, Martin, E, Jayasekera, NP, Blume, C, Swindle, EJ, Gozzard, N, Holgate, ST, Howarth, PH, Davies, DE, Collins, JE (2013). TNF-α-mediated bronchial barrier disruption and regulation by src-family kinase activation. *Journal of Allergy and Clinical Immunology* 132: 665-675.

95. Hasan, Z, Jamil, B, Ashraf, M, Islam, M, Dojki, M, Irfan, M, Hussain, R (2009). Differential live *Mycobacterium tuberculosis*-, *M. bovis* BCG-, recombinant ESAT6-, and Culture Filtrate Protein10-induced immunity in tuberculosis. *Clinical and Vaccine Immunology* 16(7): 991-998.

96. Haugland, R (2005). The handbook: A guide to fluorescent probes and labeling technologies. *Invitrogen* pp: 10-32.

97. Henderson, IR, Navarro-Garcia, F, Desvaux, M, Fernandez, RC, Ala'Aldeen, D (2004). Type V protein secretion pathway: the autotransporter story. *Microbiology and Molecular Biology Rev* 68(4): 692-744.

98. Hermanns, MI, Unger, RE, Kehe, K, Peters, K, Kirkpatrick, CJ (2004). Lung epithelial cell lines in coculture with human pulmonary microvascualr endothelial cells: development of an alveolo-capillary barrier *in vitro. Laboratory Investigation* 84(6): 736-752.

99. Hervas-Stubbs, S, Majlesi, L, Simsova, M, Morova, J, Rojas, MJ, Nouzé, C, Brodin, P, Sebo, P, Leclerc, C (2006). High frequency of $CD4^+$ T cells specific for the TB10.4 protein correlates with protection against *Mycobacterium tuberculosis* infection. *Infection and Immunity* 74(6): 3396-3407.

100. Hill, PC, Brookes, RH, Fox, A, Fielding, K, Jeffries, DJ, Jackson-Sillah, D, Lugos, MD, Owiafe, P, Donkor, SA, Hammond, AS, Otu, J, Corrah, T, Adegbola, RA, McAdam, KP (2004). Large-scale evaluation of enzyme-linked immunospot assay and skin test for diagnosis of *Mycobacterium tuberculosis* infection against a gradient of exposure in The Gambia. *Clinical Infectious Diseases* 38(7): 966-973.

101. Holland, IB, Schmitt, L, Young, J (2005). Type I protein secretion in bacteria, the ABC-transporter dependent pathway (review). *Molecular Membrane Biology* 22(1-2): 29-39.

102. Houben, ENG, Korotkov, KV, Bitter, W (2014). Take five-Type VII secretion systems of *Mycobacteria*. *Biochimica et Biophysica Acta* 1843: 1707-1716.

103. Houben, ENG, Walburger, A, Ferrari, G, Nguyen, L, Thompson, CJ, Miess, C, Vogel, G, Mueller, B, Pieters, J (2009). Differential expression of a virulence factor in pathogenic and non-pathogenic mycobacteria. *Molecular Microbiology* 72(1): 41-52.

104. Huebner, RE (1996). BCG vaccination in the control of tuberculosis. *Current Topics in Microbiology and Immunology (Tuberculosis)* 215: 263-282.

105. Hsu, T, Hinigley-Wilson, SM, Chen, B, Dai, AZ, Morin, PM, Marks, CB, Padiyar, J, Goulding, C, Gingery, M, Eisenberg, D, Russell, RG, Derrick, SC, Collins, FM, Morris, SL, King, CH, Jacobs, WR (2003). The primary mechanism of attenuation of Bacillus Calmette-Guerin is a loss of secreted lytic function required for invasion of lung interstitial tissue. *Proceedings of the National Academy of Science USA* 100: 12420-12425.

106. Ilghari, D, Lightbody, KL, Veverka, V, Waters, LC, Muskett, FW, Renshaw, PS, Carr, MD (2011). Solution structure of the *Mycobacterium tuberculosis* EsxG.EsxH complex: Functional implications and comparisons with other *M. tuberculosis* Esx family complexes. *The Journal of Biological Chemistry* 286(34): 29993-30002.

107. Jepson, A, Fowler, A, Banya, W, Singh, M, Bennett, S, (2001). Genetic regulation of acquired immune responses to antigens of *Mycobacterium tuberculosis*: a study of twins in West Africa. *Infection and Immunity* 69: 3989-3994.

108. Johnson, TL, Abendroth, J, Hol, WGJ, Sandkvist, M (2006). Type II secretion: from structure to function (minireview). *FEMS Microbiology Letter* 255: 175-186.

109. Junge, S, Brenner, B, Lepple-Wienhues, A, Nilius, B, Lang, F, Linderkamp, O, Gulbin, E (1999). Intracellular mechanisms of L-selectin induced capping. *Cell Signal* 11: 301-308.

110. Kaufmann, SHE, Hussey, G, Lambert, P-H (2010). New vaccines for tuberculosis. The Lancet 375 (9729): 1852-1854.

111. Kellar, KL, Gehrke, J, Weis, SE, Mahmutovic-Mayhew, A, Davila, B, Zajdowicz, MJ, Scarborough, R, LoBue, PA, Lardizabal, AA, Daley, CL, Reves, RR, Bernardo, J, Campbell, BH, Whitworth, WC, Mazurek, GH (2011). Multiple cytokines are released when blood from patients with tuberculosis is stimulated with *Mycobacterium tuberculosis* antigens. *PLoS One* 6(11): e26545.

112. Kim, KJ, Cheek, JM, Crandall, ED (1991). Contribution of Na^+ and Cl^- fluxes to net ion transport by alveolar epithelium. *Respiratory Physiology* 85: 245-256.

113. Kinhikar, AG, Verma, I, Chandra, D, Singh, KK, Weldingh, K, Andersen, P, Hsu, T, Jacobs, WR, Lal, S (2010). Potential role for ESAT6 in dissemination of *M. tuberculosis* via human lung epithelial cells. *Molecular Microbiology* 75(1): 92-106.

114. Kim, JY, Sajjan, US, Krasan, GP, LiPuma, JJ (2005). Disruption of tight juntions during traversal of the respiratory epithelium by *Burkholderia cenocepacia*. *Infection and Immunity* 73(11): 7107-7112.

115. Klingberg, TD, Pedersen, MH, Cencic, A, Budde, BB (2005). Application of measurements of transepithelial electrical resistance of intestinal epithelial cell monolayers to evaluate probiotic activity. *Applied and Environmental Microbiology* 71(11): 7528-7530.

116. Koo, IC, Wang, C, Raghavan, S, Morisaki, JH, Cox, JS, Brown, EJ (2008). ESX-1-dependent cytolysis in lysosome secretion and inflammasome activation during mycobacterial infection. *Cellular Microbiology* 10: 1866-1878.

117. Krawczyk, C, Penninger, JM (2001). Molecular controls of antigen receptor clustering and autoimmunity. *Trends in Cellular Biology* 11(5): 212-220.

118. Kurashima, K, Mukaida, N, Fujimura, M, Yasui, M, Nakazumi, Y, Matsuda, T, Matsushima, K (1997). Elevated chemokine levels in bronchoalveolar lavage fluid of tuberculosis patients. *American Journal of Respiratory and Critical Care Medicine* 155: 1474-1477.

119. Kurenuma, T, Kawamura, I, Hara, H, Uchiyama, R, Daim, S, Dewamitta, SR, Sakai, S, Tsuchiya, K, Nomura, T, Mitsuyama, M (2009). The RD1 locus in the *Mycobacterium tuberculosis* genome contributes to activation of caspase-1 via induction of potassium ion efflux in infected macrophages. *Infection and Immunity* 77(9): 3992-4001.

120. Kusek, ME, Pazos, MA, Pirzai, W, Hurley, BP (2014). *In vitro* coculture assay to assess pathogen induced neutrophil trans-epithelial migration. *Journal of Visualized Experiments* 83: 50832.

121. Kwon, OJ, Jose, PJ, Robbins, RA, Schall, TJ, Williams, TJ, Barnes, PJ (1995). Glucocorticoid inhibition of RANTES expression in human lung epithelial cells. *The American Journal of Respiratory Cell and Molecular Biology* 12(5): 488-496.

122. Labbé, K, Saleh, M (2008). Cell death in the host response to infection. *Cell Death Differ* 15: 1339-1349.

123. Lalor, MK, Floyd, S, Gorak-Stolinska, P, Ben-Smith, Anne, Weir, RE, Smith, SG, Newport, MJ, Blitz, R, Mvula, H, Branson, K, McGrath, N, Crampin, AC, Fine,

PE, Dockrell, HM (2011). BCG vaccination induces different cytokine profiles following infant BCG vaccination in the UK and Malawi. *The Journal of Infectious Diseases* 204: 1075-1085.

124. Lalvani, A, Brookes, R, Wilkinson, RJ, Malin, AS, Pathan, AA, Andersen, P, Dockrell, H, Pasvol, G, Hill, AVS (1998). Human cytolytic and interferon gamma-secreting CD8+ T lymphocytes specific for *Mycobacterium tuberculosis*. *Proceeding of National Academy of Science, USA* 95: 270-275.

125. Lee, HK, Iwasaki A (2007). Innate control of adaptive immunity: dendritic cells and beyond. *Seminars in Immunology* 19: 48-55.

126. Lee, W, VanderVen, BC, Fahey, RJ, Russell, DG (2013). Intracellular *Mycobacterium tuberculosis* exploits host-derived fatty acids to limit metabolic stress. *The Journal of Biological Chemistry* 288(10): 6788-6800.

127. Levine, SJ (1995). Bronchial epithelial cell-cytokine interactions in airway inflammation. *Journal of Investig Med* 43(3): 241-249.

128. Lew, JM, Kapopoulou, A, Jones, LM, Cole, ST (2011). TubercuList-10 years after. *Tuberculosis* 91: 1-7.

129. Lewis, KN, Liao, R, Guinn, KM, Hickey, MJ, Smith, S, Behr, MA, Sherman, DR (2003). Deletion of RD1 from *Mycobacterium tuberculosis* mimics bacilli Calmette-Guerin attenuation. *Journal of Infectious Diseases* 187: 117-123.

130. Lightbody, KL, Ilghari, D, Waters, LC, Carey, G, Bailey, MA, Williamson, RA, Renshaw, PS, Carr, MD (2008). Molecular features governing the stability and specificity of functional complex formation by *Mycobacterium tuberculosis* CFP-10/ESAT-6 family proteins. *Journal of Biological Chemistry* 283: 17681-17690.

131. Lightbody, KL, Renshaw, PS, Collins, ML, Wright, RL, Hunt, DM, Gordon, SV, Hewinson, RG, Buxton, RS, Williamson, RA, Carr, MD (2004).

Characterization of complex formation between members of the *Mycobacterium tuberculosis* complex CFP-10/ESAT-6 protein family: Towards an understanding of the rules governing complex formation and thereby functional flexibility. *FEMS Microbiology Letters* 238: 255-262.

132. Lin, Y, Zhang, M, Barnes, PF (1998). Chemokines production by a human alveolar epithelial cell line in response to Mycobacterium tuberculosis. *Infection and Immunity* 66(3): 1121-1126.

133. Linden, A (1996). Increased interleukin-8 release by β-adrenoceptor activation in human transformed bronchial epithelial cells. British Journal of Pharmacology 119: 402-406.

134. Louis-Jeune C, Andrade-Navarro MA, Perez-Iratxeta C (2012). Prediction of protein secondary structure from circular dichroism using theoretically derived spectra. *Proteins* 80(2): 374-381.

135. Lugo-Villarino, G, Vérollet, C, Maridonneau-Parini, I, Neyrolles, O (2011). Macrophage polarization: convergence point targeted by *Mycobacterium tuberculosis* and HIV. *Frontiers in Immunology* 2 (Article 43).

136. Maciag, A, Dainese, E, Rodriguez, GM, Milano, A, Provvedi, R, Pasca, MR, Smith, I, Palu, G, Riccardi, G, Manganelli, R (2007). Global analysis of the *Mycobacterium tuberculosis* Zur (FurB) regulon. *Journal of Bacteriology* 189: 730-740.

137. Mahairas, GG, Sabo, PJ, Hickey, MJ, Singh, DC, Stover, CK (1996). Molecular analysis of genetic differences between *Mycobacterium bovis* BCG and virulent *M. bovis. Journal of Bacteriology* 178: 1274-1282.

138. Majlessi, L, Brodin, P, Brosch, R, Rojas, MJ, Khun, H, Huerre, M, Cole, ST, Leclerc (2005). Influence of ESAT-6 secretion system 1 (RD1) of *Mycobacterium*

tuberculosis on the interaction between mycobacteria and the host immune system. *Journal of Immunology* 174: 3570-3579.

139. Majlessi, L, Rojas, MJ, Brodin, P, Leclerc, C (2003). CD8+-T-cell responses of *Mycobacterium*-infected mice to a newly identified major histocompatibility complex class I-restricted epitope shared by proteins of the ESAT-6 family. *Infection and Immunity* 71: 7173-7177.

140. Manca, C, Tsenova, L, Bergtold, A, Freeman, S, Tovey, M, Musser, JM, Bary III, CE, Freedman, VH, Kaplan, G (2001). Virulence of a *Mycobacterium tuberculosis* clinical isolate in mice is determine by failure to induce Th1 type immunity and is associated with induction of IFN-alpha/ beta. *Proceedings of the National Academy of Science USA* 98: 5752-5757.

141. Martin, LD, Rochelle, LG, Fischer, BM, Krunkosky, TM, Adler, KB (1997). Airway epithelium as an effector of inflammation: molecular regulation of secondary mediators. *European Respiratory Journal* 10(9): 2139-2146.

142. Massion, PP, Hébert, CA, Leong, S, Chan, B, Inoue, H, Grattan, K, Sheppard, D, Nadel, JA (1995). *Staphylococcus aureus* stimulates neutrophil recruitment by stimulating interleukin-8 production in dog trachea. *American Journal of Physiology* 268 (12): L85-L94.

143. Mathema, B, Kurepina, N, Faloows, D, Kreiswirth, BN (2008). Lessons from molecular epidemiology and comparative genomics. *Seminars in Respiratory and Critical Care Medicine* 29(5): 467-480.

144. McDonough, K, Kress, Y (1995). Cytotoxicity for lung epithelial cells is a virulence-associated phenotype of *Mycobacterium tuberculosis*. *Infection and Immunity* 63: 4802-4811.

145. McGuire, AM, Weiner, B, Park, st, Wapinski, I, Raman, S, Dolganov, G, Peterson, M, Riley, R, Zucker, J, Abeel, T, White, J, Sisk, P, Stolte, C, Koehrsen, M, Yamamoto, RT, Iacobelli-Martinez, M, Kidd, MJ, Maer, AM, Schoolnik, GK, Regev, A, Galagan, J (2012). Comparative analysis of *Mycobacterium* and related *Actinomycetes* yields insight into the evolution of *Mycobacterium tuberculosis pathogenesis. BMC Genomics* 13: 120-147.

146. Medie, FM, Champion, MM, Williams, EA, DiGiuseppe Champion, PA (2014). Homeostasis of N-α-terminal acetylation of EsxA correlates with virulence in *Mycobacterium marinum*. *Infection and Immunity* 82(1): 4572-4586.

147. Mehra, A, Zahra, A, Thompson, V, Sirisaengtaksin, N, Wells, A, Porto, M, Köster, S, Penberthy, K, Kubota, Y, Dricot, A, Rogan, D, Vidal, M, Hill, DE, Bean, AJ, Philips, JA (2013). *Mycobacterium tuberculosis* type VII secreted effector EsxH targets host ESCRT to impair trafficking. *PLOS Pathogens* 9(10): e1003734.

148. Mehta, PK, Karls, RK, White, EH, Ades, EW, Quinn, FD (2006). Entry and intracellular replication of *Mycobacterium tuberculosis* in cultured human microvascular endothelial cell. *Microbial Pathogenesis* 41(2-3): 119-124.

149. Mishra, BB, Moura-Alves, P, Sonawane, A, Hacohen, H, Griffiths, G, Moita, LF, Anes, E (2010). *Mycobacterium tuberculosis* protein ESAT-6 is a potent activator of the NLRP3/ASC inflammasome. *Cellular Microbiology* 12: 1046-1063.

150. Montero, MT, Matilla, J, Gomez-Mampaso, E, Lasuncion, MA (2004). Geranylgeraniol regulates negatively caspase-1 autoprocessing: implication in the Th1 response against *Mycobacterium tuberculosis. Journal of Immunology* 173: 4936-4944.

151. Mougous, JD, Cuff, ME, Raunser, S, Shen, A, Zhou, M, Gifford, CA, Goodman, AL, Joachimiak, G, Ordoñez, CL, Lory, S, Walz, T, Joachimiak, A, Mekalanos, JJ (2006). A virulence locus of *Pseudomonas aeruginosa* encodes a protein secretion apparatus. *Science* 312: 1526-1530.

152. Mukaida, N (2003). Pathophysiological roles of interleukin-8/CXCL8 in pulmonary diseases. *American Journal of Physiological and Lung Cell Molecular Physiology* 284: L566-L577.

153. Okkels, LM, Andersen, P (2004). Protein-protein interactions of proteins from the ESAT-6 family of *Mycobacterium tuberculosis*. *Journal of Bacteriology* 186: 2487-2491.

154. Oomen, CJ, van Ulsen, P, van Gelder, P, Feijen, M, Tommassen, J, Gros, P (2004). Structure of the translocator domain of a bacterial autotransporter. *EMBO J* 23(6): 1257-1266.

155. Pace, CN, Vajdos, F, Fee, L, Grimsley, G, Gray, T (1995). How to measure and predict the molar absorption coefficient of a protein. *Protein Science* 4(11): 2411-2423.

156. Packer, LM, Williams, SJ, Callaghan, S, Gotley, DC, McGuckin, MA (2004). Expression of the cell surface mucin gene family in adenocarcinomas. *International Journal of Oncology* 25(4): 1119-1126.

157. Pallen, MJ (2002). The ESAT-6/WXG100 superfamily-and a new Gram-positive secretion system? *Trends in Microbiology* 10: 209-212.

158. Pandey, A, Mann, M (2000). Proteomics to study genes and genomes. *Nature* 405: 837-846.

159. Pareek, M, Baussano, I, Abubakar, I, Dye, C, Lalvani, A (2012). Evaluation of immigrant tuberculosis screening in industrialized countries. *Emerging and Infectious Diseases* 18(9): 1422-1429.

160. Pethe, K (2000). Characterization of the heparin-binding site of the mycobacterial heparin-binding hemagglutinin adhesion. *Journal of Biological Chemistry* 275: 14273-14280.

161. Philipp, WJ, Nair, S, Guglielmi, G, Lagranderie, M, Gicquel, B, Cole, ST (1996). Physical mapping of *Mycobacterium bovis* BCG Pasteur reveals differences from the genome map of *Mycobacterium tuberculosis* H37Rv and from *M. bovis. Microbiology* 142: 3135-3145.

162. Podinovskaia, M, Lee, W, Cadwell, S, Russell, DG (2013). Infection of macrophages with *Mycobacterium tuberculosis* induces global modifications to phagosomal function. *Cell Microbiology* 15(6): 843-859.

163. Pukatzki, S, Ma, AT, Revel, AT, Sturtevant, D, Mekalanos, JJ (2007). Type VI secretin system translocate a phage tail spike-like protein into target cells where it is cross-links actin. *Proceedings of the National Academy of Science USA* 104(39): 15508-15513.

164. Pym, AS, Brodin, P, Brosch, R, Huerre, M, Cole, ST (2002). Loss of RD1 contributed to the attenuation of the live tuberculosis vaccines *Mycobacterium bovis* BCG and *Mycobacterium microti*. *Molecular Microbiology* 46: 709-717.

165. Rajaram, MVS, Ni, B, Dodd, CE, Schlesinger, LS (2014). Macrophage immunoregulatory pathways in tuberculosis (review). *Seminars in Immunology* 26: 471-485.

166. Ramakrishnan, L, Falkow, S (1994). *Mycobacterium marinum* persists in cultured mammalian cells in a temperature-restricted fashion. *Infection and Immunity* 62: 3222-3229.

167. Randhawa, AK, Shey, MS, Keyser, A, Peixoto, B, Wells, RD, de Kock, M, Lerumo, L, Hughes, J, Hussey, G, Hawkridge, A, Kaplan, G, Hanekom, WA, Hawn, TR, the South African Tuberculosis Vaccine Initiative Team (2011). Association of human TLR1 and TLR6 deficiency with altered immune responses to BCG vaccination in South African infants. *PLoS Pathogens* 7(8): e10002174.

168. Rao, SP, Alonso, S, Rand, L, Dick, T, Pethe, K (2008). The protonmotive force is required for maintaining ATP homeostasis and viability of hypoxic, non-replicating *Mycobacterium tuberculosis. Proceedings of the National Academy of Science USA* 105: 11945-11950.

169. Renshaw, PS, Lightbody, KL, Veverka, V, Muskett, FW, Kelly, G, Frenkiel, TA, Gordon, SV, Hewinson, RG, Burke, B, Norman, J, Williamson RA, Carr, MD (2005). Structure and function of the complex formed by the tuberculosis virulence factors CFP-10 and ESAT-6. *The EMBO Journal* 24*:* 2491-2498.

170. Renshaw, PS, Panagiotidou, P, Whelan, A, Gordon, SV, Hewinson, RG, Williamson, RA, Carr, MD (2002). Conclusive evidence that the major T-cell antigens of the *Mycobacterium tuberculosis* complex ESAT-6 and CFP-10 form a tight, 1:1 complex and characterization of the structural properties of ESAT-6, CFP-10, and the ESAT-6.CFP-10 complex. *The Journal of Biological Chemistry* 277(24): 21598-21603.

171. Rezaee, F, Meednu, N, Emo, JA, Saatian, B, Chapman, TJ, Naydenov, NG, De Benedetto, A, Beck, LA, Ivanov, AI, Georas, SN (2011). Polyinosinic: polycytidylic acid induces protein kinase D-dependent disassembly of apical

junctions and barrier dysfunction in airway epithelial cells. *Journal of Allergy and Clinical Immunology* 128(6): 1216-1224.

172. Rodriguez, GM, Voskuil, MI, Gold, B, Schoolnik, GK, Smith, I (2002). ideR, an essential gene in *Mycobacterium tuberculosis*: role of IdeR in iron-dependent gene expression, iron metabolism, and oxidative stress response. *Infection and Immunity* 70: 3371-3381.

173. Rohde, KH, Abramovitch, RB, Russell (2007). *Mycobacterium tuberculosis* invasion of macrophages: Linking bacterial gene to environmental cues. *Cell Host & Microbe* 2: 352-364.

174. Russell, DG (2001). *Mycobacterium tuberculosis*: here today, and here tomorrow. *Nature Rev Molecular Cell Biology* 2: 569-577.

175. Russell, DG (2011). *Mycobacterium tuberculosis* and the innate discourse of a chronic infection. *Immunological Reviews* 240: 252-268.

176. Ryndak, MB, Singh, KK, Peng, Z, Laal, S (2015). Transcriptional profile of *Mycobacterium tuberculosis* replicating in type II alveolar epithelial cells. *PLoS One* 10(4): e0123745.

177. Samten, B, Wang, X, Barnes, PF, (2009). *Mycobacterium tuberculosis* ESX-1 system-secreted protein ESAT-6 but not CFP-10 inhibits human T-cell immune responses. *Tuberculosis* 89: 574-576.

178. Sassetti, CM, Rubin, EJ (2003). Genetic requirements for mycobacterial survival during infection. *Proceedings of the National Academy of Science USA* 100: 12989-12994.

179. Schnappinger, D, Ehrt, S, Voskuil, MI, Liu, Y, Mangan, JA, Monahan, IM, Dolganov, G, Efron, B, Butcher, PD, Nathan C, Schoolnik, GK (2003). Transcriptional adaptation of *Mycobacterium tuberculosis* within macrophages:

Insights into the phagosomal environment. *The Journal of Experimental Medicine* 198(5): 693-704.

180. Schorey, JS, Holsti, MA, Ratliff, TL, Allen, PM, Brown, EJ (1996). Characterization of the fibronectin-attachment protein of *Mycobacterium avium* reveals a fibronectin-binding motif conserved among mycobacteria. Molecular *Microbiology* 21(2): 321-329.

181. Sears, CL (2000). Molecular physiology and pathophysiology of tight junctions V. Assault of tight junction by enteric pathogens. American Journal of Physiology-Gastrointestinal and Liver Physiology 279: G1129-G1134.

182. Serafini, A, Boldrin, F, Palù, G, Manganelli, R (2009). Characterization of a *Mycobacterium tuberculosis* ESX-3 conditional mutant: essentiality and rescue by iron and zinc. *Journal of Bacteriology* 191: 6340-6344.

183. Shimoji, Y, Ng, V, Matsumura, K, Fischetti, VA, Rambukkana, A (1999). A 21 kDa surface protein of *Mycobacterium leprae* binds peripheral nerve laminin-2 and mediates Schawnn cell invasion. *Proceedings of the National Academy of Science USA* 96:9857-9862.

184. Siegrist, MS, Unnikrishnan, M, McConnell, MJ, Borowsky, M, Cheng, TY, Siddiqi, N, Fortune, SM, Moody, BM (2009). Mycobacterial Esx-3 is required for mycobactin-mediated iron acquisition. *Proceedings of the National Academy of Science USA* 106: 18792-18797.

185. Simeone, R, Bobard, A, Lippmann, J, Bitter, W, Majlessi, L, Brosch, R, Enniga, J (2012). Phagosomal rupture by *Mycobacterium tuberculosis* results in toxicity and host cell death. *PLoS Pathogens* 8(2): e1002507.

186. Simeone, R, Bottai, D, Brosch, R (2009). ESX/type VII secretion system and their role in host-pathogen interaction. *Current Opinion in Microbiology* 12: 4-10.

187. Skøjt, RLV, Brock, I, Arend, SM, Munk, ME, Theisen, M, Ottenhoff, THM, Andersen, P (2002). Epitope mapping of the immunodominant antigen TB10.4 and the two homologous proteins TB10.3 and Tb12.9, which constitute a subfamily of the *esat-6* gene family. *Infection and Immunity* 70: 5446-5453.

188. Skøjt, RLV, Oettinger, T, Rosenkrands, I, Ravn, P, Brock, I, Jacobsen, S, Andersen, P (2000). Comparative evaluation of low-molecular-mass proteins from *Mycobacterium tuberculosis* identifies members of the ESAT-6 family as immunodominant T-cell antigens. *Infection and Immunity* 68: 214-220.

189. Slayden, RA, Knudson, DL, Belisle, JT (2006). Identification of cell cycle regulators in *Mycobacterium tuberculosis* by inhibition of septum formation and global transcriptional analysis. *Microbiology* (152): 1789-1797.

190. Smith, J, Manoranjan, J, Pan, M, Bohsali, A, Xu, J, Liu, J, McDonald, KL, Szyk, A, LaRonde-LeBlanc, N, Gao, LY (2008). Evidence for pore formation in host cell membranes by ESX-1-secreted ESAT-6 and its role in *Mycobacterium marinum* escape from the vacuole. *Infection and Immunity* 76(12): 5478-5487.

191. Söderström, TS, Nyberg, SD, Eriksson, E (2005). CD95 capping is ROCK-dependent and dispensable for apoptosis. *Journal of Cell Science* 118: 2211-2223.

192. Sorensen, AL, Nagai, S, Houen, G, Andersen, P, Andersen, AB (1995). Purification and characterization of a low-molecular-mass T-cell antigen secreted by *Mycobacterium tuberculosis*. *Infection and Immunity* 63: 1710-7.

193. Stadnyk, AW (1994). Cytokine production by epithelial cells. FASEB J 8(13): 1041-1047.

194. Stamm, LM, Morisaki, JH, Gao, LY, Jeng, RL, McDonald, KL, Roth, R (2003). *Mycobacterium marinum* escapes from phagosomes and is propelled by actin-based motility. *Journal of Experimental Medicine* 198: 1361-1368.

195. Stanley, SA, Raghavan, S, Hwang, WW, Cox, JS (2003). Acute infection and macrophage subversion by *Mycobacterium tuberculosis* require a specialized secretion system. *Proceedings of the National Academy of Science USA* 100: 13001-13006.

196. Stoop, EJM, Bitter, W, van der Sar, AM (2012). Tubercle bacilli rely on a type VII army for pathogenicity. *Trends in Microbiology* 20: 477-484.

197. Sweeney, KA, Dao, DN, Goldberg, MF, Hsu, T, Venkataswamy, MM, Henao-Tamayo, M, Ordway, D, Sellers, RS, Jain, P, Chen, B, Chen, M, Kim, J, Lukose, R, Chan, J, Orme, IM, Porcelli, SA, Jacobs Jr, WR (2012). A recombinant *Mycobacterium smegmatis* induces potent bactericidal immunity against *Mycobacterium tuberculosis*. *Nature Medicine* 17(10): 1261-1268. 2011

198. Swindle, EJ, Collins, JE, Davies, DE (2009). Breakdown in epithelial barrier function in patients with asthma: Identification of novel therapeutic approaches. Journal of Allergy and Clinical Immunolgy 124 (1): 23-34.

199. Teitelbaum, R, Schubert, W, Gunther, L, Kress, Y, Macaluso, F, Pollard, JW, McMurray, DN, Bloom, BR (1999). The M cell as a portal of entry to the lung for the bacterial pathogen *Mycobacterium tuberculosis. Immunity* 10:641-650.

200. Tekaia, F, Gordon, SV, Garnier, T, Brosch, R, Barrell, BG, Cole, SR (1999). Analysis of the proteome of *Mycobacterium tuberculosis* in silico. *Tubercle and Lung Disease* 79(6): 329-342.

201. Tinaztepe, E, Wei, JR, Raynowska, J, Portal-Celhay, C, Thompson, V, Philips, JA (2016). Role of metal-dependent regulation of ESX-3 secretion in

intracellular survival of *Mycobacteirum tuberculosis. Infection and Immunity* 84(8): 2255-2263.

202. Tsai, KN, Chan, EC, Tsai, TY, Chen, KT, Chen, CY, Hung, K, Chen, CM (2009). Cytotoxic effect of recombinant Mycobacterium tuberculosis CFP-10/ESAT-6 protein on the crucial pathways of WI-38 cells. *Journal of Biomedicine and Biotechnology* 2009: ID 917084.

203. Tufariello, JM, Chapman, JR, Kerantzas, CA, Wong, KW, Vilchèze, C, Jones, CM, Cole, LE, Tinaztepe, E, Thompson, V, Fenyo, D, Niederweis, M, Ueberheide, B, Philips, JA, Jacobs Jr., WR (2016). Separable roles for Mycobacterium tuberculosis ESX-3 effectors in iron acquisition and virulence. Proceedings of the National Academy of Science USA 113(3): E348-E357.

204. Ulrichs, T, Kaufmann, SHE (2006). New insights into the function of granulomas in human tuberculosis. *Journal of Pathology* 208(2): 261-269.

205. Uplekar, S, Heym, B, Friocourt, V, Rougemont, J, Cole, ST (2011). Comparative genomics of *esx* genes from clinical isolates of *Mycobacterium tuberculosis* provides evidence for gene conversion and epitope variation. *Infection and Immunity* 79(10): 4042-4049.

206. Van der Wel, N, Hava, D, Houben, D, Fluitsma, D, van Zon, M, Pierson, J, Brenner, M, Peters, PJ (2007). *M. tuberculosis* and *M. leprae* translocate from the phagolysosome to the cytosol in myeloid cells. *Cell* 129: 1287-1298.

207. Van Furth, R, Cohn, ZA, Hirsch, JG, Humphrey, JH, Spector, WG, Langevoort, HL (1972). The mononuclear phagocyte system: a new classification of macrophages, monocytes, and their precursor cells. *Bull World Health Organ* 46(6): 845-852.

208. Van Pinxteren, LA, Cassidy, JP, Smedegaard, BH, Agger, EM, Andersen, P (2000). Control of latent Mycobacterium tuberculosis infection is dependent on CD8 T cells. *European Journal of Immunology* 30: 3689-3698.

209. Verrall, AJ, Netea, MG, Alisjahbana, B, Hill, PC, van Crevel, R (2013). Early clearance of *Mycobacterium tuberculosis*: A new frontier in prevention. *Immunology* 141: 506-513.

210. Voss, S, Hallstrom, T, Saleh, M, Burchhardt, G, Pribyl, T, Singh, B, Riesbeck, K, Zipfel, PF, Hammerschmidt, S (2013). The choline-binding protein PspC of *Streptococcus pneumoniae* interacts with the C-terminal heparin-binding domain of vitronectin. *Journal of Biological Chemistry* 288: 15614-15627.

211. Walters, G, Bussow, K, Cahill, D, Lueking, A, Lehrach, H (2000). Protein arrays for gene expression and molecular interaction screening. *Current Opinion in Microbiology* 3; 298-302.

212. Wang, X, Barnes, PF, Dobos-Elder, KM, Townsend, JC, Chung, YT, Shams, H, Weis, SE, Samten, B (2009). ESAT-6 inhibits production of IFN-γ by *Mycobacterium tuberculosis*-responsive human T cells. *Journal of Immunology* 182: 3668-3677.

213. Wang, X, Barnes, PF, Huang, F, Alvarez, IB, Neuenschwander, PF, Sherman, DR, Samten, B (2012). Early secreted antigenic target of 6kDa protein of *Mycobacterium tuberculosis* primes dendritic cells to stimulate Th17 and inhibit Th1 immune responses. *Journal of Immunology* 189: 3092-3103.

214. Ware, LB, Matthay, MA (2001). Alveolar fluid clearance is impaired in the majority of patients with acute lung injury and the acute respiratory distress syndrome. *The American Journal of Respiratory and Critical Care Medicine* 163: 1376-1383.

215. Warner, DF, Mizrahi, V (2006). Tuberculosis chemotherapy: the influence of bacillary stress and damage response pathways on drug efficacy. *Clinical Microbiology Rev* 19(3): 558-570.

216. Wassenaar, TM, Bohlin, J, Binnewies, TT, Ussery, DW (2009). Genome comparison of bacterial pathogens. *Microbial Pathogenomics* 6: 1-20.

217. Waters, CM, Savla, U, Panos, RJ (1997). KGF prevents hydrogen peroxide-induced increases in airway epithelial cell permeability. *The American Journal of Physiology* 272: L681-L689.

218. Weerdenburg, EM, Abdallah, AM, Mitra, S, de Punder, K, van der Wel, NN, Bird, S, Appelmelk, BJ, Bitter, W, van der Sar, AM (2012). ESX-5-deficient *Mycobacterium marinum* is hypervirulent in adult zebrafish. *Cell Microbiology* 14(5): 728-739.

219. Weinstein, EA, Yano, T, Li, LS, Avarbock, D, Avarbock, A, Helm, D, McColm, AA, Duncan, K, Lonsdale, JT, Rubin, H (2005). Inhibitors of type II NADH: menaquinone oxidoreductase represent a class of antitubercular drugs. *Proceedings of the National Academy of Science USA* 102(12): 4548-4553.

220. Wickremasinghe, MI, Thomas, LH, Friedland, JS (1999). Pulmonary epithelial cells are a source of IL-8 in the response to *Mycobacterium tuberculosis*: Essential role of IL-1 from infected monocytes in a NF-κβ-dependent network. *The Journal of Immunology* 163: 3936-3947.

221. Wicks, IA, Howell, ML, Hancock, T, Kohsaka, H, Olee, T, Carson, DA (2008). Bacterial lipopolysaccharide copurifies with plasmid DNA: Implications for animal models and human gene therapy. Human Gene Therapy 6(3): 317-323.

222. World Health Organization (WHO) Geneva (2013). Global Tuberculosis Report 2013.

223. Xie, Z, Siddiqi, N, Rubin, EJ (2005). Differential antibiotic susceptibilities of starved *Mycobacterium tuberculosis* isolates. *Antimicrobial Agents and Chemotherapy* 49: 627-631.

224. Xu, Y, Liu, W, Shen, H, Yan, J, Qu, D, Wang, H (2009). Recombinant Mycobacterium bovis BCG expressing the chimeric protein of antigen 85B and ESAT-6 enhances the Th1 cell-mediated response. *Clinical and Vaccine Immunology* 16(8): 1121-1126.

225. Zakham, F, Aouane, O, Ussery, D, Benjouad, A, Ennaji, MM (2012). Computational genomis-proteomics and phylogeny analysis of twenty one mycobacterial genomes (tuberculosis and non tuberculosis strains). Microbial *Informatics and Experimentation* 2: 7-16

226. Zhang, A (2009). Protein interaction networks-computational analysis. *Cambridge University Press, New York, USA* pp 11-20.

227. Zhang, Y, Broser, M, Cohen, H, Bodkin, M, Law, K, Reibman, J, Rom, WN (1995). Enhanced interleukin-8 release and gene expression in macrophages after exposure to *Mycobacterium tuberculosis* and its components. *Journal of Clinical Investigation* 95: 586-592.

228. Zhang, M, Kwang, JK, Iyer, D, Lin, Y, Belisle, J, McEnery, K, Crandall, ED, Barnes, PF (1997). Effects of *Mycobacterium tuberculosis* on the bioelectric properties of the alveolar epithelium. *Infection and Immunity* 65: 692-698.

229. Zheng, Z, Luo, Y, McMaster, GK (2006). Sensitive and quantitative measurement of gene expression directly from a small amount of whole blood. *Clinical Chemistry* 52(7): 1294-1302.

230. Zhu, H, Synder, M (2001). Protein arrays and microarrays. *Current Opinion in Chemical Biology* 5:40-45.

Theses:

1. Alharbi, S. PhD thesis 2012. Characterization of the structural properties and features of *M. tuberculosis* complex proteins linked to tuberculosis pathogenesis.

2. Iakobachvili, N. PhD thesis 2014. Mycobacterial resuscitation promoting factors: roles and mechanisms in infected macrophages.

3. Ray, A. PhD thesis 2010. Expression and localization of the *Mycobacterium marinum* potential virulence factor, Mpm70 during infection: evidence for a post-phagosomal role in pathogenesis.

4. Renshaw, PS. PhD thesis 2002. Structural characterization of CFP-10 and ESAT-6, potent T-cell antigens of the *Mycobacterium tuberculosis* complex: implications for pathogenesis and virulence.

Websites:

www.bdbiosciences.com/go/humancdmarkers

www.proteinatlas.org/tissue